Controlled molecular architectures via ring opening metathesis polymerisation

Panagiotis Dounis

Controlled Molecular Architectures via Ring Opening Metathesis Polymerisation

by

Panagiotis Dounis, M.Sc. (Dunelm)

A thesis submitted in part fulfillment of the requirements for the degree of

Doctor of Philosophy at the University of Durham

February MCMXCIV

Abstract

Controlled Molecular Architectures via Ring Opening Metathesis Polymerisation

This thesis describes studies into the ring opening metathesis polymerisation (ROMP) of some monocyclic alkenes, the living polymerisation of cyclopentene and the preparation of novel block copolymers and novel polyethylene architectures using living poly(1-pentenylene) as the precursor polymer.

Chapter 1 reviews general aspects of ring opening metathesis polymerisation of relevance to the themes of this thesis.

Chapter 2 describes the ROMP of *cis,cis*-cycloocta-1,5-diene, cyclopentene, cycloheptene, cyclooctene, cyclodecene and cyclododecene using a series of well-defined initiators of general formula $M(N\text{-}2,6\text{-}i\text{-}Pr_2\text{-}C_6H_3)(CHR)(OR')_2$ where M=Mo or W, the characterisation of the resulting polymers using ^1H-, ^{13}C-NMR and IR spectroscopy, differential scanning calorimetry and gel permeation chromatography and an analysis of their ^{13}C-NMR spectroscopic data in terms of the γ-gauche effect.

Chapter 3 reports on a ^1H-NMR study of the synthesis of poly(bis(trifluoromethyl)norbornadiene)-*block*-poly(1-octenylene) and the synthesis and characterisation of poly(1-pentenylene)-*block*-polyacetylene-*block*-poly(1-pentenylene).

Chapter 4 describes the synthesis of narrow molecular weight distribution linear and three-branched star polyethylenes via ROMP of cyclopentene initiated by a well-defined tungsten based initiator at low temperature and subsequent capping with mono-, di- and trifunctional aldehydes.

Chapter 5 presents an investigation on routes to a well-defined difunctional ROMP initiator which could potentially be used for the synthesis of polyethylene networks.

Finally, Chapter 6 summarises the conclusions and outlines some suggestions for future work.

Acknowledgements

The work in this thesis would not have been possible without the contribution of many friends and colleagues whom I would like to thank.

Professor Feast for his continuous guidance, support and encouragement.

Dr. Brian Wilson and Dr. Ezat Khosravi for their helpful and patient advice; Prof. Vernon Gibson for sharing his expert knowledge of transition metal chemistry; Dr. Alan Kenwright for help with interpretation and presentation of the NMR spectra and Mrs Julia Say for recording them. Gordon Forrest for his help with the GPC and DSC. Ray Hart and Gordon Haswell for providing me with the glassware, and all the staff of the Chemistry Department for their assistance during the past three years. All my colleagues in the IRC for helpful discussions and for generating an "interesting" working environment. Steve for his patience with my lead guitar abilities, the Killa Kortz and B minor. John for his financial advice, the occasional tab and his job.

Nicholas for his views and ideas on life, the universe and everything; Nikitas for being a valuable friend and an excellent DJ partner; Kalliope and Marina for the feminine perspective and Antonis for his help and friendship.

My parents for their loving care and support.

And Carole-Anne for her help, the encouraging smile and for making the chemistry a lot more exciting ☺.

Memorandum

The work reported in this thesis was carried out at the Interdisciplinary Research Centre in Polymer Science and Technology at Durham University between October 1990 and December 1993. This work has not been submitted for any other degree and is the original work of the author except where acknowledged by reference.

Statement of Copyright

Financial Support

The Science and Engineering Research Council and the Interdisciplinary Research Centre in Polymer Science and Technology are gratefully acknowledged for providing a grant for the work described herein.

Contents

APPENDIXES

CHAPTER 1: General Introduction and Background

1.1. Definition and historical background of ring opening metathesis polymerisation (ROMP)

The Olefin Metathesis reaction is a catalytically induced bond reorganisation reaction involving the breaking and making of carbon-carbon double bonds. The total number and the type of chemical bonds is unchanged during the process.

In the presence of heterogeneous catalysts prepared from tungsten and molybdenum hexacarbonyls, the reaction, for acyclic olefins, leads to the exchange of alkylidene units. This was first reported in 1964 by Banks and Bailey[1], and was termed "olefin disproportionation".

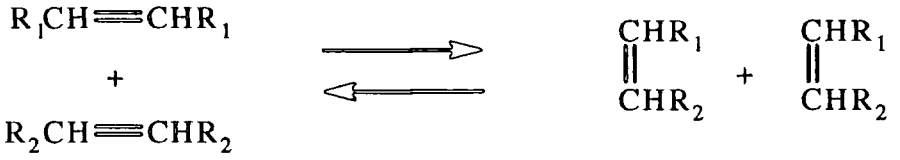

For cyclic olefins the metathesis reaction leads to ring scission and the formation of linear polymers:

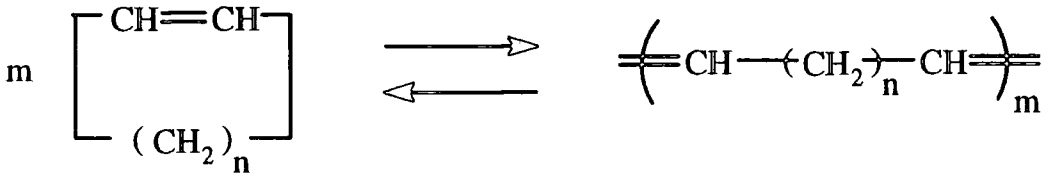

In 1967, Calderon et al[2] were the first to use the term 'olefin metathesis' for the overall result of these reactions, realising that both the ring opening of cyclic alkenes to yield unsaturated polymers and the olefin disproportionation reaction were governed by the same mechanism. Probably the first example of an olefin metathesis reaction catalysed by a transition metal was reported by Anderson and Merckling[3] in 1955. They successfully polymerised bicyclo[2.2.1]hept-2-ene using a mixture of titanium tetrachloride and either ethylmagnesium bromide or lithium

tetrabutylaluminium. It appears that there was some confusion concerning the structure of the polymeric product but Truett and co-workers[4,5] showed that the catalyst system used by Anderson and Merkling worked by ring opening. Shortly after these solution phase polymerisations had been reported, Eleuterio[6] described a catalyst prepared from molybdenum oxide on alumina, activated by hydrogen reduction and further reacted with aluminium hydride, which was able to polymerise a variety of monocyclic, bicyclic and tricyclic olefins by ring opening. In the case of cyclopentene *trans*-poly(1-pentenylene) was formed, but only in low yield. In 1963, Dall'Asta and Natta,[7] demonstrated the possibility of producing stereoregular polymers from cycloalkenes. They showed that cyclobutene was polymerised to predominantly or exclusively *cis*- or *trans*-poly(1-butenylene) by using different catalyst systems at various temperatures; for example $TiCl_4$ / Et_3Al (1/3) in n-heptane at -50°C gave high *cis*-poly(1-butenylene), $TiCl_4$ / Et_3Al (1/2) in toluene at -20°C gave 65% *trans*-poly(1-butenylene) and $RuCl_3$ in EtOH at 20°C gave all *trans*-poly(1-butenylene). Subsequently the same authors,[8] investigated tungsten and molybdenum halides in combination with organoaluminium compounds as catalysts for the ring-opening polymerisation of cyclopentene under mild conditions. They were able to obtain high *trans*-poly(1-pentenylene) by using WCl_6 / Et_3Al at -30°C. As mentioned earlier, a significant contribution to the evolution of the olefin metathesis concept was made in 1967 by Calderon et al,[9,10,11] who converted 2-pentene into a mixture of 2-butene and 3-hexene, using a catalyst derived from tungsten hexachloride (or the product of the reaction of equimolar amounts of tungsten hexachloride and an alcohol), and an organoaluminium compound. This was important because it demonstrated that ring-opening reactions and olefin disproportionation belong to the same class of reaction and are affected by similar transition metal-based catalyst systems.

The olefin metathesis reaction has been extensively reviewed and is the subject of recent books.[12-16] The following sections briefly review the main features of olefin metathesis which are relevant to the work described in this thesis.

1.2. Initiating systems

The initiating systems used for ROMP are based on the transition metals of groups IVA to VIII of the periodic table. The compounds of Ti, Zr, V, Ta, Cr, Mo, W, Re, Ru and Os are frequently cited and effective initiators can be classified as shown below.

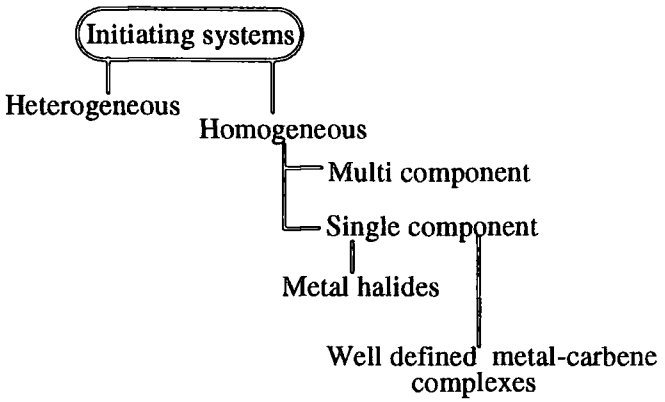

For a given monomer the effectiveness of the initiator depends on the structure of that monomer and the reaction conditions. Highly strained rings such as those found in norbornene or cyclobutene will polymerise when the reaction is initiated with Ti, V, Ru, Os and Ir derived systems, while less strained monocyclic alkenes, such as cyclopentene, demand more active initiating systems such as those derived from W or Mo compounds.[17]

1.2.1. Heterogeneous systems

These are generally transition metal oxides, sulfides or carbonyls which are absorbed on to a high surface area support, such as alumina or silica. These systems are used to catalyse the metathesis reactions of acyclic olefins but only rarely used for the initiation of ROMP.

1.2.2. Homogeneous systems

These are used in the liquid phase, either in solution or in neat monomer. The most effective systems are generally based on W, Mo and Re compounds.[12]

1.2.2.a. Multi-component

These initiator systems are usually generated from the reaction of a transition metal halide such as WCl_6 or $MoCl_5$ with an alkyl or aryl substituted metal such as $C_2H_5AlCl_2$, $(CH_3)_4Sn$ or $(C_6H_5)_4Sn$. They are usually refered to as "classical initiators". In some systems a third component such as an alcohol or another oxygen containing compound is added to enhance the activity. The metal carbene which is believed to be the initiating species in such systems (see later), is postulated to be formed in a reaction between these two components.[18] The rate at which active species are formed varies in different systems; thus, for example the $WCl_6/(CH_3)_4Sn$ (1:1) system takes several minutes until it reaches maximum activity, while the $WCl_6/C_2H_5AlCl_2/C_2H_5OH$ (1:4:1) system generates active species much faster, and the addition of monomer to the reaction mixture is recommended before the addition of $C_2H_5AlCl_2$.[19]

1.2.2.b. Single component

The Casey[21,22] and Fischer[23] carbenes were the first stable and active metal-carbene species that were shown to be capable of inducing olefin metathesis.

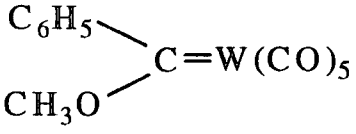

Fischer carbene

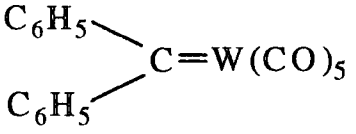

Casey carbene

Kress and Osborn[20] described well-defined metal-carbenes which, although inactive themselves, gave highly active initiating systems in the presence of $AlBr_3$ or $GaBr_3$. The interaction between the Lewis acid and the well-defined transition metal carbene can occur in two ways (see below) both of which result in the formation of active initiators.

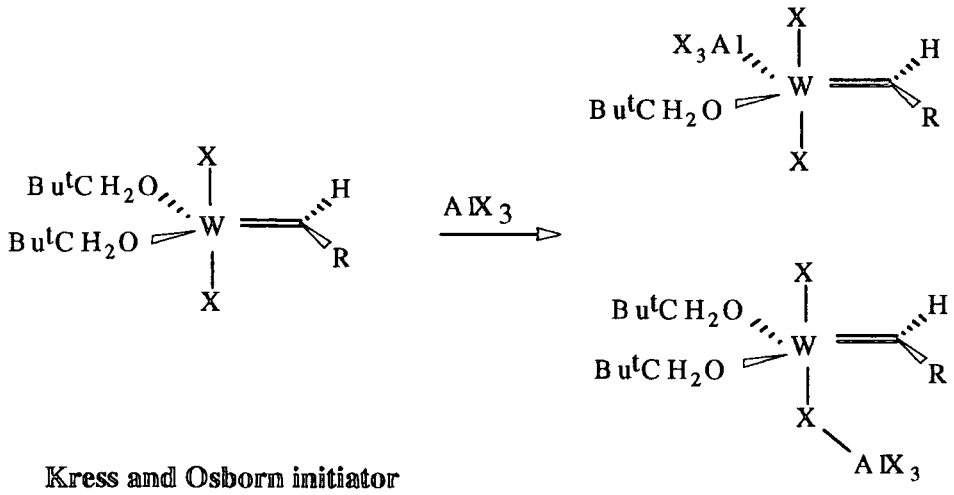

Kress and Osborn initiator

R.H.Grubbs and L.R.Gilliom reported[38] the preparation of titanium based initiators which were able to ROM polymerise norbornene and give living polynorbornene with narrow molecular weight distribution. These initiators, illustrated below, are unique among metathesis systems in that the metallacyclobutane appears to be the most stable form of the chain-carrying species rather than the metal carbene.

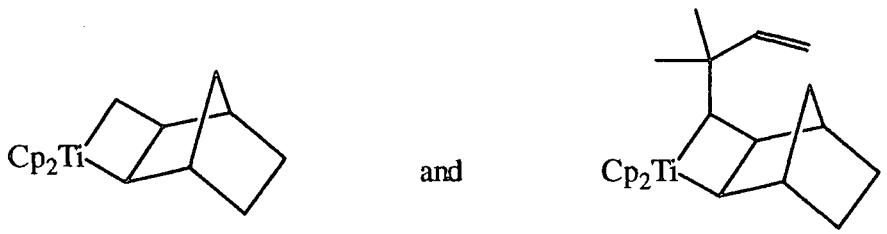

Grubbs titanacyclobutanes - well defined ROMP initiators

Schrock and coworkers introduced a particularly valuable group of initiators based on four co-ordinated metal-carbene complexes containing bulky ligands. For W and Mo centered complexes a suitable combination is two tertiary butoxides and a 2,6-diisopropylphenyl imido ligand (see figure below) in addition to the active alkylidene. Substitution of the methyl groups on the alkoxides with the more electronegative trifluoromethyl groups lead to more active initiating systems.[24,25] This increased reactivity is believed to be due to the trifluoromethyl groups drawing

electron density away from the metal centre, making it more electrophilic and a better acceptor for the incoming π-donor olefin. This effect is illustrated for the tungsten initiator by the observation that when OR is $OCMe(CF_3)_2$ the initiator will readily metathesise acyclic olefins but when OR is O-^{t}Bu it does not react readily with acyclic olefins.

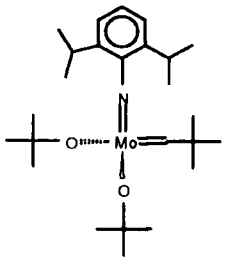

$Mo(NAr)(CH^tBu)(O^tBu)_2$

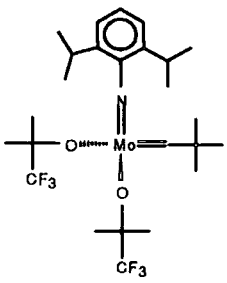

$Mo(NAr)(CH^tBu)(OC(CH_3)_2CF_3)_2$

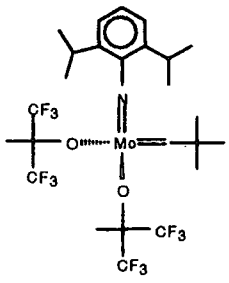

$Mo(NAr)(CH^tBu)(OCCH_3(CF_3)_2)_2$

Mo-based Schrock type initiators

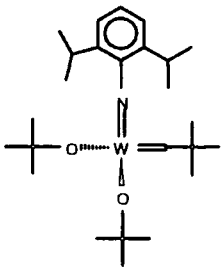

$W(NAr)(CH^tBu)(O^tBu)_2$

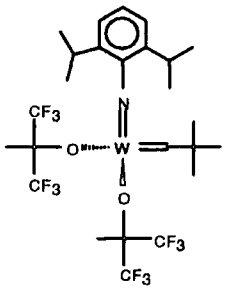

$W(NAr)(CH^tBu)(OCCH_3(CF_3)_2)_2$

W-based Schrock initiators

The representation of the bonding situation in Schrock and Fischer type metal carbene complexes of the general type $L_nM{=}CR_2$ presents some potential for complexity and possible confusion, particularly in relation to the bonding of the $:CR_2$ group to the metal[26] (see Figure 1.2.a). Carbenes, $L_nM{=}CR_2$, have "Fischer character" for low oxidation state, late transition metals, having π–acceptor ligands L, and π-donor substituents R, such as ^-OMe or $^-NMe_2$, on the carbene carbon. Such a carbene behaves as if it carries a δ^+ charge on the carbon, that is to say it is electrophilic. "Schrock character" is shown by carbenes bound to higher-oxidation

state, early transition metals, having non-π-acceptor ligands, and non-π-donor R groups. In this case, the carbene carbon behaves as a nucleophile, having a δ^- charge on the carbon.

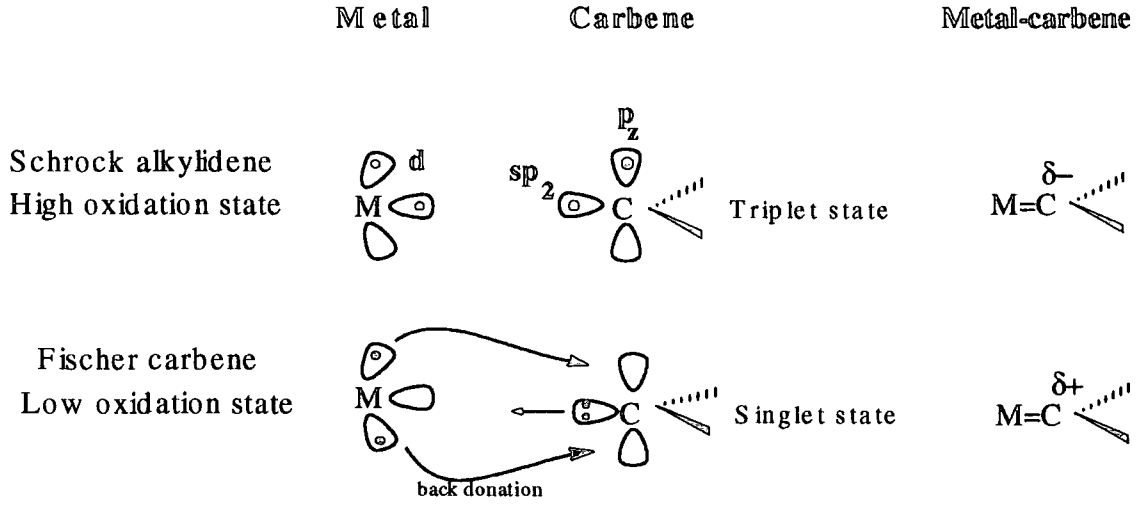

Figure 1.2.a **Metal-carbene bonding in Schrock and Fischer type complexes**

The process of defining and expanding the range of well defined metal carbenes which are active in metathesis reactions have been very fruitful during the last decade and the process appears likely to continue. For example Grubbs[27] recently reported the preparation of a stable ruthenium metal carbene initiating species which is able to initiate the 'living' ROMP of strained cyclic olefins, even in the presence of protic solvents such as ethanol or water.

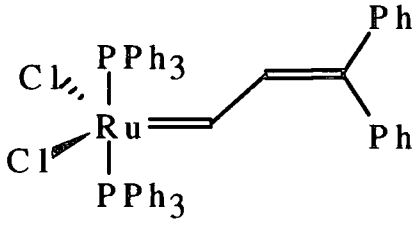

Grubbs Ru metal carbene

1.2.2.c. Transition metal halides

Compounds with neither a preformed metal carbene nor an alkyl or aryl containing species, such as WCl_6, $ReCl_5$ and $OsCl_3$ can initiate ROMP and they are also refered to as 'classical initiators'. In such systems it is believed that the metal carbene is generated by the reaction of the monomer with the transition metal. Activators such as oxygen, water or ethanol are sometimes required in order for this reaction to occur.[28] The ruthenium, osmium and iridium trichloride trihydrates ($MCl_3 \cdot 3H_2O$) can initiate ROMP of strained monomers, such as norbornenes and oxanorbornenes, in protic media (water or ethanol) unlike most other initiating systems which cannot tolerate even traces of these solvents.

1.3 A comparison of classical and well defined initiators.

The classical, ill-defined initiators have certain disadvantages in comparison with the well-defined systems including:

-limited tolerance to functional groups on the monomer,

-lack of molecular weight and molecular weight distribution control due to intra- or intermolecular reactions with the double bonds in the chain itself and

-an element of irreproducibility

There is a degree of control in the reactivity of the well-defined initiators, for example by choosing the suitable ligands, in contrast to classical systems whose reactivity cannot be systematically controlled with any precision.

Classical systems only rarely produce stereoregular polymers[29] while the use of well defined initiators has allowed the synthesis of some highly stereoregular, virtually monodisperse polymers and well defined block copolymers. Thus, for example, 'fine tuning' of the reactivity of the Schrock initiators by altering the electronegativity of the ligands can lead to polymer structures with controlled stereoregularities.[30]

Overall it seems that the key to well defined living ROMP is the careful design of isolable, well characterised initiating systems.

1.4. Mechanism of ring opening metathesis polymerisation

Initially a pairwise mechanism was proposed. According to that suggestion, two olefin units are associated with the metal atom in such a way that the double bonds may change position (see below). In the case of cyclic olefins the size of the ring is doubled by this step-growth process and repetition leads to macrocyclic compounds. The main objections to this mechanism are associated with the severe steric hinderance involved at the metal centre[31,32] and the observation of the formation of high molecular weight polymer in the presence of monomer even at low conversions which is characteristic of chain growth polymerisations. This pairwise mechanism was discarded in favour of the *metal carbene chain mechanism*, a non-pairwise mechanism proposed initially by Herrison and Chauvin,[33] involving a metal carbene as the chain carrier.

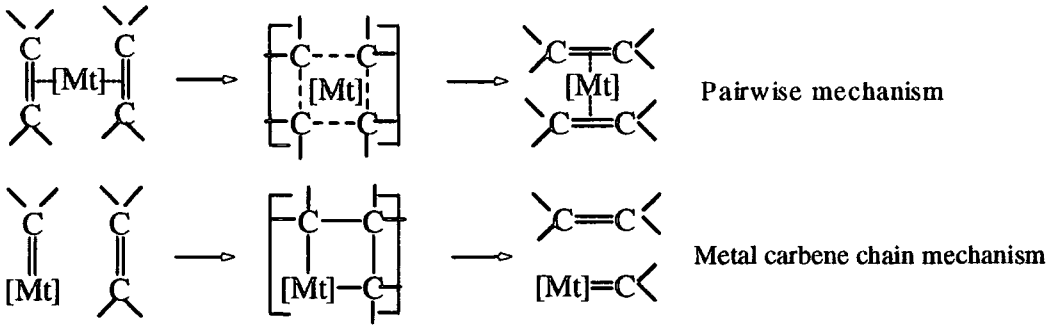

The metal carbene mechanism involves the formation of an intermediate metallacyclobutane which then cleaves to produce a new metal carbene and an alkene and it is the currently accepted mechanism for the olefin metathesis reaction. Polymerisation of cyclic olefins via ROMP, like other chain processes, proceeds via initiation, propagation and termination.

1.4.1. Initiation

There is good evidence for the involvement of a metal carbene in the initiation step. The fact that preformed metal carbenes like the Fischer carbene or the Schrock

alkylidenes initiate the chain reaction suggests, but does not prove, that these species are involved.

For the classical initiators, the reaction between the metal halide and the alkylating agent is believed to produce the initiating alkylidene. The metathesis reaction[18] of $CH_3CH{=}CH(CH_2)_4CH{=}CHCH_3$ catalysed by $WCl_6/(CD_3)_4Sn$ to give cyclohexene and 2-butene,

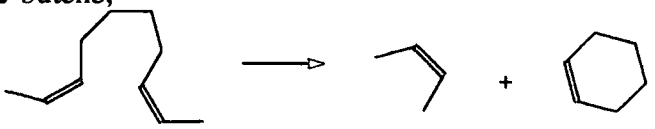

gives, as an initial product, $CH_3CH{=}CD_2$ which is consistent with the hypothesis that the initiating species involved is $[W]{=}CD_2$, formed according to the scheme shown below.

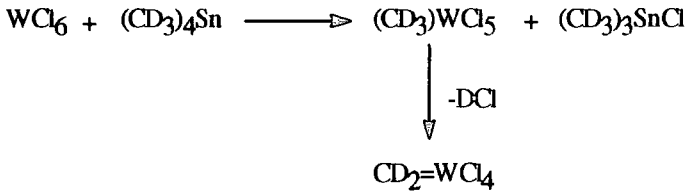

A study of this initiator system by Thorn Csyani[34-36] using UV spectroscopy gave support to this hypothesis, although these authors proposed a detailed and somewhat different scheme for the formation of the metal carbene; see below.

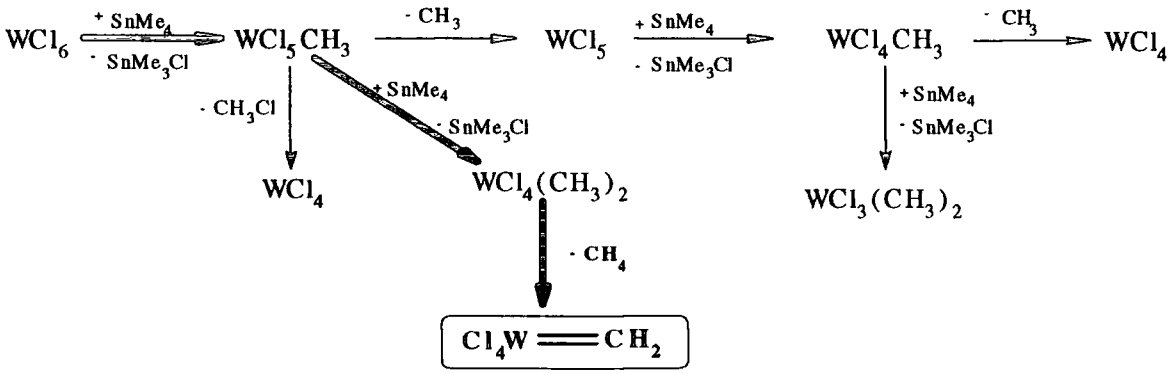

For the well defined initiators the initiating step is the one that involves the first insertion of monomer. When a strained double bond binds to a metal centre there is a relief of strain as a result of the lengthening of the double bond and a relaxation of the

angle at the vinylic carbons from 120° (suitable for sp^2 hybridisation) to closer to 109° (suitable for sp^3 hybridisation)[26]. This is followed by the formation of a metallacyclobutane which then cleaves, either productively to give the first insertion product and the first propagating alkylidene or non-productively (degeneratively) to give the initiating alkylidene and the initial olefin, see Figure 1.4.a .

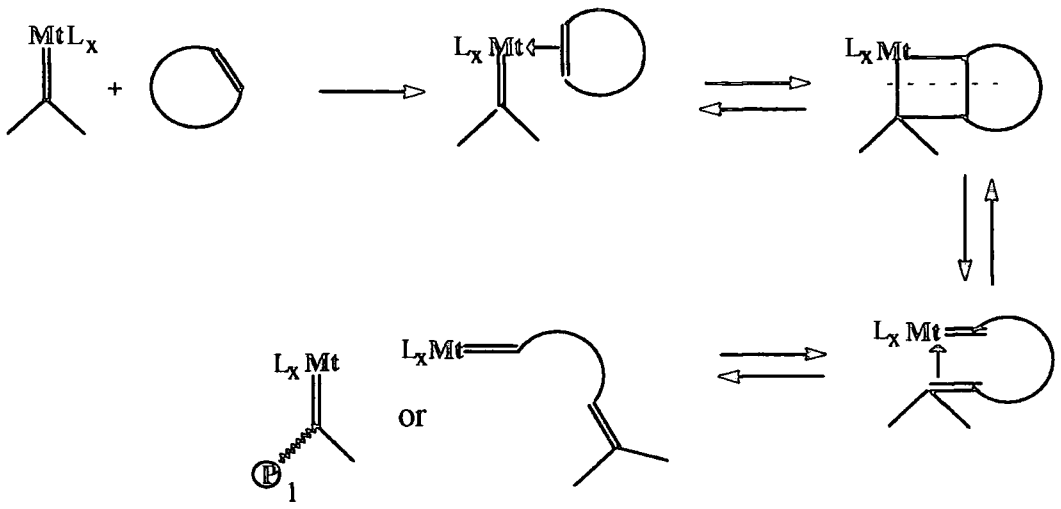

Figure 1.4.a Ring opening metathesis polymerisation initiation

1.4.2. Propagation

For well defined initiators the propagation step is similar to the initiation step but the substituents at the metal carbene carbon are different. Again a metallacyclobutane forms as an intermediate which cleaves as shown in Figure 1.4.b reproducing the metal carbene at the end of the chain.

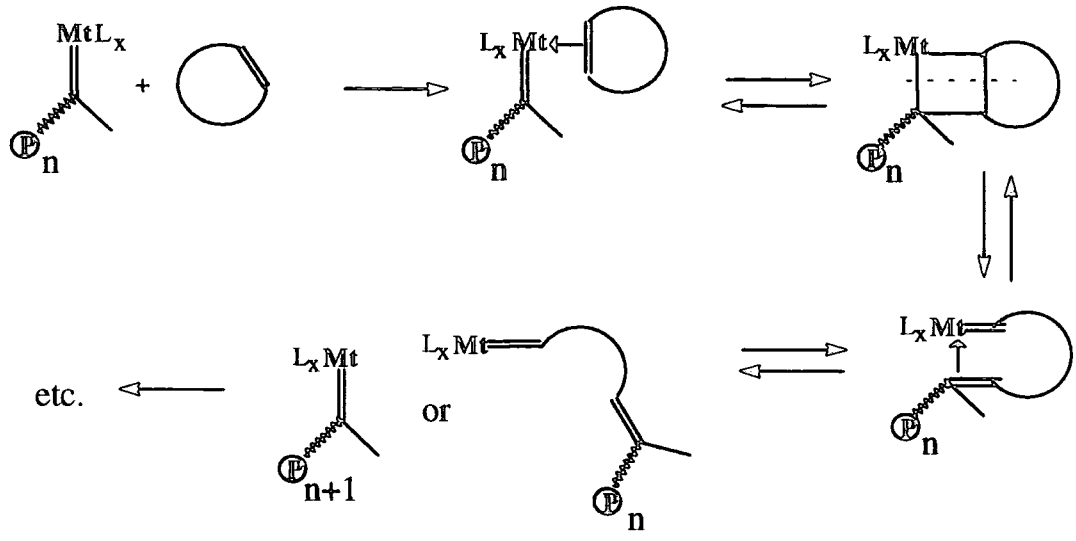

Figure 1.4.b Ring opening metathesis polymerisation propagation

There is plentiful evidence to support the formation of a metallacyclobutane as an intermediate in ROMP. Green *et al*[37] observed that the reaction of a stable metallacyclobutane by thermolysis or photolysis gave a metal carbene and an olefin as products. Further evidence comes from the work of Grubbs and Gillion[38] who have shown that well defined titanacyclobutanes can initiate the ROMP of norbornene, as shown in Figure 1.4.c below, creating a 'living' chain end. In this case it is the intermediate metal carbene complex that cannot be detected by NMR, but the structure of the resulting polymer and the product of the capping reaction with benzophenone verifies its presence.

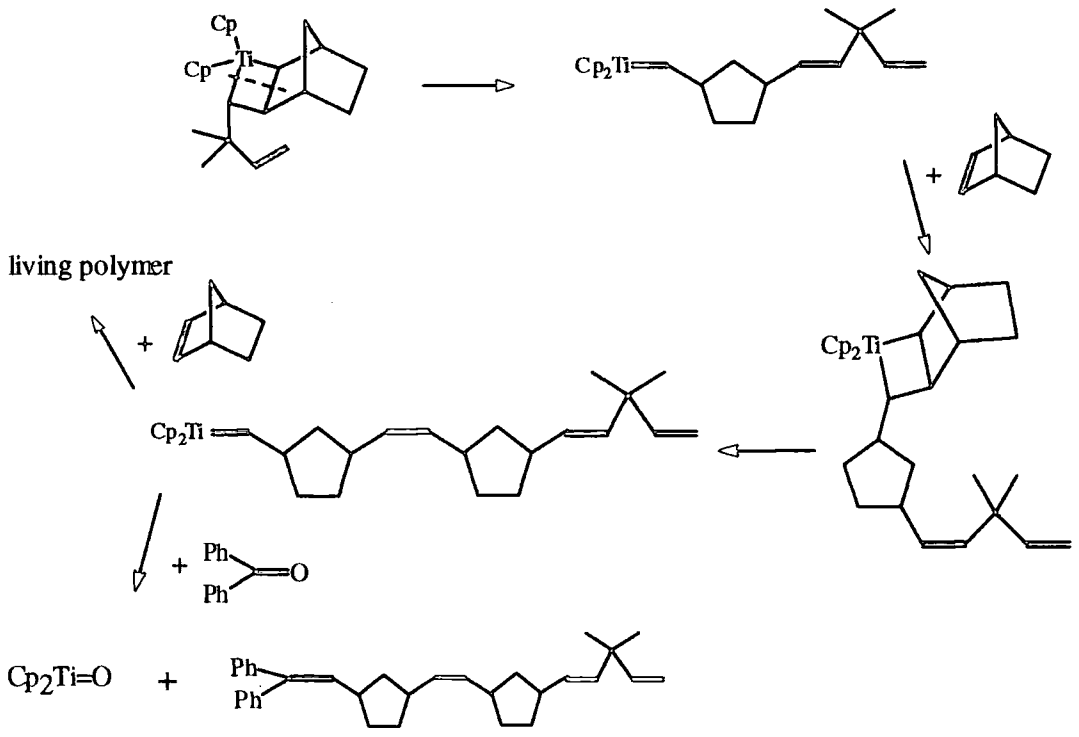

Figure 1.4.c **Polymerisation of norbornene initiated by a well defined-titanacyclobutane**

Finally the isolation and characterisation using x-ray crystallography of relatively stable metallacyclobutanes like the tungstacycle made from $W(CH^tBu)(NAr)(O^tBu)_2$ and 2,3-bis(trifluoromethyl)norbornadiene[39] is an unambiguous piece of evidence supporting the intermediate metallacyclobutane theory. Tungstacycles show in general greater stability than molybdacycles.

1.4.3. 'Living' polymerisation

The basic criterion for a polymerisation to be considered 'living' is the absence of a termination step. As a result polymerisation proceeds until all the monomer is consumed and if more monomer is introduced, the active end continues the polymerisation. Another requirement for a 'living' polymerisation is that the number average molecular weight of the resultant polymer is a linear function of conversion; as a result the molecular weight of the polymer can be controlled by the stoichiometry of the reaction.

These properties of 'living' systems are advantageous in the design and synthesis of structures with well defined molecular architectures. The addition of a second monomer after the first is consumed, yields polymers that contain blocks of each homopolymer connected to one another via covalent links, this is the classical approach to the synthesis of well-defined block copolymers. This can be extendend by the introduction of functional groups at the end of the chain during the controlled termination step (discussed later in this chapter), which can be used to introduce specific polymer blocks into well controlled macromolecular architectures such as combs, stars and networks. Some previous experimental work based on these properties of a living polymerisation is outlined here, by way of illustration.

Schrock et al obtained a series of norbornene-*block*-substituted norbornene A-B block copolymers such as polynorbornene-*block*-5,6-dicarbomethoxy-2-norbornene[39,40] using the $Mo(CH^tBu)(NAr)(O^tBu)_2$ initiator.

Grubbs[41] and Stelzer[42] prepared A-B-A type triblock copolymers using the titanium based initiating system $Cp_2Ti{=}CH_2$ (see chapter 3).

End capping of the living polymer with functional aldehydes produces a polymer with this functionality at the end of the chain.[43]

1.4.4. Termination

An irreversible reaction that destroys the propagating metal carbene may occur during the course of polymerisation. These reactions result in the termination of the chain growth and some examples which have been identified are discussed here. Proton transfer from compounds such as alcohol or water is an extremely common method by which the active species may be destroyed, as is reaction with dioxygen. Many classical and well defined initiating species are extremely sensitive to atmospheric moisture and air and require very careful handling as a consequence. However, some initiators such as $RuCl_3{\cdot}3H_2O$, not only can tolerate protic solvents but their activity may even be enhanced by them. Formation of a cyclopropane is

another possible reaction between the metal carbene and an olefin, see below, which is chain terminating.

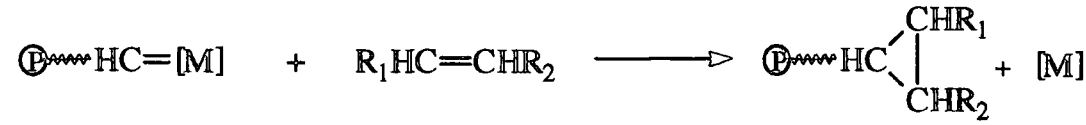

β-Hydrogen abstraction is another possible, but as yet unidentified process which would terminate propagation.

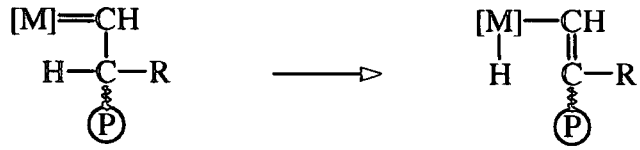

Most metal carbenes react readily with aldehydes and/or certain ketones in a Wittig-like capping reaction to yield the metal oxide and the end-capped polymer. This reaction may lead to unwanted chain growth termination where such carbonyl compounds are impurities, but can be used constructively to add functional groups at the chain end, by changing the nature of the R group on the aldehyde.[43]

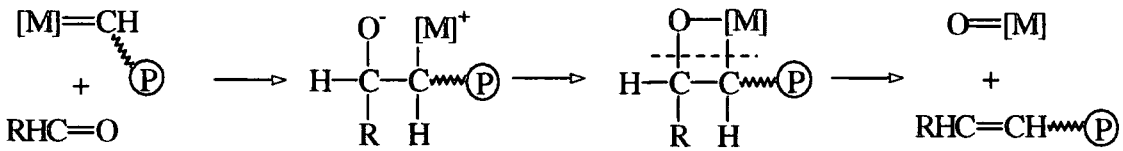

A reaction which is related to termination, namely reversible binding of Lewis bases to the active species, has been used to advantage by Grubbs[44] in the synthesis of narrow PDI poly(1-butenylene). Trimethylphosphine, binds reversibly to the initiating and propagating active species making them less available for the polymerisation reaction. Because trimethylphosphine tends to bind stronger to the propagating rather than the initiating alkylidene, for steric reasons, it has been used to improve the kinetic rates of initiation and propagation in the polymerisation of cyclobutene. Complete initiation before propagation has been achieved, resulting in well-controlled molecular weights and PDI's of 1.05-1.1.

1.4.5. Chain transfer

Chain transfer reactions are not terminating reactions because they do not destroy the propagating species. They can be subdivided into the two classes shown below.

1.4.5.a. Intra- and intermolecular metathesis reactions.

The propagating metal carbene can react intramolecularly with one of the double bonds in the same polymer chain, to produce a cyclic oligomer and transfer the active species as shown below. This process is also known as backbiting.

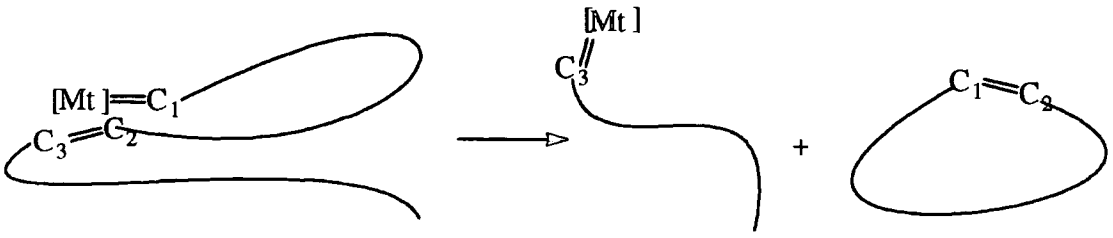

The chain end carbene can also react intermolecularly with the double bond in a different polymer chain to produce a linear polymer chain and transfer of the active species as shown below.

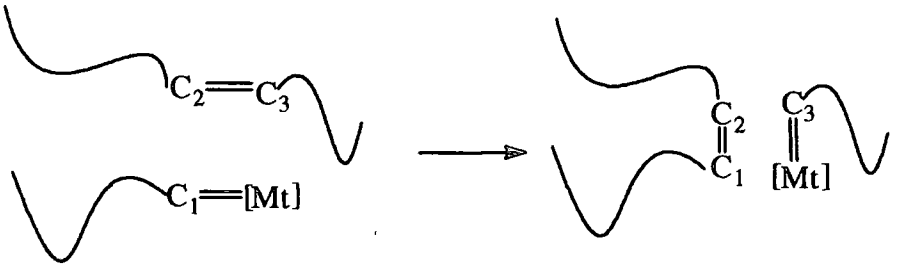

The operation of these chain transfer reactions leads to broad molecular weight distributions and lack of molecular weight control. Also this non-productive metathesis reaction decreases the availability of the active chain end for propagation.

1.4.5.b. Acyclic olefins - controlled chain transfer.

The cross metathesis between acyclic olefins and an active chain end results in the formation of a linear polymer and transfer of the active species as shown below.

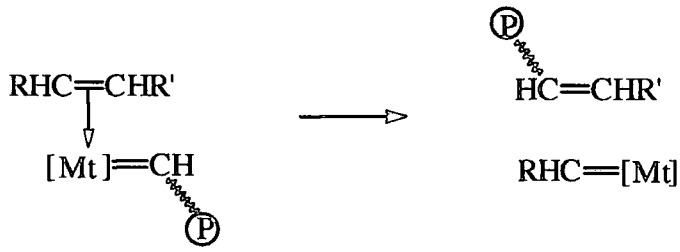

This reaction can be used to control the molecular weight of the polymer produced from a cyclic monomer (M). The acyclic olefin is termed a chain transfer agent (CTA) and in general an increase in the ratio [CTA]/[M] results in a reduction of molecular weight of the polymer. However the effectiveness of acyclic olefins in reducing the molecular weight depends on their structure, the catalyst system and also upon the bias towards *cis* vinylidene formation in the polymerisation, the process being more effective in reactions which give high *trans* polymers.[45,46] Terminal olefins have been reported to be more effective as CTAs, although internal olefins and styrene[43a] have also been used in the polymerisations of cyclopentene and norbornene monomers.

1.5. Copolymers via ROMP

Copolymers resulting from the ring opening metathesis polymerisation of cyclic olefins can either have a statistical (random) or blocky distribution. In general the polymerisation of a mixture of monomers yields a random copolymer with a composition that is dependent on the reactivity ratios of the monomers and the catalyst system used. Many copolymers, such as cyclopentene-*co*-norbornene, cyclopentene-*co*-5-substituted norbornene and norbornene-*co*-norbornene derivative copolymers have been prepared using W, Ru and Re based classical initiators.[47,48,49] Living ROMP can be used for the preparation of block copolymers by the successive addition of monomers as discussed earlier.

1.6. ROMP thermodynamics

For any addition polymerisation reaction to occur the change in the Gibbs free energy ΔG must be ≤ 0. This change is expressed as a function of the enthalpy change ΔH, the entropy change ΔS and the temperature T in °K.

$$\Delta G = \Delta H - T\Delta S$$

The change in entropy ΔS for the ring opening polymerisation of monocyclic olefins is negative. That makes $-T\Delta S$ positive and for a favourable reaction, the change in enthalpy ΔH has to be larger than or at least equal to the $T\Delta S$ component. The temperature where $\Delta G=0$ is called the *ceiling temperature*, and above that temperature the polymerisation reaction does not occur. The enthalpy change ΔH, is dependent on the ring strain. For highly strained small monocyclic and bicyclic rings, polymerisation is allowed because of the high (negative) value of the change in enthalpy during the reaction, although the change in entropy is negative and makes a positive contribution to ΔG. For monomers possessing low ring-strain energy, that is 5, 6 and 7 membered rings the reaction entropy is the major determining factor, since the reaction enthalpy is low. For larger cycloolefins (8-12 membered rings) strain factors again are involved. It is theoretically expected and experimentally observed that polymerisation of monocyclic olefins with 3,4 and 8 or more carbon atoms on their ring, as well as strained bicyclic norbornene-like monomers, proceeds readily under a wide variety of conditions, while the polymerisation of cyclic olefins with 5,6 and 7 carbons in the ring is more sensitive to experimental conditions such as temperature and concentration. In general the most favourable thermodynamic conditions for the ROMP of cycloalkenes are high monomer concentration, low temperature and high pressure. These are similar for any chain growth addition polymerisation. Ring substitution has an adverse effect on the free energy of polymerisation, i.e. it makes it less negative. Substituents in C_4, C_8 and larger rings are usually tolerated, but in medium sized rings, small changes in the substitution pattern can have a marked effect on polymerizability.

1.7. Microstructure of polymer chains

1.7.1. Monocyclic monomers

The way that the monomer unit is incorporated into the polymer chain determines the microstructure of the resulting polymer; in this section the possible microstructures are described. For unsubstituted monocyclic olefins the polymer chain microstructure is determined only by the *cis* / *trans* ratio and the sequence of the double bonds in the chain. The easiest and most accurate way to study the microstructure of these polymers is by high resolution ^{1}H and ^{13}C-NMR spectroscopy. The configuration of the nearest and next nearest double bond affects the chemical shifts of all the carbons in the repeat unit. The methylene carbons are sensitive to double bond dyads, while the olefinic carbons are sensitive to double bond triads. The chain carbons can be located between two (or three) double bonds and they are labelled as cc, ct, tc or tt. The first letter refers to the nearest while the second letter refers to the next nearest double bond. The ct and tc carbons are equivalent, when the observed carbon is in the middle of the repeat unit. In the case of triad effects on olefinic carbons three letter labelling is used such as ttt, tcc, cct etc. The middle letter refers to the double bond to which the carbon under observation belongs, while the letters on the left and the right refer to the nearest and next nearest double bond respectively.

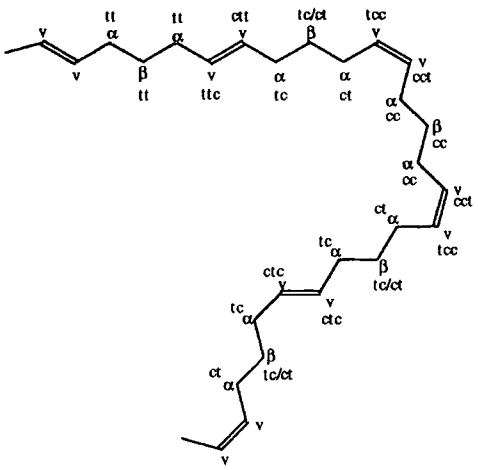

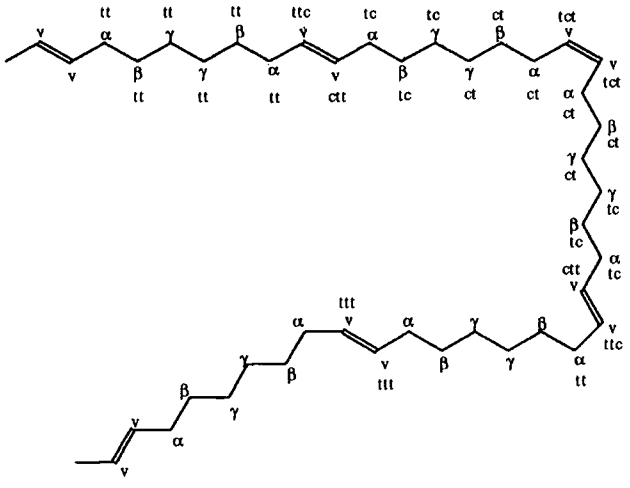

Substituted rings exhibit head / tail as well as tacticity effects. When the substituent R is on the double bond a strong head-tail (HT) bias is usually

observed.[50,51] Similarly when the substituent is on the α carbon a HT bias is likely, depending on the initiating system. When the substituent is further away from the double bond the head / tail effect is random[52].

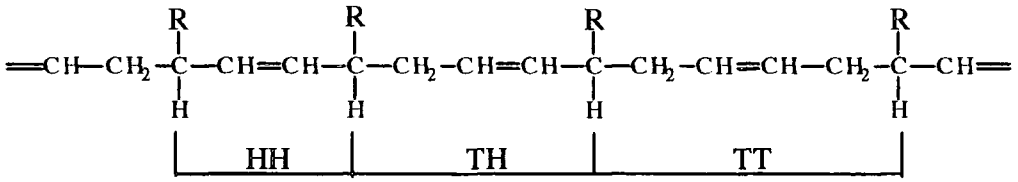

Tacticity effects may arise from the possibility of meso and racemic dyads as shown below for a polymer with all cis vinylenes.

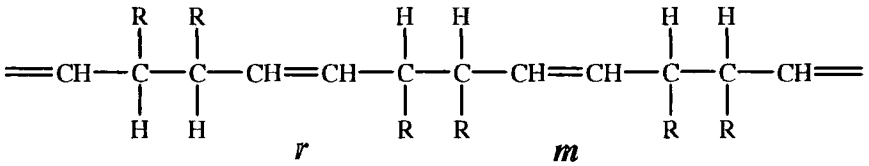

1.7.2. Bicyclic monomers

In these systems the double bonds formed during the ROMP of the cyclic olefin can be either *cis* or *trans*, and the labelling system is similar to that already described for monocyclic monomers.

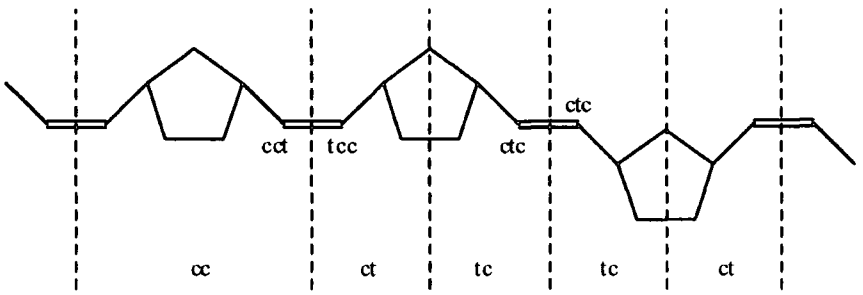

Ivin[12,53] has proposed a model for the formation of *cis/trans* double bonds based on the different ways that a norbornene ring may present itself to the reaction site, when that site is an octahedrally substituted metal carbene with one vacant coordination site.

Unsymmetrically substituted monomers result in polymers with head-head, head-tail or tail-tail structures:

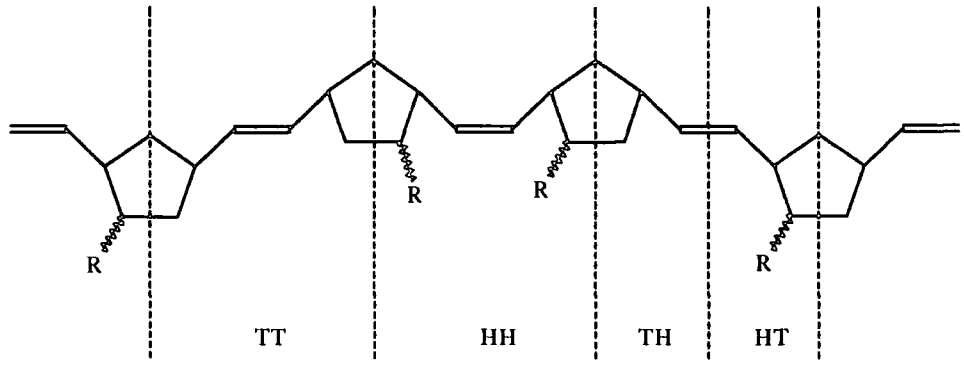

Tacticity effects may also arise from meso and racemic dyads as shown below.

cis - isotactic

cis - syndiotactic

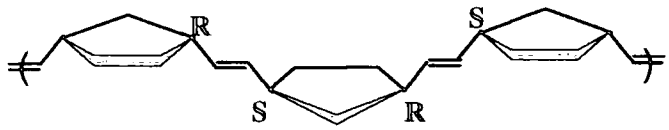

trans - isotactic

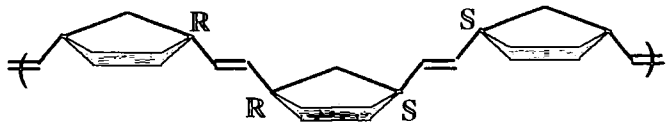

trans - syndiotactic

The carbon atoms α to the double bonds are chiral and they may have the same or opposite chiralities, which result in meso and recemic dyads respectively. Sequences of racemic dyads result in syndiotactic polymer, while sequences of meso dyads result in isotactic polymer. A statistical distribution of dyads result an atactic polymer.

From the foregoing discussion it is clear that ROMP allows, in principal, the synthesis of many polymers of different tacticities from one monomer.

This thesis describes some investigations of the synthesis and characterisation of well defined polymeric structures using living ROMP methodologies. Chapter 2 describes the synthesis and characterisation of some monocyclic alkenes, including a detailed analysis of data obtained by ^{13}C-NMR spectroscopy. Chapter 3 describes the synthesis and characterisation of poly(1-pentenylene)-*block*-polyacetylene-*block*-poly(1-pentenylene). Chapter 4 describes a route to well-defined linear and star polyethylenes via ROMP of cyclopentene. Chapter 5 describes the attempted synthesis of a difunctional ROMP initiator, which is required for the synthesis of well-defined networks via ROMP. Finally Chapter 6 outlines the conclusions and proposals for any future continuation of this work.

CHAPTER 2: Ring Opening Metathesis Polymerisation of some monocyclic alkenes using well-defined, Schrock-type initiators.

2.1. Introduction

In the presence of well-defined transition metal initiators, monocyclic alkenes, undergo ring opening metathesis polymerisation to give linear polymers containing unsaturated carbon-carbon double bond linkages. The resulting polymers are usually called polyalkenamers. The process is summarised in Figure 2.1.a.

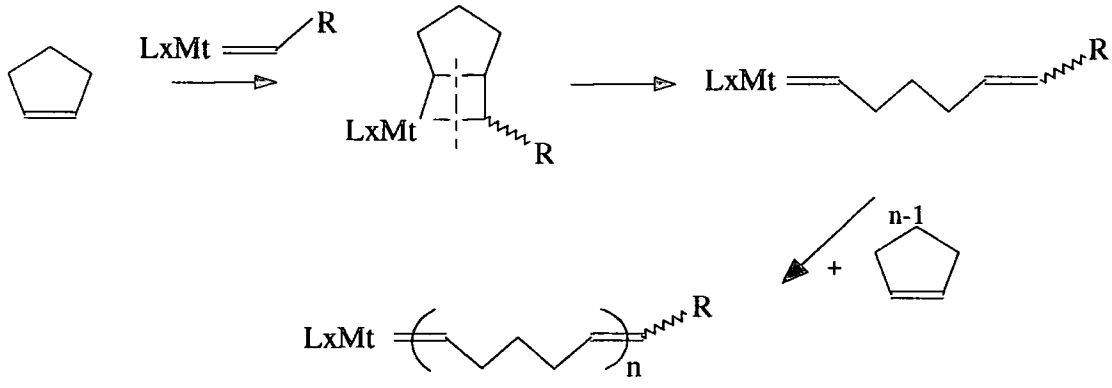

Mt = transition metal
Lx = Ligands

Figure.2.1.a The ROM polymerisation of monocyclic alkenes

These double bonds show *cis/trans* isomerism, which affects the chemical shifts of the methylene carbons in the chain. The ring strain of monocyclic alkenes with five or more carbon atoms in the ring is less than that found in bicyclic monomers, such as norbornene, where the real C-C-C angles are constrained to be considerably smaller than the ideal ones. As a result these monocyclic monomers are less susceptible to binding onto a metal centre in order to relieve their ring strain[26] in the manner described earlier (see *Introduction 1.4.1 and 1.6*). In addition the polymer chains derived from monocyclic monomers are more flexible than those derived from bicyclic monomers, which makes access of the active chain end to double bonds in

the chain easier and intramolecular secondary metathesis more probable. It is for these reasons that the ring opening polymerisation of monocyclic alkenes exhibits certain characteristics which distinguish it from the polymerisation of the bicyclic monomers. Monocyclic alkenes have been polymerised in the past using various initiating systems. The *cis* : *trans* content of the resulting polymer depends upon the system used and the reaction conditions. Some of these earlier results are recorded in Table 2.1., where the designations *cis* or *trans* indicates that predominantly, rather than exclusively, one vinylic geometry was formed.

Monomer	Initiating system/temp.	Resulting polymer
Cyclopentene	$Al(C_2H_5)_3$-$MoCl_5$/-30°C	*cis*-poly(1-pentenylene)[61]
	$Al(C_2H_5)_3$-WCl_6/-30°C	*trans*-poly(1-pentenylene)[61]
Cycloheptene	$(C_6H_5)_2C=W(CO)_5$/40°C	*cis*-poly(1-heptenylene)[63,64]
	$Al(C_2H_5)_3$-$MoCl_5$/20°C	*trans*-poly(1-heptenylene)[62]
Cyclooctene	$(C_6H_5)_2C=W(CO)_5$/40°C	*cis*-poly(1-octenylene)[63,64]
	$Al(C_2H_5)_3$-WCl_6	*trans*-poly(1-octenylene)[62]
Cyclodecene	$Al(C_2H_5)_2Cl$-WCl_6/10°C	*trans*-poly(1-decenylene)[65]
Cyclododecene	$Al(i\text{-}C_4H_9)_2Cl$-WCl_6	*trans*(70%)-poly(1-dodecenylene)[66]

Table.2.1. Polymerisation of some monocyclic alkenes using classical initiators[59]

In the work described in this chapter $W(=CH^tBu)(O^tBu)_2(NAr)$, $Mo(=CH^tBu)(OC(CH_3)_3)_2(NAr)$, $Mo(=CH^tBu)(OC(CH_3)_2CF_3)_2(NAr)$ and $Mo(=CH^tBu)(OC(CH_3)(CF_3)_2)_2(NAr)$ have been employed as the initiators for the polymerisation processes illustrated in Figure 2.1.b.

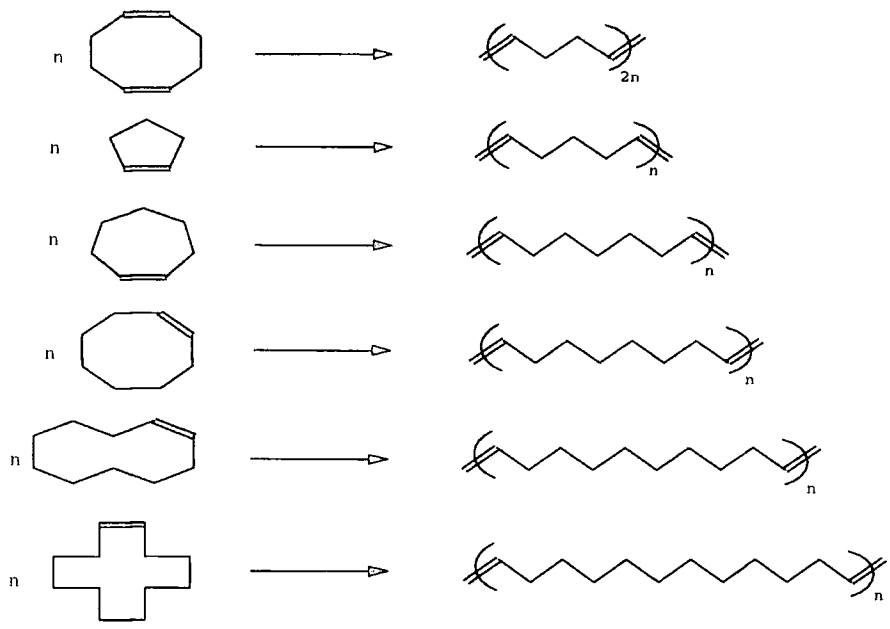

Figure 2.1.b Monocyclic monomers and resulting polymers via ROMP

Detailed analysis of their ^{13}C-NMR spectra provides a rich source of information concerning the microstructure of the polymer chains. Until very recently a full assignment of the ^{13}C-NMR spectra of polyalkenamers was restricted by the resolution attainable with available NMR equipment. The Varian VXR400 high field NMR spectrometer used throughout this work, allows the resolution and subsequent assignment of peaks for most of the carbons in the polymer chains.

In all ^{13}C-NMR spectra, recorded in the broad band ^{1}H decoupled mode, peaks for the vinylic carbons occurred between 129.4 and 130.6 ppm and for the methylene carbons between 27 and 33 ppm. The assignments are based on previous literature analyses,[12,17,54,55] the relative intensities of the signals for equivalent carbon atoms, the chemical shift differences associated with the *cis* and *trans* double bond effects and the requirement for internal consistency. Thus *cis* : *trans* ratios can be computed in all cases from the relative intensities of Cv_t : Cv_c and $C\alpha_t$: $C\alpha_c$ signals, where *t* and *c* represent a signal associated with a *trans* or *cis* double bond or double bond effect.

In the analyses presented subsequently the symbol Cv indicates the vinylic carbon,

while a Greek letter indicates a methylene carbon's relation to the vinylic unit:

$$CH{=}CH{-}CH_2{-}CH_2{-}CH_2{-}CH_2{-}CH_2$$

$$C_v \quad C_\alpha \quad C_\beta \quad C_\gamma \quad C_\delta \quad C_\varepsilon$$

The peak assignments, so derived, are summarised in Figure 2.9, page 56.

2.2 Experimental

General procedures, equipment and instrumentation are described in Appendix 1.

The initiators used throughout this work were prepared in the transition metal chemistry research group of Prof.V.C.Gibson and in our laboratories by Dr.E.Khosravi and used as supplied in solid form in inert atmosphere. The initiator solutions were prepared in the Glove Box prior to use. Two polymerisation procedures were adopted, depending on the monomer ring size.

Polymerisation of monomers with C_7 to C_{12} rings.

The monomers were dried over CaH_2 and vacuum-transferred into a pre-dried ampoule containing molecular sieves and sealed with a Young-valve. Chloroform was stirred overnight over P_2O_5, vacuum-transferred into an ampoule over molecular sieves and passed through a short column (ca.4 cm) of oven dried neutral alumina before use. All preparations were performed in the glove box at room temperature. The ratio of monomer to initiator was 300:1 and the solvent used was chloroform in all cases. The following procedure is illustrative. In the glove box the initiator was dissolved in half the chloroform. The monomer was dissolved in the other half of the chloroform, added to the initiator solution and the mixture stirred. After the completion of the reaction excess benzaldehyde was added to 'quench' the living polymer in a Wittig-like capping reaction. The polymer was purified by repeated precipitation from chloroform into methanol and then dried under vacuum.

Polymerisation of cyclopentene

A typical polymerisation of cyclopentene was performed using the reaction vessel

illustrated in Figure 2.2. The dry vessel was placed in the Glove Box and the initiator solution in chloroform was introduced into compartment B and the monomer solution in compartment A. The overall monomer concentration was 3.8M. The vessel was then taken out of the Glove Box and immersed in a cooling bath at -45°C while the greaseless joint was connected to the Vacuum/N_2 line. After 15 min the isolating Young valve between A and B was opened and the solutions allowed to mix while stirring. After reaction the living polymer was quenched by the addition of benzaldehyde which was injected into the solution at -45°C after one of the Young valves had been replaced with a Suba seal against a strong counter current of dry N_2, followed by stirring for 45 min. The polymerisation reaction times were varied as described in section 2.4.

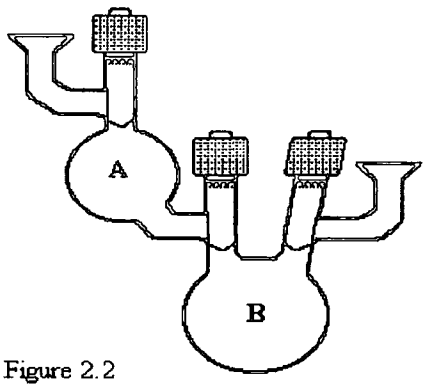

Figure 2.2

2.3. Polymerisation of cyclooctadiene to give poly(1-butenylene)

Poly(1-butenylene) can be produced by the ROM polymerisation of either cyclobutene or *cis,cis*-cycloocta-1,5-diene. The cyclobutene ring is highly strained and during its polymerisation the rate of propagation is much greater than the rate of initiation resulting in polymers with broad molecular weight distributions. In such processes the polydispersity index is generally larger than two, i.e. PDI>2. The polymerisation can be slowed by the presence of weak Lewis bases such as THF or pyridine (PDI's≈1.5)[56] and Grubbs and coworkers have established excellent control using PMe_3, PDI's≈1.02-1.1.[44b] In this study *cis,cis*-cycloocta-1,5-diene has been used as the monomer for the preparation of poly(1-butenylene) in reactions conducted at room temperature.

NMR data analysis

^{1}H-NMR

Poly(1-butenylene) 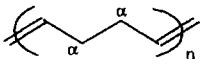

The spectrum is reproduced in Appendix 2.1 for completeness; it has been assigned previously.[12] The peak for the olefinic proton on the *cis* double bond appears at 5.38 ppm while that on a *trans* double bond appears at 5.42 ppm. The signals for the α protons next to a *cis* and next to *trans* double bond appeared at 2.03 and 2.08 ppm respectively. The integration of the signals for Hα and Hv gave a 2:1 ratio and the integration of *cis*:*trans* signals agreed with the assignment based on the ^{13}C-NMR within the limits of the resolution of the peaks.

Proton	Shift
Hv (*cis*)	5.38
Hv (*trans*)	5.42
Hα (*cis*)	2.03
Hα (*trans*)	2.08

^{13}C-NMR

Poly(1-butenylene) 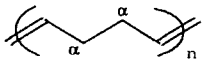

The spectrum is recorded in Appendix 2.2. The α carbons show signals for the *tt* and *tc* environments, with the signals for $C_{\alpha}tt$ separated from that for $C_{\alpha}tc$ by -0.053ppm (5.33Hz), while the signal for the *cis* configuration at 27.37 ppm occurs as an unresolved singlet. The signal for the olefinic carbons shows four peaks assigned as shown on the table, these peaks are further split possibly due to triad and even pentad effects. Since the poly(1-butenylene) was made from *cis,cis*-cycloocta-1,5-diene every other double bond has to be *cis* in the as formed polymer, hence the presence of the *tt* peak is evidence of secondary metathesis or some other form of catalysed isomerisation taking place. The ^{13}C-NMR spectrum of this and the spectra of all the other polyalkenamers discussed

Carbon	Shift (ppm)
C_v *tc*	130.06
C_v *tt*	129.94
C_v *cc*	129.54
C_v *ct*	129.38
C_{α} *tt*	32.71
C_{α} *tc*	32.66
C_{α} *c*	27.38

in this chapter are reproduced in comparative form in Figure 2.9, page 56.

GPC data

The Gel Permeation Chromatography results for polymers prepared using different initiators are shown in Appendix 2.3 and are presented below.

Initiator	Monomer : initiator ratio	Reaction time	Mn	PDI
$W(CH^tBu)(O^tBu)_2(NAr)$	300:1	20hrs	47500	2.9
$Mo(CH^tBu)(OC(CH_3)_3)_2(NAr)$	300:1	20hrs	19490	1.7
$Mo(CH^tBu)(OC(CH_3)_2CF_3)_2(NAr)$	300:1	20hrs	45000	1.6
$Mo(CH^tBu)(OC(CH_3)(CF_3)_2)_2(NAr)$	300:1	20hrs	92000	1.7

It is clear that well-defined living polymerisation has not occurred since the expected molecular weight would be 16,000 if each initiator molecule resulted in one polymer chain. Since the molecular weights are all greater than theoretical and the dispersities are ≥1.6 it is clear that propagation is significantly faster than initiation. It is also clear that in the series of molybdenum centred initiators fluorination of the alkoxide ligands increases the reactivity of the propagating chain end. The very broad distribution obtained using the tungsten centred initiator suggests a higher level of cross metathesis with in-chain vinylenes in this system. While the detail reported here with respect to these observations and those to be reported subsequently in this chapter are new, they are entirely consistent with expectation and previously reported work.[57]

Thermogravimetric analysis

All the polymers discussed in this chapter showed a similar weight loss profile which consisted of a slow loss up to about 400°C, ±50°C, followed by a catastrophic loss over the next 100 to 150°C with little or no residue. A typical example is shown in Appendix 4.8. In this experimental section the temperatures for 2% weight loss and the maximum weight loss are noted. In this case 2% weight loss occurred at 350°C

while the maximum weight loss was 97% at 530°C.

Differential Scanning Calorimetry data

The DSC traces are shown in Appendix 2.4 and show clearly that the melting temperature for these polymers increases with the *trans* content.

Initiator	*cis* : *trans* ratio[1]	Tm °C (onset)	Tm °C (max)	Heat of fusion J/g
$W(CH^tBu)(O^tBu)_2(NAr)$	80 : 20	No peak from -50 to 100°C		
$Mo(CH^tBu)(OC(CH_3)_3)_2(NAr)$	30 : 70	-13.6	-0.3	20.9
$Mo(CH^tBu)(OC(CH_3)_2CF_3)_2(NAr)$	15 : 85	31.2	34.9	16.2
$Mo(CH^tBu)(OC(CH_3)(CF_3)_2)_2(NAr)$	15 : 85	29.4	34.4	14.0

[1]Derived from analysis of the NMR data

Infrared data

The IR spectrum is recorded in Appendix 2.5.a and show peaks at 3005 cm^{-1} assigned to =C-H stretch, at 2940 and 2845 cm^{-1} to the CH_2 antisymmetric and symmetric stretching modes, at 1655 cm^{-1} to the C=C stretch, at 1450 cm^{-1} to the CH_2 bend, at 966 cm^{-1} to the *trans* =C-H out of plane bend and at 734 cm^{-1} to the CH_2 rock and/or the *cis* =C-H out of plane bend; the assignments in the finger print region below 1500 cm^{-1} are somewhat tentative but the peaks quoted are well established for the structural features to which they are assigned.

2.4. Polymerisation of cyclopentene to give poly(1-pentenylene)

The polymerisation of cyclopentene differs from that of other monocyclic alkenes as discussed in section 1.6 and 2.2. The practical consequence is that it will polymerise only under certain well-defined conditions of temperature and concentration.

Cyclopentene polymerises in a well defined living manner[58] at temperatures below -40°C in solution, when the polymerisation reaction is initiated with $W(=CH^tBu)(O^tBu)_2(NAr)$. The ^{1}H-NMR singlet resonance at 8.05 ppm

corresponding to the alkylidene proton on the initiator is gradually replaced by a triplet at 8.45 ppm (J_{HH}=7Hz) which corresponds to the propagating alkylidene proton. Above this temperature the conversion is not complete and at +40°C there is no conversion at all, i.e. initiation does not occur. The polymerisation is fully reversible.

NMR data analysis.

^{1}H-NMR data

Poly(1-pentenylene) 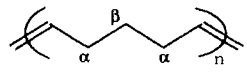

Proton	Shift (ppm)
Hv	5.38
Hα (*cis*)	2.03
Hα (*trans*)	1.98
Hβ	1.39

The spectra from which these data are derived are reproduced in Appendices 2.6. and 2.7. The signal for the β protons appears as a quintet at 1.39 ppm (J_{HH}= 7.4Hz). The peaks for the α protons were assigned with the aid of a HETCOR spectrum. The peak for the α protons next to a *cis* double bond appear at 2.03 ppm and although it is partly overlapped by the α(*trans*) signal a fine splitting of ≈7.4 Hz can still be observed. In contrast the peak for the α protons next to a *trans* double bond appears rather broad and unresolved at 1.98 ppm.

^{13}C-NMR data

Poly(1-pentenylene) 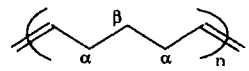

Carbon	Shift (ppm)
Cv *t*	130.30
Cv *c*	129.81
Cα *tc*	32.19
Cα *tt*	32.05
Cα *cc*	26.88
Cα *ct*	26.73
Cβ *cc*	29.82
Cβ *ct/tc*	29.68
Cβ *tt*	29.53

The spectra on which this analysis is based are shown in Appendix 2.8. The spectrum of poly(1-pentenylene) shows at least three resolved signals for both the *cis* and the *trans* olefinic carbons. This must be as a result of the effect of the configuration of

the nearest double bonds on either side of the double bond in question and will be discussed later in this chapter. The α carbons also show splitting as a result of the effect of the nearest and next nearest double bonds, the line order from low to high field being *tc*, *tt*, *cc*, *ct* and Cα *cis* being 5.3 ppm upfield from Cα *trans*. The distance between the β carbon and the double bonds on either side is the same and as a result the Cβ *ct* and Cβ *tc* peaks coincide and only three peaks are resolved.

GPC data

The reaction conversion, average molecular weight and polydispersity varies with the time of the reaction in ROMP of cycloalkenes. To study the relationship between these parameters in this case we investigated the reaction at -45°C using the apparatus shown in Figure 2.4. and a thermostated cooling bath.

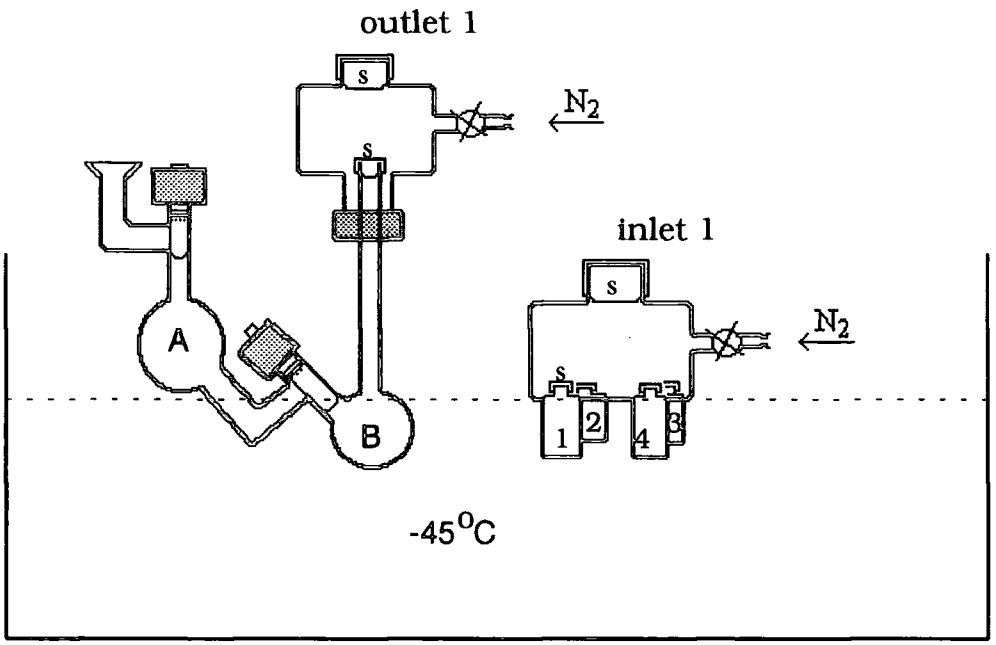

Figure 2.4 Apparatus for study of polymerisation of cyclopentene. s=Suba seal

The solvent used, chloroform, was dried and distilled prior to use and was stored in the glove box. The monomer solution (300 equivalents) was kept in the part of compartment A below the coolant level and did not mix with the initiator solution in compartment B until both solutions were cooled to -45°C (monomer concentration

3.8M). Aliquots were taken out via the two Suba seals of outlet 1 using a glass barrelled syringe and were quickly injected into a preweighed sample bottle containing benzaldehyde (also stored at -45°C) through the Suba seal of inlet 1. The sample bottles were weighed again after the end of the experiment and for the third time after the removal of the volatiles in order to calculate the yield.

	Solution injected (g)	Polymer recovered (g)
Sample 1	0.732	0.03
Sample 2	0.652	0.033
Sample 3	0.555	0.037
Sample 4	0.545	0.048

The yield was calculated using the following formula:

$$\text{Yield } (\%) = \frac{\text{Polymer recovered (g) x 100}}{\text{Solution injected (g) x Monomer concentration (w / w)}}$$

Time (hrs)	**Cumulative yield (%)**	***trans* / *cis*[2]**	**Mn[3]**	**PDI**
1.5	29	50 /50	16700	1.1
3	35	40 / 60	24000	1.2
5	46	40 / 60	26500	1.6
8	61	40 / 60	31500	1.7
24[1]	94	-	48000	1.6

[1]Result from 24 hour experiment, same conditions.

[2]Calculated from ^{13}C-NMR spectra

[3]Relative to polystyrene standards

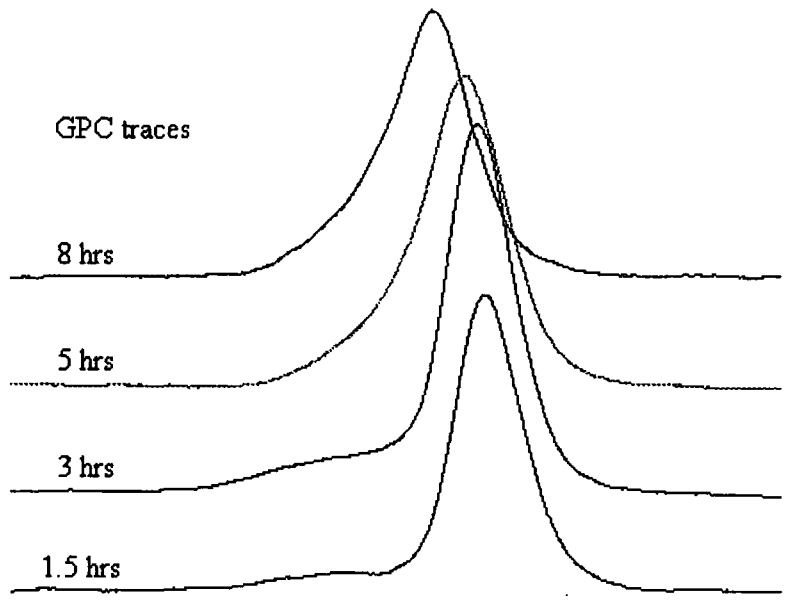

The Mn values obtained by GPC are subject to a correction factor in order to obtain the actual molecular weights. If we assume linear increase of molecular weight with percent monomer conversion in this well characterised living polymerisation, this correction factor can be calculated using the following equations, where M_n(th) is the theoretical molecular weight calculated from the monomer : initiator ratio.

$$\overline{M}_n(\text{th}) = A \times \overline{M}_n(\text{GPC})$$

i.e.

$\overline{M}_n$ (th) = Initial No of monomer equivalents × Conversion × repeat unit MW

The correction factor A is readily calculated and the results of these calculations are tabulated below.

Yield %	Mn[1]	DP (Mn)[1]	Corr. factor (Mn)
29	16700	245	0.35
35	24000	353	0.3
46	26500	390	0.45
61	31500	463	0.4
94	48000	705	0.4

[1]Relative to polystyrene standards

The variation observed in the calculated values is presumably related to increase in PDI with reaction conversion. A correction factor of 0.5 has been reported for poly(1-butenylene).[44b,50,54] In essence both our correction factor of 0.4 for poly(1-pentenylene) and Grubbs value of 0.5 for poly(1-butenylene) indicate that GPC calibrated relative to polystyrene standards overestimates M_n for these polymers.

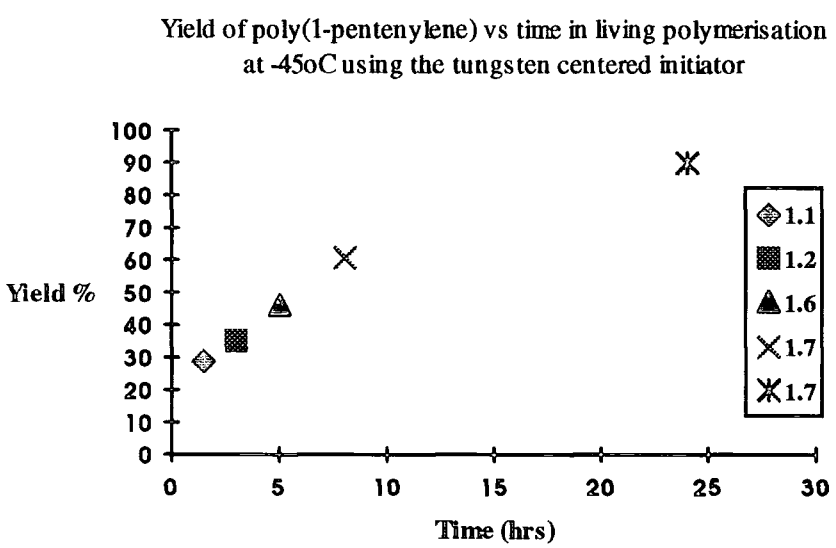

We observed that yield increases in a regular manner with time. The PDI also increases with time, which is probably a consequence of intramolecular or intermolecular secondary metathesis taking place. The Mn values which were obtained from other polymerisation reactions of cyclopentene carried out under the same conditions compared well with these results within an error band of ±10%. This error could occur because of the high sensitivity of the system to contamination and small temperature variations during sampling. The PDI values also showed some variation with a tendency to be lower in the products of reactions which were not interrupted for sampling or other reasons. For example, in our best results, a PDI value of 1.04 was obtained for a sample produced in 3 hrs, whereas a value of 1.45 was obtained for a similar reaction which ran for 20 hrs.

The ^{13}C-NMR spectra of the polymers recovered from these aliquots showed no significant change in the *cis:trans* ratio, a value of 50:50 was seen for the sample from the initial aliquot and 60:40 in the second and subsequent samples.

When the polymerisation was initiated using molybdenum centred well-defined initiators under the same conditions of temperature, concentration and monomer to

initiator ratio, the recovered polymers showed the following GPC parameters.

Initiator	Monomer : initiator ratio	Reaction time	Mn	PDI
$Mo(CH^tBu)(OC(CH_3)_3)_2(NAr)$	300 : 1	45min	371000	1.35
$Mo(CH^tBu)(OC(CH_3)_2CF_3)_2(NAr)$	300 : 1	20min	217000	1.5

These data, when compared to the results obtained using tungsten centred initiators discussed above, indicates that the use of molybdenum centred initiators gives faster propagation than initiation and that they are unsuitable for use in well defined living polymerisation of cyclopentene. The GPC traces are recorded in Appendix 2.9.

IR data

The infrared spectrum is recorded in Appendix 2.5.b and showed peaks at 3004 cm^{-1} assigned to =CH stretch, at 2922 $cm^{-1}$and 2852 cm^{-1} to antisymmetric and symmetric CH_2 stretching modes, at 1654 cm^{-1} to C=C stretch, at 1455 and 1437 cm^{-1} to CH_2 bend, at 966 cm^{-1} =C-H *trans* out of plane bend and at 721 cm^{-1} to CH_2 rocking and/or to *cis* =C-H out of plane bend.

DSC data

Polypentenamer has been the subject of extensive thermal analysis. High *trans* poly(1-pentenylene) (85-94%) has been reported[59,60] to have Tm and Tg values of 23°C and -90°C respectively, while high *cis* poly(1-pentenylene) has values of -41°C and -114°C and crystallises only after prolonged annealing at -75°C. A single scan of the material produced in this work showed two weak broad transitions at about -75 and -50°C which we tentatively assign to glass transition processes. Since the ^{13}C-NMR data indicates a blocky tendency in this polymer, this observation is not unreasonable but a detailed study has not been conducted. The DSC trace is reproduced in Appendix 2.10.

2.5. Polymerisation of cycloheptene to give poly(1-heptenylene)

The polymerisation of cycloheptene when initiated with molybdenum based well defined initiators at room temperature and 3.1M concentration in chloroform produces a high molecular weight polymer while the tungsten based initiator used with monomer concentration of 2.6M or 5.1M in the same solvent gave no polymer; there is no obvious reason for this failure to produce a polymer in this case.

NMR analysis

The spectra on which these analyses are based are reproduced in Appendix 2.11 (^{1}H) and Appendix 2.12 (^{13}C)

^{1}H-NMR data

Poly(1-heptenylene)

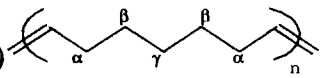

The signal for the olefinic protons on a *cis* double bond appeared at 5.38 ppm while the signal for those on a *trans* double bond appeared at 5.35. The assignment is based on the integration for the two peaks and correlation with the unambiguous assignment based on the ^{13}C-NMR spectrum. The α protons also show splitting due to *cis* or *trans* nearest double bonds. The peaks for the β and γ protons appear as one broad band centred at 1.32 ppm and integrates for six protons.

Proton	Shift
Hv (*cis*)	5.38
Hv (*trans*)	5.35
Hα (*cis*)	2.02
Hα (*trans*)	1.96
Hβ and Hγ	1.32

^{13}C-NMR data

Poly(1-heptenylene) 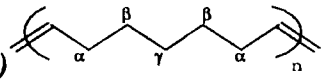

Carbon	Shift (ppm)
Cv *t*	130.31
Cv *c*	129.84
Cα *t*	32.58
Cα *c*	27.19
Cβ *cc*	29.67
Cβ *ct*	29.64
Cβ *tc*	29.56
Cβ *tt*	29.53
Cγ *cc*	28.98
Cγ *ct/tc*	28.84
Cγ *tt*	28.71

The olefinic carbons show triplet splitting for both *cis* and *trans* signals emanating from triad effects which will be discussed later in this chapter. The signal for the α carbons is influenced only by the configuration of the nearest double bond, showing two peaks with $C_{\alpha}c$ 5.4 ppm upfield from $C_{\alpha}t$. The β carbons show splitting due to the nearest and next nearest double bonds and give rise to a four line pattern which can be readily assigned on the basis of signal intensities to a sequence *cc*, *ct*, *tc*, *tt* from low to high field. The $C_{\beta}cc$ to $C_{\beta}tc$ and $C_{\beta}ct$ to $C_{\beta}tt$ splitting is 0.106 ppm. The γ carbon being equidistant from the double bonds, display a three line splitting pattern, assigned to *cc*, *ct≡tc*, *tt* sequence of environments on an analogous basis; the splitting between the three lines is the same at 0.133 ppm.

GPC data

The Gel Permeation Chromatography results for polymers prepared using different initiators are shown in Appendix 2.13 and are tabulated below.

Initiator	Monomer : initiator ratio	Reaction time	Mn[1]	PDI
Mo(CH^{t}Bu)(OC(CH$_3$)$_3$)$_2$(NAr)	1 : 300	20hrs	29000	1.5
Mo(CH^{t}Bu)(OC(CH$_3$)$_2$CF$_3$)$_2$(NAr)	1 : 300	20hrs	37400	1.5
Mo(CH^{t}Bu)(OC(CH$_3$)(CF$_3$)$_2$)$_2$(NAr)	1 : 300	20hrs	20000	1.9

[1]Relative to polystyrene standards calibration

It is clear that well defined living polymerisation is not attained under these conditions, molecular weights and/or PDIs are too large possibly indicating that propagation rates exceed initiation rates and cross metathesis occurs.

DSC data

The DSC traces are shown in Appendix 2.14 and the results are presented below.

Initiator	*cis* : *trans* ratio[1]	Tm °C (onset)	Tm °C (max.)	Heat of fusion J/g
$Mo(CH^tBu)(OC(CH_3)_3)_2(NAr)$	45 : 55	-2.6	10.6	26.0
$Mo(CH^tBu)(OC(CH_3)_2CF_3)_2(NAr)$	23 : 77	40.9	47.5	54.6
$Mo(CH^tBu)(OC(CH_3)(CF_3)_2)_2(NAr)$	20 : 80	43.3	47.5	68.9

[1]Derived from analysis of the NMR data

It can be seen that the higher the *trans* vinylene content in the polymer, the higher the melting temperature and heat of fusion. This is in line with the expectation that the *trans* geometry allows crystallisation more easily than the *cis*.

Thermogravimetric analysis

2% weight loss was observed at 435°C, while the maximum weight loss was observed at 580°C.

IR data

The infrared spectrum is recorded in Appendix 2.5.c and showed peaks at 3003 cm^{-1} assigned to =CH stretch, at 2920 cm^{-1} and 2849 cm^{-1} to antisymmetric and symmetric CH_2 stretching bands, at 1464 and 1435 cm^{-1} to CH_2 bend, at 964 cm^{-1} to =C-H *trans* out of plane bend and at 725 cm^{-1} to CH_2 rocking and/or to *cis* =C-H out of plane bend. The C=C stretch shows only a very weak absorption at approx. 1660 cm^{-1}. The assignments below 1500 cm^{-1} are somewhat tentative.

2.6. Polymerisation of cyclooctene to give poly(1-octenylene)

Cyclooctene when polymerised, at room temperature in $CHCl_3$ in 5M solution, using the tungsten based initiator gave a high *cis* polymer, while polymerisation using the molybdenum based initiators gave high *trans* polymers.

NMR data analysis

The spectra on which these analyses are based are reproduced in Appendix 2.15 (^1H) and Appendix 2.16 (^{13}C)

^1H-NMR data

Poly(1-octenylene) 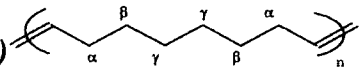

The peaks have been assigned as *cis* or *trans* according to their relative intensities and with the aid of a HETCOR spectrum (Appendix 2.17). The peaks for β and γ protons overlap but the HETCOR spectrum allows unambiguous identification since the ^{13}C spectrum can be fully assigned. The protons on the *cis* double bond appear as a slightly broadened but distinctive triplet at 5.35 while the peak for the protons on the *trans* double bond are less well resolved.

Proton	Shift
Hv (*cis*)	5.35
Hv (*trans*)	5.38
Hα (*cis*)	2.02
Hα (*trans*)	1.96
Hγ	1.29
Hβ	1.33

^{13}C-NMR data

Poly(1-octenylene)

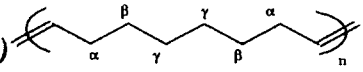

Carbon	Shift (ppm)
Cv *t*	130.33
Cv *c*	129.86
Cα *t*	32.62
Cα *c*	27.22
Cβ *c*	29.75
Cβ *t*	29.64
Cγ *cc*	29.23
Cγ *ct*	29.19
Cγ *tc*	29.09
Cγ *tt*	29.05

Adjacent double bonds in the polymer chain are still close enough to affect each other and triad splitting of the *cis* and *trans* olefinic signals is observed. The α and β carbons are only subjected to the effect of the nearest double bond giving one peak for both *cis* and *trans* with $C_{\alpha}c$ upfield from $C_{\alpha}t$ by 5.4 ppm and $C_{\beta}t$ upfield from $C_{\beta}c$ by 0.11 ppm. The γ carbons show a four line splitting pattern in the *cc*, *ct*, *tc*, *tt* sequence of environments, with $C_{\gamma}cc$ to $C_{\gamma}tc$ and $C_{\gamma}ct$ to $C_{\gamma}tt$ splitting of 0.137 ppm. The relative intensity of these peaks gives a *cis*:*trans* ratio of 90:10 when the polymerisation is initiated with a tungsten initiator, while the use of molybdenum based initiators gives high *trans* polymers under comparable reaction conditions.

GPC data

The Gel Permeation Chromatography results for polymers prepared using different initiators are shown in Appendix 2.18 and are presented below.

Initiator	Monomer : initiator ratio	Reaction time	Mn	PDI
$W(CH^tBu)(O^tBu)_2(NAr)$	300 : 1	20hrs	135000	1.4
$Mo(CH^tBu)(OC(CH_3)_3)_2(NAr)$	300 : 1	1hr	162000	1.5
$Mo(CH^tBu)(OC(CH_3)_2CF_3)_2(NAr)$	300 : 1	20hrs	320000	1.8
$Mo(CH^tBu)(OC(CH_3)(CF_3)_2)_2(NAr)$	300 : 1	20hrs	114600	2.6

Overall the molecular weights are higher and the molecular weight distributions broader than required for well defined living polymerisations, suggesting that propagation is faster than initiation in these systems under these conditions.

DSC data

The DSC traces are shown in Appendix 2.19 and show clearly that the melting temperature for these polymers increases with the *trans* content.

Initiator	*cis* : *trans* ratio[1]	Tm °C (onset)	Tm °C (max.)	Heat of fusion J/g
$W(CH^tBu)(O^tBu)_2(NAr)$	90 : 10	6.0	15.5	45.7
$Mo(CH^tBu)(OC(CH_3)_3)_2(NAr)$	30 : 70	31.0	40.1	43.5
$Mo(CH^tBu)(OC(CH_3)_2CF_3)_2(NAr)$	20 : 80	44.2	54.1	40.2
$Mo(CH^tBu)(OC(CH_3)(CF_3)_2)_2(NAr)$	15 : 85	51.8	58.1	44.6

[1]Derived from ^{13}C-NMR data

In this case, however, in contrast to the poly(1-heptenylene) case the heats of fusion of 90% *cis* and 85% *trans* polymers are very similar; it could be that the relative magnitudes of the heat of fusions in these polymers are determined by the relative importance of the vinylene and methylene sequences in determining the crystal packing. The effects appear to be rather subtle and the data set is too small to justify elaborate analysis.

Thermogravimetric analysis

2% weight loss was observed at 430°C, while the maximum weight loss was observed at 560°C.

IR data

The infrared spectrum is recorded in Appendix 2.5.d and showed peaks at 3003 cm^{-1} assigned to =CH stretch, at 2923 and 2852 cm^{-1} to antisymmetric and symmetric CH_2 stretching modes, at 1652 cm^{-1} to C=C stretch , at 1436 and 1465 cm^{-1} to CH_2 bend, at 966 cm^{-1} to *trans* =C-H out of plane bend and at 720 cm^{-1} to CH_2 rock and /or to *cis* =C-H out of plane bend.

2.7. Polymerisation of cyclodecene to give poly(1-decenylene)

The polymerisation of cyclodecene at room temperature and 3M in $CHCl_3$ when initiated with either tungsten or molybdenum based initiators gave high *trans* (up to 95%) polymer after reaction of 20 hours duration. When the polymerisation was run under the same conditions with a fluorinated Mo initiator and quenched after 15 min the resulting polymer had a *trans*:*cis* ratio of 80:20. This observation, while not representing a spectacular change, is in agreement with previous reports[12,68] of polymerisations using classical initiators where prolonged reaction times result in increased *trans* content as a result of secondary metathesis.

NMR data analysis

The spectra on which these analyses are based are reproduced in Appendix 2.20 (^1H) and Appendix 2.21 (^{13}C)

^1H-NMR

Poly(1-decenylene)

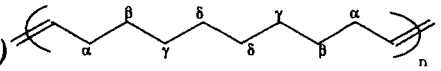

The assignments of the shifts due to *cis-trans* configurations are based on the relative intensities of the signals and on the shifts of the α and β protons of the polyalkenamers discussed earlier in this chapter. The signal at 1.26 ppm is not present in any of the ^1H-NMR of the polyalkenamers studied so far and so it must be associated with the δ protons because it is the first time they are being introduced to the repeat unit.

Proton	Shift (ppm)
Hv (*cis*)	5.34
Hv (*trans*)	5.38
Hα (*cis*)	2.01
Hα (*trans*)	1.96
Hβ, Hγ	1.32
Hδ	1.26

^{13}C-NMR data

Poly(1-decenylene)

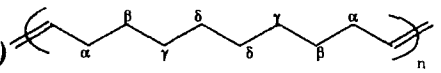

Carbon	Shift (ppm)
Cv *t*	130.34
Cv *c*	129.88
Cα *t*	32.63
Cα *c*	27.22
Cβ *c*	29.79
Cβ *t*	29.68
Cγ *c*	29.33
Cγ *t*	29.20
Cδ *c*	29.56
Cδ *t*	29.52

The olefinic carbons show no splitting due to triad effects and appear as slightly broaden singlets with C_vc 0.463 ppm upfield from C_vt. All the methylene carbons also give one signal for each configuration with respect to the nearest double bond C_αt being 5.4 ppm upfield from C_αc, C_βc being 0.11 ppm upfield from C_βt, C_γc being 0.136 ppm upfield from C_γt and C_δc being 0.035 ppm upfield from C_δt.

GPC data

The Gel Permeation Chromatography results for polymers prepared using different initiators are shown in Appendix 2.22 and are presented below.

Initiator	Monomer : initiator ratio	Reaction time	Mn	PDI
W(CH^{t}Bu)(O^{t}Bu)$_2$(NAr)	300 : 1	20hrs	38000	1.5
Mo(CH^{t}Bu)(OC(CH$_3$)$_3$)$_2$(NAr)	300 : 1	20hrs	91000	1.4
Mo(CH^{t}Bu)(OC(CH$_3$)$_2$CF$_3$)$_2$(NAr)	300 : 1	15min	112000	1.5
	300 : 1	20hrs	insoluble	
Mo(CH^{t}Bu)(OC(CH$_3$)(CF$_3$)$_2$)$_2$(NAr)	300 : 1	20hrs	insoluble	

Overall the molecular weights are higher and the molecular weight distributions broader than required for well defined living polymerisations, suggesting that propagation is faster than initiation in these systems under these conditions.

DSC data

The DSC traces are shown in Appendix 2.23 and show similar melting temperatures for polymers with similar *cis*:*trans* ratio, the higher the *trans* ratio the higher the

melting temperature.

Initiator	*cis* : *trans* ratio[1]	Tm °C (onset)	Tm °C (max.)	Heat of fusion J/g
$W(CH^tBu)(O^tBu)_2(NAr)$	20 : 80	59.9	64.0	53.6
$Mo(CH^tBu)(OC(CH_3)_3)_2(NAr)$	17 : 83	64.1	69.4	83.3
$Mo(CH^tBu)(OC(CH_3)_2CF_3)_2(NAr)$	20 : 80 5 : 95	60.4 71.2	65.6 75.2	53.2 67.8
$Mo(CH^tBu)(OC(CH_3)(CF_3)_2)_2(NAr)$	5 : 95	70.7	74.1	54.6

[1]Derived from ^{13}C NMR data

Thermogravimetric analysis

2% weight loss was observed at 425°C while the maximum weight loss was observed at 520°C.

IR data

The infrared spectrum is recorded in Appendix 2.5.e and showed peaks at 3003 cm^{-1} assigned to =CH stretch, at 2918 and 2848 cm^{-1} to antisymmetric and symmetric CH_2 stretching modes, at 1436 and 1465 cm^{-1} to CH_2 bend, at 963 cm^{-1} to *trans* =C-H out of plane bend and at 720 cm^{-1} to CH_2 rock and/or to *cis* =C-H out of plane bend. The peak for C=C stretching appeared very weak in the spectrum.

2.8. Polymerisation of cyclododecene to give poly(1-dodecenylene)

The polymerisation of cyclododecene at room temperature and 3M in $CHCl_3$ when initiated with either tungsten or molybdenum based initiators gave high *trans* (up to 95%) polymer after reaction of 20 hours duration. When the polymerisation was run under the same conditions with a fluorinated Mo initiator and quenched after 15 min the resulting polymer had a *trans*:*cis* ratio of 80:20.

NMR data analysis

The spectra on which these analyses are based are reproduced in Appendix 2.24 (^{1}H) and Appendix 2.25 (^{13}C)

^{1}H-NMR data

Poly(1-dodecenylene) 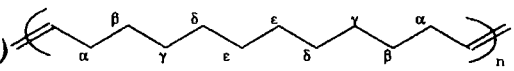

The peaks for the *cis* and *trans* configurations of the vinylic protons are found at 5.35 and 5.38 ppm respectively. The α -CH_2- protons appear at 1.96 ppm for the *trans* and 2.02 ppm for the *cis*. The assignments are based on the relative intensities of the signals and correlation with the unambiguous assignments based on the ^{13}C NMR spectrum. The peaks at 1.31 ppm are assigned to the β and γ protons, while the peaks at 1.26 ppm are assigned to the δ and ε protons in analogy with ^{1}H-NMR spectra of polyalkenamers discussed previously in this chapter.

Proton	Shift (ppm)
Hv (*cis*)	5.35
Hv (*trans*)	5.38
Hα (*trans*)	1.96
Hα (*cis*)	2.02
Hβ–γ	1.31
Hδ–ε	1.26

^{13}C-NMR data

Poly(1-dodecenylene) 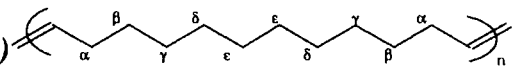

The signals due to the olefinic carbons for both the *cis* and *trans* geometries of the double bonds appear as slightly broadened singlets with C_vc upfield 0.462 ppm from C_vc. The methylene carbons also give one peak for each configuration of the double bond with $C_\alpha c$ upfield 5.4 ppm from $C_\alpha t$, $C_\beta t$ upfield 0.11 ppm from $C_\beta c$, $C_\gamma t$ upfield 0.137 ppm from $C_\gamma c$, $C_\delta t$ upfield 0.035 ppm from $C_\delta c$. The ε carbon gives one peak at 29.771 ppm but no other peak can be seen either because the

Carbon	Shift (ppm)
Cv *t*	130.44
Cv *c*	129.98
Cα *t*	32.73
Cα *c*	27.32
Cβ *c*	29.90
Cβ *t*	29.79
Cγ *c*	29.44
Cγ *t*	29.31
Cδ *c*	29.69
Cδ *t*	29.66
Cε	29.77

resolution is insufficient or the peaks overlap with other resonances.

GPC data

The Gel Permeation Chromatography results for polymers prepared using different initiators are shown in Appendix 2.26 and are tabulated below.

Initiator	Monomer : initiator ratio	Reaction time	Mn	PDI
$W(CH^tBu)(O^tBu)_2(NAr)$	300 : 1	3hrs	82800	1.8
$Mo(CH^tBu)(OC(CH_3)_3)_2(NAr)$	300 : 1	3hrs	160000	1.7
$Mo(CH^tBu)(OC(CH_3)_2CF_3)_2(NAr)$	300 : 1	15min	132000	1.7
	300 : 1	20hrs	insoluble	
$Mo(CH^tBu)(OC(CH_3)(CF_3)_2)_2(NAr)$	300 : 1	20hrs	insoluble	

It is clear that the molecular weights and their distributions are higher than required for well defined living polymerisation in all cases, suggesting that propagation is faster than initiation.

DSC data

The DSC traces are shown in Appendix 2.27 and show similar melting temperatures for polymers with similar *cis*:*trans* ratio.

Initiator	*cis* : *trans* ratio[1]	Tm °C (onset)	Tm. °C (max.)	Heat of fusion J/g
$W(CH^tBu)(O^tBu)_2(NAr)$	20 : 80	63.0	67.2	52.5
$Mo(CH^tBu)(OC(CH_3)_3)_2(NAr)$	15 : 85	64.9	69.2	56.1
$Mo(CH^tBu)(OC(CH_3)_2CF_3)_2(NAr)$	20 : 80	62.7	68.8	57.6
	5 : 95	67.6	72.0	60.4
$Mo(CH^tBu)(OC(CH_3)(CF_3)_2)_2(NAr)$	15 : 85	63.9	71.4	58.2

[1]Derived from ^{13}C-NMR data

Thermogravimetric analysis

2% weight loss was observed at 420°C while the maximum weight loss was observed

at 520°C.

IR data

The infrared spectrum is recorded in Appendix 2.5.f and showed peaks at 3005 cm^{-1} assigned to =CH stretch, at 2919 $cm^{-1}$and 2849 cm^{-1} to antisymmetric and symmetric CH_2 stretching modes, at 1462 and 1439 cm^{-1} to CH_2 bend, at 963 cm^{-1} =C-H *trans* to out of plane bend and at 719 and 729 cm^{-1} to CH_2 rocking and the *cis* =C-H out of plane bend.

2.9. Discussion

2.9.1. General remarks. In the ^{13}C-NMR spectra, shown in Figure 2.9, p.56, the peaks associated with *cis* double bonds appear upfield from the analogous *trans* peaks for both Cv and Cα, and downfield for Cβ, Cγ and Cδ. The magnitudes of the shift differences are illustrated in the table below.

Carbon	Cv	Cα	Cβ	Cγ	Cδ
cis to *trans* splitting (ppm)	0.46 - 0.5	5.4	0.11	0.136	0.035

The methylene carbon shifts experience a nearest and next nearest vinylene neighbour effect until there are eight methylene units between vinylenes. This gives rise to a set of four lines defined by the environments *cc*,*ct*,*tc* and *tt*, with *tt* being nearest to TMS. When a methylene carbon is symmetrically placed with respect to the double bonds the *ct* and *tc* peaks coincide and the splitting pattern changes to *cc*, *ct*/*tc* and *tt*, again with *tt* nearest to TMS.

2.9.2. Olefinic triads effect. The splitting of the olefinic signals due to triads (ccc, ttt etc.) decreases as the length of the repeat unit increases.

Polymer	*ttt→ctt* or *ttc* (ppm)	*ccc→tcc* or *cct* (ppm)
Poly(pentenylene)	0.04	0.08
Poly(heptenylene)	0.03	0.03
Poly(octenylene)	0.02	0.02

The assignment of these peaks is based on the observation that the splitting pattern for this effect generally appears to consist of one intense peak and two smaller peaks of the same intensities on either side, for both the *cis* and the *trans* signals. Since the polymers examined were highly blocky we assign the more intense peak as ttt (or ccc). The ttc (or cct) and ctt (or tcc) peaks should by definition have the same intensities since the presence of a ttc carbon requires the presence of a ctt one. The ctc and tct peaks are expected to be of relatively low intensity and to be overlapped by the ttt and ccc peaks respectively, because the nearest and next nearest double bond effect is symmetrical.

2.9.3. Polyalkenamers and the γ-*gauche* effect.

Large chemical shift effects due to the geometry of the nearest double bond can be observed in the peaks associated with the carbon α to the double bond in all the polymers studied. This is as expected; indeed it is probably the most reliable parameter for assigning *cis/trans* vinylene content in these kind of materials. A shift of about 5.5 ppm to lower frequency (higher field) is observed on changing from *trans* to *cis*, see Figure 2.9. However there are two very clear anomalies in the set of ^{13}C-NMR spectra collected in Figure 2.9; thus, the chemical shifts of the *cis* and *trans* vinylic and α-carbons are very similar throughout the set with the exception of the vinylic carbons in poly(1-butenylene) and the α-carbons in poly(1-pentenylene). In both cases the relevant signals display significant upfield shifts. In the case of

poly(1-pentenylene) the peaks for the α-carbons are shifted upfield by about -0.4 ppm with respect to the α-carbon shifts in all the other polyalkenamer spectra and split due to the effect of the next nearest double bond by +0.133 ppm for the *tt* to *tc* signals and +0.151 ppm for the *ct* to *cc* signals. This is a large effect in comparison to the *tt* to *tc* splitting of -0.05 ppm for the α-carbons in poly(1-butenylene), where the next nearest double bond is only two bonds away. These observations can be accounted for in terms of a phenomenon which has been extensively documented by Tonelli and is known as the "γ-*gauche* effect".[67]

This predicts that the chemical shift of a specific carbon, namely the observed carbon C^0, see Figure 2.9.3a and b, will be influenced by the probability that the carbon atom three bonds away, that is gamma with respect to C^0, occurs in a *gauche* conformation with respect to the "observed carbon". In the case of poly(1-pentenylene) the γ-carbon (C^γ), that is the carbon three bonds away from the allylic carbon (C_α), is the sp^2 carbon at the near end of the next nearest double bond and it is reasonable to assume that the relative population of the *trans* and *gauche* isomeric states will be significantly different in this case from that where the γ-carbon is a methylene. The relevant carbon-carbon bond rotation barrier will be lower and the energy difference between *gauche* and *trans* smaller, giving a relatively higher *gauche* content. The foregoing discussion allows for a rationalisation of the gross upfield shift; the splitting of $C_\alpha t$ and $C_\alpha c$ signals into *tc/tt* and *cc/ct* pairs is a consequence of the difference in shift effect from γ-*gauche* carbons in *trans* and *cis* double bonds.

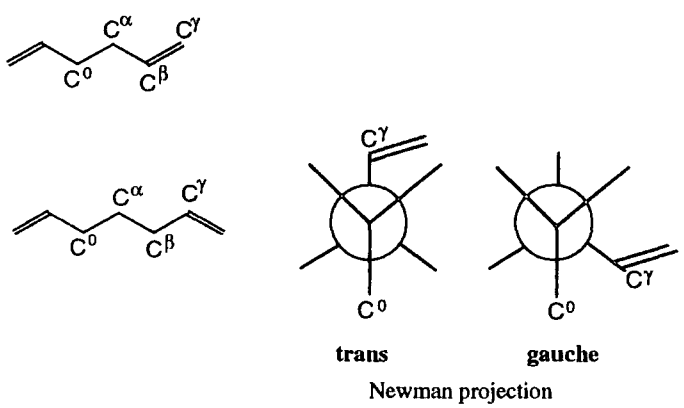

Fig 2.9.3.a The observed carbon is α to the double bond $C^0=C_\alpha$

In the case of poly(1-butenylene), a different rotational isomeric state (RIS) model must apply since the carbon three bonds away from the α carbon is now at the far end of the next nearest double bond. This means that the carbon two bonds away from the α carbon, see Fig. 2.9.3.a, is now also sp^2 hybridised, and the configuration of the double bond has a negligible effect on the probability of the carbon three bonds away being *gauche*, indeed the terms trans and *gauche* are not strictly applicable in this case. This interpretation is supported by the fact that upfield shift (-0.2 to -0.3 ppm) and large effects due to the next nearest double bond are also seen for the vinylic carbons Cv of poly(1-butenylene) (Fig 2.9.3.b) as well as for the Cγ carbon of poly(1-heptenylene) (although this shift is rather small), where the carbon three bonds away is again the near end of the next nearest double bond. We observe that when the next nearest double bond is *trans* in these cases the γ-*gauche* effect is enhanced (i.e. these peaks are shifted towards lower frequencies) as a result of the higher probability of the γ carbon being in the *gauche* conformation.

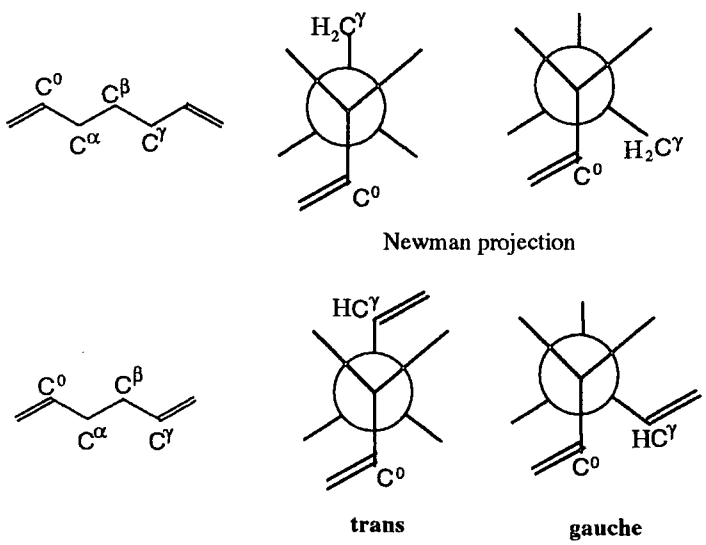

Fig.2.9.3.b. The observed carbon is the vinylic carbon $C^0=C_v$

This analysis in terms of the γ-*gauche* effect allows us to explain minor shifts and multiplicities in the ^{13}C-NMR spectra of polyalkenamers which have not previously received comment. This matter may be susceptible to further investigation through molecular modelling if this technique proves capable of predicting the relative abundances of *trans* and *gauche* conformations in different polyalkenamers. A study of this kind requires a large effort and has not been possible to date, but is recommended by the author for future work.

2.9.4. Secondary metathesis.

The existence of a *tt* peak in the ^{13}C-NMR spectrum of poly(1-butenylene) made from the ROMP of 1,5-*cis,cis*-cyclooctadiene as well as the results of the two experiments with cyclodecene and cyclododecene which are tabulated here, give evidence of either intra- or intermolecular secondary metathesis taking place, biased towards the formation of *trans* double bonds.

Polymer	Reaction time	*cis*:*trans* double bonds
Poly(1-decenylene)	15min	20 :80
	20 hrs	5 : 95
Poly(1-dodecenylene)	15min	20 : 80
	20 hrs	5 : 95

These results, while not representing spectacular changes, are in agreement with previously reported[12,68] ROM polymerisations of monocyclic alkenes using classical initiators, where prolonged reaction times result in increased *trans* content as a result of secondary metathesis.

2.9.5. DSC data analysis.

The observed T_ms for these polymers are dependent on the *cis*:*trans* ratio. The higher the *trans* content the higher the melting temperature, and the higher the double bond content in the polymer chain the more acute is this effect. So, for example, in the case of poly(1-butenylene) the melting point changes dramatically with small changes in the *cis* and *trans* ratio while, at the other end of this scale, in poly(1-dodecenylene) the melting point changes are smaller as shown on Figure 2.9.5 overleaf. The data shown in this chart are only indicative of the effect and the lines drawn are intended only as a "guide to the eye", there are far too few data points for an analysis and no linear dependence of the melting temperature on the *cis* content is implied.

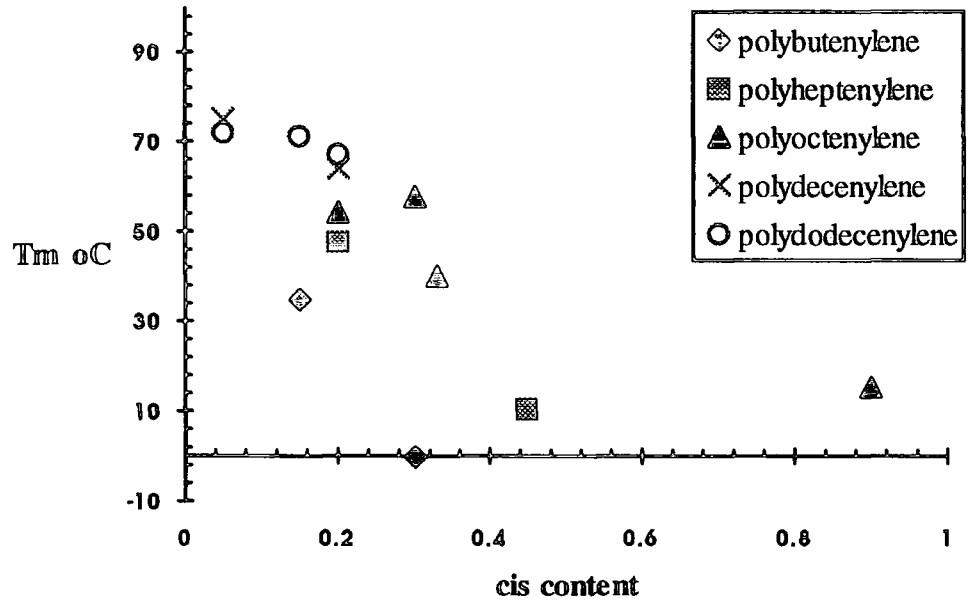

Figure 2.9.5. Melting temperature vs. *cis* content data in some polyalkenamers

2.9.6 Summary of results: Some of the most important characteristics of the polyalkenamers prepared during this study and discussed earlier in this chapter are tabulated below.

Initiator / Monomer	[W]	[Mo]	$[Mo]_{F3}$	$[Mo]_{F6}$	
Cyclooctadiene	80 : 20*	30 : 70*	15 : 85*	15 : 85*	*cis:trans ratio*
	2.9	1.7	1.6	1.7	*PDI*
	440	190	416	840	*DP*
	--	-0.3	34.9	34.4	T_m° *C*
Cyclopentene	55 : 45	55 : 45	45 : 55		*cis:trans ratio*
	1.06	1.35	1.5		*PDI*
	320	5400	3180		*DP*
Cycloheptene	No polymer recovered	45 : 55*	25 : 75*	20 : 80*	*cis:trans ratio*
		1.5	1.5	1.87	*PDI*
		300	390	210	*DP*
		10.6	47.5	47.5	T_m° *C*
Cyclooctene	90 : 10*	30 : 70	20 : 80*	15 : 85*	*cis:trans ratio*
	1.39	1.5	1.8	2.6	*PDI*
	1220	1460	2900	1040	*DP*
	15.5	40.1	54.1	58.1	T_m° *C*
Cyclodecene	20 : 80*	17 : 83*	5 : 95*	5 : 95*	*cis:trans ratio*
	1.55	1.4	-	-	*PDI*
	273	660	-	-	*DP*
	64.0	69.4	75.2	74.1	T_m° *C*
Cyclododecene	20 : 80	15 : 85	5 : 95*	15 : 85*	*cis:trans ratio*
	1.78	1.73	-	-	*PDI*
	500	950	-	-	*DP*
	67.2	69.2	72.0	71.3	T_m° *C*

*Polymerisation quenched after 20hrs

Table 2.9.6. Summary of polymerisation data

All the reactions were performed in chloroform at room temperature, except for the polymerisation of cyclopentene at -45°C, with monomer:initiator ratio 300:1; the GPC results are relative to polystyrene standards and the *cis:trans* ratio were derived from analysis of ^{13}C-NMR spectra recorded at 100.577 MHz in $CDCl_3$.

It is difficult to deduce any really secure generalisations concerning the polymerisation of cycloalkenes from the set of data collected in Table 2.9.6. Since the

poly(1-pentenylene) was made at low temperature it can not sensibly be compared with the other results which were produced from room temperature polymerisations. It is noteworthy that with the tungsten centred initiator both cycloocta-2,5-diene and cyclooctene give predominantly *cis* vinylenes, whereas both the ten and twelve membered rings give predominantly *trans* double bonds under apparently similar conditions. The reason for this is not clear but may reside in subtleties involving the conformation preferences and energetics of the monomers and derived metallacyclobutanes. Another discernible trend in the molybdenum based initiators is that fluorination in the alkoxy ligand favours *trans* double bonds in the polymer, whether this arises in the primary polymerisation or as a result of secondary metathesis is unclear in this case but the same trend is observed in polymerisations of norbornenes where secondary metathesis is unlikely for steric reasons.

For the work described in other parts of the thesis we wanted to make use of well defined living polyalkenamers for the synthesis of novel hydrocarbon polymer topologies. Part of the reason for the investigation described in this chapter was to see if a more convenient living system than poly(1-pentenylene) at -45°C was available via the use of a range of well defined initiators and a range of cycloalkenes. In the event it became clear that there were no such systems accessible with the available reagents investigated.

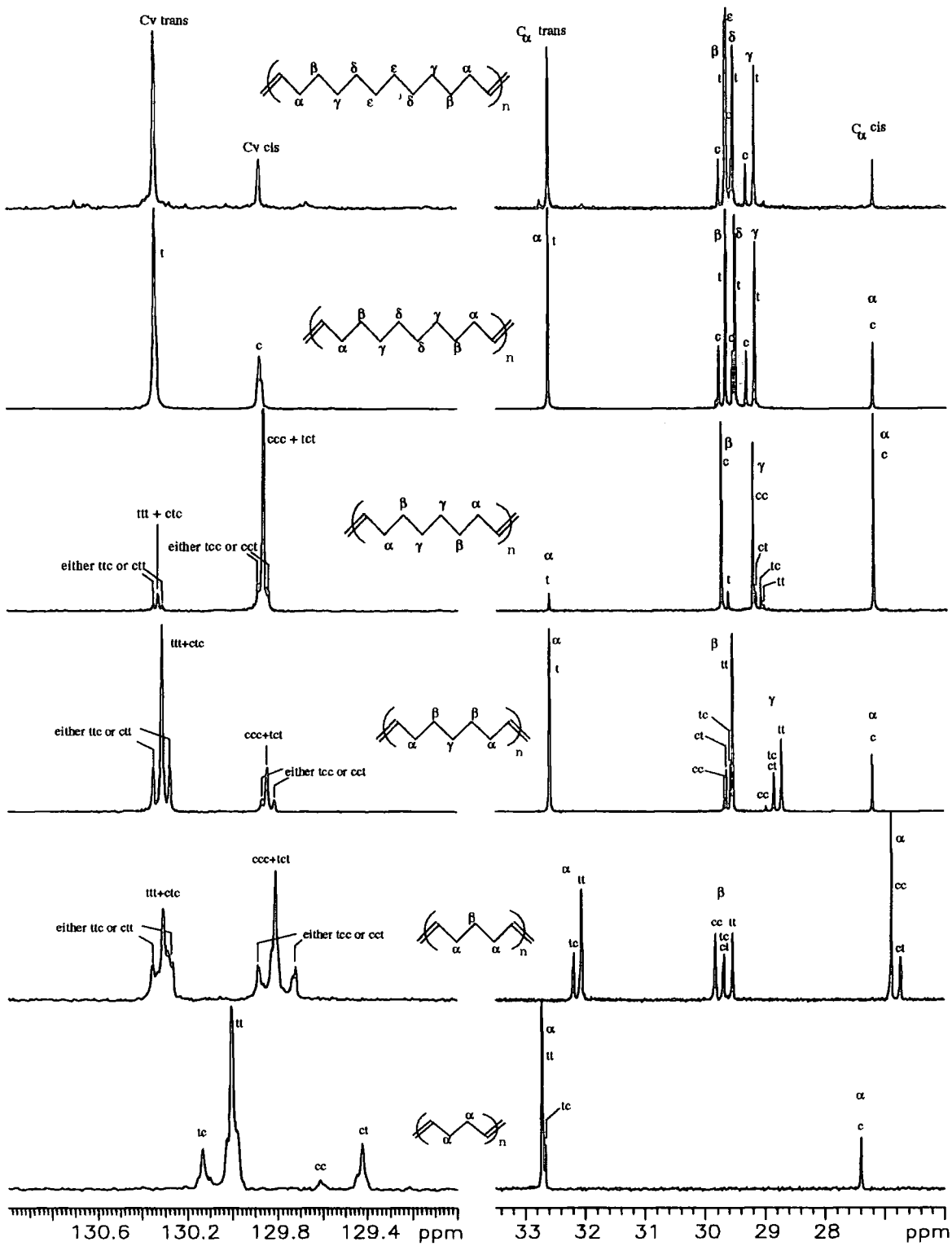

Figure 2.9 **^{13}C-NMR spectra of the polyalkenamers discussed in this chapter**

CHAPTER 3: Novel block copolymers via ROMP

3.1. Introduction

In a living polymerisation process after the first monomer (A) has been consumed the chain end is still active and the polymer can then either be quenched by the addition of a suitable reagent or a second monomer (B) may be added to yield, in favourable cases, an A-B block copolymer (A-*block*-B or A-*b*-B). This procedure can be repeated to produce polymers with well-defined blocks of homopolymers as illustrated below.

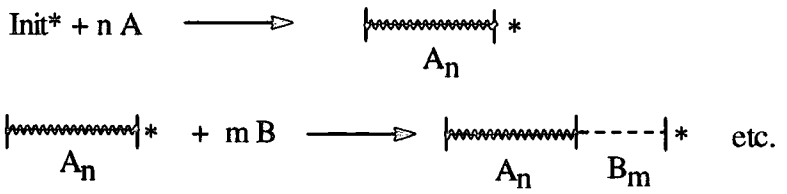

An alternative method for the preparation of block copolymers is reaction between functional groups at the ends of two different polymers, as shown below.

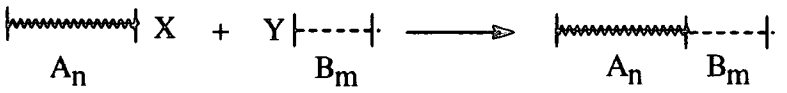

ROMP initiated with well defined transition metal complexes has been used for the preparation of several block copolymers (see chapter 1). Polyacetylene-*block*-polynorbornene-*block*-polyacetylene has been prepared[42] using a titanium based difunctional initiator and the "Durham precursor route"[69,70] to polyacetylene. Also polynorbornene-*block*-polyacetylene copolymers have been prepared using $Mo(CH^tBu)(NAr)(O^tBu)_2$ as the initiator.[71]

In this work an attempt to prepare an A-B-A block copolymer, where the A blocks are long aliphatic chains and the B block is a sequence of approximately 20 conjugated double bonds, that is poly(1-pentenylene)-*block*-polyacetylene-*block*-

poly(1-pentenylene), is described. This study was undertaken since such a block copolymer was desirable for investigations of the forces experienced by individual polymer chains being stretched in solution. The study of this process is a research interest in the group of Professor D.N.Batchelder of the Physics department at Leeds University and the target molecule fits within the theme of the author's research into the application of living ROMP in the synthesis of polymers with novel well defined architectures. The high molecular weight linear polymer with a short conjugated sequence exactly at its centre would be an ideal probe for this work since shifts in the Raman spectrum of the polyene sequence can be correlated with the distortion of the sequence and consequently with the force experienced by it and by the polymer chain of which it is a part. The aliphatic blocks in the desired A-B-A block copolymer does not have to be poly(1-pentenylene) and some work investigating the synthesis of poly(bistrifluoromethylnorbornadiene)-*block*-poly(1-octenylene) as a preliminary model for the use of poly(1-octenylene) as the A-block polymer is also discussed here.

3.2. Preparation of poly(bistrifluoromethylnorbornadiene) - *block* - poly(1-octenylene)

The reaction sequence for this synthesis is shown schematically overleaf.

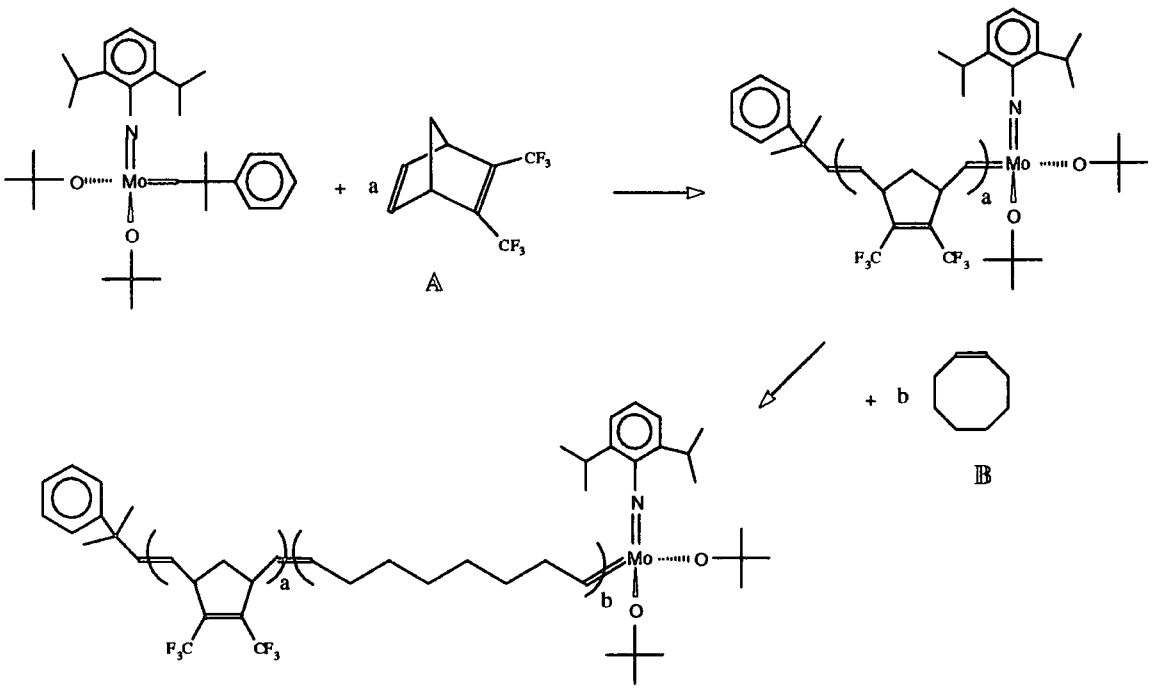

Bis(trifluoromethyl)norbornadiene (monomer A) polymerises in a living manner when initiated with $Mo(NAr)(C(CH_3)_2Ph)(O\text{-}t\text{-}Bu)_2$ in THF-d_8 at room temperature.[72] When all monomer A was consumed, as shown by ^{1}H-NMR, cyclooctene (monomer B) was added to the living polymer solution and allowed to react until it was all converted to polymer.

^{1}H-NMR data

The polymerisation was performed in a plastic topped sample bottle with a micro magnetic stirrer follower, in the Glove Box at room temperature. In order to record the ^{1}H-NMR spectra the reaction solution was periodically transferred into an NMR tube sealed with Parafilm. The results of this study are outlined here and the sequential spectra are shown in Appendices 3.1 a, b, c, d and e.

One hour after the addition of 10 equivalents of (bistrifluoromethyl)norbornadiene to a $Mo(NAr)(C(CH_3)_2Ph)(O\text{-}t\text{-}Bu)_2$ solution in THF-d_8 the singlet peak at 11.29 ppm, due to the initial alkylidene proton, was completely replaced by a doublet at 11.45 ppm (J_{HH}= 8 Hz) due to the proton of the propagating alkylidene. At the same time peaks for the polymer had appeared. The doublet at 5.8 (J_{HH}= 16 Hz) and the

doublet of doublets at 5.44 ppm (J_{HH}= 8 Hz and 16 Hz) are the signals from the olefinic protons on the first double bond of the chain, which has trans configuration. Integration for these peaks in comparison to the broad singlet from the vinylic protons in the remainder of the chain at 5.6 ppm indicates a degree of polymerisation of 10 and suggest that a well-controlled living polymerisation process is taking place. At this stage all monomer A was consumed and ten equivalents of cyclooctene (monomer B) were added. The intensity of the doublet from the propagating alkylidene started to diminish but the expected triplet in the alkylidene region was not observed as a well resolved signal although there was a new unresolved peak of low intensity at 11.28 ppm which may be associated with the proton of the propagating alkylidene on the poly(1-octenylene) block. The intensity of the peaks for poly(1-octenylene) increased and there was a corresponding decrease in the intensity of the peaks associated with cyclooctene. The reaction was monitored until no signals were observed in the alkylidene region and until all monomer B was converted to polymer. At this stage a small amount of benzaldehyde was added to terminate the polymerisation. The shifts for the characteristic protons of the living A-block, the B-block and the cyclooctene monomer are tabulated overleaf.

Bis(trifluoromethyl) norbornadiene living polymer (A block)	Shift (ppm)	Multiplicity	Integral
[Mo]=$\underline{H}$C-propagating alkylidene	11.45	doublet	1
-C$\underline{H}$(CH_3)$_2$ living end of chain	3.82	septet	-
PhC(CH_3)$_2$C$\underline{H}$:CH-inactive end of chain	5.8	doublet	1
PhC(CH_3)$_2$CH:C$\underline{H}$-inactive end of chain	5.44	doublet of doublets	1
$\underline{H}_{olefinic}$	5.62	broad	20
$\underline{H}_{allylic}$	3.65	broad	20
C$\underline{H}_2$ (syn and anti)	2.6 1.6	m doublet	10 10

Peaks of very low intensity for some unreacted monomer A are present at 7.02 ($\underline{H}_{olefinic}$), 3.97 ($\underline{H}_{allylic}$) and 2.1 and 2.33 ppm (C$\underline{H}_2$ syn and anti) in the first spectrum (Appendix 3.1.a), but were not visible in any subsequent spectra.

Polyoctenylene (B block)	Shift (ppm)	Multiplicity	Integral
Hv	5.36 cis-trans	m	1
Hα	2.02 cis-trans	m	2
Hβ–γ	1.37	m	4

Cyclooctene	Shift (ppm)	Multiplicity	Integral
CH_v	5.6	m	1
$CH_{\alpha 2}$	2.18	m	2
CH_2	1.56	m	4

GPC data

The resulting polymer was recovered by evaporation of the solvent; it was then redissolved in THF and its gel permeation chromatogram recorded, using a dual refractometer/viscometer detector system and calibration with polystyrene standards. The molecular weights for the homopolymers are overestimated by a factor of ca.2 using this analytical procedure and there is some uncertainty concerning the GPC behaviour of block copolymers, nevertheless the measured M_n values appear to be at least a factor of two higher than would be expected for perfect well behaved living polymerisation.

PDI	1.31
M_n	13900
M_w	18200

The above results indicate that the addition of cyclooctene (monomer B) to the well defined living A block (bistrifluoromethyl)norbornadiene proceeds in a less than ideal manner since a higher than expected molecular weight and a broader molecular weight distribution is observed. The GPC trace is recorded in Appendix 3.2.

DSC data

Trans(bistrifluoromethyl)norbornadiene homopolymer displays a Tg at 93°C and Tm at 200°C,[72] while the T_m of poly(1-octenylene) varies considerably depending on the configuration of the double bonds and is reported to be in the region of 5-50°C, see Chapter 2. The DSC trace of the block copolymer, Appendix 3.3 shows three broad endothermic transitions with peaks at about 196, 174 and 25°C. The transitions at 196 and 25°C can be provisionally assigned to melting of the poly(bis(trifluoromethyl)norbornadiene) and poly(1-octenylene) crystalline domains, but the peak at 174°C is difficult to rationalise. There is also a marked change in the base line slope at about 93°C which corresponds to Tg for the

poly(bis(trifluoromethyl)norbornadiene) although the actual trace in not very convincing. We concluded from this brief study and the studies reported in Chapter 2 that using cyclooctene to generate the A blocks in the target A-B-A block copolymer was not a practical proposition.

3.3. Preparation of poly(1-pentenylene)-*block*-polyacetylene-*block*-poly(1-pentenylene)

The aim of this study was to prepare an A-B-A block copolymer which consists of a long poly(1-pentenylene) block (A), followed by a short polyacetylene sequence (B), followed by a long poly(1-pentenylene) block (A). We have seen in chapter 2 that $W(CH^tBu)(O^tBu)_2(NAr)$ in chloroform at -45°C initiates the living, well-defined polymerisation of cyclopentene (monomer A). The same system is also capable of initiating the ring opening polymerisation of 7,8-bis(trifluoromethyl)tricyclo[4.2.2.$0^{2,5}$]deca-3,7,9-triene (I) (monomer B), to produce a precursor polymer which on heating under vacuum at 70°C for 1/2 hour eliminates 1,2-(bistrifluoromethyl)benzene as a result of a retro-Diels-Alder reaction to yield polyacetylene. As both polymerisation processes are living, subsequent addition of monomer B, after monomer A has been consumed, should result in the formation of an living A-B block copolymer. Further addition of monomer A after monomer B has been consumed should result in the formation of an A-B-A block copolymer. In order to achieve complete conversion of cyclopentene, reaction times >24 hours are necessary. It was realised that there might be practical problems in realising the above copolymerisation as there is a tendency for cyclopentene to undergo intermolecular side reactions during the polymerisation, resulting in broader molecular weight distributions (see chapter 2) or the formation of crosslinked material (see chapter 4), when the polymerisation times are longer than 8 hrs. In order to avoid these unfavourable side reactions, the whole reaction vessel was

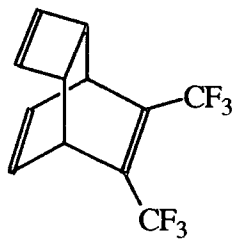

or

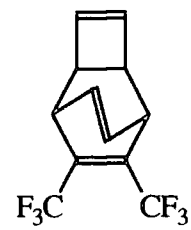

(I)

evacuated at -45°C after 4 hours reaction which removed solvent and unreacted cyclopentene. Pure solvent was returned to the reaction vessel giving well defined living poly(1-pentenylene). As concluded in chapter 2, the polymerisation of cyclopentene at a fixed concentration (3.8M) in $CHCl_3$ at -45°C gave a polymer which had a molecular weight dependent on the monomer to initiator ratio and the reaction time and so the molecular weight of the living poly(1-pentenylene) obtained by the procedure described above could be predicted to ±10%.

In a typical experiment a solution of 400 equivalents of cyclopentene was mixed with 1 equivalent of initiator under the above conditions and allowed to react for 4 hours. Then the reaction vessel was placed under vacuum and any unreacted cyclopentene was removed from the reaction mixture together with chloroform. The dry living polymer was redissolved in chloroform at -45°C and then 10 equivalents of monomer B in $CHCl_3$ were added via cannula transfer under N_2. The mixture was allowed to react for at least 1 hour to ensure complete conversion of monomer B to polymer. The last batch of 400 equivalents monomer A, dissolved in chloroform at a concentration of 3.8M, was added and allowed to react for 4 hours. Finally, excess benzaldehyde was added to terminate the polymerisation in a Wittig-like capping reaction. The final product was put under vacuum in order to remove the solvent, any unreacted cyclopentene and excess benzaldehyde. The resulting polymer was heated under vacuum at 70°C for 1/2 hour in order to eliminate 1,2-(bistrifluoromethyl)benzene from the repeat units of the B-block, resulting in the formation of polyacetylene. The deep-red polymer was soluble in chloroform, toluene and heptane. The reaction path is shown schematically overleaf.

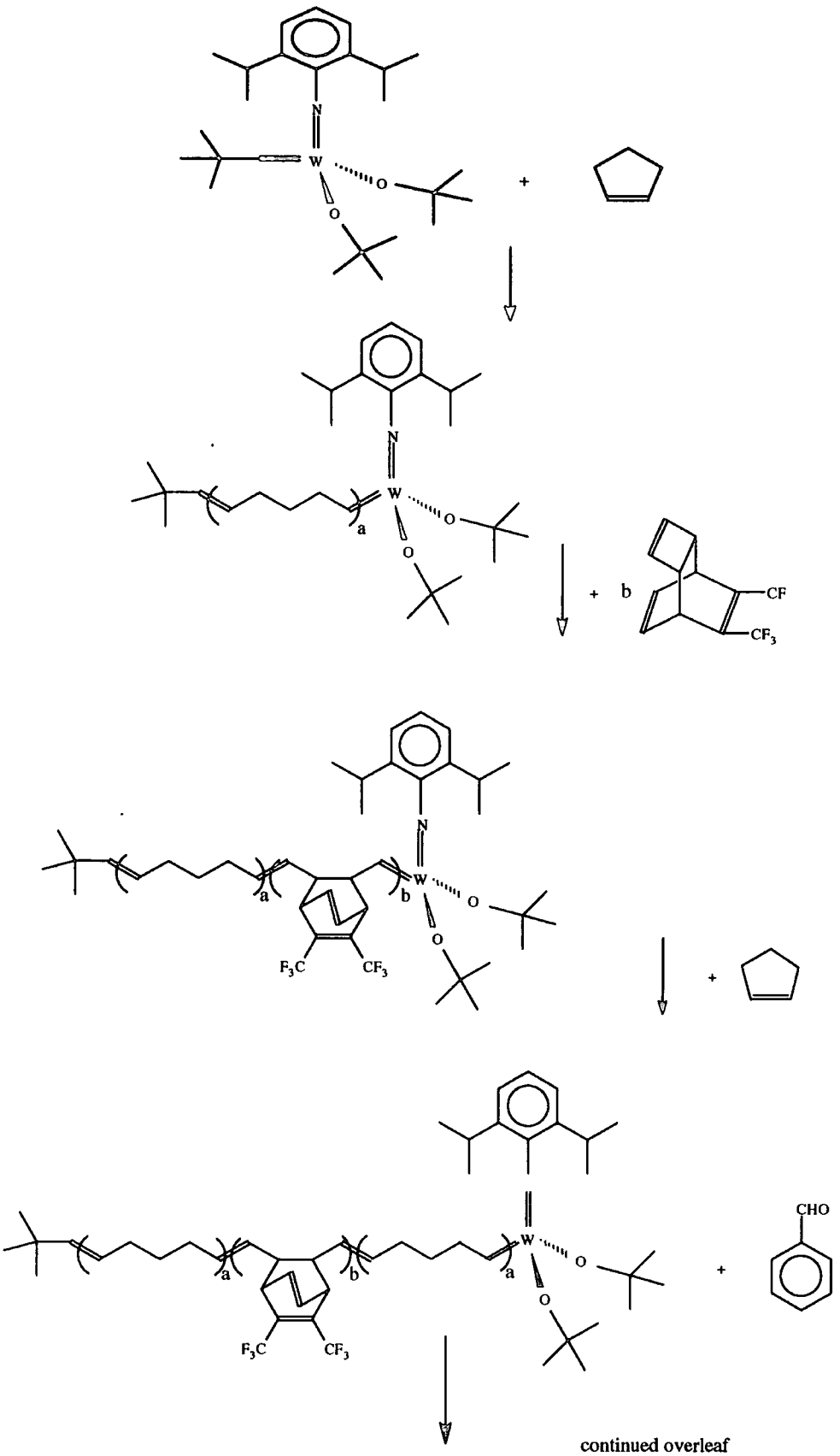

continued overleaf

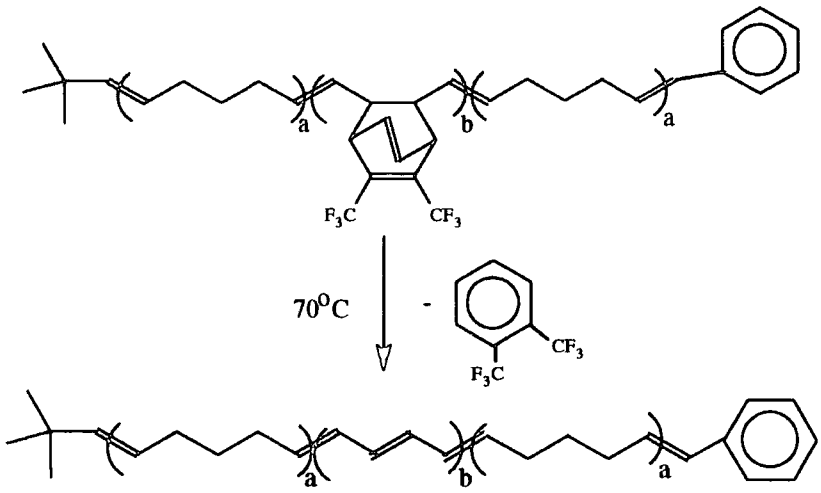

NMR data

The ^{13}C and ^{1}H-NMR spectra of the final A-B-A block copolymer were essentially identical to those obtained for poly(1-pentenylene) (see Chapter 2). The ^{1}H signals due to the protons on the polyacetylene block should constitute between 1 and 2% of the total signal and would be expected to coincide with the signals from the vinylic protons of the poly(1-pentenylene) protons. This also applies to the carbons of the polyacetylene block which are not visible in the ^{13}C-NMR spectrum. The spectra are illustrated in Appendices 3.4 and 3.5.

UV-Vis spectroscopy

Conjugation of double bonds lowers the energy required for the $\pi \rightarrow \pi^*$ transition and the absorption related to this electronic transition moves to longer wavelengths with increasing conjugation lengths.

The UV-Vis spectra of a solution of the poly(1-pentenylene)-*block*-polyacetylene-*block*-poly(1-pentenylene) copolymer, in spectroscopic grade toluene and heptane, reproduced in Appendices 3.6.a and b, showed a distribution of absorption peaks from 260nm in the 'near' UV region to 600nm in the visible region. The wavelength of maximum absorption (λ_{max}) was at 450nm while the absorption edge was at 600nm in both solutions. The absorption peaks observed are tabulated overleaf.

Solution in toluene absorption (nm)	Solution in heptane absorption (nm)
294	261
333	319
348	334
366	350
392	381
416	403
450	436
473	470

Schrock and Krouse[73] investigated the behaviour of polynorbornene-*block*-polyacetylene and polynorbornene-*block*-polyacetylene-*block*-polynorbornene polymers, using UV/Vis spectroscopy. They observed that the A-B block copolymers showed broad unresolved peaks corresponding to generally smaller conjugation lengths than the number of double bonds in the polyene sequence and in the case of A-B-A block copolymers (only) they also observed well resolved peaks characteristic of triene (240-300 nm), pentaene (310-380 nm), heptaene (380-410 nm) and nonaene (410-450). They proposed that polyenes that are generated in the triblocks are restricted in the extent to which their double bonds can be brought into conjugation by twisting of the polyene chains , whereas in the diblocks the polyene chains are relatively mobile and can be brought into conjugation more easily. The spectrum of the poly(1-pentenylene)-*block*-polyacetylene-*block*-poly(1-pentenylene) copolymer, shows well resolved peaks corresponding to conjugation lengths of three, five, seven, nine and eleven and the absorption edge at about 600 nm, suggesting that polyene sequences of up to 20 double bonds may be present in this block copolymer. The spectrum shows similar features to the spectrum for the 50-10-50 polynorbornene-*block*-polyacetylene-*block*-polynorbornene (21ene) in the work of Schrock and Krouse. The number 50-10-50 refers to the degree of polymerisation of the A-B-A blocks of the copolymer. We also observe a shift of the absorption peaks as an effect of the different solvents used.

Raman spectroscopy

In a conjugated trans polyene the carbon-carbon single and double bond stretches are Raman active. The conjugation length dependence of Raman scattering in a series of linear polyenes and the implications for polyacetylene have been studied by Schaffer and coworkers.[74] In that work it was observed that a linear decrease of the Raman shift occurs with the increase of the conjugation length. For linear polyenes the equation that describes this relationship is $\omega = (A+B/N)$ cm^{-1}, where N is the number of double bonds and ω is the wavelength of the Raman peak. For the carbon-carbon single bond stretch (R_1), they showed that A=1082 and B=476 while for the carbon-carbon double bond (R_2), A=1438 and B=830. Calculation based on these equations gives for N=20 a theoretical shift of 1106 cm^{-1} and 1480 cm^{-1} for R_1 and R_2 respectively.

The Raman spectrum of the A-B-A block copolymer prepared in this work, reproduced in Appendix 3.7, showed two peaks at 1106 cm^{-1} for the carbon-carbon single bond stretch (R_1) and at 1488 cm^{-1} for the carbon-carbon double bond stretch (R_2), which agrees with the calculated values and suggests an average conjugation length of 20 double bonds in the central block of the polymer has been achieved .

Infrared spectroscopy

The infrared spectrum of the A-B-A block copolymer was identical with that of pure poly(1-pentenylene) except for the introduction of two low intensity peaks at 1597 and 1556 cm^{-1} in the -CH=CH- stretching region which is consistent with the expected structure. The overlaid IR spectra of poly(1-pentenylene) and poly(1-pentenylene)-*block*-polyacetylene-*block*-poly(1-pentenylene) are shown in Appendix 3.8.

Gel Permeation Chromatography

A typical polymerisation of cyclopentene initiated with 1/400 equivalents $W(NAr)(CHC(CH_3)_3)(O^tBu)_2$ in $CHCl_3$ (concentration 3.8M based on monomer) at

-45°C for 4 hours gives Mn ≈ 21000 (relative to polystyrene standards calibration) (see Chapter 2) and a polydispersity index (Mw/Mn) of 1.1.

The gel permeation chromatogram for the A-B-A block copolymer shows a Mn of 36400 and a PDI of 1.2. and is illustrated in Appendix 3.9. Since the addition of 10 units of monomer B is not expected to alter significantly the Mn value, this result suggests that after the consumption of monomer B, which has been detected and confirmed by means of UV and Raman studies, the subsequent addition of 400 equivalents of monomer A to the reaction mixture yielded an A-B-A block copolymer. The addition of the last block of monomer A is not expected to follow the same kinetic pattern as the first block of monomer A since the "initiating" system is different. The tungsten vinylalkylidenes that may be present in the reaction system, as a result of the retro-Diels Alder reaction, are reported[3] to be less stable than their Mo analogues and therefore may effect the polymerisation of monomer A. However since the reaction was carried out at -45°C the retro-Diels Alder reaction was inhibited and therefore the tungsten vinylalkylidenes will be present in very low concentrations.

However, it is clear that the living polymerisation of cyclopentene in the conditions described above was followed by the polymerisation of 10 equivalents of 7,8-bis(trifluoromethyl)tricyclo[4.2.2.$0^{2,5}$]deca-3,7,9-triene as the B block (which after the retro-Diels Alder reaction gave rise to a polyene sequence of up to 20 double bonds) and although the addition of the last block of cyclopentene does not appear to be as well defined as that of the first block, it can be confirmed by GPC analysis and comparison with the results already discussed in Chapter 2.

Conclusions

The foregoing discussion shows that the required A-B-A block copolymer was produced, although, because of the uncertainties associated with the introduction of the second A block, the overall symmetry of the structure could not be guaranteed with confidence. The block copolymer was soluble in chloroform, toluene and heptane as initially produced, sadly during transport from the authors laboratory to

the Leeds Physics laboratory a solid film of the polymer became insoluble and so the intended investigation by our physicist colleagues was not carried out. The synthesis was difficult and the results described above were achieved after several unsuccessful attempts. On reflection there may be better approaches to the synthesis of the required A-B-A block copolymer and these are discussed in Chapter 6 which deals with suggestions for further work.

CHAPTER 4: A route to low polydispersity linear and star polyethylenes via ring opening metathesis polymerisation

4.1. Introduction

Living ROM is a controlled polymerisation reaction and in favourable circumstances can allow the construction of well defined macromolecular structures with a high level of precision. Linear homopolymers and block copolymers with narrow molecular weight distributions, star polymers and comb copolymers[75] have been prepared via ROMP.

In principle, linear, low polydispersity poly(1-pentenylene) can be used as the precursor to linear narrow molecular weight distribution polyethylene. At present polyethylene of low polydispersity is usually produced by the hydrogenation of 1,4-polybutadiene prepared by the anionic polymerisation of 1,3-butadiene. This approach inevitably results in polyethylene containing C_2 branches as a consequence of the small amount of 1,2 polymerisation which always occurs even in the best regulated 1,4-polymerisations of butadiene. Linear low polydispersity polyethylene is of interest for detailed studies of the physical behaviour of the material and consequently has always been an important synthetic goal. In this study we have investigated the possibility of using poly(1-pentenylene) as the precursor polymer to achieve this target.

Star structures, because of their finite size, are expected to resemble linear polymers rather more than networks; thus, for example, they are usually soluble in the same solvents as their linear analogues. However, their architectures have profound effects on their solid state physical and mechanical properties, and on their solution and melt properties.[80]

Highly branched polymeric structures have been synthesised[76] via ROMP by the addition of a few equivalents of the norbornadiene dimer (exo-trans-exo-pentacyclo[8.2.1.$1^{4,7}$.$0^{2,9}$.$0^{3,8}$]tetradeca-5,11-diene) to living polynorbornene. The living polymer was then cleaved from the metal in a Wittig-like reaction with

benzaldehyde. The scheme below illustrates some of the possible reactions in that system, which lead to a multibranched polynorbornene which has been described as a "star polymer".

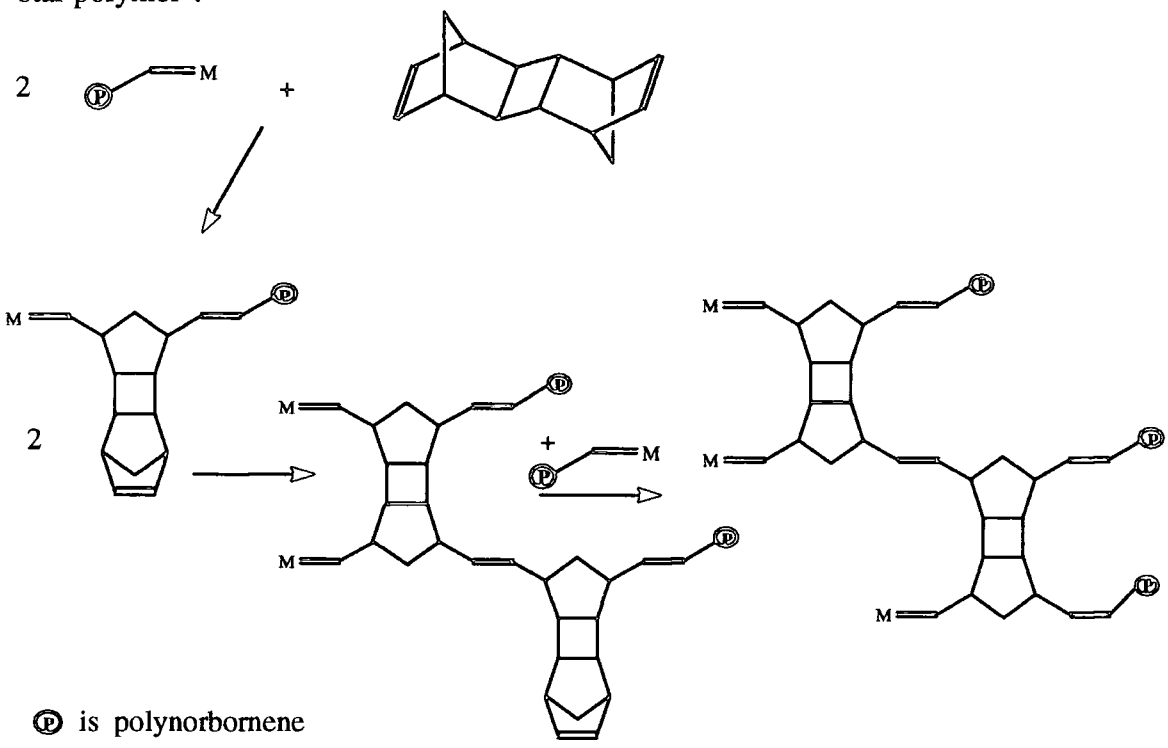

In this method of synthesis the number of branches is neither fixed nor predictable and it is dependent on various parameters, including reactant ratios, concentrations, temperature and probably on stirring and diffusion rates. In this chapter we describe an attempt to establish a well controlled method for the synthesis of star polymers via living ROMP.

4.2. Star poly(1-pentenylenes) and polyethylenes via living ROMP

Our route to star polyethylene via living ROMP is outlined schematically below, and it is advantageous compared to the method described in the previous section because both the number and length of the branches is defined. The first step is the preparation of living poly(1-pentenylene) as described in chapter 2.

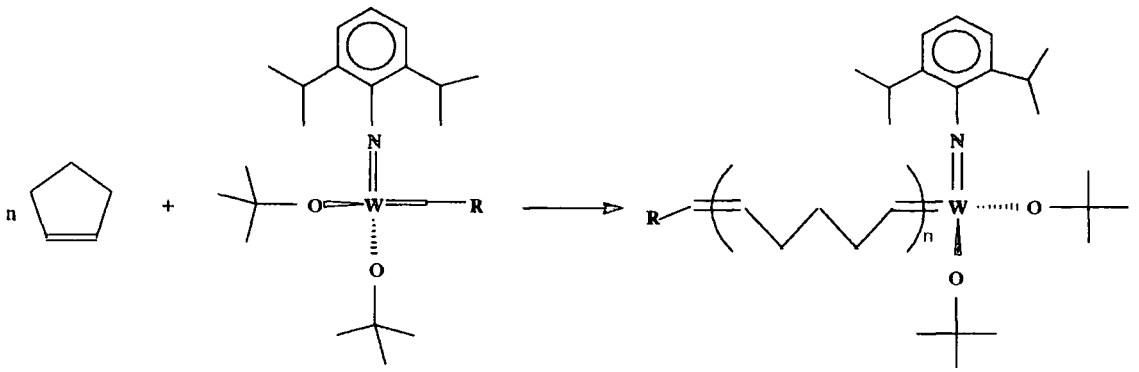

Living poly(1-pentenylene)

The ring opening metathesis polymerisation of cyclopentene at -45°C can give living polymers of narrow molecular weight distribution. The Wittig-like capping reaction of the living polymer chain-end with a monofunctional aldehyde, such as benzaldehyde, produces linear poly(1-pentenylene) (**I**), as illustrated below. The product can be obtained in high structural purity and with a narrow molecular weight distribution.

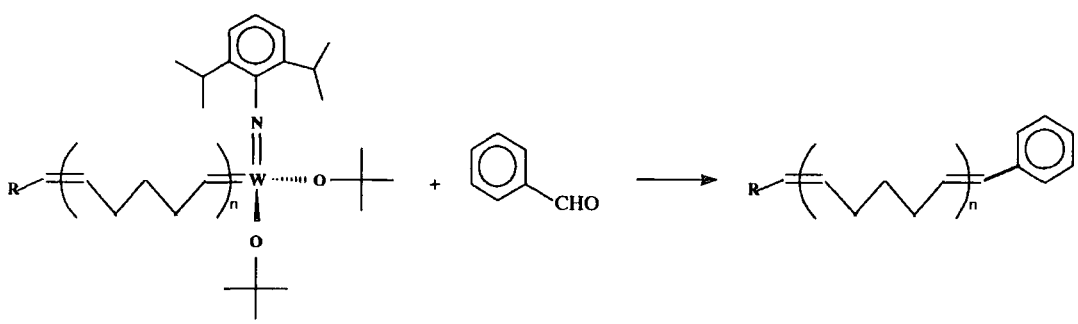

(I)

The introduction of difunctional or trifunctional aldehydes for the termination step, results in polymers which have, respectively, two and three times the molecular weight of the linear polymer produced when the reaction is terminated with benzaldehyde. This is a result of the capping reaction between the active chain-end species of the living polymer with each of the functional groups of these aldehydes. The structures arising from these reactions, are in the case of difunctional aldehydes a linear polymer with $M_n=2xM^L_n$ (**II**), while in the case of trifunctional aldehydes a structure with a localised core (benzene ring) from which three polymer chains or arms emanate, and $M_n=3xM^L_n$ (**III**), where M^L_n is the M_n of the living polymer just before the addition of the aldehyde, as shown in Figure 4.2.a.

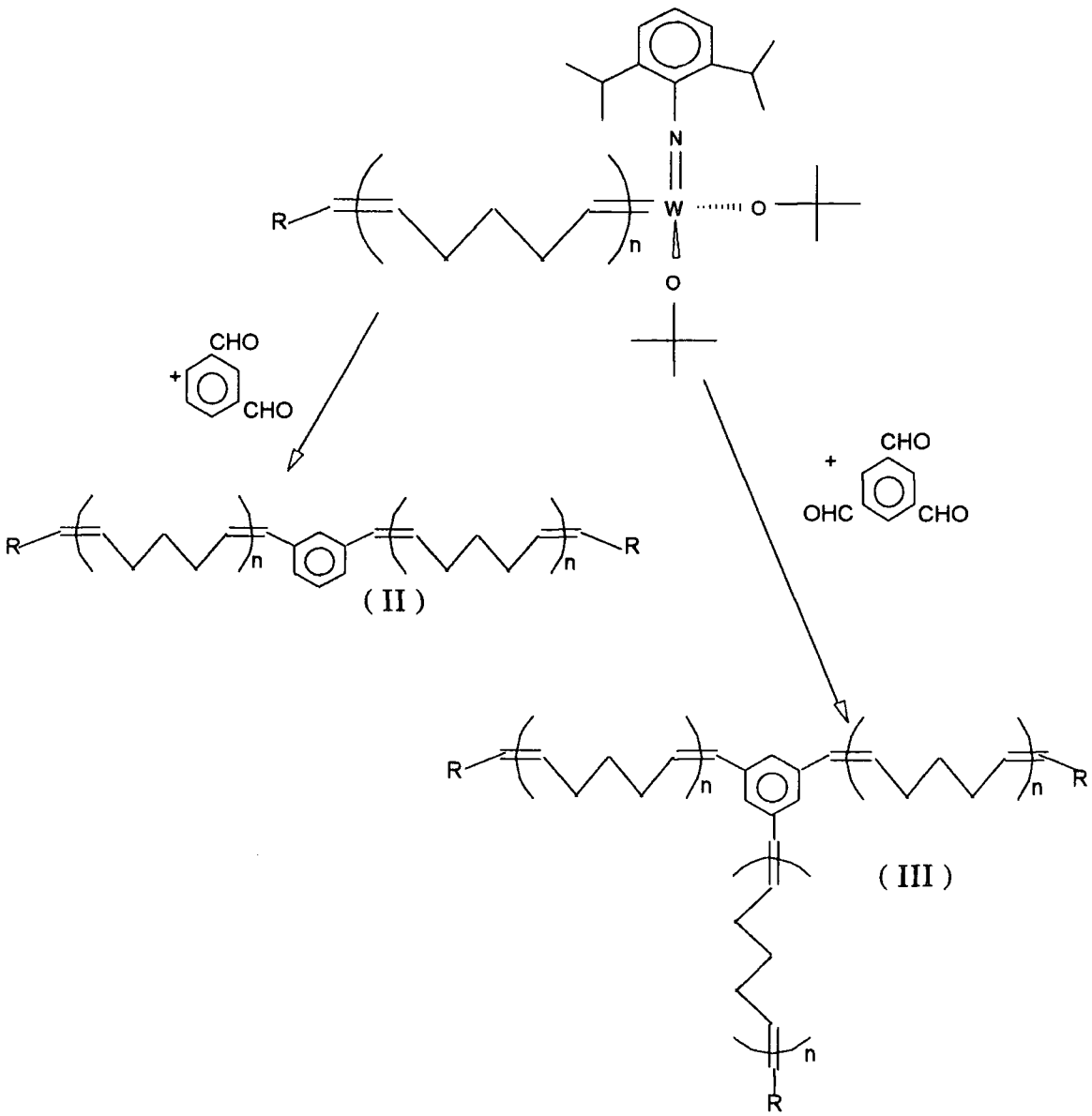

Figure 4.2.a Capping reaction between living poly(1-pentenylene) and multifunctional aromatic aldehydes

The resulting precursor polymers were soluble and were characterised by convensional GPC analysis of solutions in chloroform. The stationary phase was a polystyrene / divinylbenzene gel; a refractive index detector was used and the system calibrated with polystyrene standards. A correction factor of ≈ 0.4 was calculated (see chapter 2) for this system; this correction factor is in the same range as a previously reported correction factor for a similar polymer (poly(1-butenylene)).[44b,50,54] The

poly(1-pentenylene) linear and star precursor polymers were hydrogenated using excess *p*-toluenesulfonyl hydrazide to produce linear and star polyethylenes as shown in Figure 4.2.b, and described in detail below.

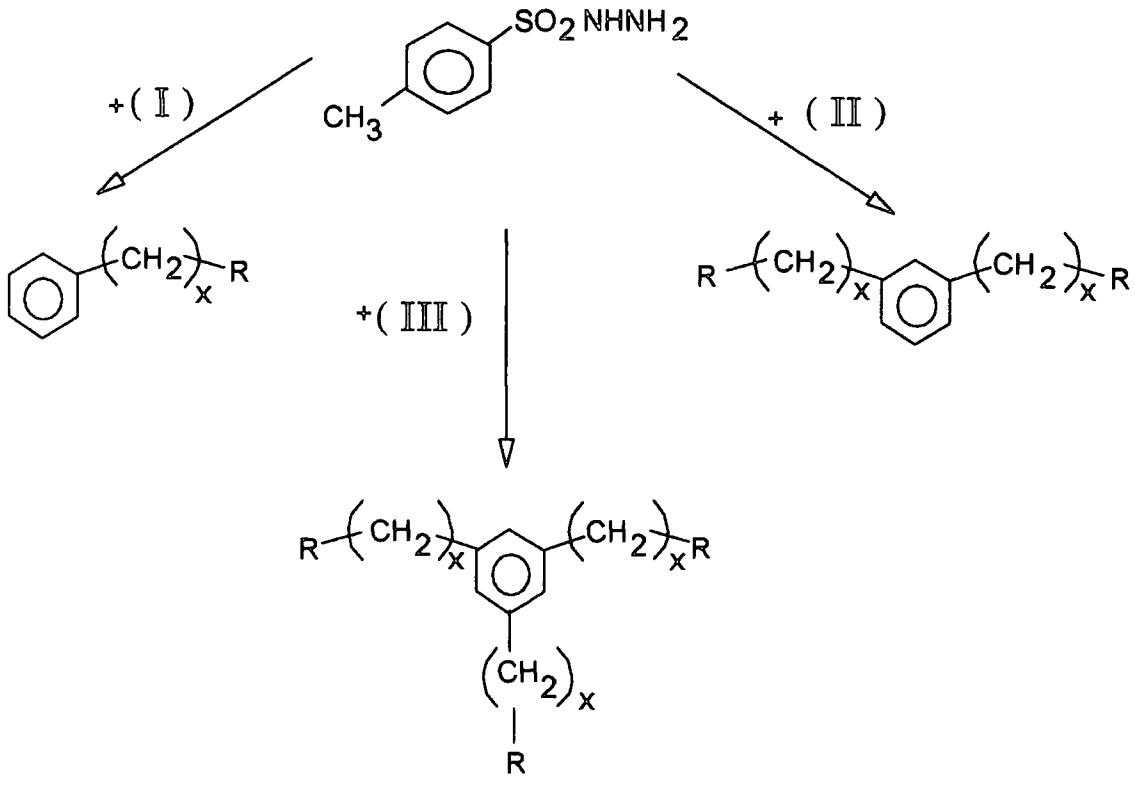

Figure 4.2.b Hydrogenation of the precursor poly(1-pentenylenes) to produce polyethylenes

4.3. Preparation and purification of difunctional and trifunctional aldehydes

Since the Wittig-like capping reaction is used to build these novel macromolecular structures, the structure and functionality of the capping reagent determines the architectures of the resulting polymeric structures. In this study we used benzaldehyde, isophthalaldehyde, glutaraldehyde and 1,3,5-benzenetricarboxaldehyde, to produce linear, "double" linear and "3-branched" star structures. The preparations of these materials for the capping reaction are described below, together with details of their purification and characterisation.

4.3.1. Purification of isophthalic dialdehyde and glutaraldehyde

Isophthalic dialdehyde (1,3-benzenedicarboxaldehyde) was purchased from Lancaster Synthesis and purified by recrystallisation from methanol. It was then sublimed and stored under dry, oxygen free nitrogen. The product was pure as judged by high resolution ^{1}H-NMR which displayed signals at 10.13 (2H, -CHO), 8.39 (1H, t J_{HH}= 1.6 Hz), 8.16 (2H, dd J_{HH}= 1.6 and 7.6 Hz) and 7.74 (1H, t, J_{HH}= 7.6 Hz) with a good S/N and no trace of other peaks except for those due to solvent.

Glutaric dialdehyde (50% solution in water, electron microscopy grade) was kindly provided by the University of Durham Biology department. It was extracted from the aqueous solution with diethyl ether and dried over $MgSO_4$. Diethyl ether was removed in a rotary evaporator and the residue was fractionally distilled to give pure glutaric dialdehyde.The ^{1}H-NMR spectrum showed signals at 9.72 (1H, -CHO), 2.49 (2H, -CH_2-, t J_{HH}= 7.0 Hz) and 1.89 ppm (1H, quintet J_{HH}= 7.0 Hz) with a good S/N and no trace of impurities. The product was then stored under dry, oxygen free nitrogen at -40°C.

4.3.2. Preparation of 1,3,5-Benzenetricarboxaldehyde

The synthesis of 1,3,5-benzenetricarboxaldehyde was based on previously reported work,[77-79] and the path followed is shown schematically below. Previous workers reported m.p., ^{1}H NMR and IR spectra for this compound. In this work we have characterised the sample using ^{1}H and ^{13}C NMR with high S/N in order to estimate the purity attained.

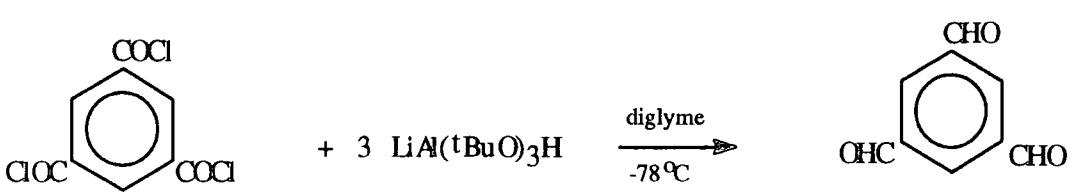

The reduction of 1,3,5-benzenetricarbonyl chloride using lithium aluminium tri-tert-butoxyhydride, in diglyme at -78°C, produced 1,3,5-benzenetricarboxaldehyde in 56% yield, see experimental later in this section.

Characterisation

The samples were dissolved in $CDCl_3$ and NMR spectra were recorded at 199.975 MHz for ^{1}H-NMR and 50.3 MHz for ^{13}C-NMR. The major signal shifts, intensities and assignements are recorded in the tables below and are consistent with the expected structure.

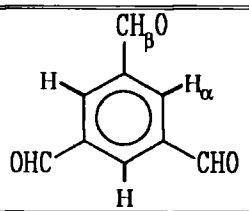	^{1}H-NMR of 1,3,5-benzenetricarboxaldehyde in $CDCl_3$		
Proton	**Shift (ppm)**	**Multiplicity**	**Integral**
α	8.65	singlet	1
β	10.21	singlet	1

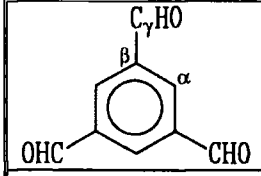	^{13}C-NMR in $CDCl_3$
Carbon	**Shift (ppm)**
α	134.8
β	137.8
γ	189.8

However in is clear from the spectra recorded in Appendices 4.1. and 4.2 that there are minor peaks present at 10.20 (Aryl CHO), 8.85 (d, Aryl H) and 8.74 ppm (d, aryl H) which, although reduced in intensity by repeated recrystallisation and sublimation, could not be entirely eliminated. These signals are consistent with the presence of a partially reduced material in which there are two aldehyde units and one residual carbonyl chloride and in support of this hypothesis a shoulder can be seen at the high frequency side of the carbonyl absorption in the IR spectrum (Appendix 4.3). Although these data are not good enough to make an unambiguous assignment of the

impurity's structure, it is reasonable to propose as a working hypothesis that there is a difunctional aromatic aldehyde present in this material. Careful expansion and analysis of the ^1H NMR spectrum indicates that if this hypothesis is true, the difunctional aromatic aldehyde is present to the extend of ca. 15 mole %. Although it was disappointing not to get a higher level of purity it was decided to use this material in subsequent capping experiments.

Infrared data

The major peak in the infrared spectrum obtained on KBr disc (Appendix 4.3) were assigned as follows: 3369 cm^{-1} C=O overtone, 3061 cm^{-1} C-H aromatic, 2871 cm^{-1} O=C-H, 1695 cm^{-1} C=O, 1594 cm^{-1} C=C aromatic,1454 and 1377 cm^{-1} skeletal vibrations which are consistent with the proposed structure.

Mass Spectroscopy

The Electron Impact (EI+) mass spectrum (Appendix 4.4) showed the molecular ion at m/e 162 (99.78 %) with the expected base peak at m/e M-1 mass units. Other peaks of high intensity occured at 133 $[C_6H_3(CHO)_2]^+$, 105 $[C_6H_4(CHO)]^+$. There was no indication of chlorine bearing species in the mass spectrum and consequently no support for our hypothesis concerning the nature of the impuriy. The small peak at m/e 177 (i.e.M+15) may possibly be indicative of a trace of oxidised product.

Experimental

$LiAl(tBuO)_3H$ (8.6g, 0.034 moles) was dissolved in diglyme (100 ml) in an ampoule. 1,3,5-Benzenetricarbonyl chloride (3g, 0.0113 moles) was also dissolved in diglyme (100 ml) in an ampoule and then cooled down to -78°C (acetone-dry ice bath). The $LiAl(tBuO)_3H$ solution was added dropwise to the 1,3,5-benzenetricarbonyl chloride solution with stirring in order to avoid any major temperature rise. The solution colour turned from white to orange-red. After the completion of the addition the cooling bath was removed and the mixture allowed to warm to room temperature.

The mixture was poured onto crushed ice and the white solid which precipitated was extracted with hot ethanol, the solvent was removed using a rotary evaporator and the crude product was purified by several recrystalizations from acetone, followed by sublimation to give 1,3,5-benzenetricarboxaldehyde (m.p. 155°C, yield 56 %). The product was stored under dry, oxygen free nitrogen.

4.4. Preparation of living polypentenamer

The polymerisation of cyclopentene (described also in Chapter 2), initiated by W(CH-t-Bu)(NAr)(O-t-Bu)$_2$ at -45°C, exhibits characteristics of an ideal living polymerisation; i.e. well defined kinetics, linear increase of molecular weight with percent monomer conversion, irreversible propagation steps, the absence of chain termination and transfer steps and the rate constant of initiation is greater than that of propagation.

The same apparatus, techniques and conditions were used for the first step of the preparation of linear and star polyethylenes. The **general experimental procedure** for the preparation of poly(1-pentenylenes) is outlined below and is also discussed in Chapter 2. In the Glove Box the reaction vessel, shown left, was loaded with the initiator solution (0.029g, 0.049 mmoles in 2 ml $CHCl_3$) and a stirrer bar in compartment B and the monomer solution (1g, 0.0147 moles in 2 ml $CHCl_3$) in compartment A. It was then sealed, taken out of the box, connected to the vacuum/N_2 line and put into a cooling bath at -45°C. The solutions were allowed to cool for 1/2 hour and then the Young's valve that separates the two compartments was opened and the two solutions allowed to mix. After the required polymerisation time had elapsed, one of the Young's valves was removed under a strong positive flow of N_2 and

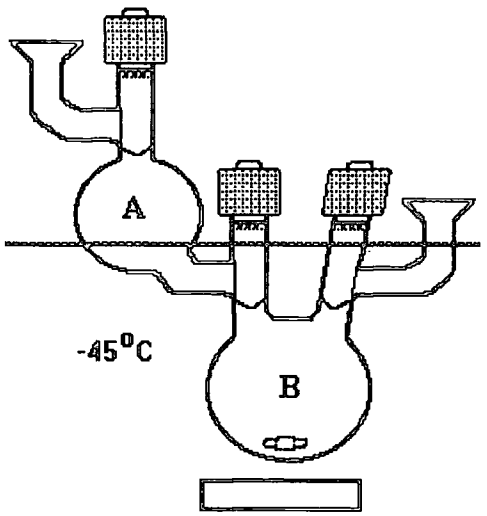

replaced with a suba seal. The quenching agent solution was added via cannula transfer under N_2, and the reaction mixture was stirred for a further 2hrs at -45°C. The use of this apparatus reduced the possibility of contamination and also any major temperature rises during the transfer of the monomer and aldehyde solutions.

4.5. End capping reactions

The following experiment was designed to study the effect of different aldehydes as the capping agent. In the Glove Box three identical reaction vessels (see above) were loaded with the same amounts of monomer and initiator solutions. The monomer concentration was 3.8M in $CHCl_3$. The solutions were allowed to react at -45°C and after 3 hours benzaldehyde added to the first ampoule, isophthalaldehyde to the second and 1,3,5-benzenetricarboxaldehyde to the third; the solutions were left to react for an additional 45min. After recovery by precipitation from chloroform into a ten fold excess of methanol and drying the yield of (I) after 3 hours reaction time was found to be 44% while (II) and (III) under the same conditions gave 56 and 55% yields respectively (see Figure 4.2.a and text in section 4.2 for definition of (I), (II) and (III).

GPC data

These polymers were soluble and were characterised by GPC, using PL_{gel} columns and an RI detector; the results are shown in Table 4.5.

Poly(1-pentenylene) capped with:	M_n	M_w	PDI	DP
Benzaldehyde (I)	23360	26800	1.15	340
Isophtalaldehyde (II)	40220	62167	1.55	590
1,3,5-Benzene tricarboxaldehyde (III)	67900	109209	1.61	998

Table 4.5 Raw uncorrected data for polymers (I),(II) and (III), relative to polystyrene standards calibration.

These materials were all obtained by capping living polypentenamer with aromatic aldehydes after 3 hours reaction. Earlier studies have established that at this stage we have a narrow polydispersity but incomplete consumption of monomer. If the reaction is allowed to proceed to completion (ca. 24 hours at -45°C, see Chapter 2) there is inevitably some broadening of the molecular weight distribution, so quenching at 3 hours was selected as the optimum time. The values quoted in the table are uncorrected, but since we are only concerned with the relative molecular weight and polydispersities of materials obtained by quenching with capping agents of different functionalities this is not important. The GPC traces reproduced here (full details are shown in Appendix 4.5) show a narrow peak for the mono-capped linear poly(1-pentenylene) (I) while the peak for the di-capped (II) is clearly bimodal, apparently corresponding to partially and completely reacted dialdehyde and the peak for the star poly(1-pentenylene) (III) appears to be broad but symmetrical. It is clear that capping the living poly(1-pentenylene) with excess benzaldehyde gives the well defined narrow polydispersity polymer (I) as expected. To make the doubled and tripled molecular weight polymers (II) and (III) requires exact stoichiometric balance between the aldehyde and the living chain ends and it is clear that for bimodal polymer (II) this was not fully realised. It is clear from the trace reproduced here that the low molecular weight peak corresponds to singly capped polymer and the second peak is the anticipated dimer. There are several possible reasons for this outcome; these experiments were conducted on a small scale and weighing with precision in a Glove Box is difficult, which may have lead to inaccurate stoichiometric balance; the capping reagent may not have been completely soluble at the temperature of reaction and it is also possible that the

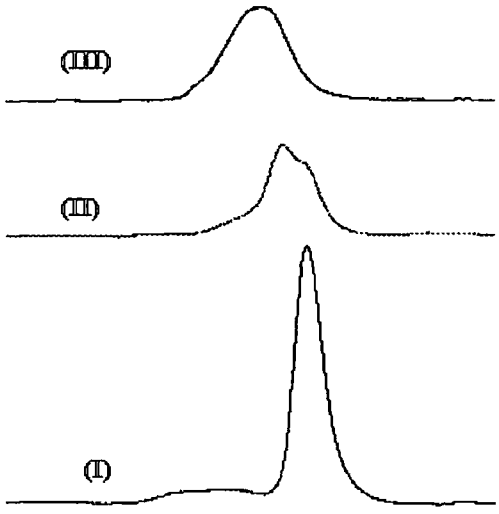

duration and mixing efficiency at the capping stage was inadequate for the purposes of these experiments.

The three branched polymer showed a symmetric but broad GPC peak and it is clear that in this case there is essentially no monocapped polymer present. In theory the complete linking of arms into stars with constant functionality (*f*) leads to narrowing of the molecular weight distribution according to the equation below.[80]

$$(Mw/Mn)_{star} = 1 + [\,(Mw/Mn)_{arm} - 1\,] / f$$

Thus if ideal behaviour had been attained we should have a PDI value of 1.05; however as disscused above we know that the capping agent was impure and probably contaminated with a difunctional aldehyde to the extent of ca.15 mole %. It is therefore reasonable to assume that the broadening of the molecular weight distribution in this case is partly due to the presence of this impurity, as well as due to the reasons already discussed for the case of the difunctional aromatic aldehyde.

Nevertheless if we consider simply the Mn's for (I), (II) and (III) in Table 4.5, it is clear that, although imperfectly accomplished, the process outlined in Figure 4.2.a has been realised. Optimisation to produce perfect well defined stars would require both more materials and more time than was available to the author.

NMR data

The ^{1}H-NMR and ^{13}C-NMR spectra of linear and star poly(1-pentenylene) were identical. The spectra for the star polymer are reproduced in Appendices 4.6 and 4.7 and the peak assignements are tabulated overleaf.

Carbon	Shift (ppm)
Cv t	130.35
Cv c	129.85
Cα tc	32.23
Cα tt	32.09
Cα cc	26.91
Cα ct	26.77
Cβ cc	29.87
Cβ ct/tc	29.72
Cβ tt	29.57

^{13}C-NMR data

Proton	Shift (ppm)
Ho	5.38
Hα (cis)	2.03
Hα (trans)	1.98
Hβ	1.39

^{1}H-NMR data

The chain-end groups are not expected to be detected in the NMR spectra since the chains we examine here are too long to permit such an observation.

Thermogravimetric analysis

Samples of linear and star poly(1-pentenylene) showed the same TGA pattern, with a 2% weight loss at 360°C and maximum weight loss at 480°C as shown in Appendix 4.8.

4.6. Other poly(1-pentenylenes) prepared using similar techniques

Other experiments that yielded precursor poly(1-pentenylene) of various molecular weights and architectures are described in this section. The molecular weight distribution of poly(1-pentenylene) was controlled by changing the initiator : monomer ratio and the reaction times.

The experimental techniques and apparatus used were the same as disscussed in the previous section; the experimental conditions and the resulting polymers are presented briefly below.

4.6.1. Linear poly(1-pentenylenes)

The polymerisation of cyclopentene, as discussed earlier in this chapter, was followed by the addition of the appropriate aldehyde to give linear structures with the following characteristics:

Polymer	Ratio monomer: initiator	Polymerisation reaction time	Aldehyde	Mn	Mw	PDI
(IV)	1000 : 1	24 hrs	benzaldehyde	124000	140100	1.13
(V)	600 : 1	5 hrs	glutaraldehyde	61500	94500	1.5

The GPC trace of polymer (IV), as recovered after precipitation from chloroform into excess methanol and drying, is illustrated below (trace $(IV)_1$), and shows a narrow main peak corresponding to the expected linear polymer and a broader peak

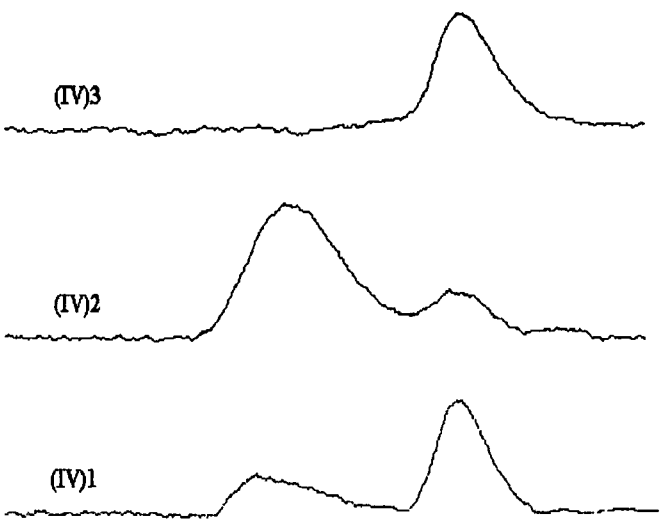

corresponding to polymer of about 10-14 times this molecular weight. This higher molecular weight material may be the product of some kind of cross linking between the polymer chains and it can be easily separated from the lower molecular weight material by fractionation. The GPC traces obtained after fractionation of polymer (IV) are also illustrated here, where trace $(IV)_2$ shows the high molecular weight, broad polydispersity fraction and trace (IV)3 shows the low molecular weight, narrow polydispersity fraction (see also Appendix 4.9). Fractionation was achieved by dissolving the polymer in chloroform, transferring the solution into a separating funnel, and slowly adding methanol until the solution was cloudy. The separating

funnel and contents were then warmed up until the solution was clear again and left to equilibrate at room temperature for 24 hrs. The high molecular weight fraction came out of solution in the top layer, while the low molecular weight fraction stayed in solution. The low molecular weight fraction was separated, the volume of solvent was reduced by evaporation and the polymer was recovered by precipitation into excess methanol and dried under vacuum.

Polymer (Ⅴ) was formed after the capping reaction between the living polymer chains and 1/2 equivalent of glutaraldehyde. A characteristic of this system is that the resulting polymer is a linear poly(1-pentenylene) with 2n+1 repeat units in the chain and identical (R) chain ends as shown schematically below.

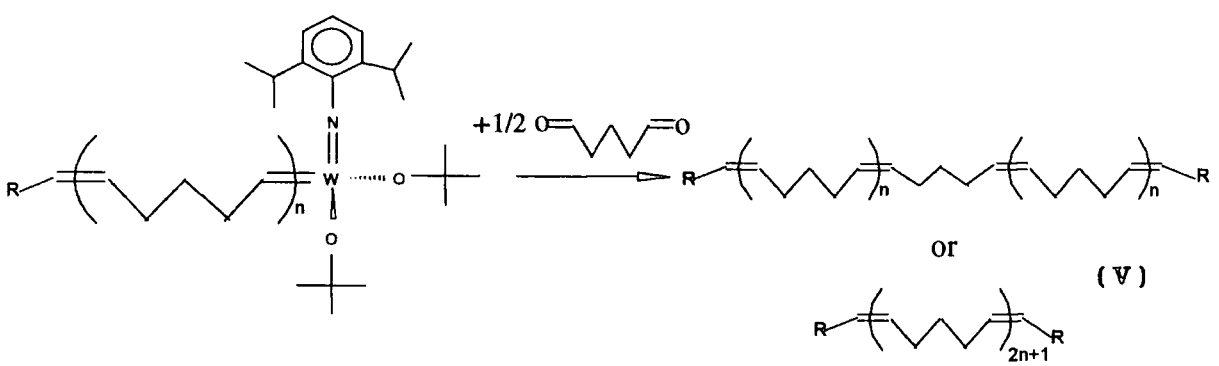

Cyclopentene (600 equivalents, 0.0147 moles, 1g) was polymerised at -45°C using W(CH-t-Bu)(NAr)(O-t-Bu)$_2$ (0.0245 mmoles, 14 mg) as the initiator and an aliquot was taken out of the reaction vessel after 5hrs. The GPC analysis of this aliquot showed Mn=33800, Mw=37200 and PDI=1.1. A solution of 1/2 equivalent of glutaraldehyde (0.0122 mmoles, 1.2 mg) in 1 ml $CHCl_3$ was prepared in the Glove Box and sealed under N_2. It was then taken out of the box, cannula transferred under N_2 into the living polymer solution at -45°C, just after the first aliquot was taken out, and allowed to react for 1.5 hrs.

The GPC analysis on the final product showed Mn=61500, Mw=94500 and PDI=1.5.

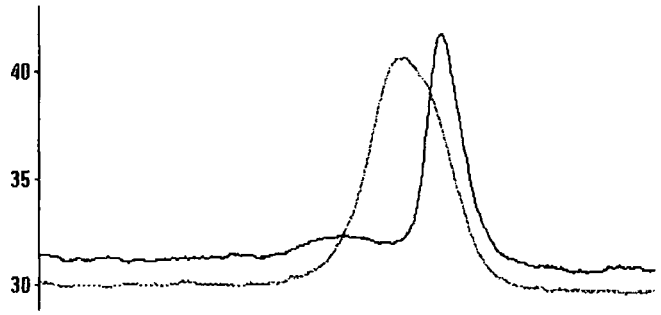

It is clear that the Mn value is double that of the living polymer just before quenching. However, the overlaid GPC traces (also Appendix 4.10) suggest the presence of polymer chains that did not double their molecular weight, an expected result in this case because glutaraldehyde was in slight excess after some living polymer was removed from the reaction vessel for analysis. The presence of these monocapped polymer chains in the solution has as a result the broadening of the molecular weight distribution. Exact stoichiometry in this case should lead to well defined narrow polydispersity linear polypentenylene.

4.6.2. Star poly(1-pentenylenes)

Three-branched star structures with various molecular weights have also been synthesised. The reaction conditions and the GPC results are summarised in the table below. The GPC traces are shown in Appendix 4.11 for polymer (VI) and in Appendix 4.12 for polymer (VII).

Polymer	Ratio monomer: initiator	Polymerisation reaction time	Aldehyde	Mn	Mw	PDI
(VI)	600 : 1	4 hrs	trialdehyde[1]	53000	78000	1.5
(VII)	600 :1	20 hrs	trialdehyde[1]	95300	147000	1.5

[1] 1,3,5-Benzenetricarboxaldehyde

The results described above demonstrate that control over the molecular weight can be achieved by variation of the monomer to initiator ratio and the polymerisation reaction times as discussed in previous sections.

4.7. Hydrogenation of poly(1-pentenylene) derived structures to give linear, narrow molecular weight distribution polyethylene and star polyethylenes

The hydrogenation of linear low polydispersity poly(1-pentenylene) using p-toluenesulfonylhydrazide is expected to yield linear polyethylene with approximately the same molecular weight and molecular weight distribution. The same considerations apply to poly(1-pentenylenes) with different topologies, they will presumably maintain their architectures, chain lengths and molecular weight distributions after the hydrogenation. The resulting polyethylenes were not soluble in $CHCl_3$ or THF and GPC analysis of these samples was not possible with systems available to the author.

IR analysis

Infrared spectroscopy can provide information about the presence of residual double bonds in the polymer after hydrogenation. Solvent (hot p-xylene) cast films of the resulting polyethylenes were used for these experiments. The overlaid spectra of the precursor poly(1-pentenylene) and the resulting polyethylene show complete conversion (see Appendix 4.13). The peaks at 1654 cm^{-1}(C=C stretch), at 966 cm^{-1} (=C-H trans out of plane bend) and at 3004 cm^{-1} (=CH stretch) visible in the poly(1-pentenylene) spectrum do not appear in the spectrum of the hydrogenated polymer. The spectrum of the resulting polyethylene consists only of the peaks at 2922 cm^{-1} and 2852 cm^{-1} (antisymmetric and symmetric CH_2 stretch), at 1455 and 1437 cm^{-1} (CH_2 bend), at 721 cm^{-1} (CH_2 rock), as well as of weak absorption peaks in the region around 1000-1300 cm^{-1}.

Differential Scanning Calorimetry data

The linear and star polyethylenes were studied using a Perkin-Elmer DSC 7 instrument, to determine their melting points and their degrees of crystallinity. The melting process appears as an endothermic peak on the *heat flow* vs. *temperature* plot. The melting point is reported both as the onset value which is found by drawing a line through the steepest point on the forward edge of the melting peak and extrapolating it to the temperature axis, and as the value of the peak on the temperature axis at the point of maximum intensity. The percentage degree of crystallinity (*% dc*) is based on

$$\%dc = \frac{\Delta H}{\Delta H^0} \times 100$$

the heat of fusion measurement, which is defined as the area under the endotherm and described by the above equation. Where ΔH is the heat of fusion for the observed polymer and ΔH^0 is the heat of fusion of the 100% crystalline polymer. For the linear and star polyethylenes studied here the *% dc* was calculated assuming a heat of fusion ΔH^0 of 293 J/g[81,82] for 100% crystalline PE. The melting points of the linear and star PE's appear to be in the same range and they are tabulated below.

Melting points and % crystallinity for **star** polyethylenes produced in this work:

Mn*	**Mw***	**PDI***	**T_m max °C**	**T_m onset °C**	**Crystallinity** *dc (%)*
49800	70600	1.42	129.2	124.3	46 (App.4.14)
62800	97000	1.54	131.1	123.1	59 (App.4.15)
95300	147000	1.54	131.1	124.4	56 (App.4.16)

Melting points and % crystallinity for **linear** polyethylenes produced in this work:

Mn*	**Mw***	**PDI***	**T_m max °C**	**T_m onset °C**	**Crystallinity** *dc (%)*
21640	23020	1.06	129.7	126.2	58 (App.4.17)
124000	140100	1.13	120.3	111.6	25 (App.4.18)

*Values for the precursor monomers

The melting range of these polymers is within the range expected for linear polyethylene produced by classical Ziegler chemistry. The broader the molecular weight distribution the broader the melting range appears to be. The results for the higher molecular weight linear polyethylene are clearly somewhat anomalous, indeed the sample was subjected to prolonged solvent extraction to see if there was a removable impurity (e.g. residual hydrazide or biproduct) and the IR spectrum was scrutinised for traces of residual double bonds; in neither case was any evidence for impurity or structural defect detected but their presence at an undetectable level may be sufficient to account for the T_m lowering observed.

4.7.1. Experimental

The hydrogenation of the precursor polypentenylenes was achieved after treatment with p-toluenesulfonyl hydrazide.[83,84] In a typical experiment, poly(1-pentenylene) (1g, 0.015 repeat unit moles) was dissolved in 150 ml p-xylene in a 250 ml 2-neck rbf and heated in an oil bath at 120°C while stirring. p-Toluenesulfonyl hydrazide (22.3 g, 0.12 moles, 8x excess) was added, and the solution was left to stir for 2 hrs. The hot solution was added slowly to excess methanol and polyethylene precipitated as white powder. Methanol was removed via a filter cannula and the PE powder was dried under vacuum for several hours. Recovered polymer 0.98g (98% yield).

4.8. Conclusions

The polymerisation of cyclopentene using W(CH-t-Bu)(NAr)(O-t-Bu)$_2$ as the initiator can produce narrow molecular weight distribution linear living poly(1-pentenylene), which, after quenching with the appropriate aldehyde, yields poly(1-pentenylenes) with the expected structures and appropriate multiples of the initial molecular weight. If exact stoichiometry can be achieved this should lead to structures with narrower molecular weight distributions than the linear starting polymer; although the general principal was demonstrated, the molecular weight distribution narrowing was not observed in this work probably as a result of not

obtaining precise stoichiometry control in rather small scale reactions and in not obtaining 100% pure capping agents. Hydrogenation of these polymers produces the corresponding polyethylenes. Linear polyethylenes with PDI≈1.04 and star polyethylenes have been prepared via this route.

CHAPTER 5: An investigation of routes to well defined difunctional ROMP initiators - a possible route to polyethylene networks

5.1. Introduction

The preparation of star polyethylenes via ROMP using the end capping reaction is described in Chapter 4. The same principal, involving a trifunctional aldehyde as the capping reagent, when applied to poly(1-pentenylene) with two living ends, one at each end of the polymer chain would ideally give rise to a well-defined polyethylene network as shown schematically below.

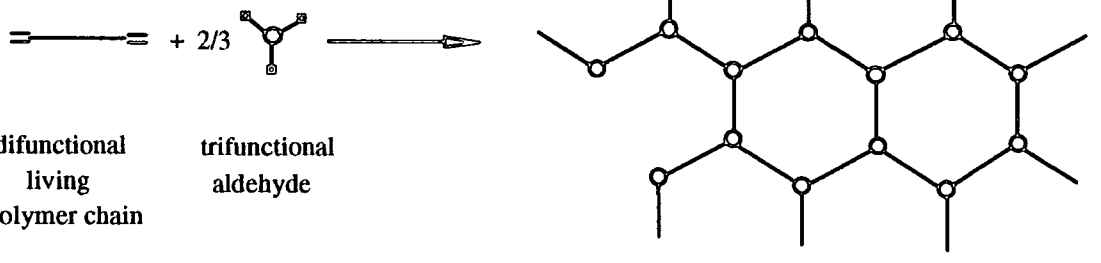

difunctional living polymer chain

trifunctional aldehyde

well defined network

Since poly(1-pentenylene) with narrow molecular weight distributions can be prepared, the distance between the network junctions would, at least in principle, be closely defined. Of course this is an idealised two dimensional picture; entanglements, free ends and loops are the inevitable consequence of the statistics of assembling a network consisting of flexible chains coupled to network junctions in this way. It is obvious from the above that the preparation of a difunctional initiator has to be the first step towards the synthesis of such networks. A titanium based difunctional initiator has already been prepared, characterised and used for the ROMP of norbornene but it is not active enough to initiate the polymerisation of cyclopentene.[38,42,85]

5.2. A "blocked chain-end reactivity" approach to difunctional ROMP initiators.

It is known from the literature that the attempted ROMP of 7-isopropylidene-2,3-dicarbomethoxynorbornadiene initiated by the molybdenum based Schrock initiator, shown below, resulted only in the formation of the first insertion product, which was isolated and characterised by X-ray crystallography.[39] The first insertion product would not polymerise this monomer further, probably for steric reasons since the isopropylidene unit in the 1:1 adduct is close to the molybdenum atom and hinders approach by this bulky monomer. It would however initiate the polymerisation of norbornene which is less sterically hindered and probably a better π-donor.

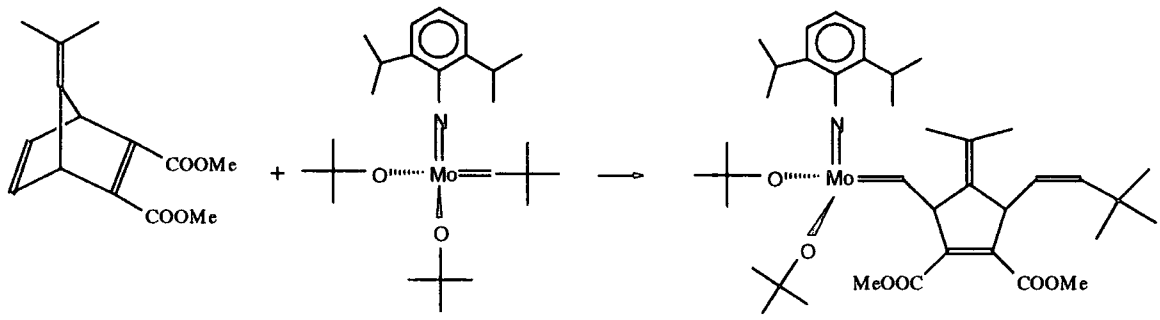

The preparation of the difunctional analogue of 7-isopropylidene-2,3-dicarbomethoxy norbornadiene (see section 5.2.2 below) and its subsequent ROMP, could be a route to the difunctional initiator required, if the reaction yields only the first insertion product. The first step towards this preparation is the synthesis of the corresponding difulvene, which can then undergo Diels-Alder reaction with dimethyl acetylenedicarboxylate to yield the required norbornadiene dimer (structure **(2)**, section 5.2.2).

5.2.1. Preparation of 1,4-cyclohexanedicyclopentadienylidene (1)

Pyrrolidine has been proved to be a very effective reagent to promote fulvene formation between cyclopentadiene and a number of ketones and aldehydes.[86]

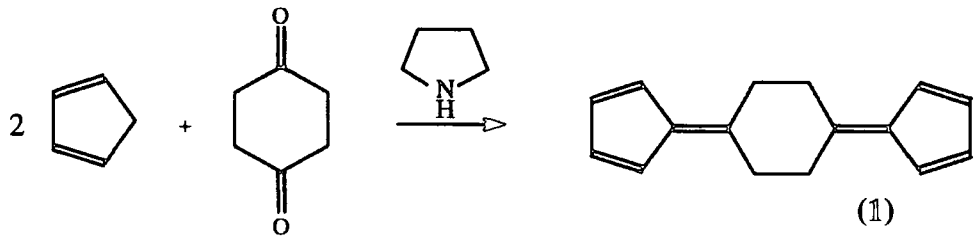

(1)

In this experiment two equivalents of cyclopentadiene were allowed to react with 1,4-cyclohexanedione, in the presence of pyrrolidine, with methanol as the solvent, to give 1,4-cyclohexanedicyclopentadienylidene (1). The experimental procedure is described in detail later in this chapter.

NMR data

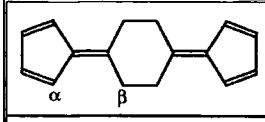	^{1}H-NMR spectrum in $CDCl_3$ at 399.952 MHz		
Proton	**Shift (ppm)**	**Multiplicity**	**Integral**
α	6.57	multiplet	1
β	2.91	singlet	1

The ^{1}H-NMR spectrum of the product showed one peak for the -C<u>H</u>$_2$- protons at 2.91 ppm, and a multiple peak from 6.52 - 6.62 ppm, for the =C<u>H</u>- protons. The spectrum is shown in Appendix 5.1.

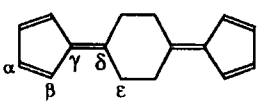	^{13}C-NMR spectrum in $CDCl_3$
Carbon	**Shift (ppm)**
α	131.7
β	120.1
γ	140.6
δ	153.2
ε	33.6

The proton-decoupled ^{13}C-NMR, shown in Appendix 5.2, showed five signals, for the five non-equivalent carbons C_α to C_ε. The assignments are based on the chemical shifts, relative intensities of the peaks and the literature values for dimethyl fulvene.[87] The peak at 33.6 ppm corresponds to the CH_2 carbons, the peaks at 153.2

and 140.6 are of low intensity and are assigned to the quartenary carbon atoms; according to the literature, they are assigned to δ and γ carbons respectively. The remaining two peaks at 131.7 and 120.1 ppm are assigned to carbons α and β respectively.

IR data

The IR spectrum, shown in Appendix 5.13, showed peaks at 3099 and 3066 cm^{-1} which were assigned to the C_{sp2}-H stretch. The peaks from 2971 to 2838 cm^{-1} were assigned to the CH_2 stretch, the peak at 1642 cm^{-1} to the C=C stretch, the peak at 775 cm^{-1} to the out of plane CH bend and the peak at 727 cm^{-1} to CH_2 rocking. The IR spectrum corresponds to the proposed structure. The model compound, 6,6-pentamethylenefulvene, has been reported[86] to give peaks at 3100, 3070, 2930, 2855, 1638, 1370, 1348, 856, 762, 680, and 605 cm^{-1}.

Mass Spectroscopy data

The Electron Impact (EI+) spectrum showed the base peak at m/e 208 which corresponds to the parent ion. Other peaks at m/e 193 $[M-CH_3]+$, 77 $[C_6H_5]+$ and 65 $[C_5H_5]+$ (cyclopentadienyl cation). The Chemical Ionisation (CI+) spectrum showed the base peak at m/e 209 [M+1] and other very low intensity peaks which were not assigned. The spectra are reproduced in Appendix 5.14.

Experimental:

Reagents:

Cyclopentadiene was freshly prepared by thermal cracking of dicyclopentadiene[88] which was purchased from Aldrich.

Pyrrolidine was purchased from BDH and freshly distilled under nitrogen.

1,4-Cyclohexanedione was purchased from Aldrich and was purified by recrystallisation from toluene.

Procedure:

1,4-Cyclohexadione (3 g, 0.027 moles) was put in a 2-necked round bottom flask and dissolved in methanol (26 ml). Cyclopentadiene (7 g, 0.054 moles) was added and the resulting clear solution was stirred under nitrogen. Then pyrrolidine (2.9 g, 0.041 moles) was added and the solution turned first yellow, then brick-red. After about 3 minutes solid began to precipitate out of solution. The mixture was stirred for 30 min and then acetic acid (2.7 g, 0.045moles) was added. Diethyl ether and distilled water were added to the mixture and then it was placed into a separating funnel. The organic layer was separated and the aqueous layer was extracted twice with diethyl ether. The combined organic extracts were washed with brine, separated and then dried over $MgSO_4$. The solvent was removed using a rotary evaporator and the orange-red solid (1.83 g, 0.088 moles) was collected and dried under vacuum. Yield 33%.

5.2.2. Synthesis of the Diels -Alder adduct with dimethyl acetylenedicarboxylate

The Diels-Alder reaction between (1) and slightly over two equivalents of dimethyl acetylenedicarboxylate in toluene, yielded the adduct (2). The procedure followed was similar to that established for the preparation of 7-isopropylidene-2,3-dicarbomethoxynorbornadiene[89] and it is described in detail later in this chapter.

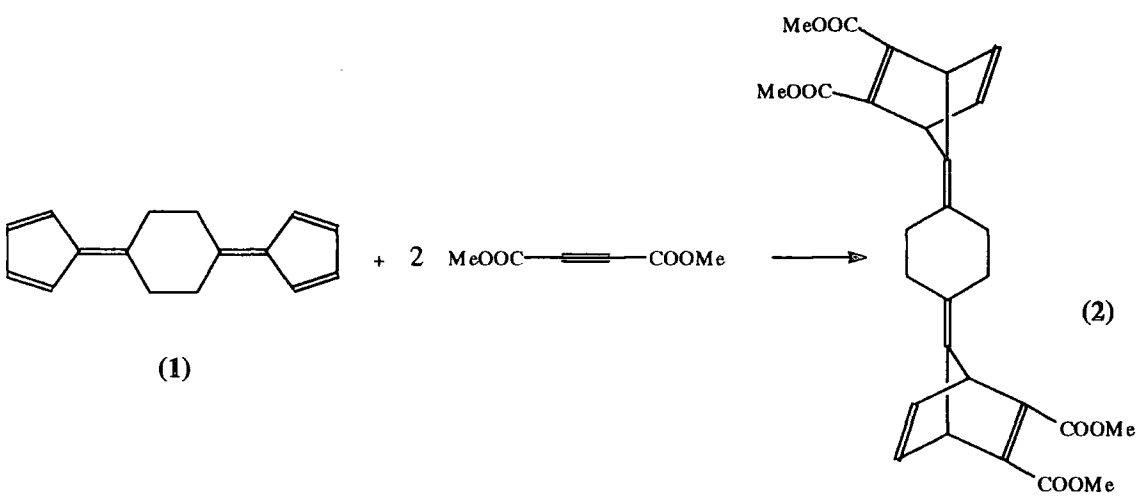

(1) (2)

While attempting to observe the m.p. of the product, the colour of the compound turned from light yellow to brick red, at 230°C, possibly as a result of the retro-Diels-Alder reaction.

NMR data

The α and β protons, as shown below, form an AA'XX' system and generate a complicated splitting pattern due to long range coupling. $J_{\alpha\beta}$ is almost certainly the largest observable coupling (≈2.4 Hz), but the four bond $J_{\alpha\beta'}$ is also large due to the 'W' conformation of the intervening bonds (≈1.9 Hz).

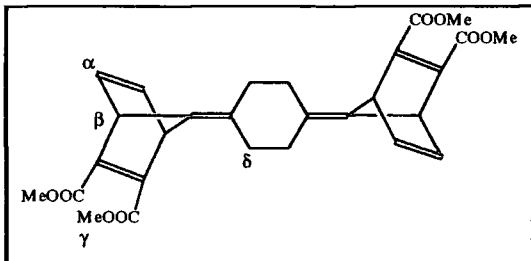

^{1}H-NMR in $CDCl_3$ at 399.997 MHz

Proton	Shift (ppm)	Multiplicity	Integral
α	6.99	doublet of doublets $J_{\alpha\beta}$=2.4Hz	1
β	4.42	doublet of doublets $J_{\alpha\beta}$=2.4Hz	1
γ	3.79	singlet	3
δ	1.92	multiplet	2

The δ protons also produce a complicated splitting pattern due to conformational effects (some are expected to be equatorial and some axial) and long range coupling effects. The methyl protons give a singlet at 3.79 ppm. The spectrum is reproduced in Appendix 5.3.

The ^{13}C-NMR spectrum, reproduced in Appendix 5.4, showed eight peaks for the eight non-equivalent carbons of the molecule, C_α to C_θ, as shown in the table overleaf.

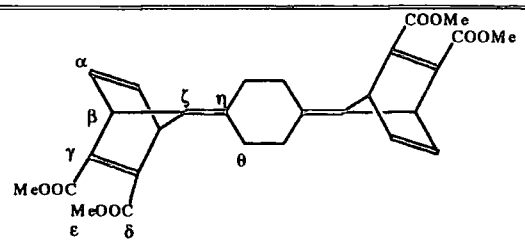

^{13}C-NMR

Carbon	Shift (ppm)
α	142.3
β	52.1
γ	106.4
δ	164.9
ε	52.9
ζ	159.8
η	151.7
θ	28.9

These were assigned with the aid of an APT spectrum and literature assignments for 7-isopropylidene-2,3-dicarbomethoxynorbornadiene. The APT spectrum, which is reproduced in Appendix 5.5, showed the peak for the CH_3 carbon at 52.9 ppm, the peak for the CH_2 carbon at 28.9, and two peaks for the α and β CH carbons at 142.3 and 52.1 ppm respectively. The peaks due to non-protonated (quartenary) carbons at 151.7, 159.8 and 164.9 ppm are assigned to η, ζ and δ carbons respectively. These assignments are tabulated above. The fact that only eight carbon signals can be observed for this product is consistent with it being a single isomer. In the drawings in this manuscript it is indicated as the anti isomer but it could equally well be the syn isomer from the spectroscopic data. Since the recovered yield was only 11% it is very likely that one isomer was preferentially concentrated and purified during the workup.

IR data

The IR spectrum (KBr disc) (see Appendix 5.15) shows absorption peaks at 2953 and 2845 cm^{-1} which were assigned to the C-H stretch, peaks at 1737 and 1706 cm^{-1} to the C=O stretch, the peak at 1623 cm^{-1} to a C=C stretch and also peaks at 1436, 1256, 1100 cm^{-1}, due to skeletal vibrations, which are consistent with the proposed

structure. The doubling of the carbonyl absorption may be a solid state effect or a consequence of splitting between formally degenerate vibrational energy levels (Fermi resonance).

Mass spectrum

The calculated molecular weight for the Diels-Alder adduct is 492. The CI+ spectrum showed the base peak at m/e 493 [M+1], a small peak at 510 [$M+NH_4^+$] and other peaks of low intensity. The EI+ spectrum showed a peak of high intensity at m/e 460 [M-OMe and -H] and a complex fragmentation pattern. There are no peaks which correspond to simple retro-Diels-Alder fragmentation processes and the pathways adopted appear to be dominated by fragmentations initiated at the ester units. These spectra are illustrated in Appendix 5.16.

Experimental

Reagents: *Dimethyl acetylenedicarboxylate* was used as supplied from Aldrich.

1,4-Cyclohexanedicyclopentadienylidene was prepared as described in section 5.2.1.

Procedure: In a 2-necked round bottom flask, a 1,4-cyclohexanedicyclopentadienylidene (1g, 0.0048 moles) solution in toluene (10ml) was mixed with an excess of 2 equivalents of dimethyl acetylenedicarboxylate (1.7g, 0.012 moles) solution in toluene (10ml) and left to react overnight with stirring at room temperature under nitrogen. Then the solvent was removed using a rotary evaporator, the oily residue was poured into methanol and white powder precipitated out of solution. The white powder was purified further by washing with ice cold methanol, then filtered and dried to give (**2**) (0.220g, 11% yield).

5.2.3. The ROMP of (2) using $Mo(=CHC(CH_3)_2C_6H_5)(NAr)(O\text{-}t\text{-}Bu)_2$ as the initiator

As mentioned above the ROMP of 7-isopropylidene-2,3-dicarbomethoxynorbornadiene when initiated with $Mo(CH^tBu)(NAr)(O\text{-}t\text{-}Bu)_2$ yields only the first insertion product. In this study ^{1}H-NMR spectroscopy was used to investigate the result of the reaction when the difunctional analogue (2) is used.

Solutions of initiator and (2) at a ratio of 2:1 were mixed in a sample bottle at room temperature in the Glove Box, using C_6D_6 (0.8 ml) as the solvent and transferred to an NMR tube, which was then sealed. The first ^{1}H-NMR spectrum (I) was recorded 10 min after the mixing was complete, and showed the singlet for the alkylidene proton of the initiator at 11.32 ppm and the septet for the isopropyl -CH proton on the NAr ligand at 3.99 ppm. Two peaks at 4.42 and 6.99 ppm are due to the -CH protons of the monomer (see 5.2.2), while the peak at 3.38 ppm is due to the methyl protons of the ester groups of the monomer. The monomer did not dissolve completely in benzene and this is probably the reason why the signals do not resolve very well and the integration does not correspond to the actual ratio of monomer to initiator. If we assume that the ROM reaction occurs at both norbornadiene rings of a single molecule, then the first insertion product is expected to be that shown on Fig.5.2.3.a.

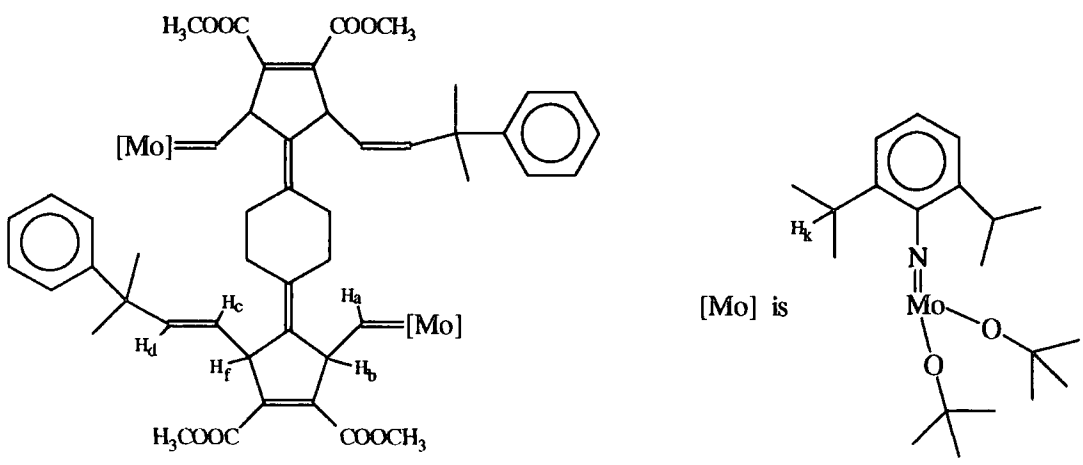

Figure 5.2.3.a The first insertion product after the ROM of (2), another isomer is also possible

The singlet for the alkylidene proton on the initiator, should be replaced by a doublet due to the propagating proton H_a which now couples with proton H_b on the ring. On the other hand the protons around the neophylidene substituted double bond should appear in the spectrum, while the methyl protons on the ester groups should loose their equivalence due to the change of environment in the structure shown above as compared to the symmetry of the monomer. The sequence of ^1H NMR spectra recorded, as discussed in the text below, appear in Figure 5.3.2.b. After six hours two doublets appear (spectrum (II)) at 11.00 and 10.84 ppm, assigned to non-equivalent alkylidene protons; the doublet splitting is due to the coupling to the allylic proton. The appearance of two different signals can be attributed either to the fact that one of them belongs to a partly reacted monomer and the other to a fully reacted monomer, or to different arrangements of the [Mo] and neophylidene groups in space. Another possibility is that one of these signals is due to second insertion of monomer. Low intensity doublets also appear in the region between these two peaks, at 10.92 and 10.98 ppm. At least one new septet appears at 4.16 ppm, as well as three more intense signals for the CH_3 protons, which are no longer equivalent, at 3.35, 3.43 and 3.48 ppm, two doublets for the H_b protons at 6.5 and 6.3 ppm, a number of doublets for the H_c and H_d protons between 5.5 and 5.85 ppm arising also from possible cis-trans isomerism on the double bond. The H_f protons gave two doublets at 2.4 and 2.8 ppm. The NMR tube remained sealed and 24 hours later another NMR spectrum was recorded at 50°C (III).

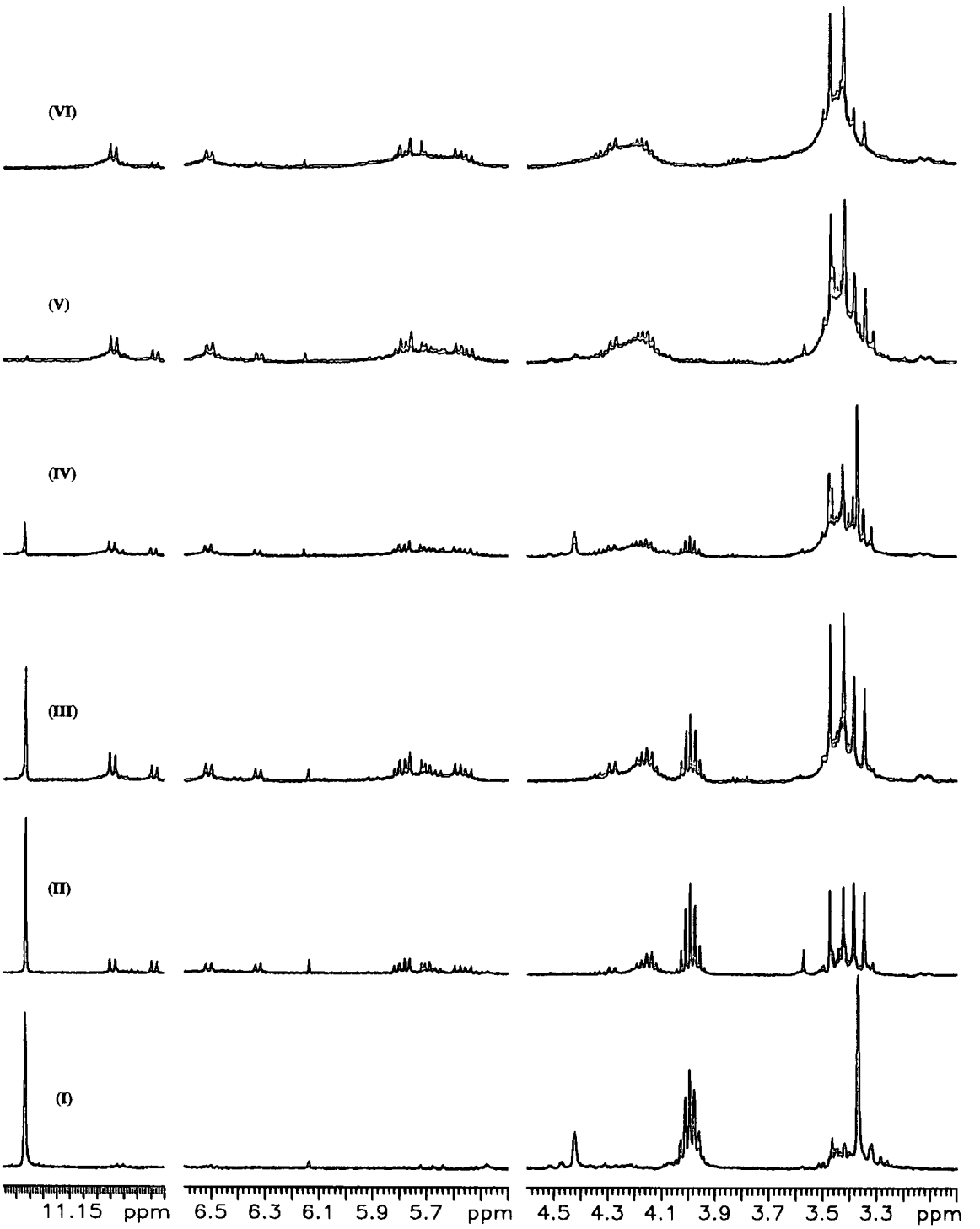

Figure 5.2.3.b ^{1}H NMR spectra of the ROMP reaction of (2)

The intensity of the new peaks described above seemed to increase with time while the intensity for the peaks associated with the initiator and the monomer seemed to decrease. In spectrum (III) the peaks for the -CH groups of the monomer no longer appear in the spectrum and at that stage, the NMR tube was returned to the Glove

Box, opened and one more equivalent of monomer was added, the tube sealed and the ^1H NMR recorded (IV). More signals appear in almost all the regions of interest in the spectrum and a broadening of the lines is observed. In spectrum (V) most of the peaks appear too broad and unresolved to assign but it is already clear that the freshly added monomer has been consumed. In the alkylidene region the integral of the signal for the initiating alkylidene has decreased to 1/10 of that for the propagating ones. Finally at spectrum (VI) there is no signal for the initiating alkylidene proton at 11.31 and the rest of the signals are broad unresolved peaks making the full unambiguous assignment of the spectrum problematic. It is possible that the broadening of the signals is the result of second and subsequent insertions of monomer in the system. The fact is that this NMR experiment proved inconclusive with regard to the nature of the reaction product. The solution changes from yellow to deep red during the course of the reaction.

The same experiment when performed in $CDCl_3$ showed three new doublets appearing at 10.72, 10.76, 10.81 ppm and about 14 signals for the CH_3 protons from 3.62 to 3.86 ppm resulting in an even more complicated NMR spectrum.

Although it was not possible to completely assign the structures involved it is clear that this bis-norbornadiene derivative undergoes polymerisation rather than formation of the 1:2 adduct desired.

5.3. Modification of existing initiators

A different approach to the same objective could be the preparation of difunctional initiators using the cross metathesis reaction between the $Mo(CH^tBu)(OC(CH_3)(CF_3)_2)_2(NAr)$ (from now on termed $[Mo]_{F6}$) initiator and a difunctional styrene compound. The reaction of 1,4-divinylbenzene with 2 equivalents of $[Mo]_{F6}$ in ethylene glycol dimethyl ether (DME) has been reported[90] to give the product of cross metathesis at both vinyl groups as shown below.

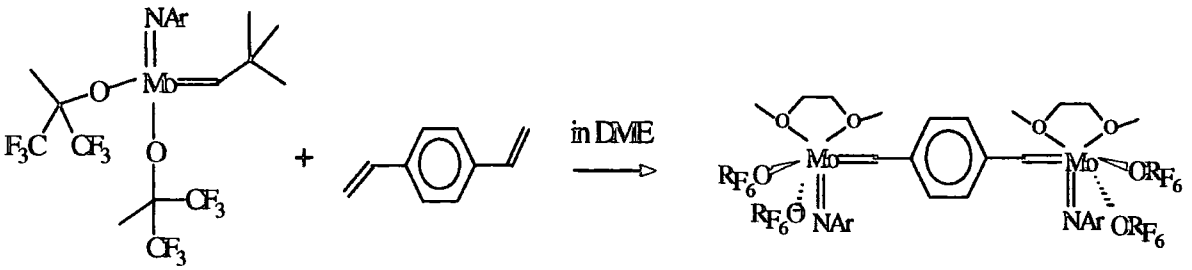

DME is a Lewis base which binds as a donor ligand onto Mo to stabilise the structure sterically, presumably by inhibiting the approach of another molecule and hence the resulting bimolecular decomposition.

The isolation of pure 1,4-divinylbenzene requires relatively complicated chemical and physical purification procedures.[91] Also four coordinate alkylidene complexes are inherently unstable towards bimolecular decomposition. The introduction of a CH_3 group on the double bond was thought to be desirable not only because the resulting alkylidene would be more stable for steric reasons, but also because the purification of m- and p-diisopropenylbenzene is easier compared to the procedure required for 1,4-divinylbenzene (*see* experimental, later in this chapter). The question arising is if this CH_3 group would sterically inhibit the approach of monomer molecules and consequently hinder the ROMP reaction.

5.3.1. Synthesis of $Mo(C(CH_3)Ph)(NAr)(OC(CH_3)(CF_3)_2)_2$.

This complex was synthesised as the model compound, via the metathesis reaction between excess α-methyl styrene and the $[Mo]_{F6}$ initiator.

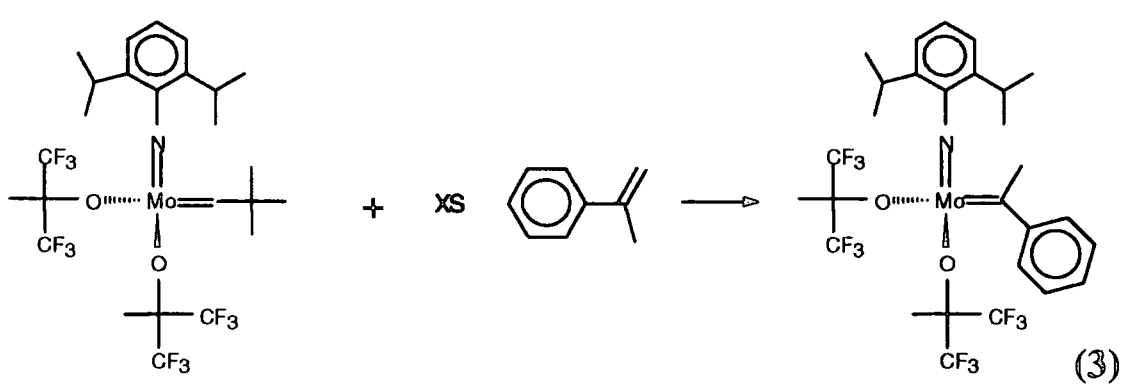

(3)

The reaction was followed by ^{1}H-NMR to monitor the slow replacement of the neopentylidene ligand by the methylphenylalkylidene from α-methyl styrene. The colour of the solution changes from yellow to deep red during the reaction.

^{1}H-NMR analysis

As in the new complex (3) there is no proton attached to the carbene carbon, the signal due to the alkylidene proton at 12.13 ppm in $[Mo]_{F6}$ slowly disappears, as shown in the sequence of spectra, (O) to (IV), in Figure 5.6.a. On the other hand a singlet at 3.29 ppm appears, apparently due to the [Mo]=CC$\underline{H}_3$Ph protons, and a new septet at 3.67 ppm corresponding to the CH proton of the isopropyl groups on the NAr ligand of the new species (the initial septet appears at 3.57 ppm). The integration ratio of these two signals is 3:2 as expected. At 5.95 ppm a doublet of doublets arising from an AB system is seen. This is the signal due to the CH_2=C$\underline{H}$(CCH_3) proton which couples with the vinylic CH_2 protons of the 3,3-dimethylbut-1-ene which is the by-product of the reaction. The signals for the CH_2 protons of this compound are at 4.98 ppm and in this case are partly overlapped by the peak for the vinylic protons of α-methyl styrene. The reaction proceeds until all the Mo_{F6} initiator is consumed. The volatiles, that is the solvent, α-methyl styrene and 3,3-dimethylbut-1-ene were removed under vacuum, to give Mo(C(CH_3)Ph)(NAr)(OC(CH_3)(CF_3)$_2$)$_2$ (3). The ^{1}H-NMR spectrum of (3) is shown in Appendix 5.6.

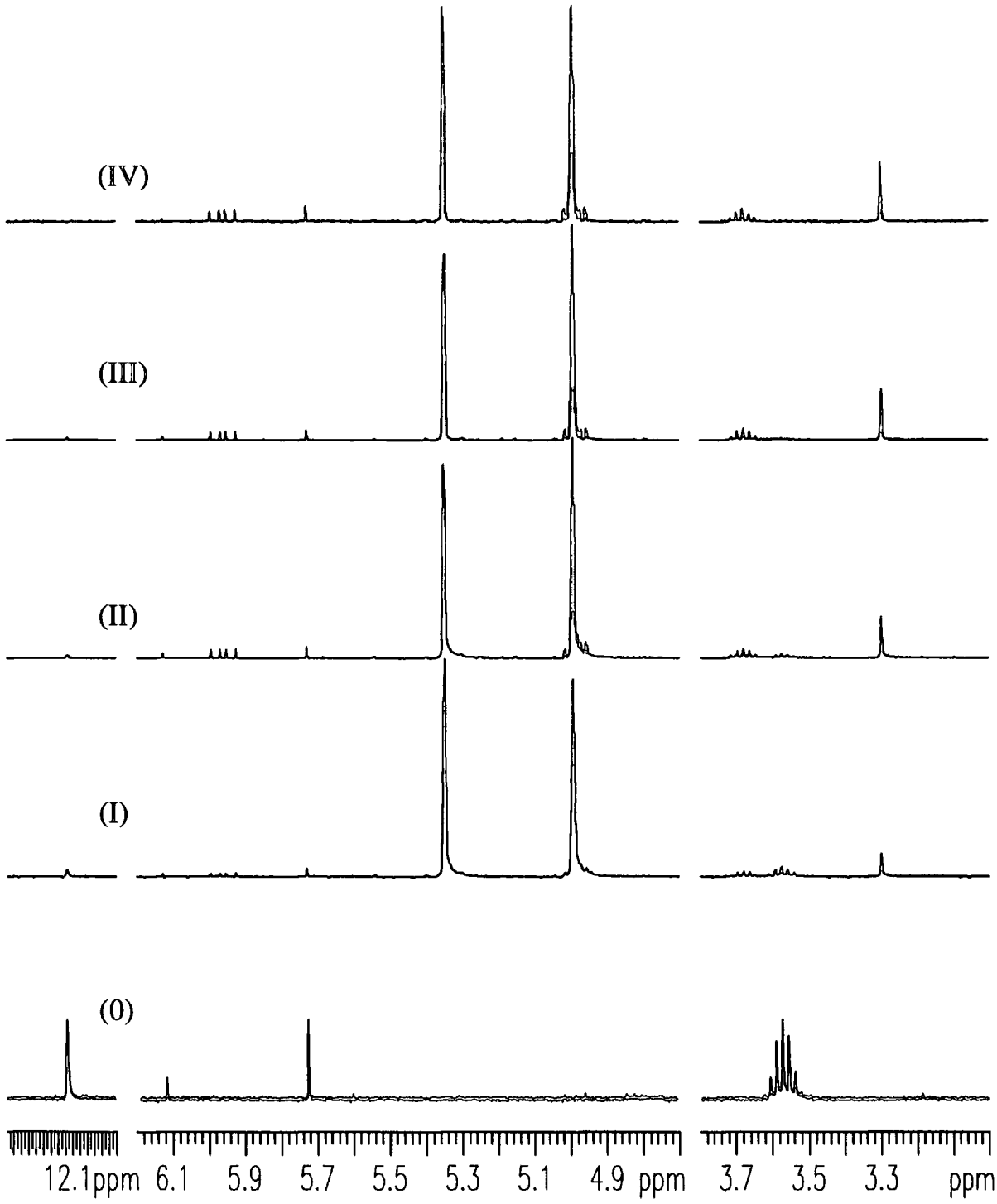

Figure 5.6.a ^{1}H NMR spectra during the reaction of Mo_{F6} with α-methyl styrene

The resulting complex was used for the polymerisation of norbornene, cyclooctene and bistrifluoromethylnorbornadiene (see section 5.4).

5.3.2. Attempted synthesis of meta- and para- $((CF_3)_2(CH_3)CO)_2(NAr)Mo{=}C(CH_3)\text{-}C_6H_4\text{-}(CH_3)C{=}Mo(NAr)(COCH_3(CF_3)_2)$.

Because the metathesis reaction described above is very slow if the α-methyl styrene is not in excess, and also for a more controlled monitoring of the resulting species by NMR, we chose the reaction path shown below.

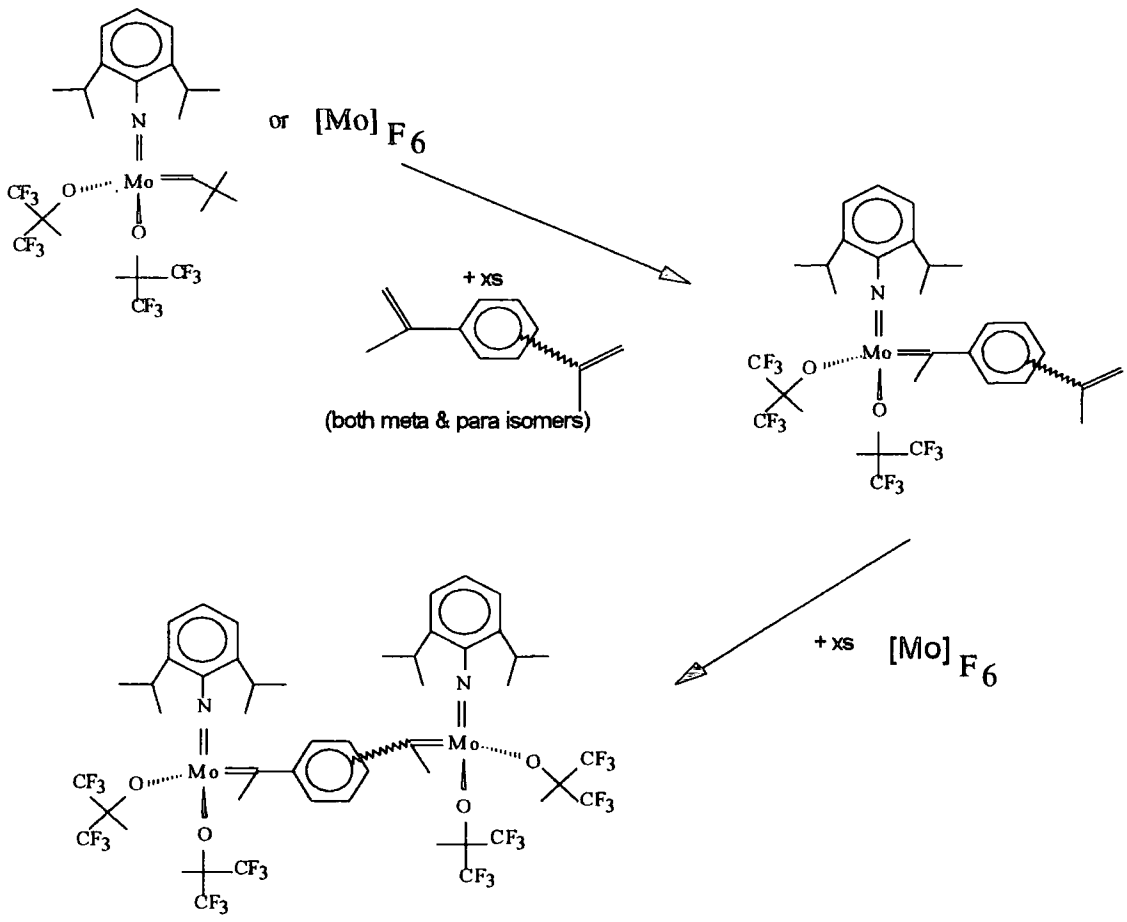

Excess *meta* or *para*-isopropenylbenzene was used for the reaction with $[Mo]_{F6}$ and the resulting product was isolated and allowed to react with excess $[Mo]_{F6}$. Both reactions were followed by ^{1}H-NMR spectroscopy and the results are discussed in sections 5.3.3 to 5.3.6.

5.3.3 Synthesis of $Mo(=C(CH_3)\text{-}m\text{-}C_6H_4C(CH_3)=CH_2)(NAr)(OC(CH_3)(CF_3)_2)_2$

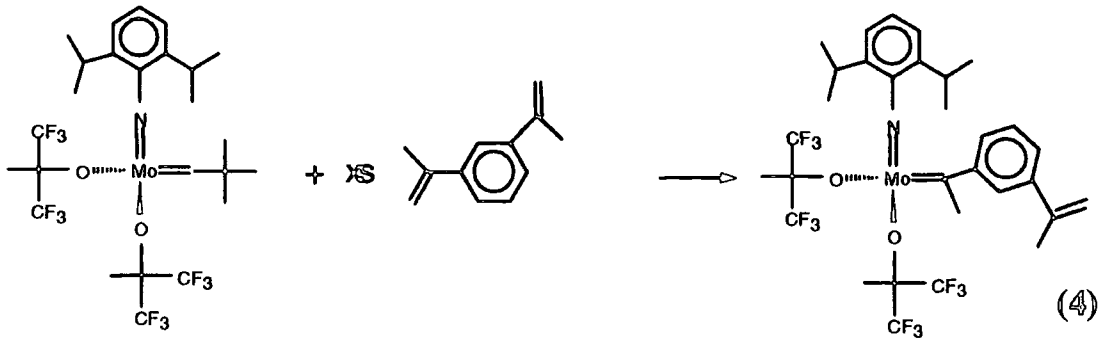

(4)

The reaction of 1,3-diisopropenylbenzene with $Mo(CH^tBu)(OC(CH_3)(CF_3)_2)_2(NAr)$ in benzene at room temperature is relatively fast and total conversion to (4) is achieved within 15 hrs when 1,3-isopropenylbenzene is in excess. When a 1:2 molar ratio was mixed the conversion was much slower.

NMR data

The singlet for the CH_3 protons of 1,3-diisopropenylbenzene appears at 1.99 ppm, while two singlets for the vinylic protons appear at 5.01 and 5.37 ppm. The sterically hindered proton on the 2 position of the benzene ring gives a signal at 7.65 ppm. The signal for the alkylidene proton on the $[Mo]_{F6}$ initiator is a singlet at 12.12 ppm, while the septet at 3.57 ppm is due to the CH protons on the isopropyl substituent of the NAr ligand.

When the reaction takes place, the signal for the alkylidene proton disappears and a signal for the $Mo=C(C\underline{H}_3)$- appears at 3.31 ppm. At the same time, a new septet appears at 3.67 ppm corresponding to the new species. The two protons on the unreacted vinyl of the 1,3-diisopropenylbenzene now appear slightly downfield at 4.91 and 4.82 ppm. The sterically hindered proton on the benzene ring of the molybdenum monosubstituted diisopropenylbenzene gives a signal shifted to 7.78 ppm. These characteristic new resonances which appear in the spectrum, strongly suggest that the reaction proceeds as proposed. Another observation to support this assumption is the

signals at 4.96 and 5.95 ppm for the vinylic protons of 3,3-dimethylbut-1-ene, which is the expected by-product of the cross metathesis reaction. When the conversion was complete, according to NMR observations, the solvent, 1,3-diisopropenylbenzene and 3,3-dimethylbut-1-ene were removed to give $Mo(=C(CH_3)$-m-$C_6H_4C(CH_3)=CH_2)(NAr)(OC(CH_3)(CF_3)_2)_2$ (4), which was then redissolved in C_6D_6 and the ^{1}H-NMR and ^{13}C-NMR spectra were recorded and are shown in Appendix 5.7 and 5.8 respectively. The main assignments, shifts and integrals for the proton and carbon-13 spectra are shown in the tables below.

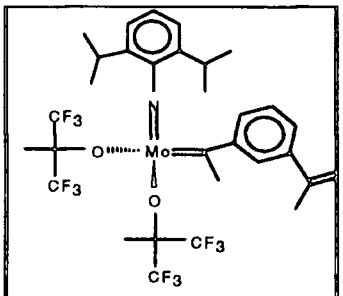

^{1}H-NMR spectrum

Proton	Shift (ppm)	Multiplicity	Integral
Mo=C$\underline{H}_3C_6H_4$-	3.31	singlet	3
OCC$\underline{H}_3(CF_3)_2$	1.25	singlet	6
-C_6H_4C(C$\underline{H}_3$):CH_2	1.67	singlet	3
-C_6H_4C:C$\underline{H}_2CH_3$	4.91	singlet (broad)	1
-C_6H_4C:C$\underline{H}_2CH_3$	4.82	singlet (broad)	1
$NC_6H_3C\underline{H}(CH_3)_2$	3.68	septet (J_{HH}=6.8Hz)	2
$NC_6H_3CH(C\underline{H}_3)_2$	1.06	doublet(J_{HH}=6.8Hz)	12
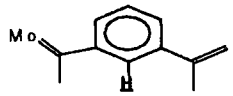	7.78	singlet (broad)	1
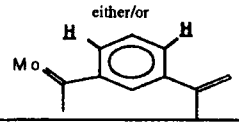	6.65	doublet of triplets (J^d_{HH}=7.6Hz)o (J^t_{HH}=1.6Hz)m	1
Other aromatics	6.8 - 7.1	multiplet	5

The ^{13}C-NMR spectrum was assigned by analogy with the ^{13}C-NMR spectrum of Mo(=CH^{t}Bu)(OC(CH$_3$)(CF$_3$)$_2$)$_2$(NAr), taking into account differences in the chemical shift consequent upon the replacement of the neopentylidene ligand by the arylmethylalkylidene ligand. Some of the characteristic peaks are tabulated here. The peak for the alkylidene carbon which should occur at very low field was not recorded in this experiment, as a result of a miscommunication with the operator. The analogous signal in the para isomer was detected at 283 ppm downfield.

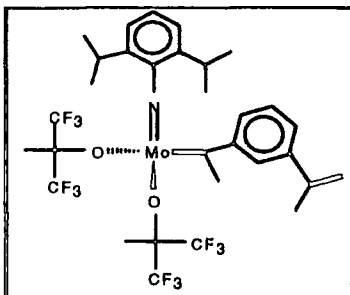

^{13}C-NMR

Carbon	Shift (ppm)
Mo=C$\underline{C}$H$_3$C$_6$H$_4$-	--
Mo=C$\underline{C}$H$_3$C$_6$H$_4$-	unassigned
O$\underline{C}$CH$_3$(CF$_3$)$_2$	82.0 (^{1}J$_{CF}$=29Hz)
OCCH$_3$($\underline{C}$F$_3$)$_2$	124.5(^{2}J$_{CF}$=288Hz)
OC$\underline{C}$H$_3$(CF$_3$)$_2$	19.5
-C$_6$H$_4$$\underline{C}$:CH$_2CH_3$	142 calc 141.6
-C$_6$H$_4$C:$\underline{C}$H$_2$CH$_3$	112.9 calc 106.9
-C$_6$H$_3$$\underline{C}$H(CH$_3$)$_2$	28.6
-C$_6$H$_3$CH($\underline{C}$H$_3$)$_2$	23.5
NC meta	123.6
NC ipso	152.9

5.3.4. Reaction of Mo(=C(CH$_3$)-m-C$_6$H$_4$C(CH$_3$)=CH$_2$)(NAr)(OC(CH$_3$)(CF$_3$)$_2$)$_2$ (4) with excess [Mo]$_{F6}$

The monosubstituted adduct (4) was mixed with excess [Mo]$_{F6}$ in benzene and allowed to react at room temperature. The ^{1}H-NMR spectra are recorded in Figure 5.3.4 (I)-(IV).

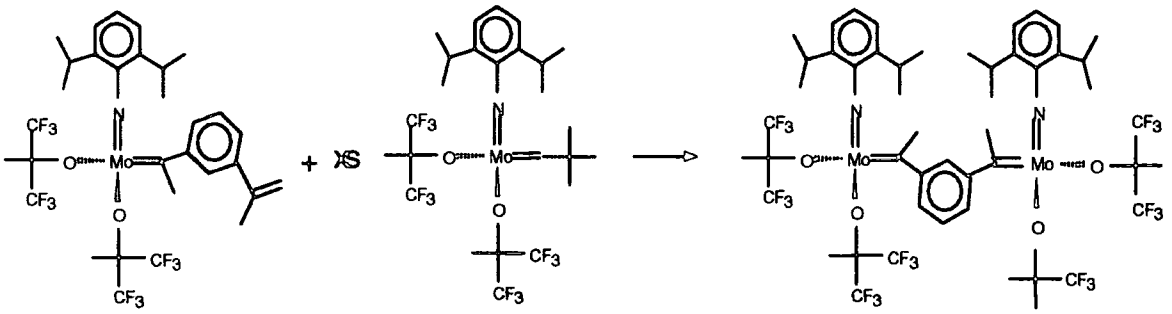

(4) (5)

Although the conversion was very slow, again the formation of 3,3-dimethylbut-1-ene is observed (peaks at 4.96 and 5.95 ppm), suggesting that cross metathesis is taking place between the free vinyl group of (4) and the metal carbene of $[Mo]_{F6}$. A new septet is observed at 3.50 ppm and a new singlet at 3.05 ppm both of which increase in intensity with time. These are assigned to the signal due to the CH protons on the isopropyl substituent of the NAr ligand and the signal due to the [Mo]=C(C$\underline{H}_3$)Ph protons of (5) respectively. The conversion to the difunctional analogue (5) was not complete 3 months after the addition at room temperature. During this period the reaction vessel was also warmed to 50°C for three days. From this analysis it appears that the required reaction has occurred but the rate is too slow to be practically useful in the generation of a difunctional initiator even if the problem of separating (5) from excess $[Mo]_{F6}$ could be solved.

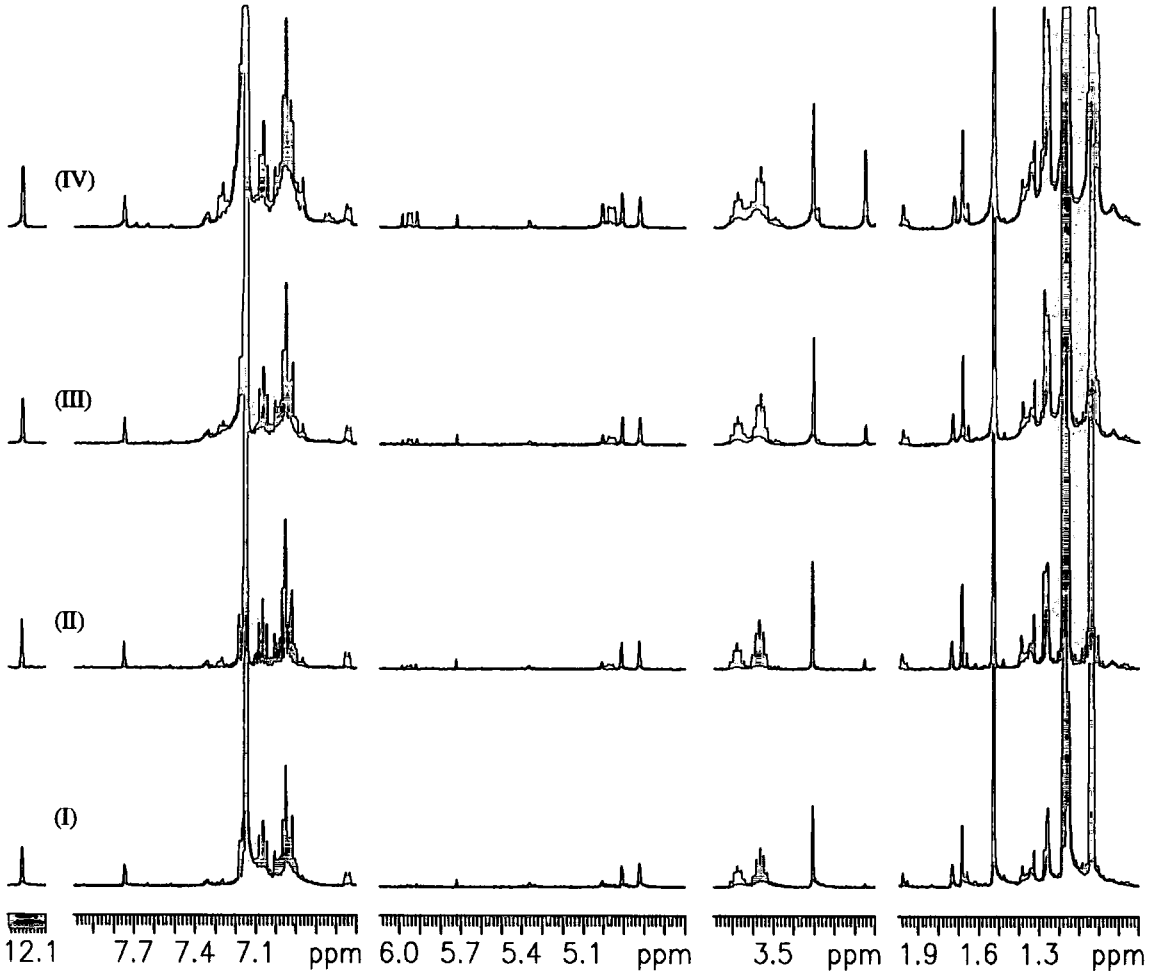

Figure 5.3.4 ^{1}H-NMR spectra of reaction of Mo(=C(CH_3)-m-C_6H_4C(CH_3)=CH_2)(NAr)(OC(CH_3)(CF_3)$_2$)$_2$ (4) with excess $[Mo]_{F6}$.

(I) after 3 hours, (II) after 1 week, (III) after 6 weeks and (IV) after 3 months

5.3.5 Synthesis of Mo(=C(CH_3)-p-C_6H_4C(CH_3)=CH_2)(NAr)(OC(CH_3)(CF_3)$_2$)$_2$

The reaction of the 1,4-diisopropenylbenzene with $[Mo]_{F6}$ was conducted under the same conditions as the reaction for the meta analogue. It was also followed by ^{1}H-NMR spectroscopy and the resulting spectra showed a complete conversion of the $[Mo]_{F6}$ initiator to Mo(=C(CH_3)-p-C_6H_4C(CH_3)=CH_2)(NAr)(OC(CH_3)(CF_3)$_2$)$_2$ (6). The change of substitution position from meta to para, although it does not seem to affect the chemical shift of the vinylic protons of the diisopropenylbenzene, affects the

shift of the analogous protons on the monosubstituted species. For the meta mono molybdenum substituted complex these peaks appear at 4.91 and 4.82 ppm as discussed in the previous section, while for the para substituted they appear at 5.18 and 4.87 ppm. Another expected variation is the absence of the peak at 7.78 ppm which in the 1,3 (meta) case was due to the proton at the 2 position. Again complete conversion is assumed to be achieved when the signal for the alkylidene proton of $[Mo]_{F6}$ can no longer be observed in the NMR spectrum.

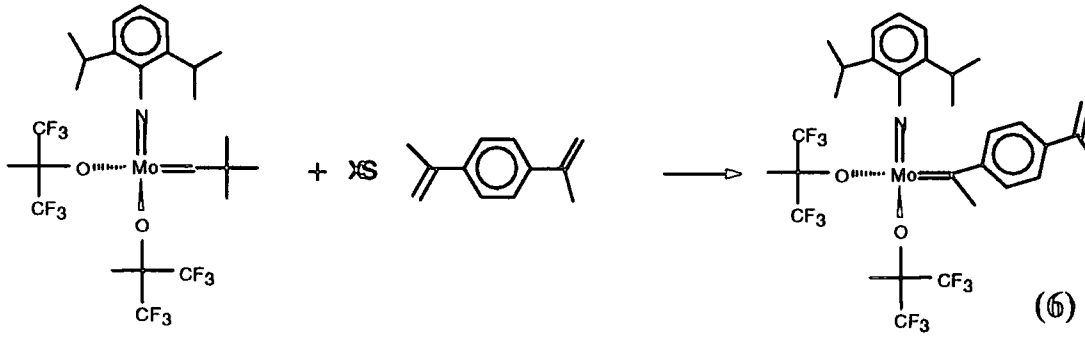

(6)

$Mo(=C(CH_3)\text{-}p\text{-}C_6H_4C(CH_3)=CH_2)(NAr)(OC(CH_3)(CF_3)_2)_2$ (6) was obtained after removal of the volatiles, that is solvent, 1,3-diisopropenylbenzene and 3,3-dimethylbut-1-ene. The deep red solid was redissolved in C_6D_6 and the ^1H-NMR and ^{13}C-NMR spectra were recorded and are shown in Appendices 5.9 and 5.10 respectively. Some of the characteristic peaks of these spectra are tabulated overleaf.

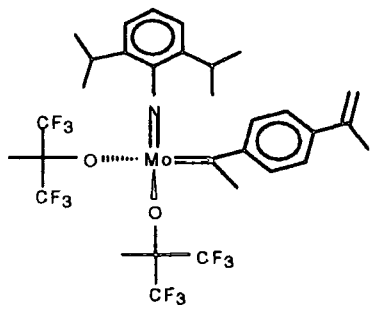

^{1}H-NMR spectrum at 399.577 MHz

Proton	Shift (ppm)	Multiplicity	Integral
Mo=C$\underline{H}_3$C$_6$H$_4$-	3.33	singlet	3
OCC$\underline{H}_3$(CF$_3$)$_2$	1.25	singlet	6
-C$_6$H$_4$C(C$\underline{H}_3$):CH$_2$	1.82	singlet	3
-C$_6$H$_4$C:C$\underline{H}_2$CH$_3$	5.18	singlet (broad)	1
-C$_6$H$_4$C:C$\underline{H}_2$CH$_3$	4.87	singlet (broad)	1
NC$_6$H$_3$C$\underline{H}$(CH$_3$)$_2$	3.72	septet	2
NC$_6$H$_3$CH(C$\underline{H}_3$)$_2$	1.17	doublet	12
Other aromatics	6.8 - 7.1	multiplet	5

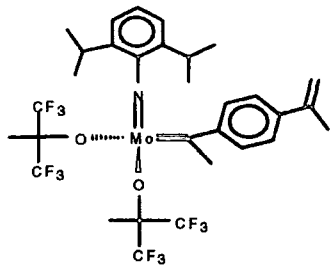

^{13}C-NMR

Carbon	Shift (ppm)
Mo=$\underline{C}CH_3C_6H_4$-	282.96
Mo=C$\underline{C}H_3C_6H_4$-	unassigned
O$\underline{C}CH_3(CF_3)_2$	82.0 (1JCF=29Hz)
OCCH$_3$($\underline{C}$F$_3$)$_2$	124.1(2JCF=288Hz)
O$\underline{C}$CH$_3$(CF$_3$)$_2$	19.5
-C$_6$H$_4\underline{C}$:CH$_2$CH$_3$	142.0 calc 141.6
-C$_6$H$_4$C:$\underline{C}$H$_2$CH$_3$	113.3 calc 106.9
-C$_6$H$_3\underline{C}$H(CH$_3$)$_2$	28.6
-C$_6$H$_3$CH($\underline{C}$H$_3$)$_2$	23.5
NC meta	123.6
NC ipso	153.0

5.3.6. Reaction of Mo(=C(CH$_3$)-p-C$_6$H$_4$C(CH$_3$)=CH$_2$)(NAr)(OC(CH$_3$)(CF$_3$)$_2$)$_2$ (6) with excess [Mo]$_{F6}$

The monosubstituted adduct (6) was mixed in the Glove Box with excess [Mo]$_{F6}$ in benzene-d$_6$ and allowed to react at room temperature.

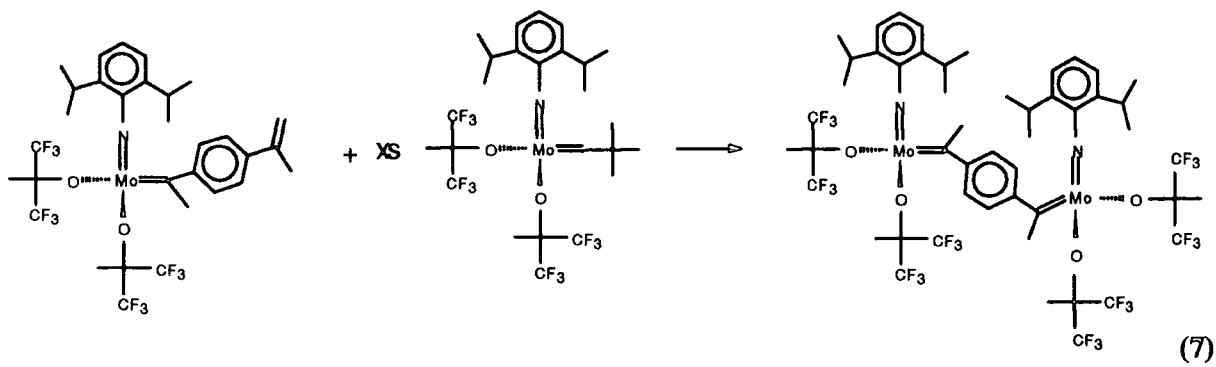

(7)

The conversion again was very slow, the reaction was monitored by ^{1}H NMR spectroscopy and the resulting spectra (I) to (IV) are reproduced in Figure 5.3.6. The

formation of 3,3-dimethylbut-1-ene (peaks at 4.96 and 5.95 ppm), suggests that cross metathesis is taking place between the free vinyl of (6) and the metal carbene of $[Mo]_{F6}$. A new septet is observed at 3.49 ppm and a new singlet at 3.13 ppm which both increase in intensity with time and which can be assigned to the signal due to the CH protons on the isopropyl substituent of the NAr ligand of (7) and the signal due to the [Mo]=C(C$\underline{H}_3$)C_6H_4- protons respectively. The conversion to the difunctional analogue (7) was not complete 3 months after the addition at room temperature.

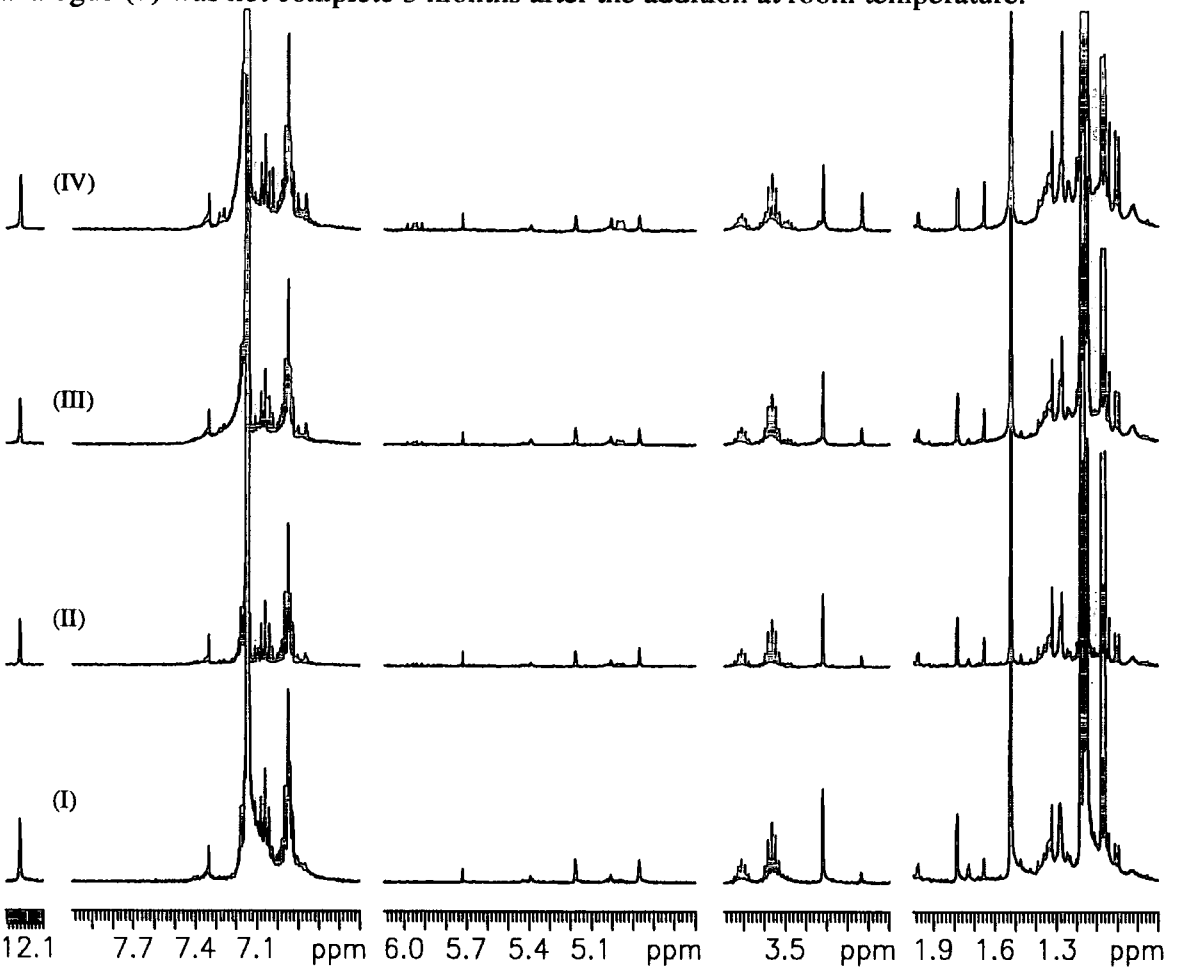

Figure 5.3.6. ^{1}H-NMR spectra of reaction of Mo(=C(CH_3)-p-$C_6H_4C(CH_3)=CH_2$)(NAr)($OCCH_3(CF_3)_2$)$_2$ (6) with excess $[Mo]_{F6}$.

(I) after 3 hours, **(II)** after 1 week, **(III)** after 6 weeks and **(IV)** after 3 months

The reaction vessel was warmed up to 50°C for three days, but no further reaction was observed. From this analysis it appears that the required reaction has occured but

the rate is too slow to be practically useful in the generation of a difunctional initiator even if the problem of separating (7) from excess $[Mo]_{F6}$ could be solved.

5.4. The ROMP of some monocyclic and bicyclic alkenes using $Mo(=C(CH_3)Ph)(NAr)(OC(CH_3)(CF_3)_2)_2$ as the initiator.

The product of the reaction between $[Mo]_{F6}$ and α-methyl styrene was used to initiate the polymerisation of cyclooctene, norbornene and (bistrifluoromethyl)norbornadiene. The solution containing the product from the reaction between $[Mo]_{F6}$ and excess α-methylstyrene (see section 5.3.1.) in C_6D_6 was divided into three fractions for the polymerisation of the above monomers. All the calculations are based on the initial amount of $[Mo]_{F6}$ and the assumption of complete conversion to the new species containing the $Mo=C(CH_3)C_6H_4$- unit.

5.4.1. Polymerisation of cyclooctene using $Mo(=C(CH_3)Ph)(NAr)(OC(CH_3)(CF_3)_2)_2$ as the initiator.

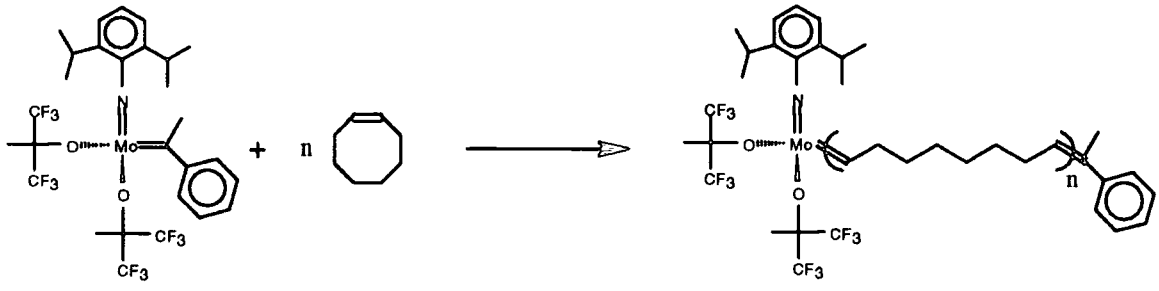

The ratio of monomer to initiator used was 1:10, in 800 μl C_6D_6. The reaction was monitored by ^{1}H-NMR and the progress of the reaction is shown in Figure 5.4.1 and discussed below. The signals for the monomer appear at 5.65 ppm associated with the vinylic protons, at 2.4 ppm associated with the CH_2 protons adjacent to the double bond, and around 1.4 ppm associated to the remaining CH_2 protons. The signal for the $Mo=C(C\underline{H}_3)Ph$ protons appears at 3.3 ppm while the septet corresponding to the

isopropyl substituent of the NAr ligand at 3.68 ppm (see earlier in this chapter) is visible in the expanded spectra but not in the reproduction of Figure 5.4.1. The peaks at 4.99 and 5.35 are due to the vinylic protons of α-methyl styrene. Thirty minutes after the addition (spectrum (I)) there was only a small amount of polymer, giving a signal for the olefinic protons at 5.46 ppm, while three days after the addition (spectrum (II)) all the monomer had been converted to poly(1-octenylene). The peaks due to the initiator were reduced in intensity but they had not disappeared completely. At this stage 10 more equivalents of monomer were added (spectrum (III)), these were consumed within three hours, then 20 more equivalents (spectrum (IV) were added and these were also rapidly consumed.

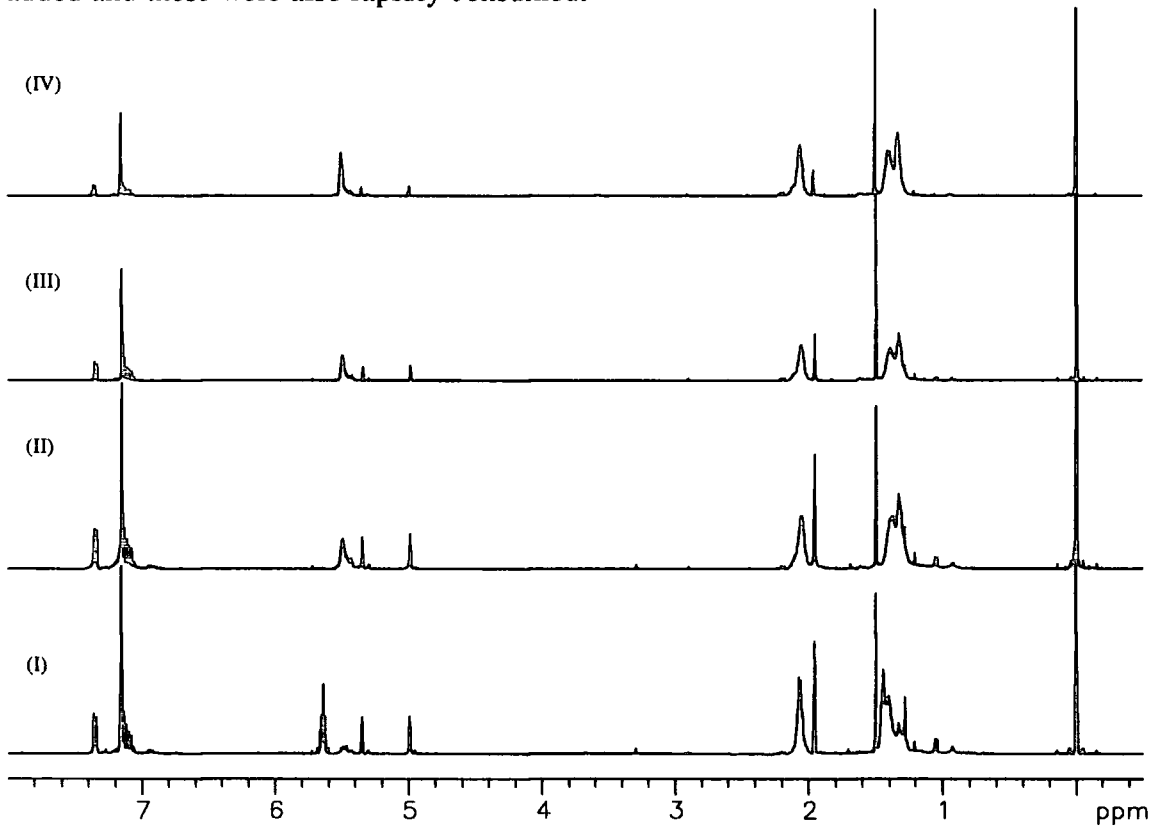

Figure 5.4.1. ^{1}H-NMR spectra during the ROMP of cyclooctene using $Mo(=C(CH_3)Ph)(NAr)(OC(CH_3)(CF_3)_2)_2$ as the initiator

The GPC trace of the product of this reaction, illustrated in Appendix 5.17, showed a main broad peak which corresponds to Mn=15190, Mw=23910, PDI=1.57 and

DP=170. It also shows narrow distinctive peaks for lower molecular weight material corresponding to oligomers with DP's 6, 5, 4, 3 and 2 possibly formed by back biting or chain transfer with the α-methyl styrene, although the former explanation is preferred since the propagating chain end appears to be very reactive and as established earlier metathesis with α-methyl styrene is very slow.

5.4.2. Polymerisation of norbornene using $Mo(=C(CH_3)Ph)(NAr)(OCCH_3(CF_3)_2)_2$ as the initiator.

The ratio of norbornene to initiator was 10:1 in 0.8 ml C_6D_6 and the polymerisation was rapid. In five minutes all the monomer had been consumed and only a small amount of the available initiator had been used. This is not surprising considering that after the first insertion the propagating species is likely to be more reactive than the initiating species because of the absence of the bulky methyl group near the active site.

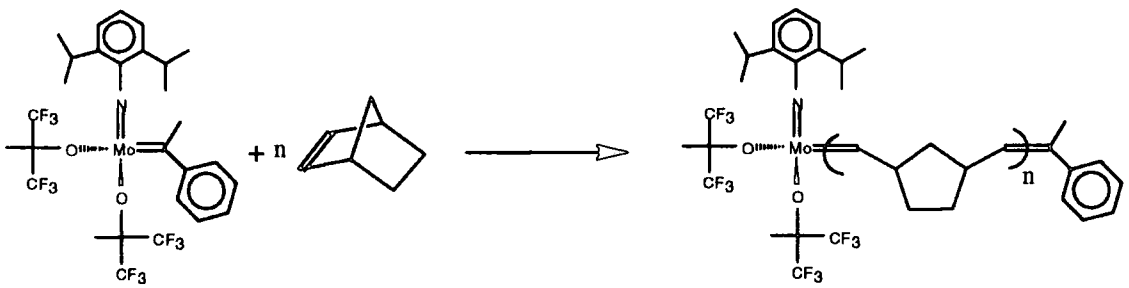

The ^{1}H-NMR spectrum, illustrated in Appendix 5.11, showed the peaks for the vinylic protons of polynorbornene at 5.35 and 5.50 ppm, associated with the *cis* and *trans* configurations respectively. The peaks for the allylic protons on the ring appear at 2.52 and 2.90 ppm associated with the protons next to a *cis* and next to a *trans* double bond respectively. From these signals the *cis* to *trans* ratio was found to be 85 : 15. The end groups cannot be detected by NMR presumably because the polymer chains are too long.

GPC data

The GPC trace, illustrated in Appendix 5.18, showed a very broad peak which, when analysed gave Mn=1610, Mw=6680 and a large amount of higher molecular weight material (Mp=11300). The PDI was 4.14 and the DP was 70.

It is clear from the ^{1}H NMR and GPC data that, in this case, the propagation rate is much faster than the initiation rate ($k_{init} << k_{prop}$).

5.4.3. Polymerisation of (bistrifluoromethyl)norbonadiene using $Mo(CCH_3Ph)(NAr)(OCCH_3(CF_3)_2)_2$ as the initiator.

The polymerisation of (bistrifluoromethyl)norbornadiene when initiated with well defined Schrock initiators is usually slower than the polymerisation of norbornene, and the rate of initiation is faster than or equal to the rate of propagation ($k_{init} \cong k_{prop}$). It has been observed[30b,72] that, when the polymerisation is initiated with the $[Mo]_{F6}$ initiator, the resulting polymer has a very high cis content (90%).

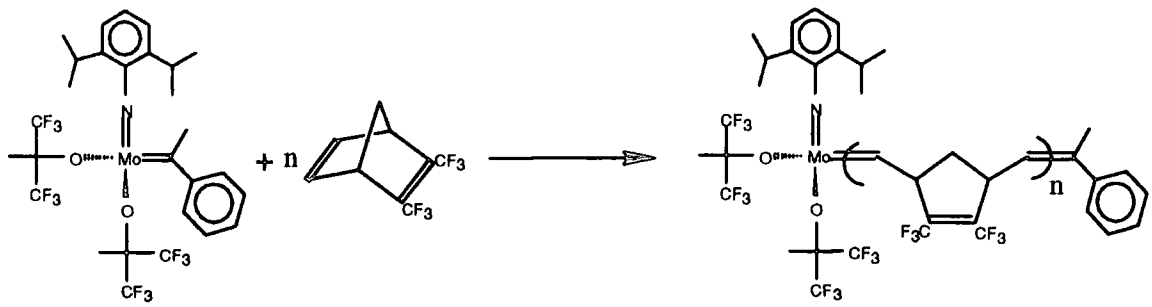

The polymerisation was performed in benzene-d_6, and the polymer formed precipitated out of solution. Some THF-d_8 was added to dissolve the polymer and the ^{1}H-NMR was recorded (see Appendix 5.12). The broad peaks from 5.4 to 5.6 are assigned to protons on mostly *cis* double bonds with the observed splitting due to tacticity effects.[92] The integration for the allylic carbons at 4.1 (next to a *cis* double bond) and 3.7 ppm (next to a *trans* double bond), suggest a *cis* : *trans* ratio of 92:8. The septet at 2.97 ppm is presumably due to the CH protons on the isopropyl substituent of the NAr ligand of the initiator, but since no peak was observed for the

alkylidene proton around 12 ppm, it is assumed that the metal has been cleaved from the chain end either via chain transfer caused by the excess α-methyl styrene or another as yet unidentified process.

GPC data

The GPC trace, illustrated in Appendix 5.19, showed a bimodal distribution, Mn=17000, Mw=19700 and PDI=1.16. The low molecular weight peak corresponds to Mp=8400 while the high molecular weight shoulder to Mp=15000. It has been observed in the past that the introduction of oxygen during the termination of living metathesis polymerisation may double the molecular weight.[93] If this is the case in this experiment the DP of the resulting polymer was 35 (based on the low molecular weight material) which is larger than would be expected in a well-defined living polymerisation process, suggesting that the initiation rate is slower than the propagation rate. Thus, the above results are all consistent with the Mo=C(CH_3)C_6H_4- initiator being somewhat less reactive than the Mo=CH-R analogues.

5.5. Experimental

Reaction of α-methyl styrene with Mo(=CH^{t}Bu)(OC(CH_3)(CF_3)$_2$)$_2$(NAr)

Solutions of Mo(=CH^{t}Bu)(OC(CH_3)(CF_3)$_2$)$_2$(NAr) (0.01 g, 0.0142 moles) in 0.5 ml C_6D_6 and α-methyl styrene (15 x molar excess, 0.00022 moles, 0.026 g) in 0.25 ml C_6D_6 were prepared in the Glove Box. The solutions were mixed, stirred for 45 min. and the colour changed from yellow to orange. At that stage the solution was transferred into an NMR tube, which was then sealed and the first ^{1}H-NMR spectrum was recorded. The sealed tube was kept at room temperature, the colour changed to deeper red with time and the progress of the reaction was recorded with subsequent ^{1}H-NMR experiments.

Reaction of 1,3-diisopropenylbenzene and 1,4-diisopropenylbenzene with Mo(=CH^{t}Bu)(OC(CH$_3$)(CF$_3$)$_2$)$_2$(NAr)

Meta- and *para*-diisopropenylbenzene were purified dy sublimation at 50°C under vacuum. The procedure and molar ratios for both reactions were the same. In the first step of the experiment using the meta analogue, a solution of Mo(=CH^{t}Bu)(OC(CH$_3$)(CF$_3$)$_2$)$_2$(NAr) (0.01 g, 0.0142 mmoles) in 0.5 ml C_6D_6 and a solution of excess 1,3-diisopropenylbenzene (5 x molar excess, 0.011 g, 0.071 mmoles) were mixed and transferred into an NMR tube. When the reaction was complete, the contents of the NMR tube were transferred in a Young valve ampoule in the glove box. The ampoule was then connected to the vacuum/N_2 line, warmed up to 40°C and the volatiles were removed under vacuum to give Mo(=C(CH$_3$)-m-C$_6$H$_4$C(CH$_3$)=CH$_2$)(NAr)(OC(CH$_3$)(CF$_3$)$_2$)$_2$. In the second part of the experiment this product (0.011 g, 0.0142 mmoles) was dissolved in 0.5 ml C_6D_6 and excess Mo(=CH^{t}Bu)(OC(CH$_3$)(CF$_3$)$_2$)$_2$(NAr) (3 x molar excess, 0.029 g, 0.0426 mmoles) in 0.5 ml C_6D_6 was added. The solution was transferred into an NMR tube and the reaction was followed by ^{1}H-NMR spectroscopy.

Polymerisation of cyclooctene, norbornene and (bistrifluoromethyl)norbornadiene using Mo(=C(CH$_3$)Ph)(NAr)(OC(CH$_3$)(CF$_3$)$_2$)$_2$ as the initiator.

All polymerisations were performed in the glove box at room temperature. The amount of initiator used was calculated as a known concentration volume fraction of the original solution in C_6D_6 and the initiator : monomer ratio was 1:10 in all cases. The monomer solution was added rapidly into the initiator solution and allowed to react while stirring. The reaction mixtures were then transferred into NMR tubes and the ^{1}H-NMR spectra were recorded.

5.6. Conclusions

Two possible routes to well defined difunctional initiators were studied in this chapter. The first, "blocked chain end reactivity" approach was based on the observations by Schrock and coworkers[39] on the attempted ROMP of 7-isopropylidene-2,3-dicarbomethoxy norbornadiene as described in section 5.2. The difunctional analogue (2) was prepared, but the attempt to isolate the 2:1 adduct from reaction with Mo(=CH-t-Bu)(NAr)(O-t-Bu)$_2$ and use it as a possible difunctional initiator, was not succesful since the monomer was polymerised futher. The second approach studied was the modification of existing well-defined Schrock type initiators, using the cross metathesis reaction with half an equivalent of both 1,3-diisopropenylbenzene and 1,4-diisopropenylbenzene to form the potential difunctional ROMP initiators as described in section 5.3.2. Although the spectroscopic data suggest the formation of the desired products, the reaction rates were too slow and complete conversion was not achieved.

CHAPTER 6: Conclusions and suggestions for future work

The work reported in this thesis is a part of a project of work in Durham aimed at the preparation of well-defined macromolecular architectures via living ring opening metathesis polymerisation.

In order to obtain novel hydrocarbon polymer topologies, by using well defined living polyalkenamers, we investigated the polymerisation of a series of monocyclic alkenes, using a range of well defined initiators, as described in Chapter 2. The polymerisations of cyclooctadiene, cycloheptene, cyclooctene, cyclodecene and cyclododecene at room temperature, using chloroform as the solvent, did not proceed in a living manner, that is the number average molecular weight of the resulting polymers was not a linear function of conversion and the molecular weight could not be controlled by the stoichiometry of the reaction. Cyclopentene polymerises in a living manner at -45°C in chloroform when the polymerisation is initiated with $W(CH^tBu)(O^tBu)_2(NAr)$ but the polydispersity index of the resulting poly(1-pentenylene) tends to increase with the reaction time as a result of intra- and/or intermolecular cross metathesis reactions. A study of this polymerisation using gel permeation chromatography showed that conversion increases in a regular manner with time and the number average molecular weight can be controlled by adjusting the monomer to initiator ratio and the reaction time. Differential scanning calorimetry studies of the polyalkenamers showed a dependence of their T_ms on the *cis* to *trans* double bond ratio in the chain. The higher the *trans* content in a polyalkenamer the higher the T_m and the higher the double bond content in a chain the more acute this effect is. This study was conducted using the polymers obtained during the polymerisations described in Chapter 2 and the data collected were not enough for a complete analysis or generalisations on the dependence of the melting temperature on the *cis* to *trans* ratio. A more detailed analysis using more polyalkenamers with a wider range of *cis* to *trans* ratios could lead to the formulation of a general rule governing this relationship. The ^{13}C-NMR study of these polyalkenamers using a high field NMR

spectrometer allowed the observation and assignment of all the large shift effects due to the geometries of the neighbouring double bonds and minor shifts due to the conformational *γ-gauche* effect which have not previously received comment. Molecular modelling techniques may be used to further investigate the possibility of predicting the relative abundances of *trans* and *gauche* conformations of a polyalkenamer, using the information concerning conformational effects obtained by ^{13}C-NMR studies as a check of the reliability of the predictions.

The synthesis of a poly(1-pentenylene)-*block*-polyacetylene-*block*-poly(1-pentenylene) polymer is discussed in Chapter 3. The preparation of the A-B block copolymer proceeds in a well controlled manner when the initiator used is $W(CH^tBu)(O^tBu)_2(NAr)$ at low temperature, but the addition of the second A block was not as well defined and the overall symmetry of the molecule could not be guaranteed with confidence. A more realistic approach to the problem may be the preparation of well defined poly(1-pentenylene)-*block*-polyacetylene living copolymer followed by the introduction of half an equivalent of a difunctional conjugated aldehyde as the capping reagent as shown schematically below.

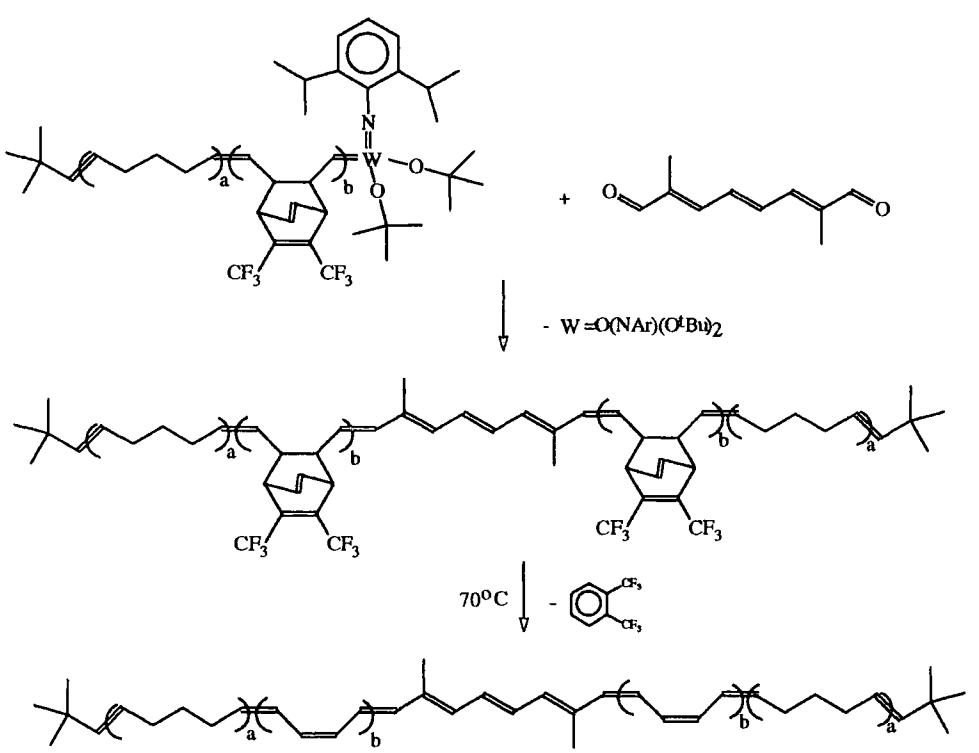

This reaction path, in favourable circumstances, may result in the formation of an A-B-C-B-A block copolymer with the conjugated polyene exactly in the middle of the chain and the number of double bonds equal to twice the number of double bonds in the B block plus the number of double bonds (C) in the conjugated difunctional aldehyde.

The preparation of linear and star polyethylenes with controlled molecular weights and polydispersities as low as 1.04 was achieved; the living polypentenamer that was obtained after the living ROMP of cyclopentene at -45°C, was cleaved from the metal centre in a Wittig-like capping reaction with mono-, di- and trifunctional aldehydes to yield linear and three-branched star poly(1-pentenylenes) with the appropriate multiples of the molecular weight of the initial living linear poly(1-pentenylene), which were then hydrogenated to yield the corresponding polyethylenes as described in Chapter 4. If exact stoichiometry had been achieved, the capping reaction with multifunctional aldehydes should lead to structures with narrower molecular weight distributions than the linear starting polymer; although the general principal was demonstrated, the molecular weight distribution narrowing was not observed in this work probably as a result of not obtaining precise stoichiometry control in rather small scale reactions and not obtaining 100% pure capping agents. Star polyethylenes with four or more branches could be prepared if a tetra- or a multifunctional aldehyde is used as the capping agent.

The introduction of a difunctional initiator and the consequent preparation of living poly(1-pentenylene) with two living ends followed by the addition of a multifunctional aldehyde, can potentially lead to the synthesis of polymeric network structures with controllable well defined distances between the junction points. Two potential routes to a well defined difunctional ROMP initiator are discussed in Chapter 5. The first route had as an objective the preparation and isolation of the 2:1 adduct of the

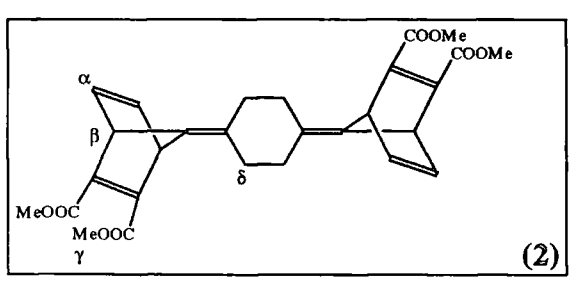

(2)

difunctional monomer (2) with Mo(=CH-t-Bu)(NAr)(O-t-Bu)$_2$ which could then potentially act as a difunctional ROMP initiator.

The synthesis of the 2:1 adduct was not possible under the conditions investigated because the monomer underwent ROMP beyond the first insertion. Another difunctional monomer that could be used for the same purpose is monomer (3). This monomer was synthesised but its purification was proved to be somewhat problematic and the synthesis is not reported in this work. Future work could deal with the preparation (using a similar path to the preparation of (2)), purification and use of (3) as a potential route to the 2:1 adduct with Mo(=CH-t-Bu)(NAr)(O-t-Bu)$_2$ which could be used as a potential difunctional ROMP initiator. The second route to a possible difunctional initiator discussed in Chapter 5 was via the cross metathesis between Mo(=CH^{t}Bu)(OC(CH$_3$)(CF$_3$)$_2$)$_2$(NAr) and meta or para-isopropenylbenzene but although spectroscopic data indicate the formation of these difunctional species the rates of the reaction, under the conditions described in Chapter 5, were too slow to be practically useful in the generation of a difunctional initiator.

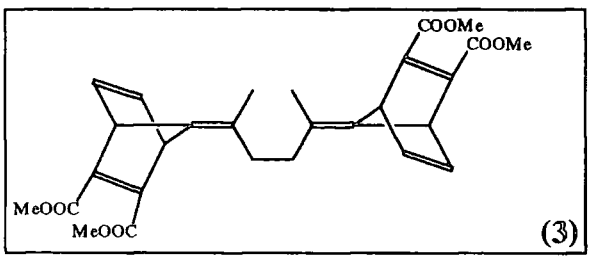

(3)

APPENDIX 1

General procedures, equipment and instrumentation

General experimental procedures

The Glove Box used throughout this work was a modified Miller Howe dry box with a fitted freezer (-40°C), the inert gas was oxygen-free nitrogen and the working conditions were 2-6 ppm oxygen and 5-7 ppm H_2O. Apparatus was transfered in and out of the box via two vacuum / nitrogen ports.

The vacuum / nitrogen line was fitted with Young valves and greaseless joints to allow handling of materials either under nitrogen or under vacuum. Vacuum was provided by an Edwards 5 Two Stage pump and dry oxygen-free nitrogen was supplied through a H_2SO_4 bubbler and a double P_2O_5 column.

The thermostated cooling bath used for the polymerisation of cyclopentene was a HAAKE F3-Q model and the cooling fluid used was methylated spirits.

Instrumentation

^{1}H and ^{13}C nuclear magnetic resonance spectra were recorded on a Varian VXR 400 NMR spectrometer at 399.952 MHz (^{1}H) and 100.577 MHz (^{13}C) and a Varian Gemini 200 NMR spectrometer at 199.532 MHz (^{1}H) and 50.289 MHz (^{13}C).

Mass Spectra were recorded on a VG Analytical Model 7070E Mass Spectrometer.

Gel Permeation Chromatography was carried out using a Waters Model 590 (refractometer, column packing PL_{gel} 5μ mixed styrene-divinyl benzene beads, solvent: chloroform) and a Viscotek Differential Refractometer/Viscometer Model 200 (column packing PL_{gel} 10μ mixed styrene-divinyl benzene beads, solvent: tetrahydrofuran)

Infrared spectra were recorded on a Perkin Elmer 1600 series FTIR.

Differential scanning calorimetry was performed using a Perkin Elmer DSC 7 differential scanning calorimeter.

Ultraviolet/Visible Spectra were recorded on a Perkin Elmer 330 Spectrophotometer.

Thermogravimetric Analysis was performed using a Stanton Redcroft TG760 thermobalance.

APPENDIX 2

Analytical data for Chapter 2

Table of appendices in Chapter 2

	Poly(1-butenylene)	Poly(1-pentenylene)	Poly(1-heptenylene)	Poly(1-octenylene)	Poly(1-decenylene)	Poly(1-dodecenylene)	Initiated by
^{1}H-NMR	2.1	2.6	2.11	2.15	2.20	2.24	W
^{13}C-NMR	2.2.a	2.8.a		2.16.a	2.21.a	2.25.a	W
	2.2.b	2.8.b	2.12.a	2.16.b	2.21.b	2.25.b	Mo^{t}Bu
	2.2.c	2.8.c	2.12.b	2.16.c	2.21.c	2.25.c	MoF_3
	2.2.d		2.12.c	2.16.d	2.21.d	2.25.d	MoF_6
HETCOR		2.7		2.17			W
GPC	2.3.a	2.9.a		2.18.a	2.22.a	2.26.a	W
	2.3.b	2.9.b	2.13.a	2.18.b	2.22.b	2.26.b	Mo^{t}Bu
	2.3.c	2.9.c	2.13.b	2.18.c	2.22.c	2.26.c	MoF_3
	2.3.d		2.13.c	2.18.d			MoF_6
DSC	2.4.a	2.10		2.19.a	2.23.a	2.27.a	W
	2.4.b		2.14.a	2.19.b	2.23.b	2.27.b	Mo^{t}Bu
	2.4.c		2.14.b	2.19.c	2.23.c	2.27.c	MoF_3
	2.4.d		2.14.c	2.19.d	2.23.d	2.27.d	MoF_6
IR	2.5.a	2.5.b	2.5.c	2.5.d	2.5.e	2.5.f	---

W is W(CH^{t}Bu)(O^{t}Bu)$_2$(NAr)
Mo^{t}Bu is Mo(CH^{t}Bu)(OC(CH$_3$)$_3$)$_2$(NAr)

MoF_3 is Mo(CH^{t}Bu)(OC(CH$_3$)$_2$CF$_3$)$_2$(NAr)
MoF_6 is Mo(CH^{t}Bu)(OC(CH$_3$)(CF$_3$)$_2$)$_2$(NAr)

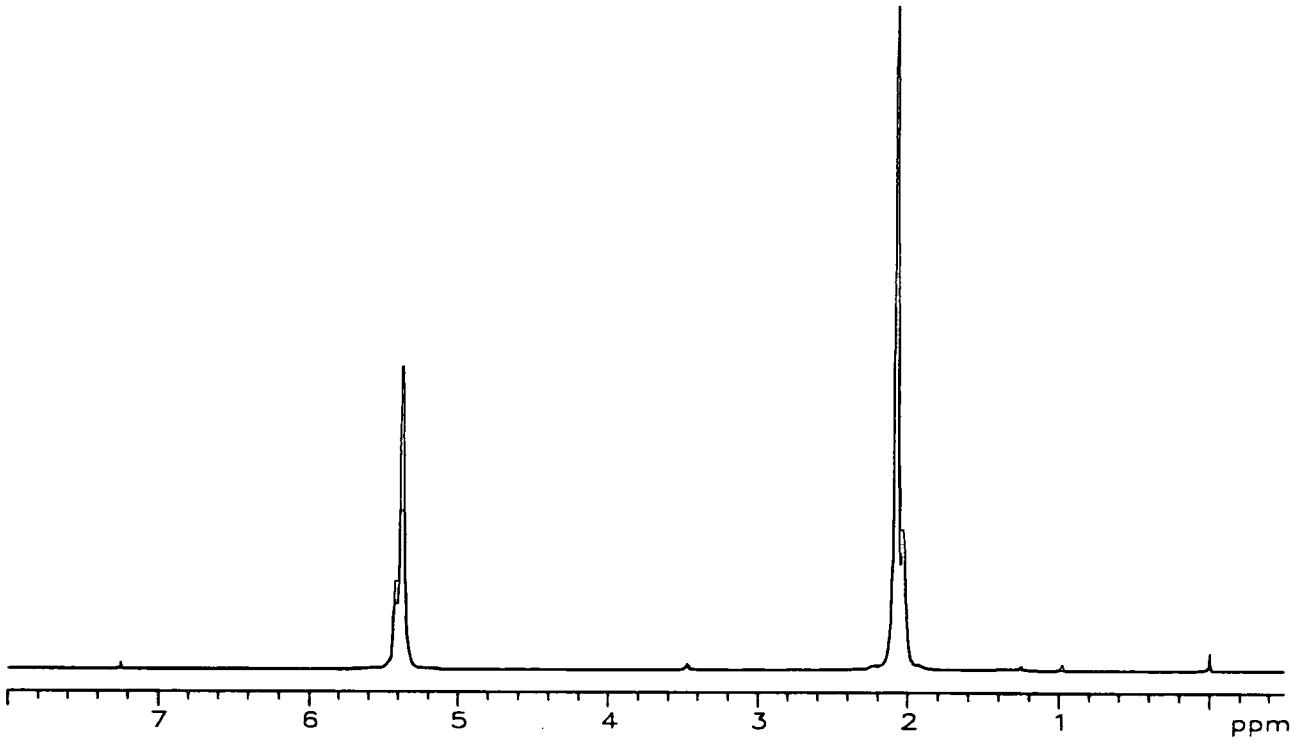

Appendix 2.1 ^{1}H-NMR spectrum of poly(1-butenylene) initiated by W(CH^{t}Bu)(O^{t}Bu)$_2$(NAr)

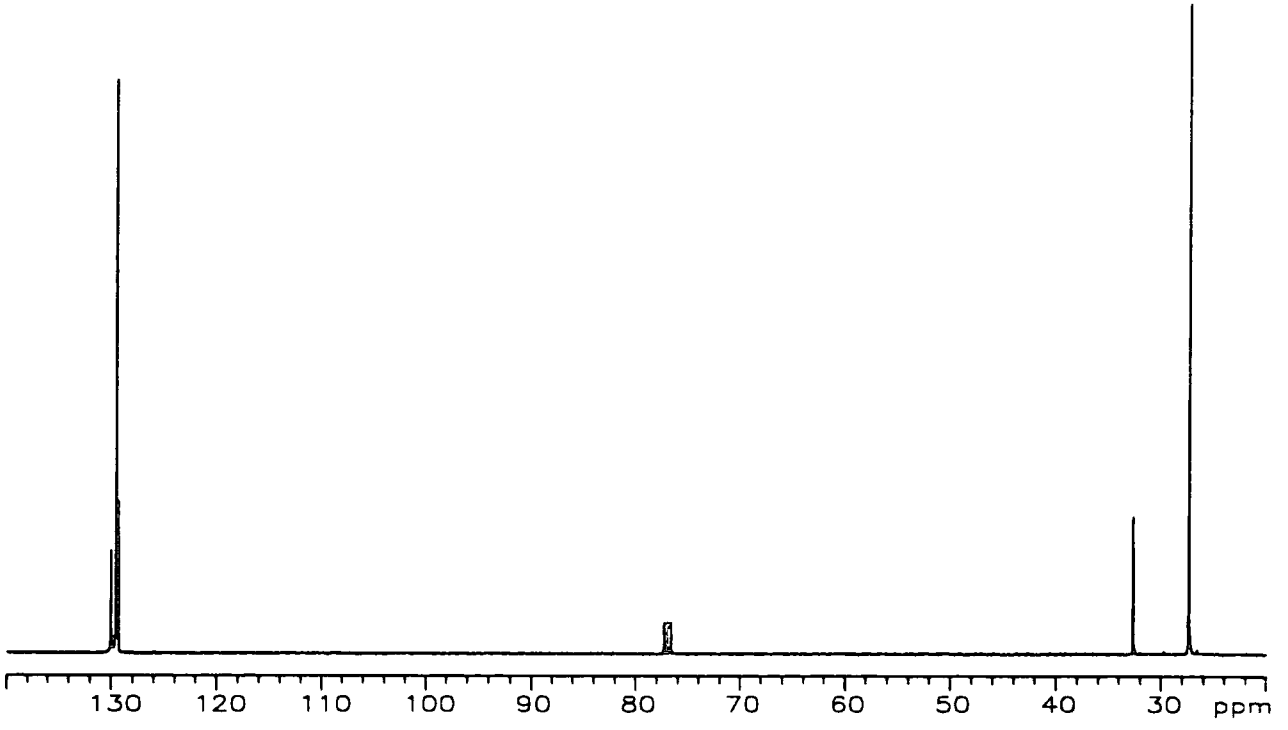

Appendix 2.2.a ^{13}C-NMR spectrum of poly(1-butenylene) initiated by W(CHtBu)(OtBu)2(NAr)

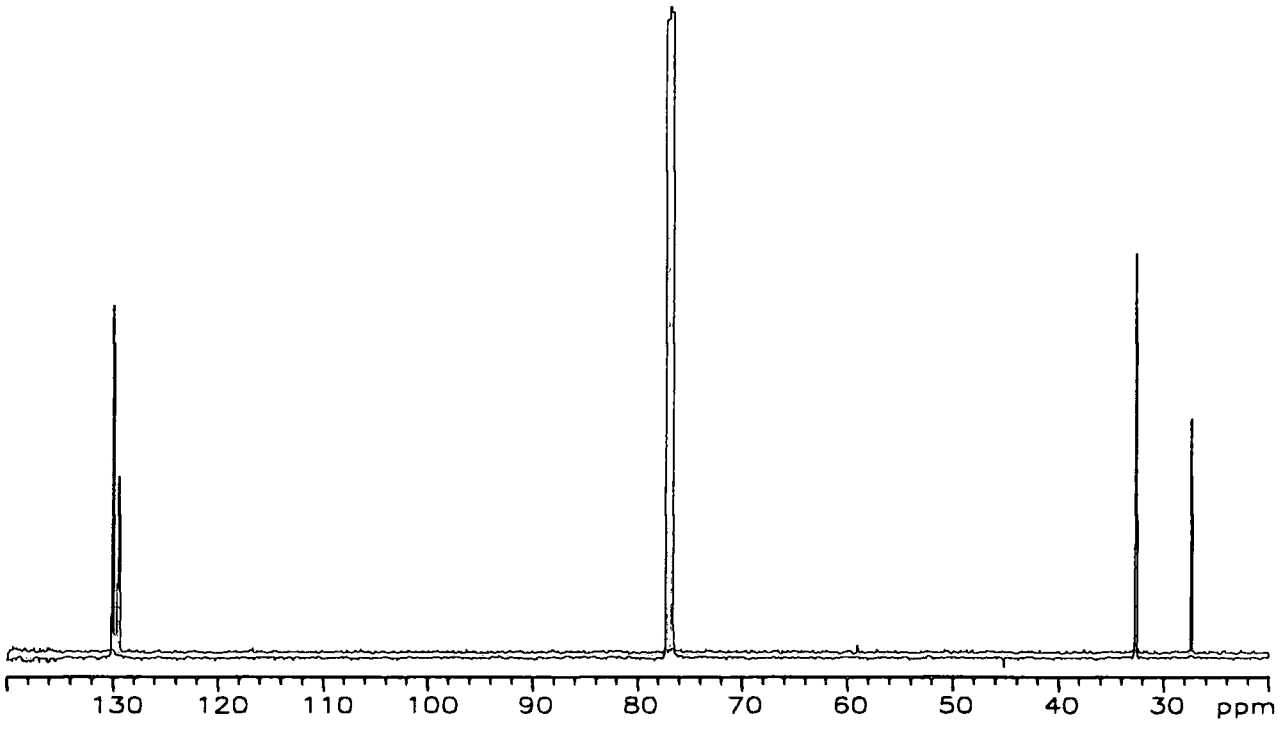

Appendix 2.2.b ^{13}C-NMR spectrum of poly(1-butenylene) initiated by $Mo(CH^tBu)(OC(CH_3)_3)_2(NAr)$

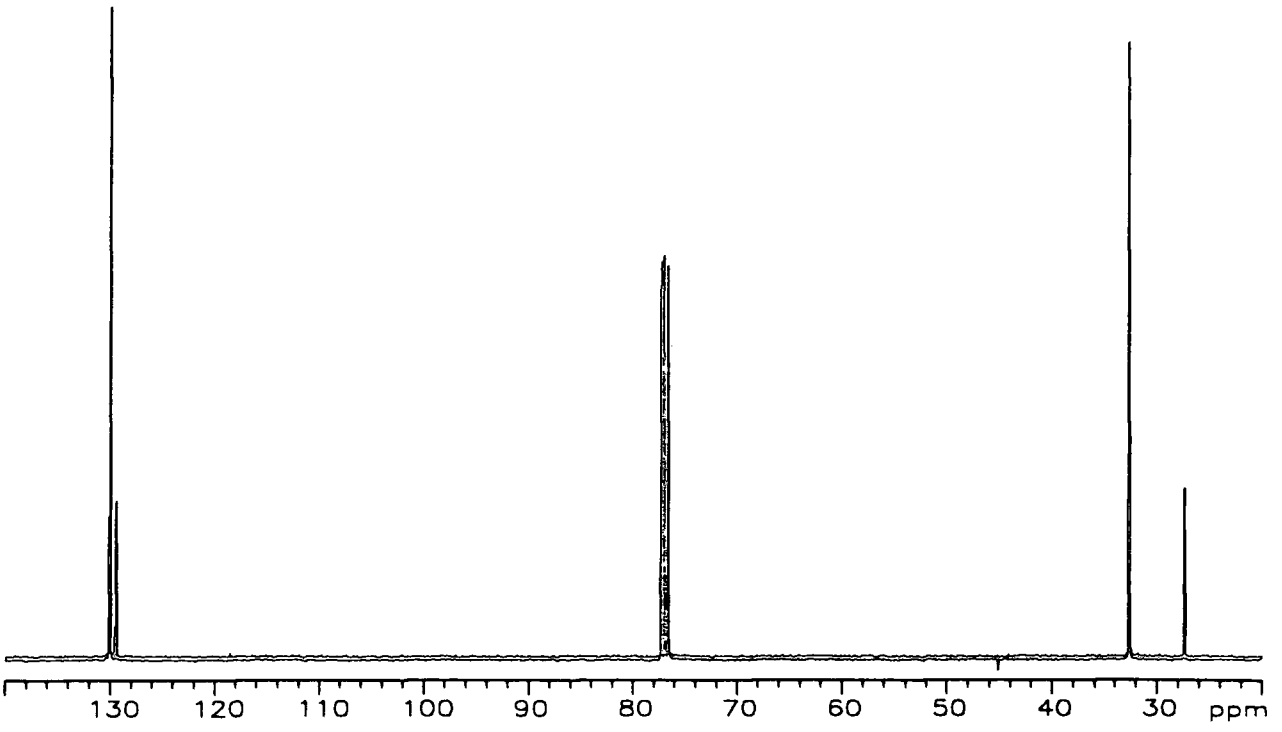

Appendix 2.2.c ^{13}C-NMR spectrum of poly(1-butenylene) initiated by $Mo(CH^tBu)(OC(CH_3)_2CF_3)_2(NAr)$

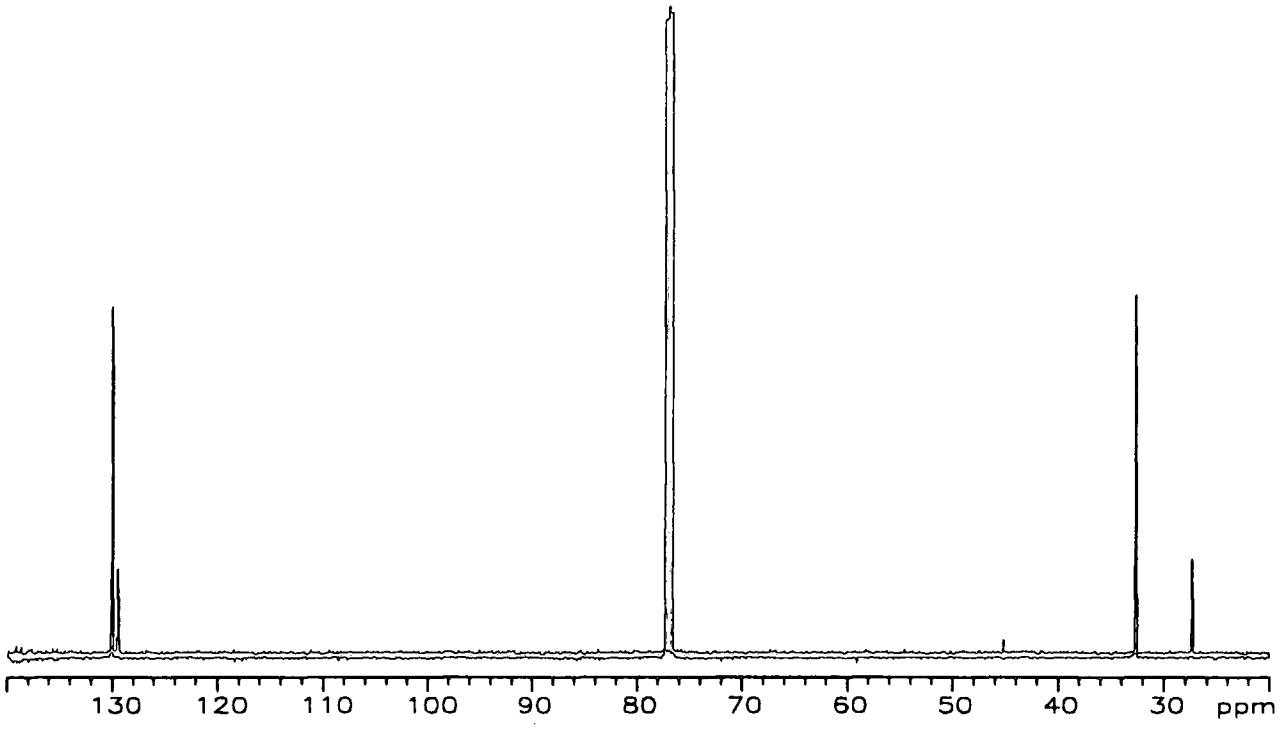

Appendix 2.2.d ^{13}C-NMR spectrum of poly(1-butenylene) initiated by $Mo(CH^tBu)(OC(CH_3)(CF_3)_2)_2(NAr)$

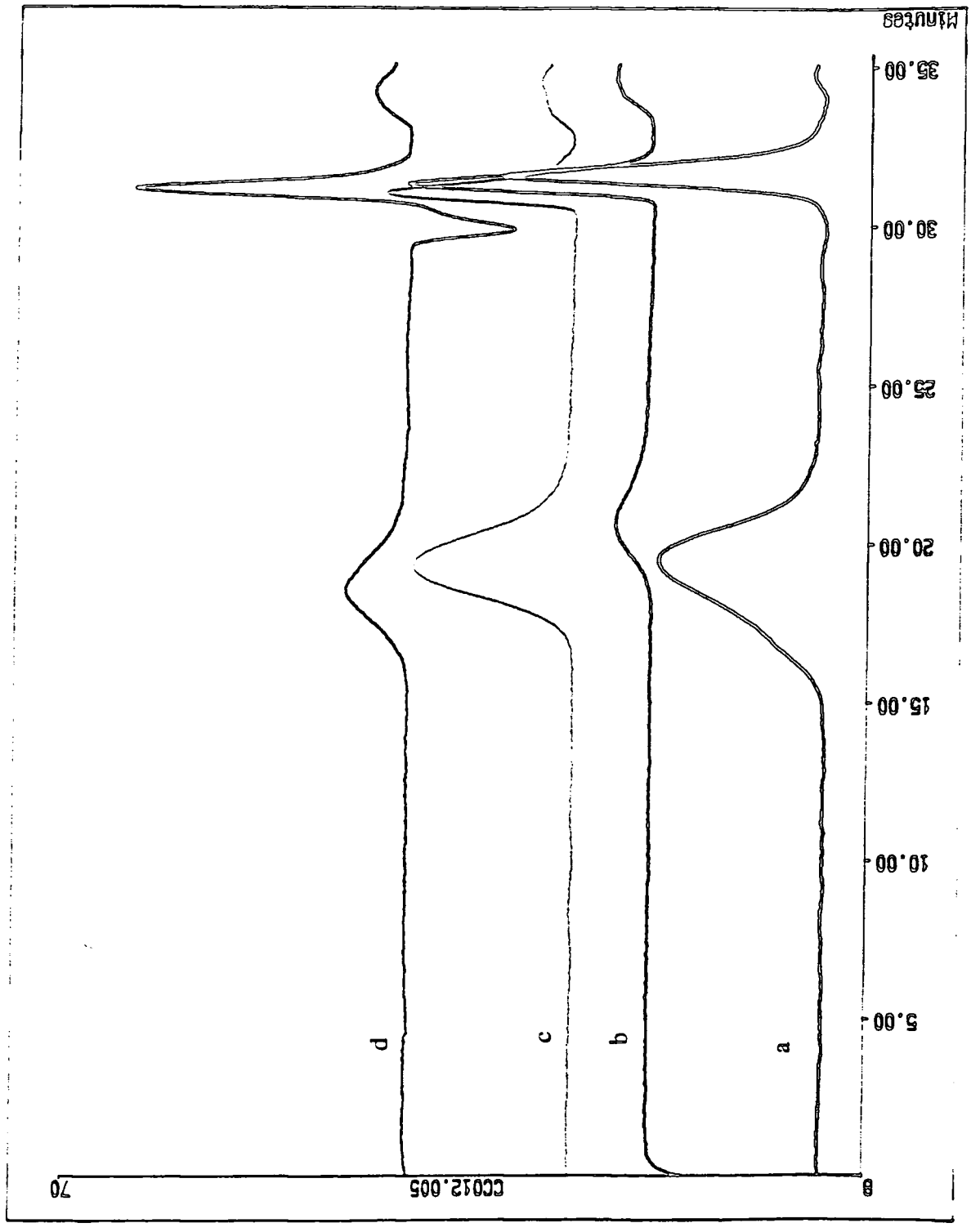

Appendix 2.3. GPC trace of poly(1-butenylene) initiated with

a $W(CH^tBu)(O^tBu)_2(NAr$

b $Mo(CH^tBu)(OC(CH_3)_3)_2(NAr)$

c $Mo(CH^tBu)(OC(CH_3)_2CF_3)_2(NAr)$

d $Mo(CH^tBu)(OC(CH_3)(CF_3)_2)_2(NAr)$

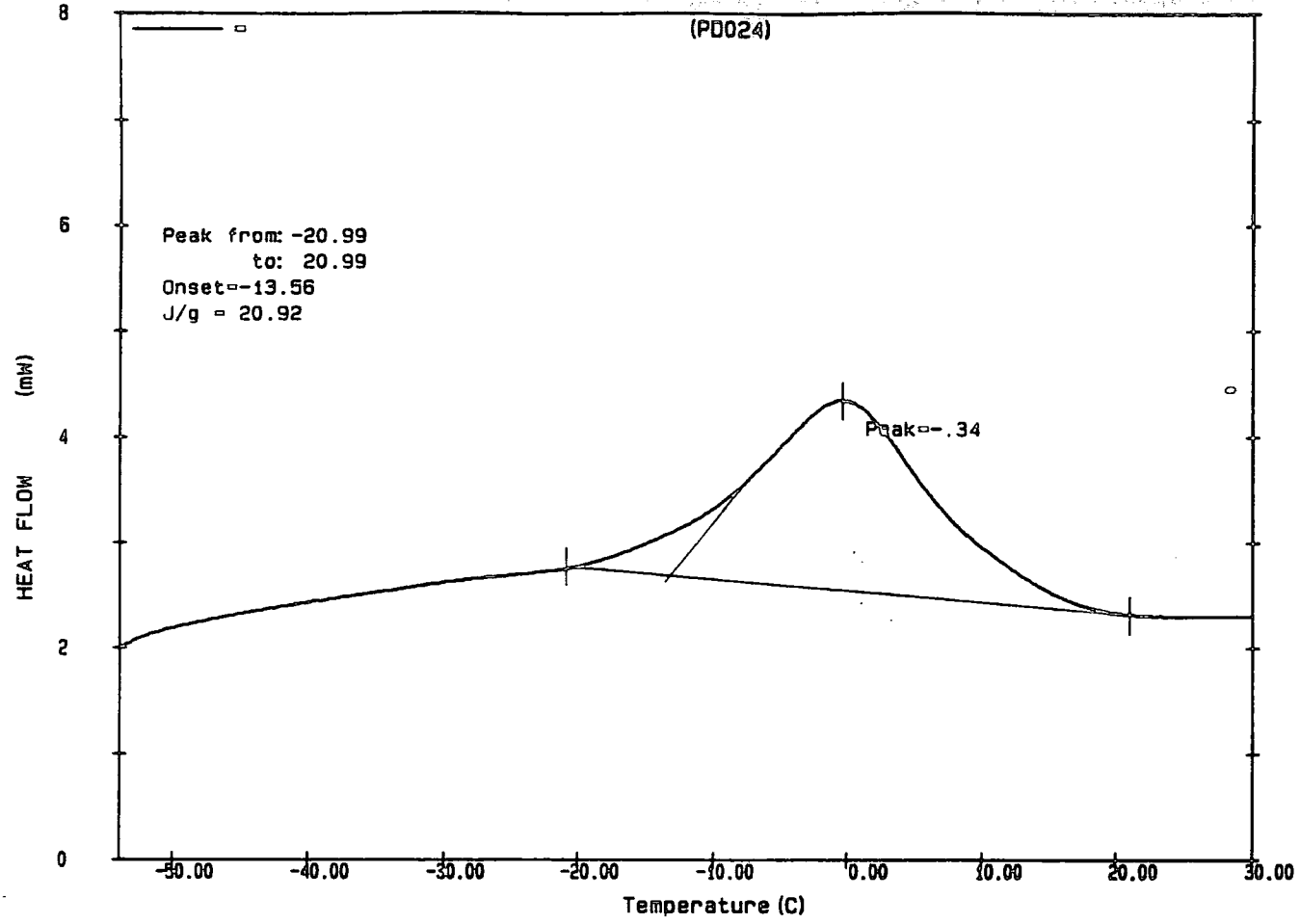

Appendix 2.4.b DSC trace of poly(1-butenylene) initiated with $Mo(CH^tBu)(OC(CH_3)_3)_2(NAr)$

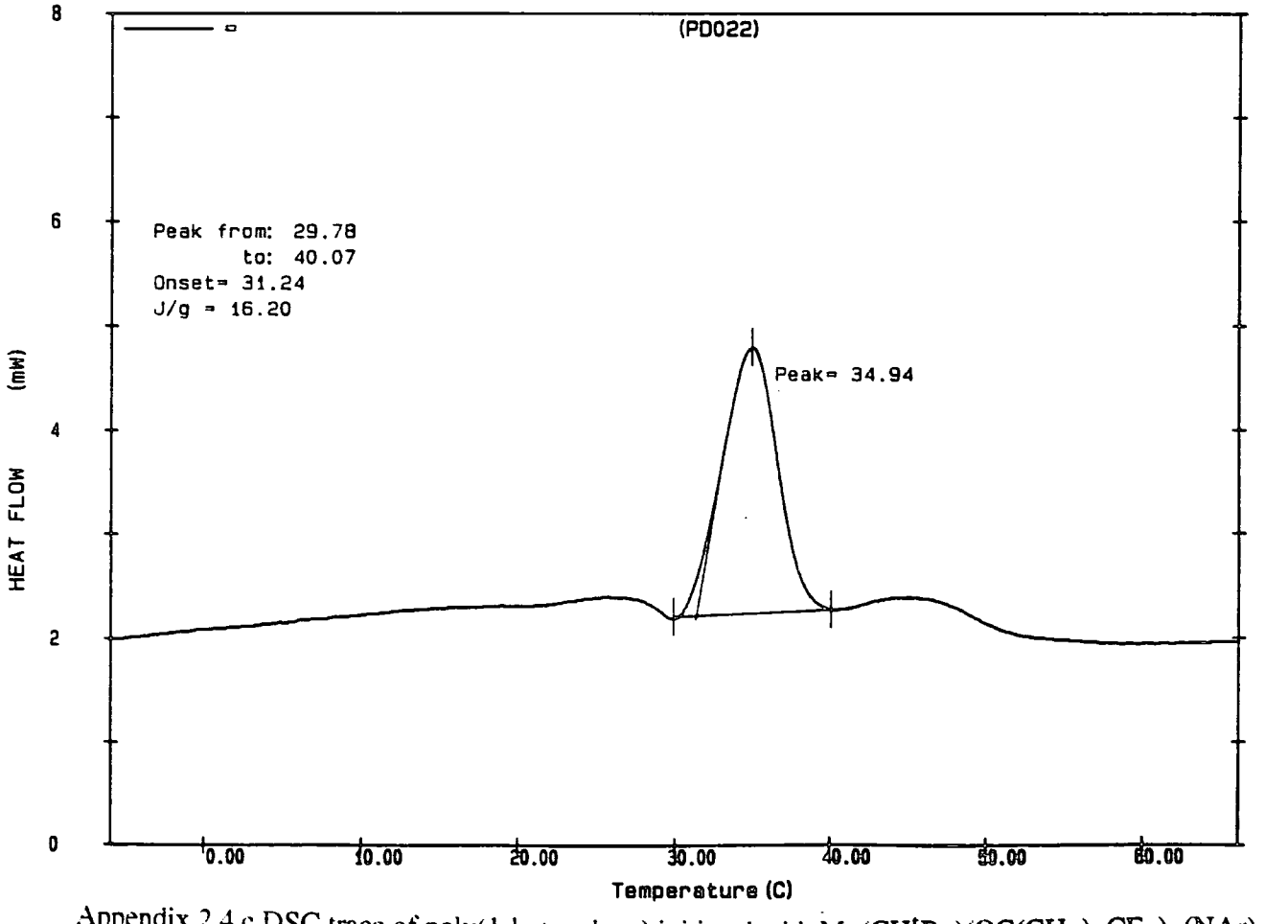

Appendix 2.4.c DSC trace of poly(1-butenylene) initiated with $Mo(CH^tBu)(OC(CH_3)_2CF_3)_2(NAr)$

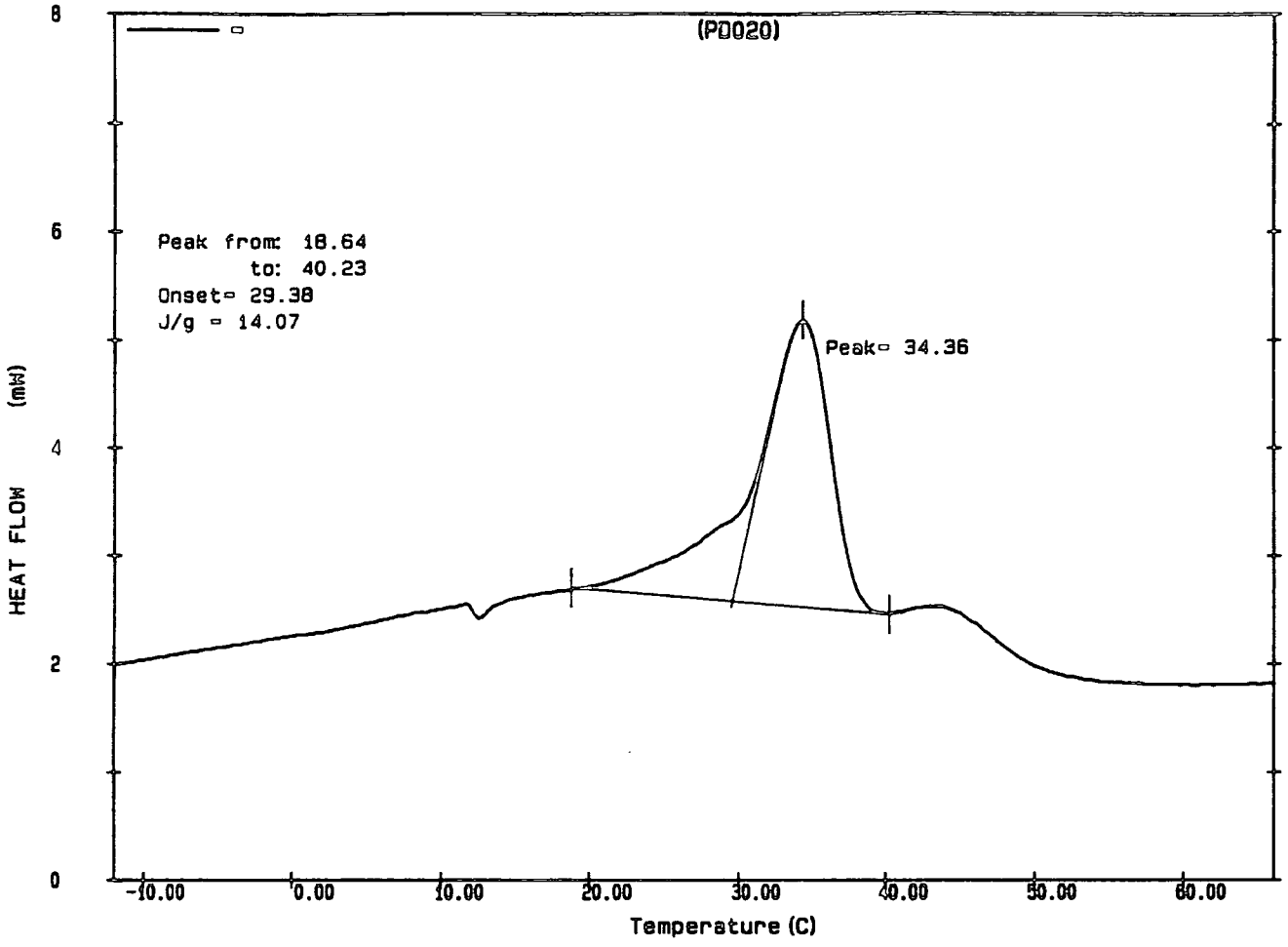

Appendix 2.4.d DSC trace of poly(1-butenylene) initiated with $Mo(CH^tBu)(OC(CH_3)(CF_3)_2)_2(NAr)$

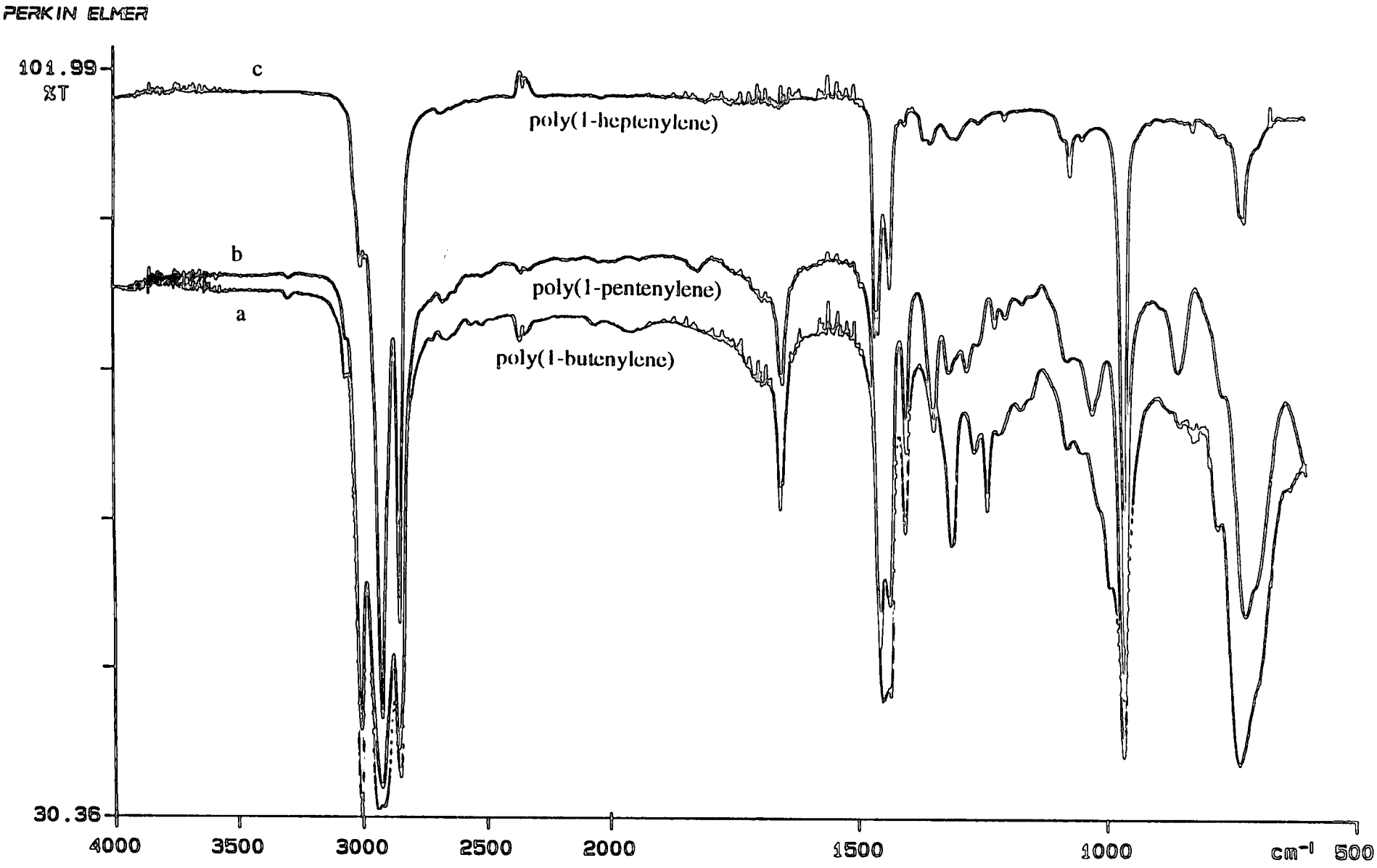

Appendix 2.5 IR spectra of a) poly(1-butenylene), b) poly(1-pentenylene), c) poly(1-heptenylene)

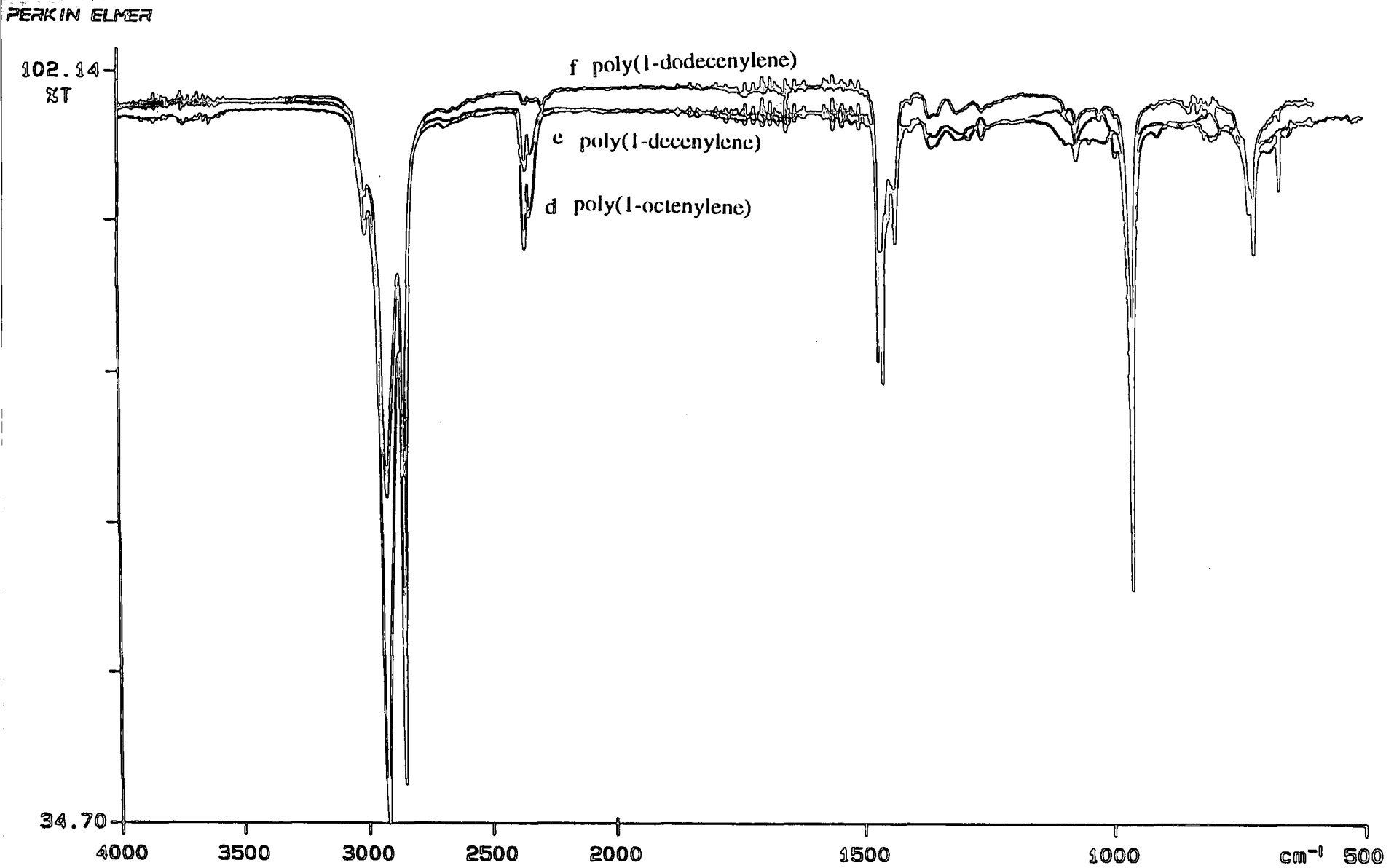

Appendix 2.5 IR spectra of d) poly(1-octenylene), e) poly(1-decenylene), f) poly(1-dodecenylene)

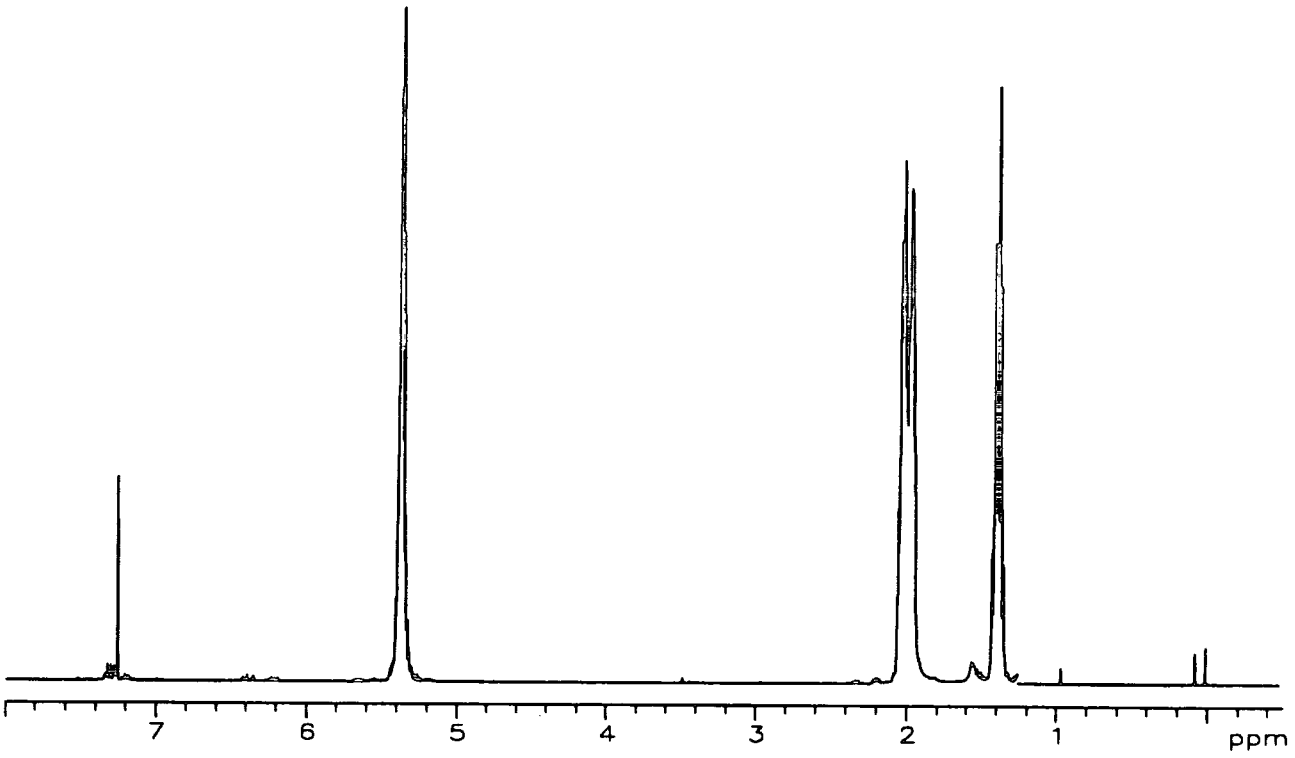

Appendix 2.6 ^{1}H-NMR spectrum of poly(1-pentenylene) initiated by W(CH^{t}Bu)(O^{t}Bu)$_2$(NAr)

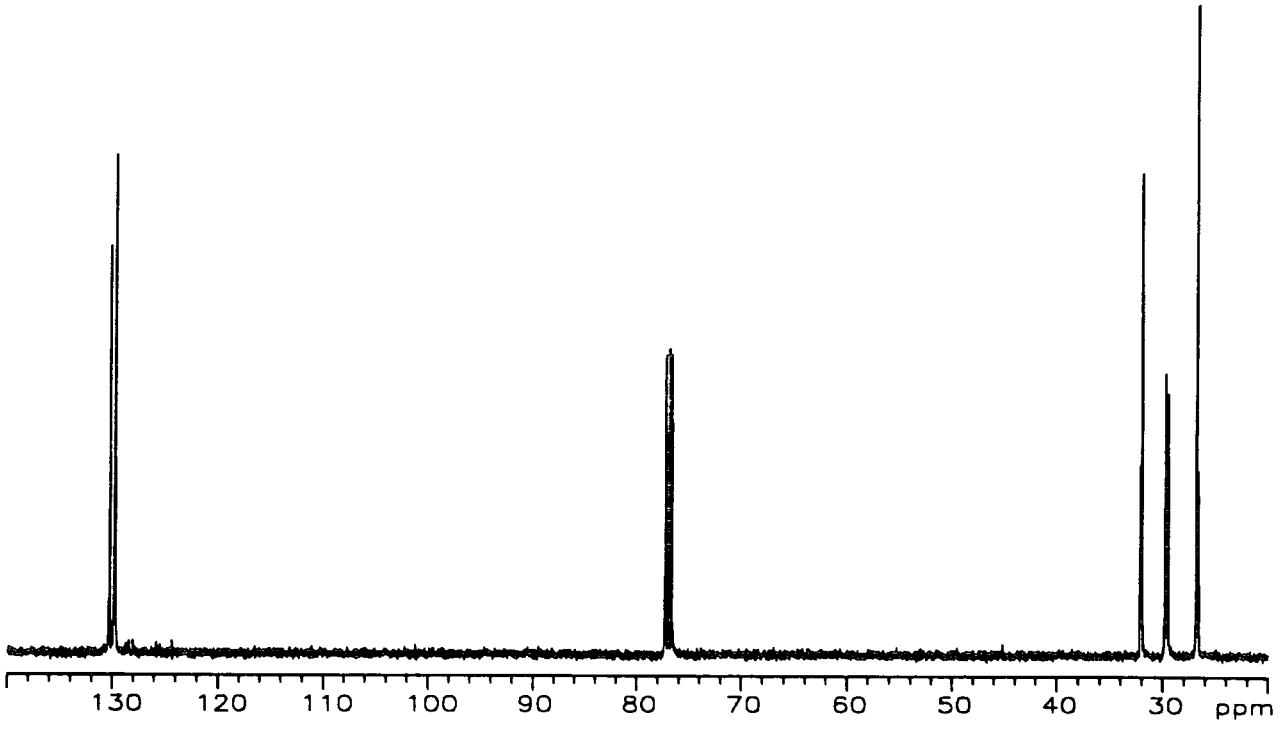

Appendix 2.8.a ^{13}C-NMR spectrum of poly(1-pentenylene) initiated by W(CHtBu)(OtBu)2(NAr)

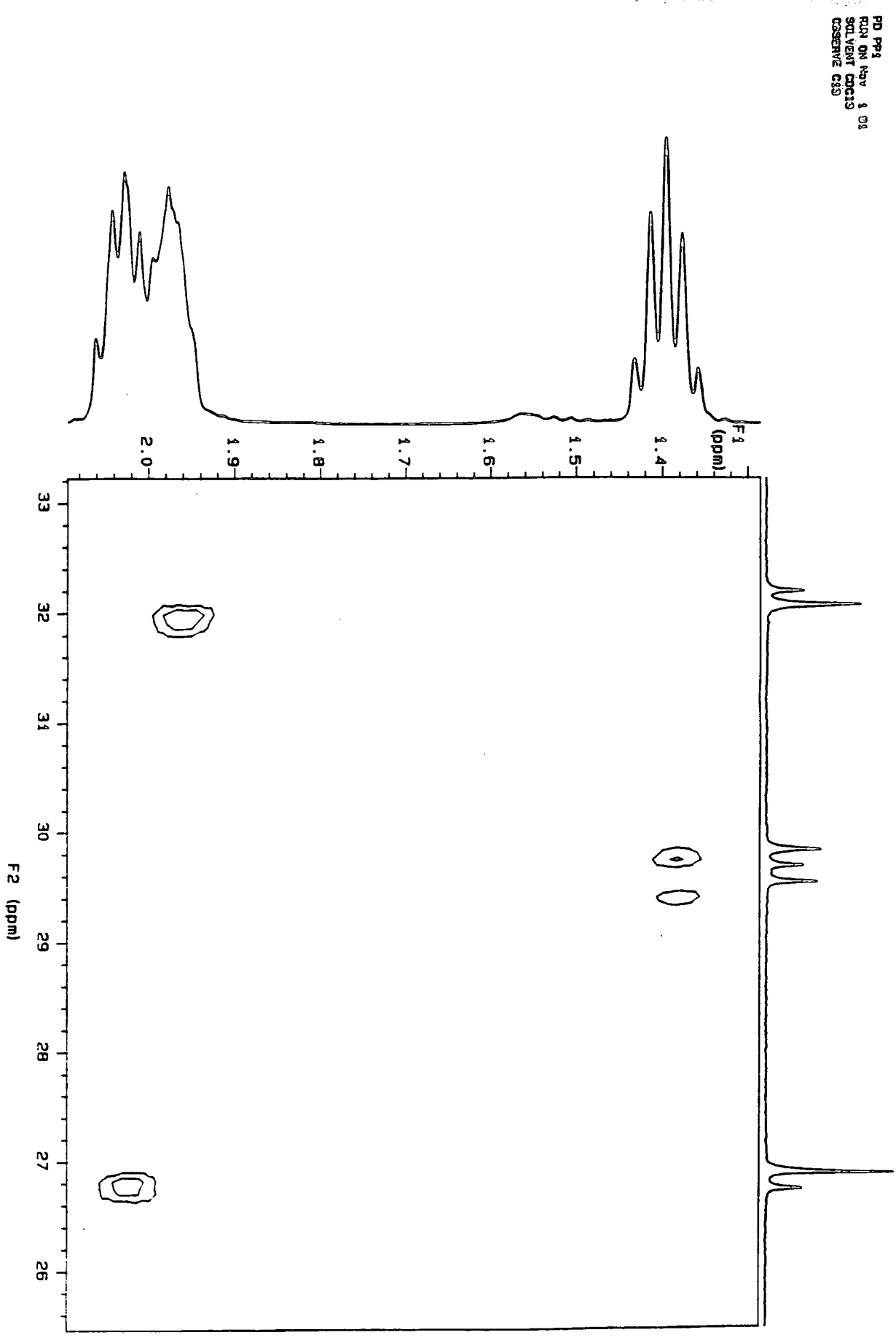

Appendix 2.7 HETCOR spectum of poly(1-pentenylene) initiated with $W(CH^tBu)(O^tBu)_2(NAr)$

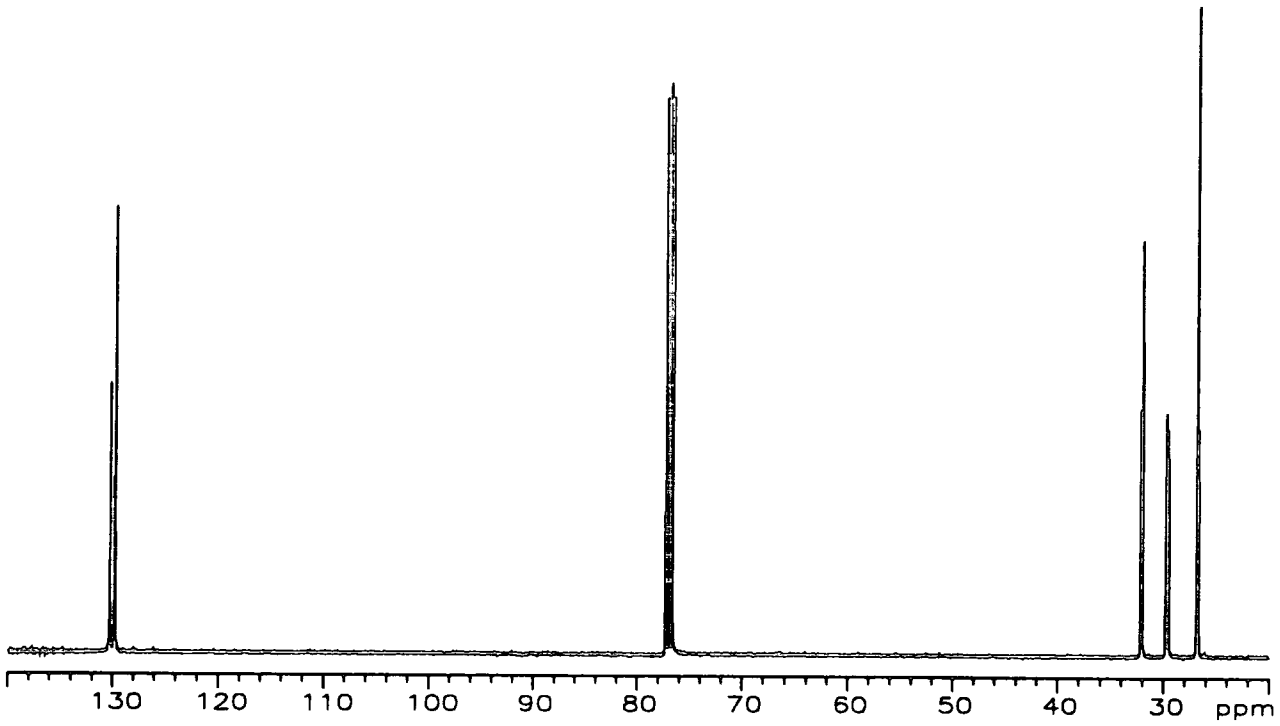

Appendix 2.8.b ^{13}C-NMR spectrum of poly(1-pentenylene) initiated by $Mo(CH^tBu)(OC(CH_3)_3)_2(NAr)$

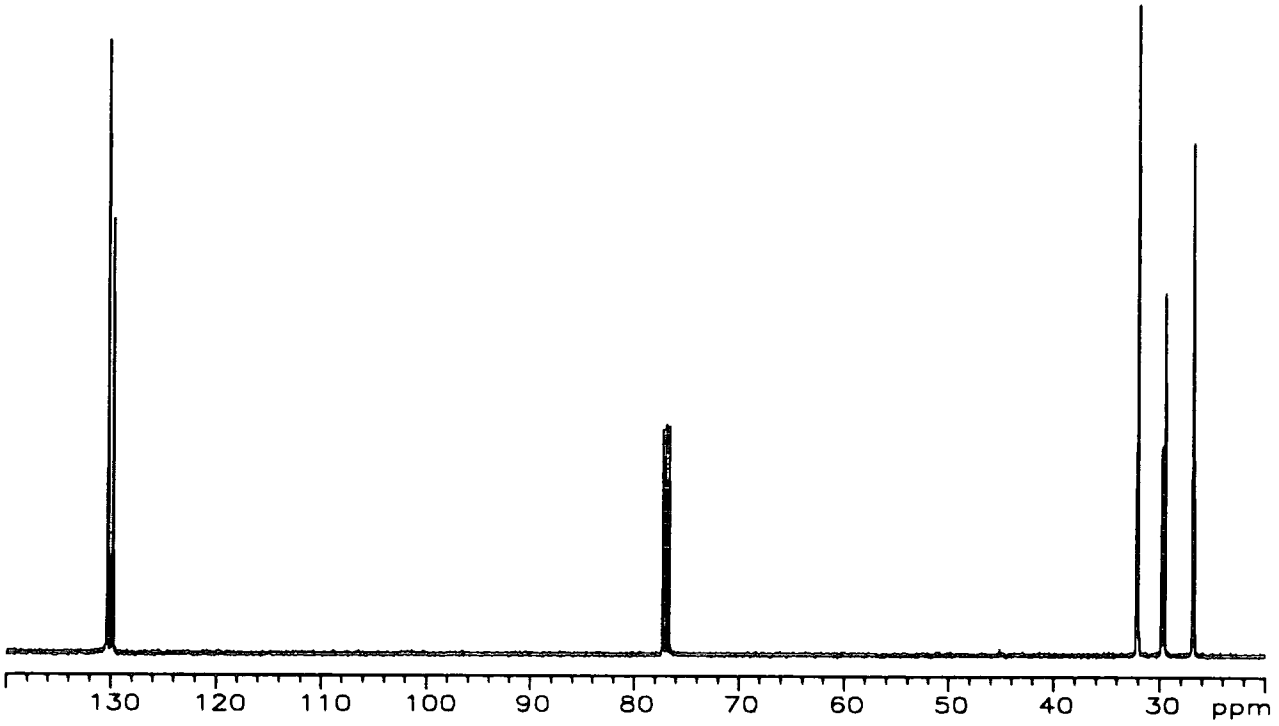

Appendix 2.8.c ^{13}C-NMR spectrum of poly(1-pentenylene) initiated by $Mo(CH^tBu)(OC(CH_3)_2CF_3)_2(NAr)$

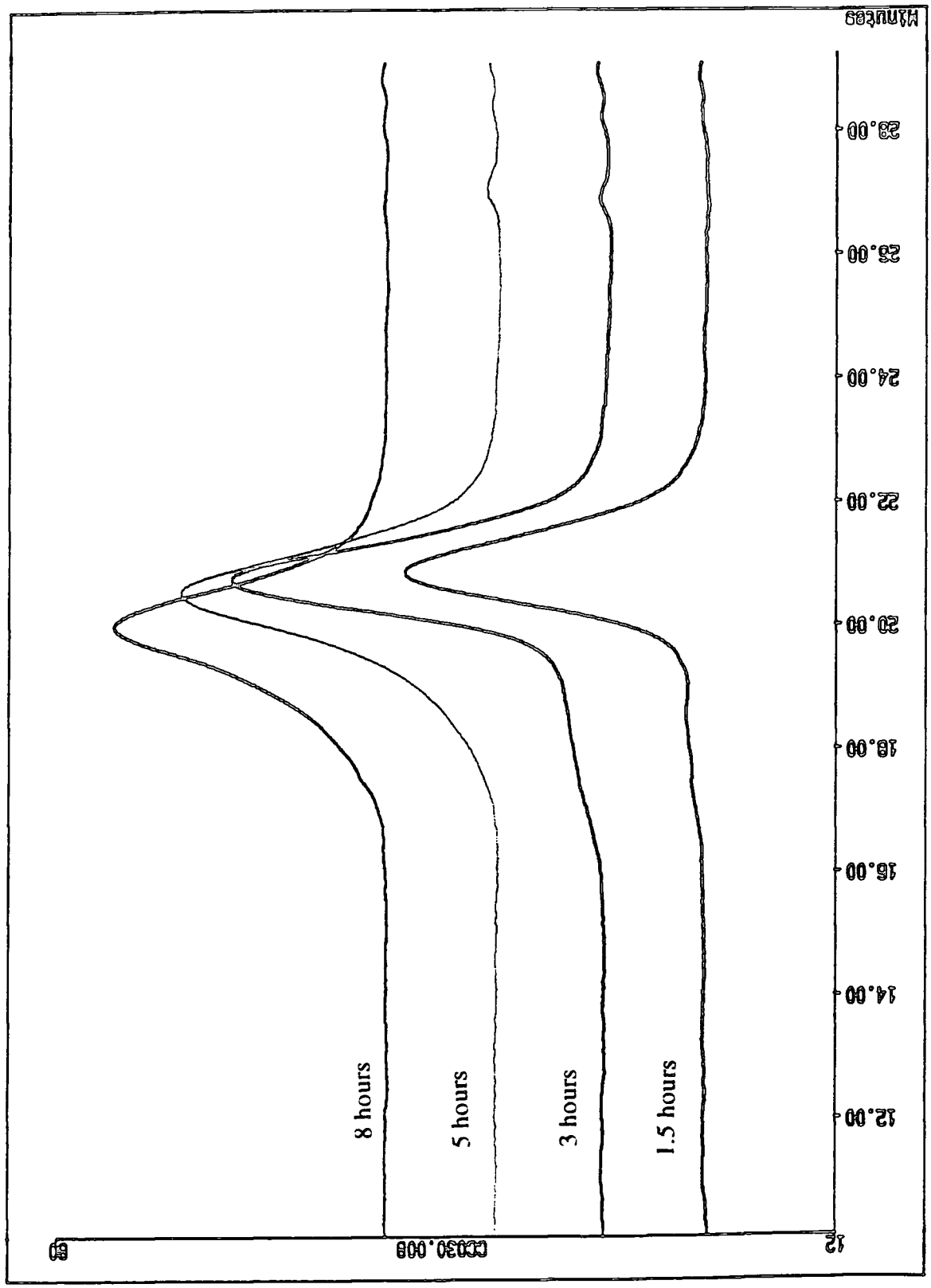

Appendix 2.9.a GPC trace of poly(1-pentenylene) initiated with $W(CH^tBu)(O^tBu)_2(NAr)$

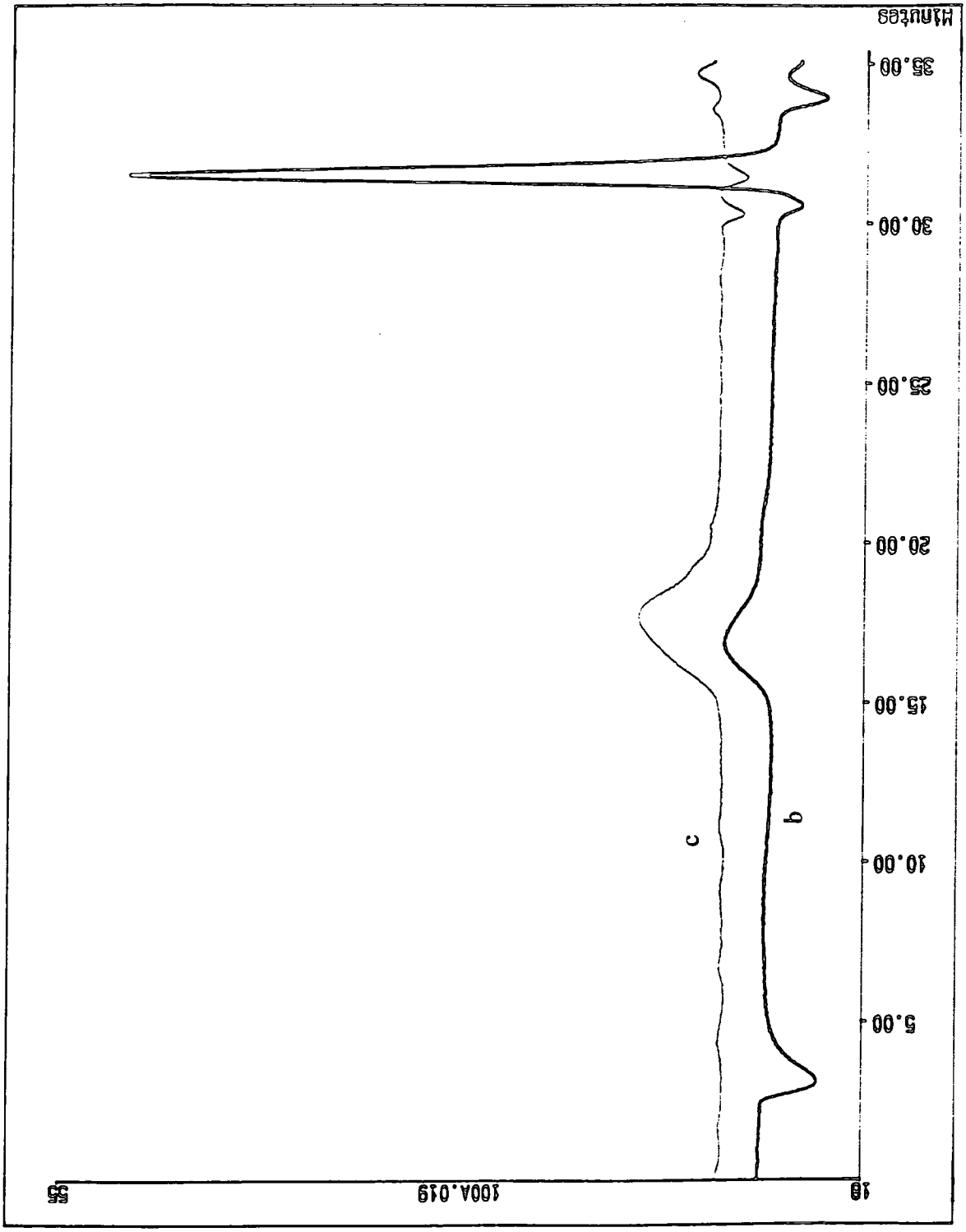

Appendix 2.9.b GPC trace of poly(1-pentenylene) initiated with $Mo(CH^tBu)(OC(CH_3)_3)_2(NAr)$

Appendix 2.9.c GPC trace of poly(1-pentenylene) initiated with $Mo(CH^tBu)(OC(CH_3)_2CF_3)_2(NAr)$

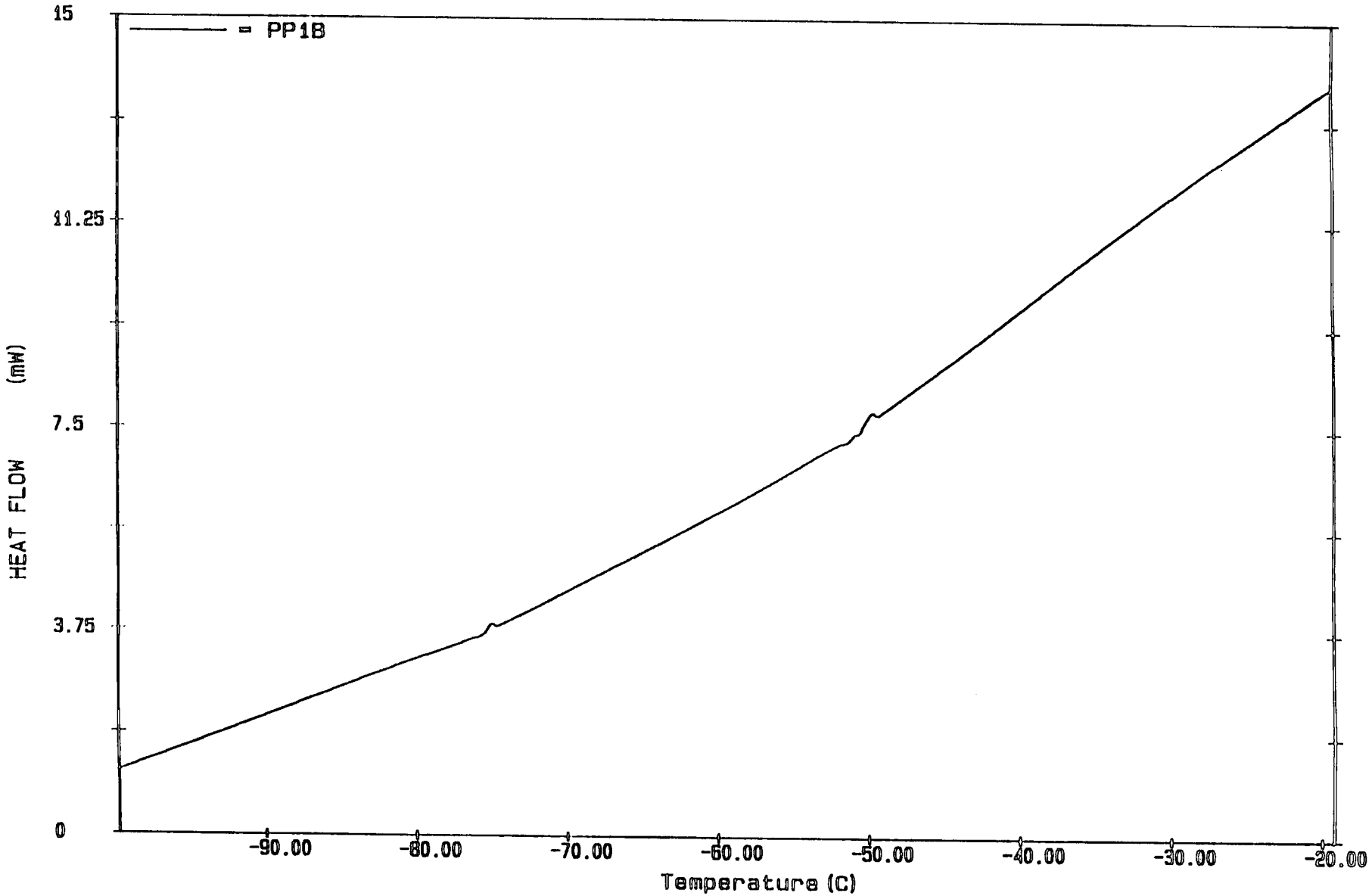

Appendix 2.10. DSC trace of poly(1-pentenylene) initiated with $W(CH^tBu)(O^tBu)_2(NAr)$

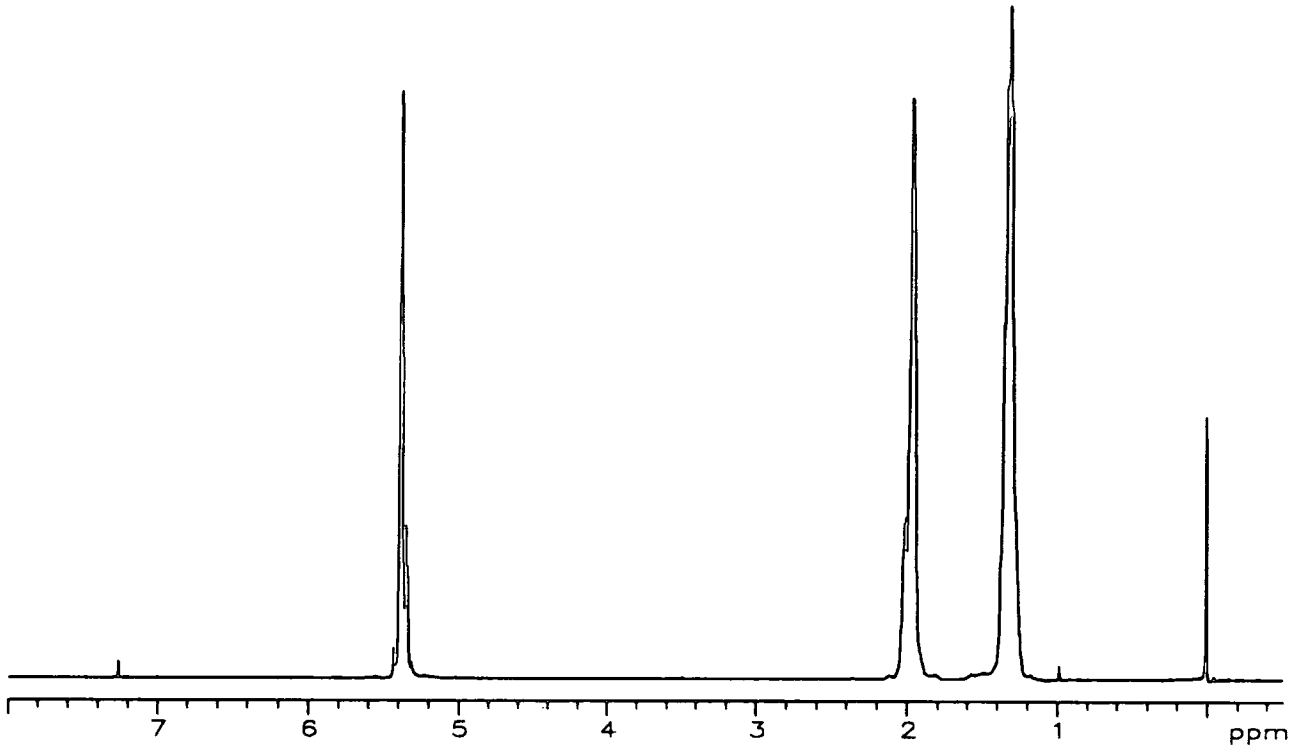

Appendix 2.11 ^{1}H-NMR spectrum of poly(1-heptenylene) initiated by W(CH^{t}Bu)(O^{t}Bu)$_2$(NAr)

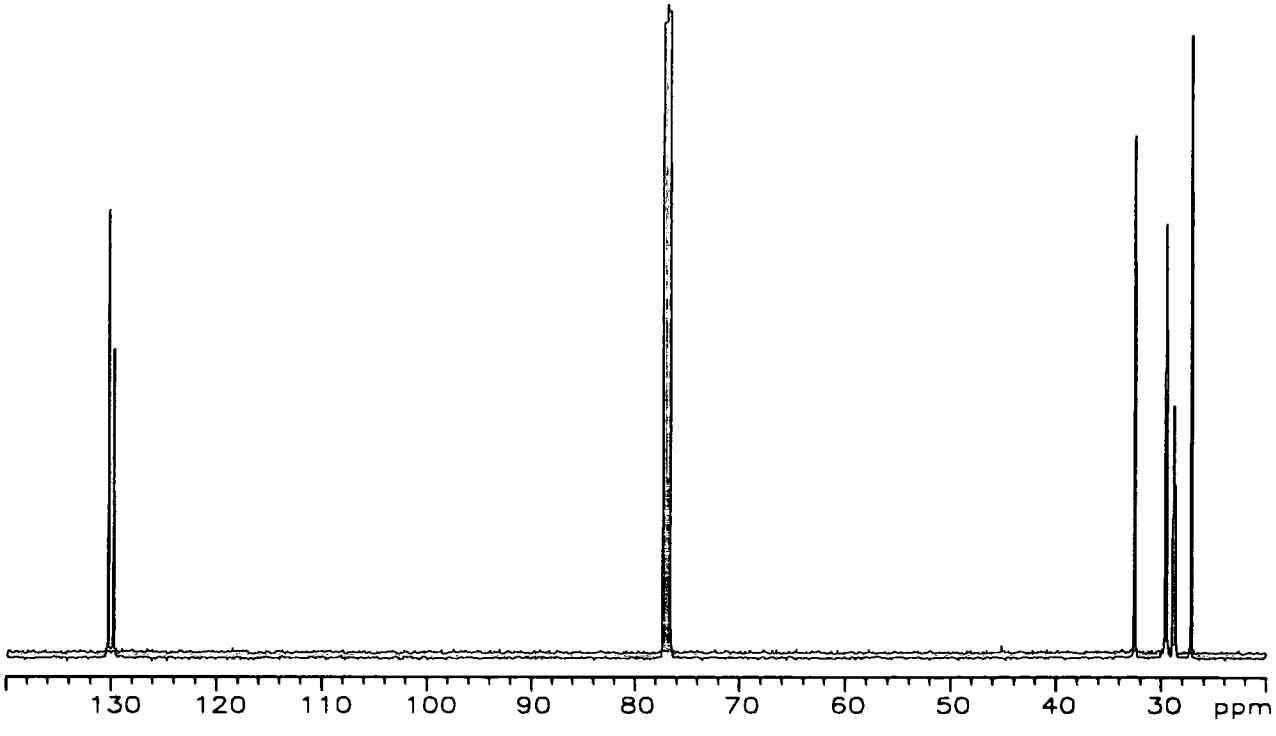

Appendix 2.12.a ^{13}C-NMR spectrum of poly(1-heptenylene) initiated by Mo(CH^{t}Bu)(OC(CH$_3$)$_3$)$_2$(NAr)

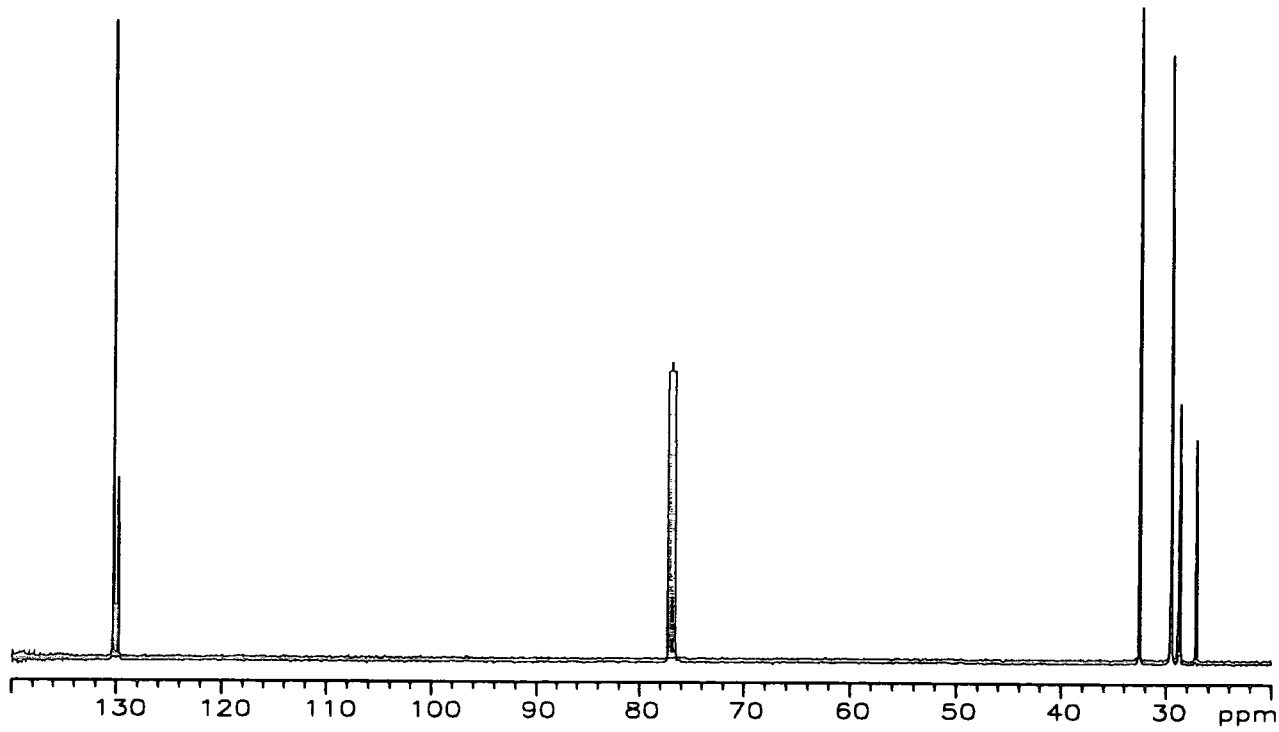

Appendix 2.12.b ^{13}C-NMR spectrum of poly(1-heptenylene) initiated by $Mo(CH^tBu)(OC(CH_3)_2CF_3)_2(NAr)$

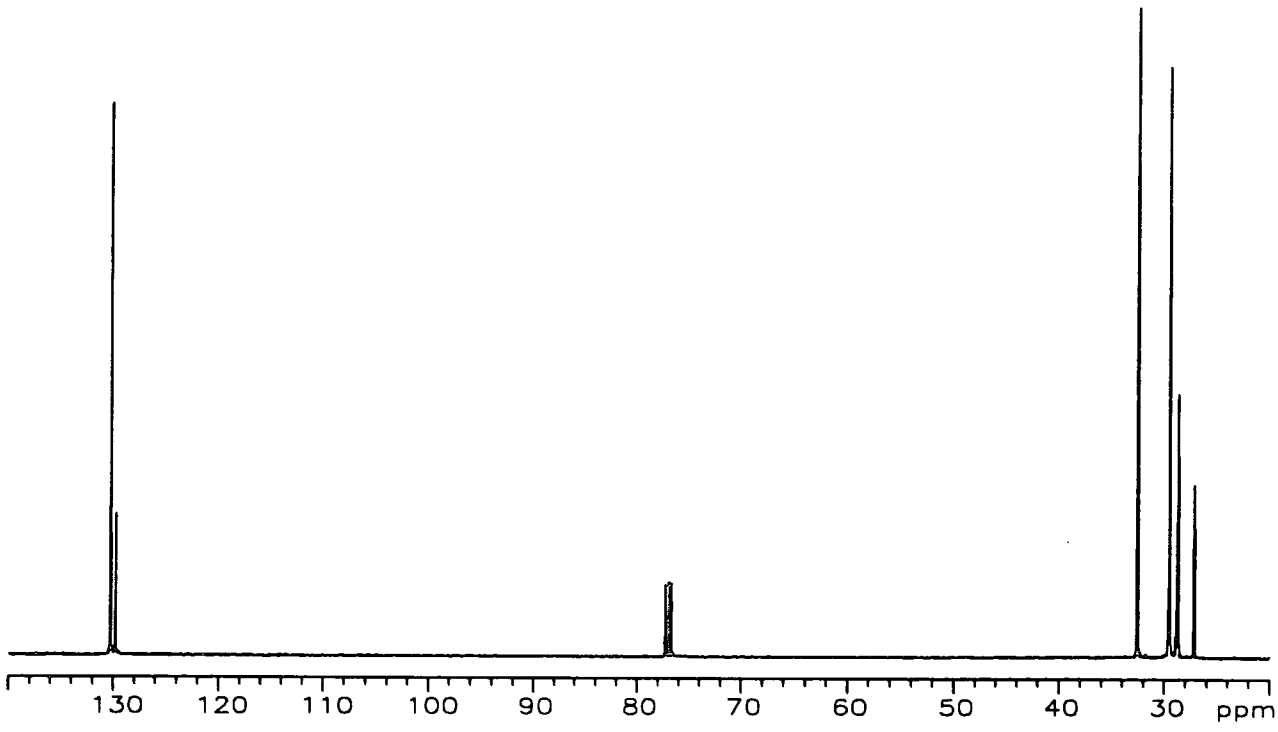

Appendix 2.12.c ^{13}C-NMR spectrum of poly(1-heptenylene) initiated by $Mo(CH^tBu)(OC(CH_3)(CF_3)_2)_2(NAr)$

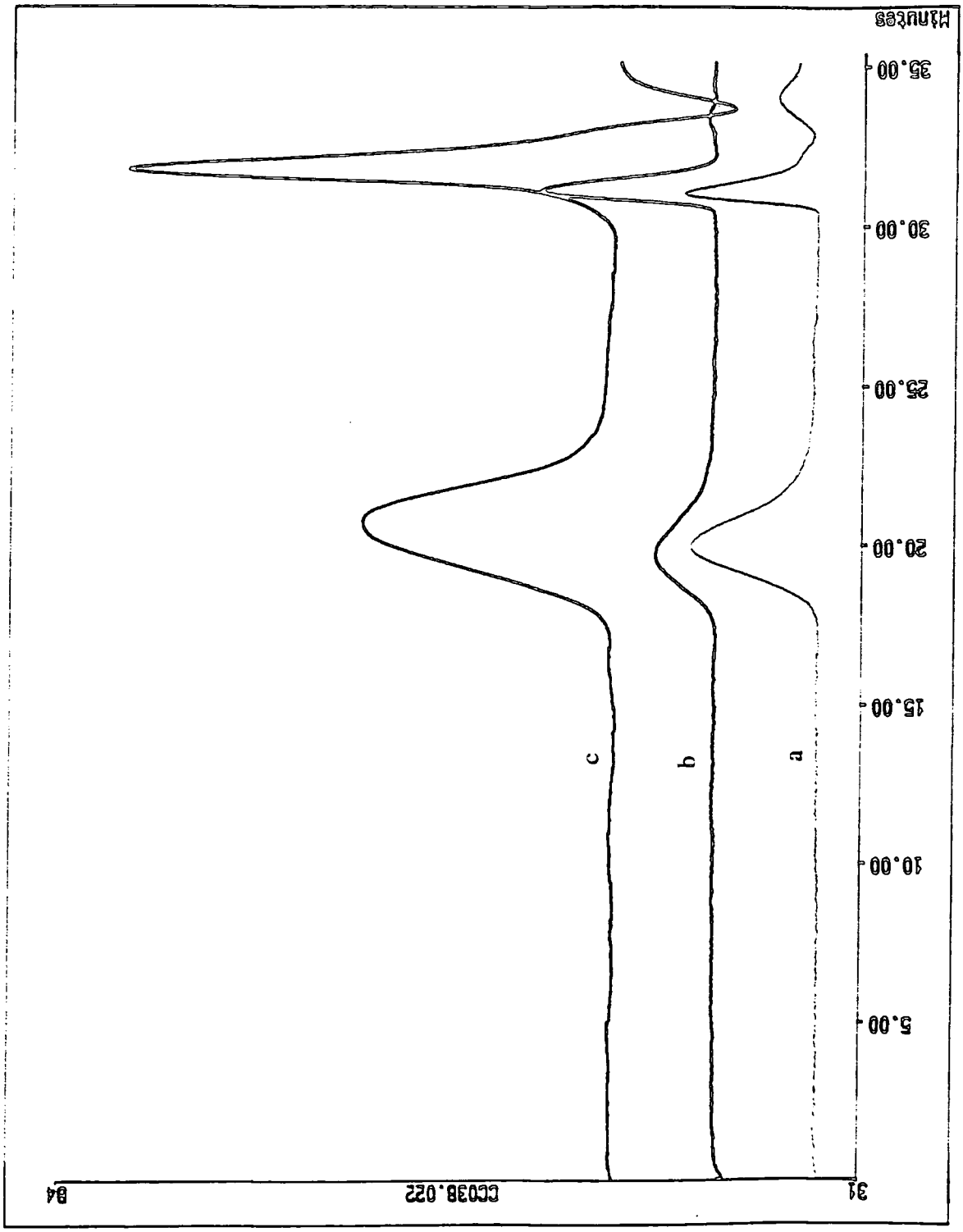

Appendix 2.13.a GPC trace of poly(1-heptenylene) initiated with $Mo(CH^tBu)(OC(CH_3)_3)_2(NAr)$

Appendix 2.13.b GPC trace of poly(1-heptenylene) initiated with $Mo(CH^tBu)(OC(CH_3)_2CF_3)_2(NAr)$

Appendix 2.13.c GPC trace of poly(1-heptenylene) initiated with $Mo(CH^tBu)(OC(CH_3)(CF_3)_2)_2(NAr)$

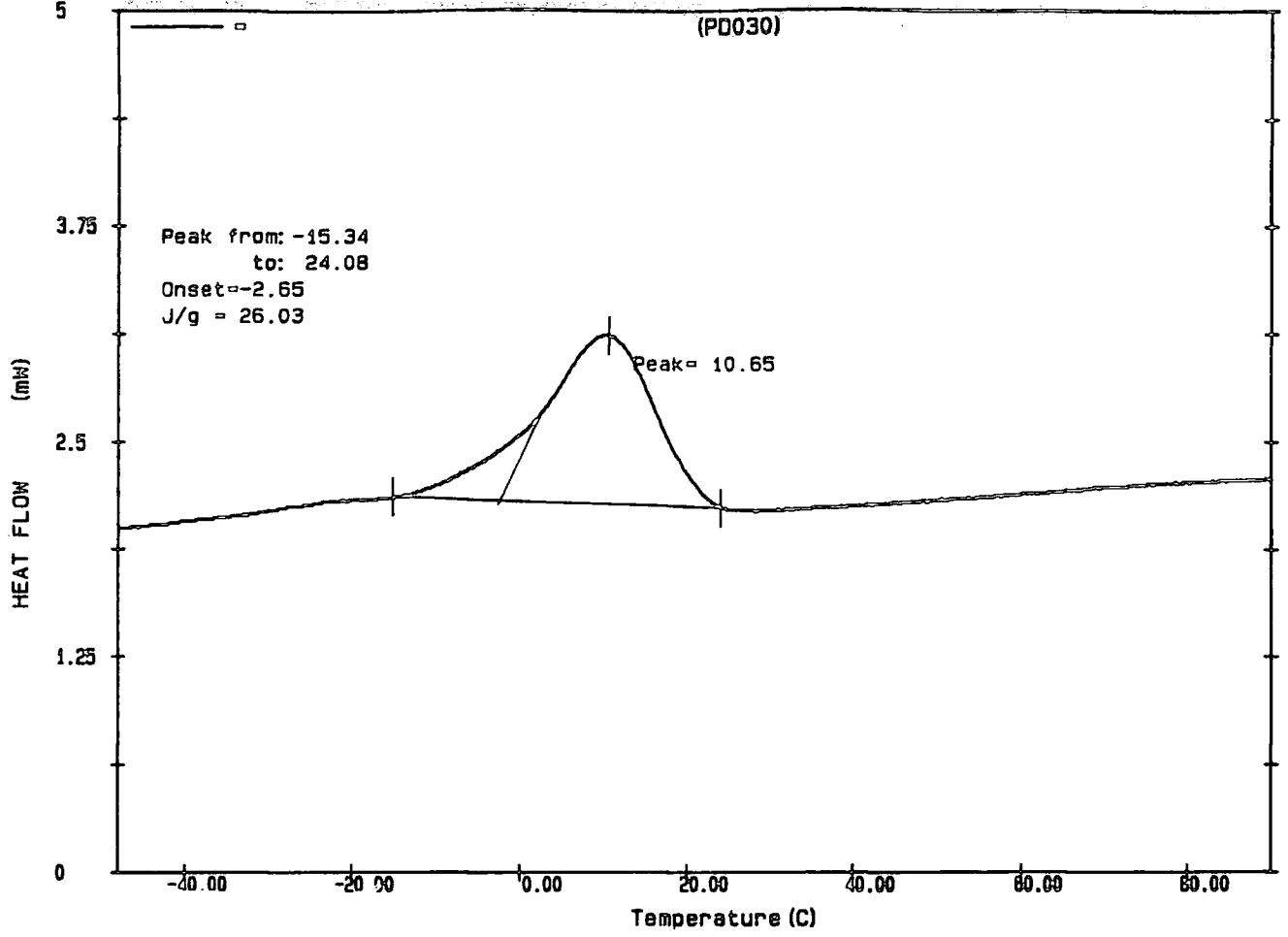

Appendix 2.14.a DSC trace of poly(1-heptenylene) initiated with $Mo(CH^tBu)(OC(CH_3)_3)_2(NAr)$

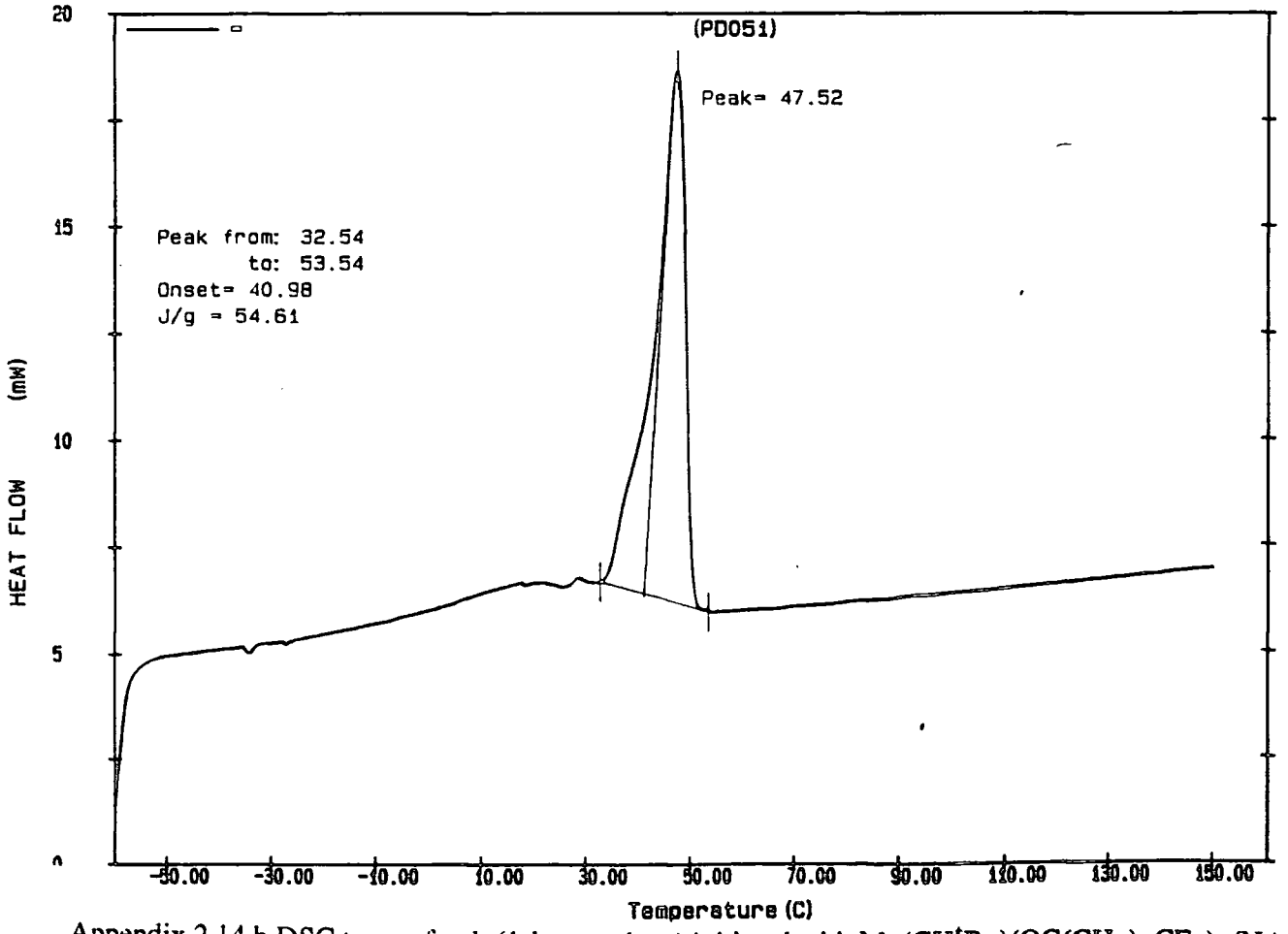

Appendix 2.14.b DSC trace of poly(1-heptenylene) initiated with $Mo(CH^tBu)(OC(CH_3)_2CF_3)_2(NAr)$

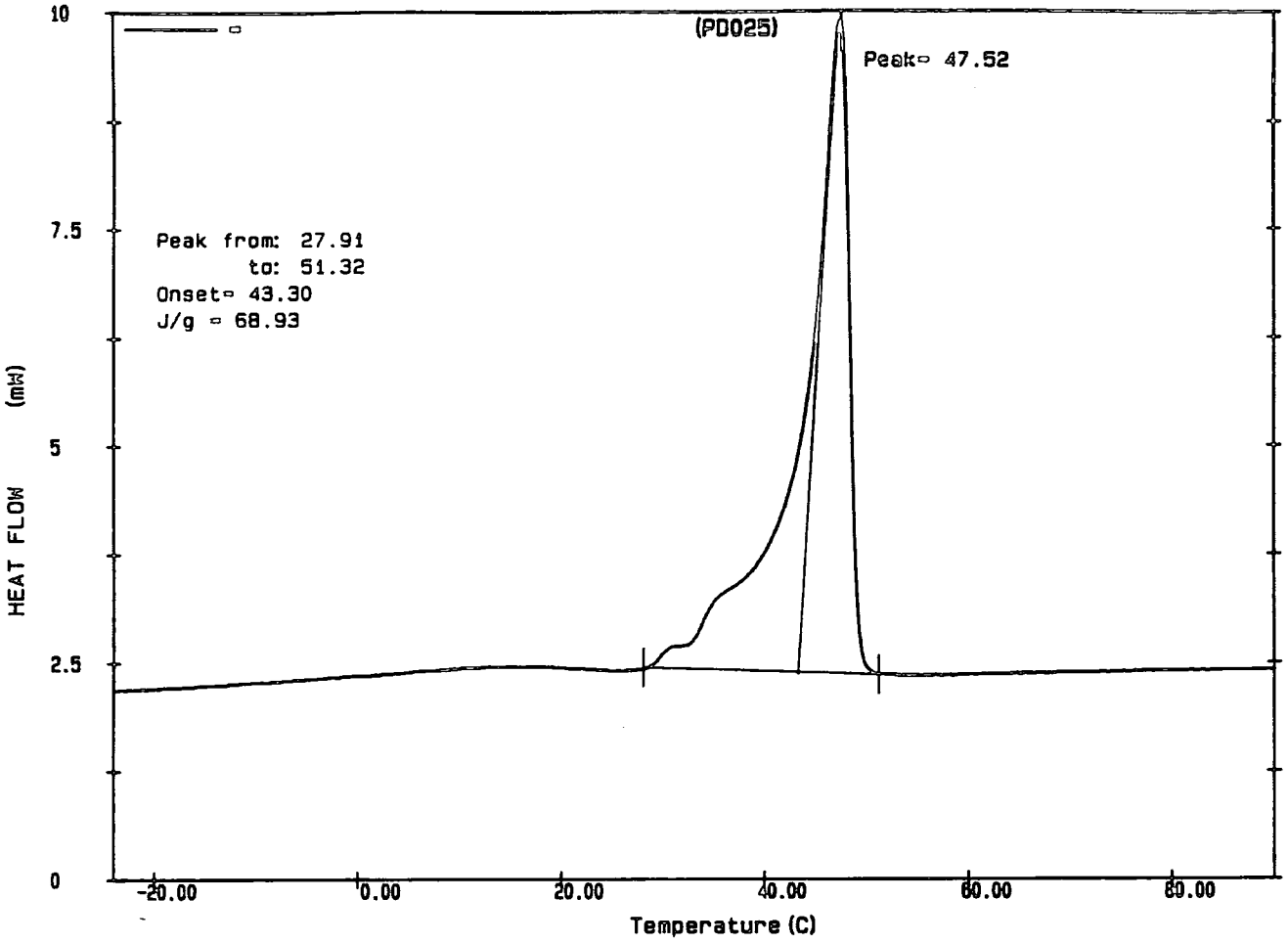

Appendix 2.14.c DSC trace of poly(1-heptenylene) initiated with $Mo(CH^tBu)(OC(CH_3)(CF_3)_2)_2(NAr)$

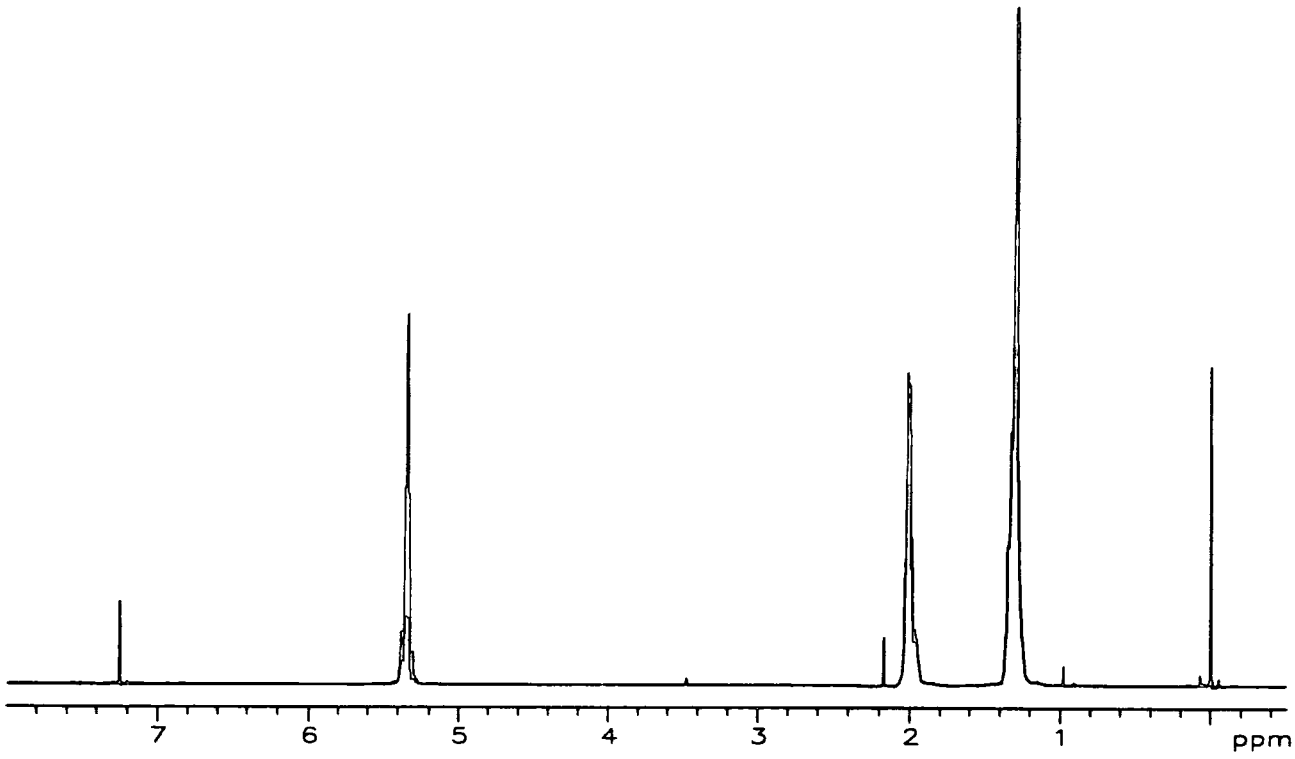

Appendix 2.15 ^{1}H-NMR spectrum of poly(1-octenylene) initiated by W(CH^{t}Bu)(O^{t}Bu)$_2$(NAr)

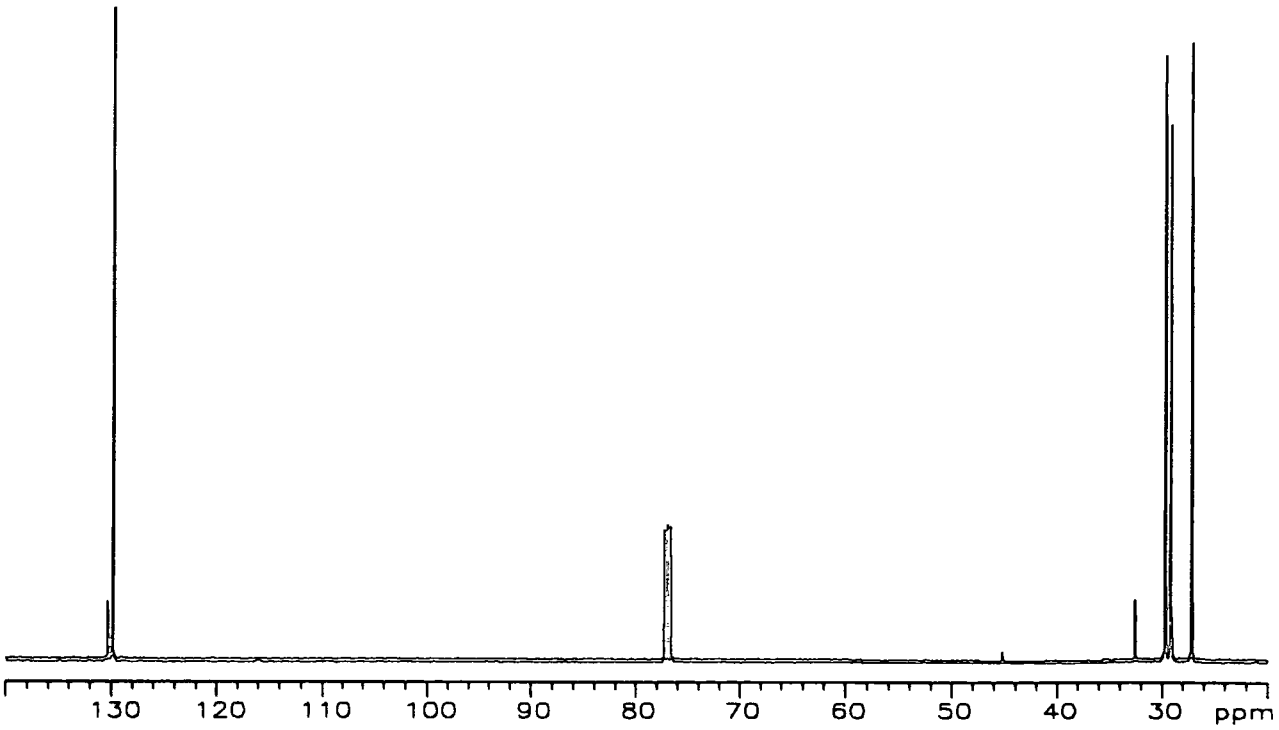

Appendix 2.16.a ^{13}C-NMR spectrum of poly(1-octenylene) initiated by W(CHtBu)(OtBu)2(NAr)

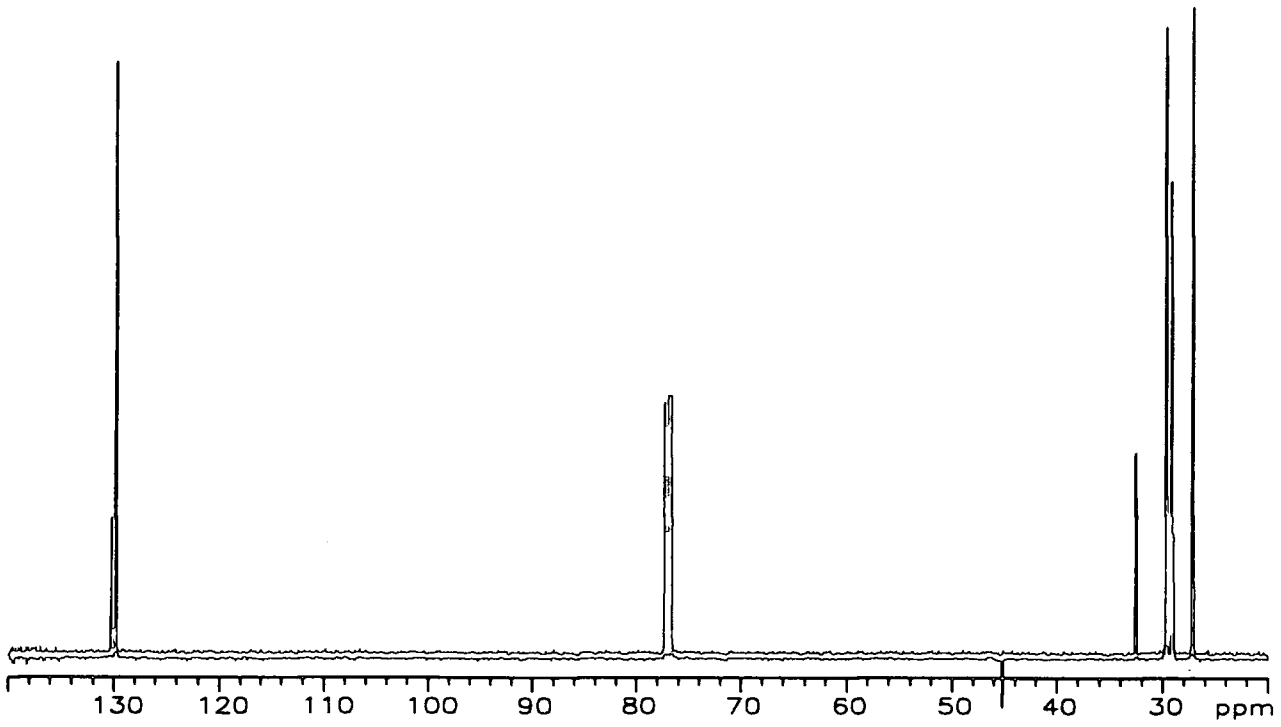

Appendix 2.16.b ^{13}C-NMR spectrum of poly(1-octenylene) initiated by $Mo(CH^tBu)(OC(CH_3)_3)_2(NAr)$

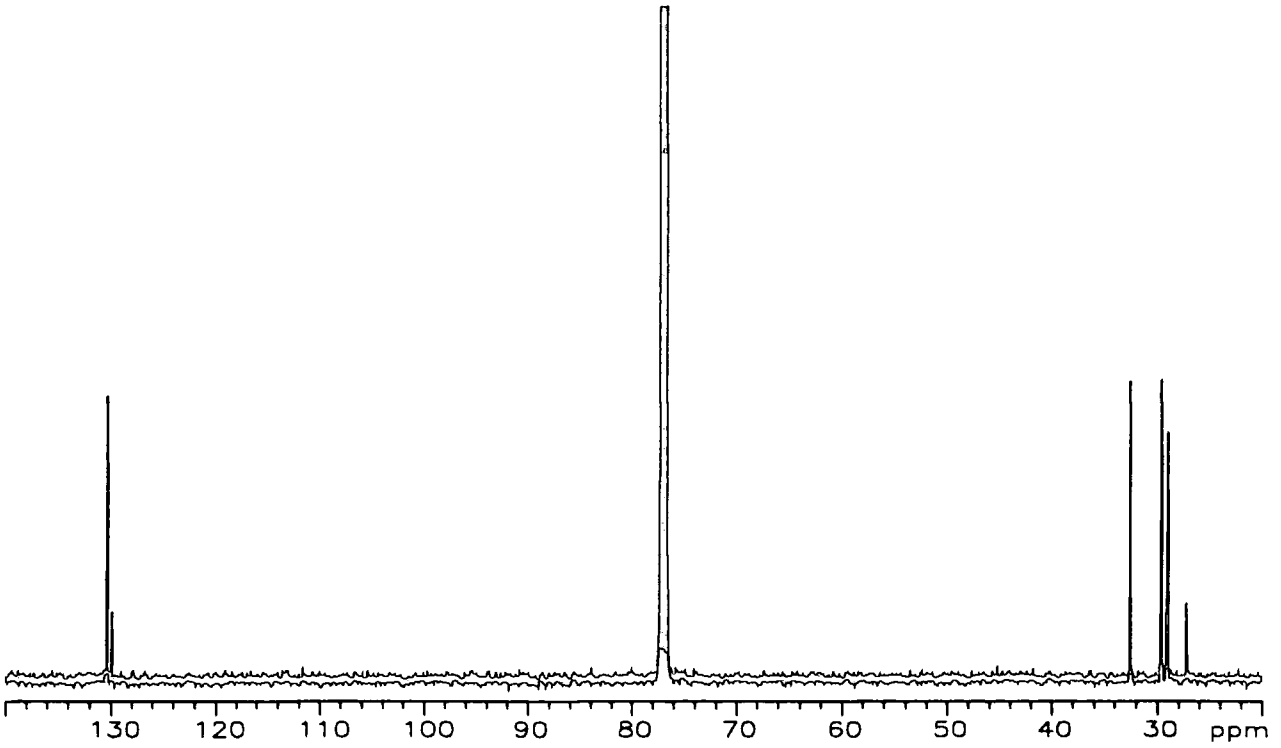

Appendix 2.16.c ^{13}C-NMR spectrum of poly(1-octenylene) initiated by $Mo(CH^tBu)(OC(CH_3)_2CF_3)_2(NAr)$

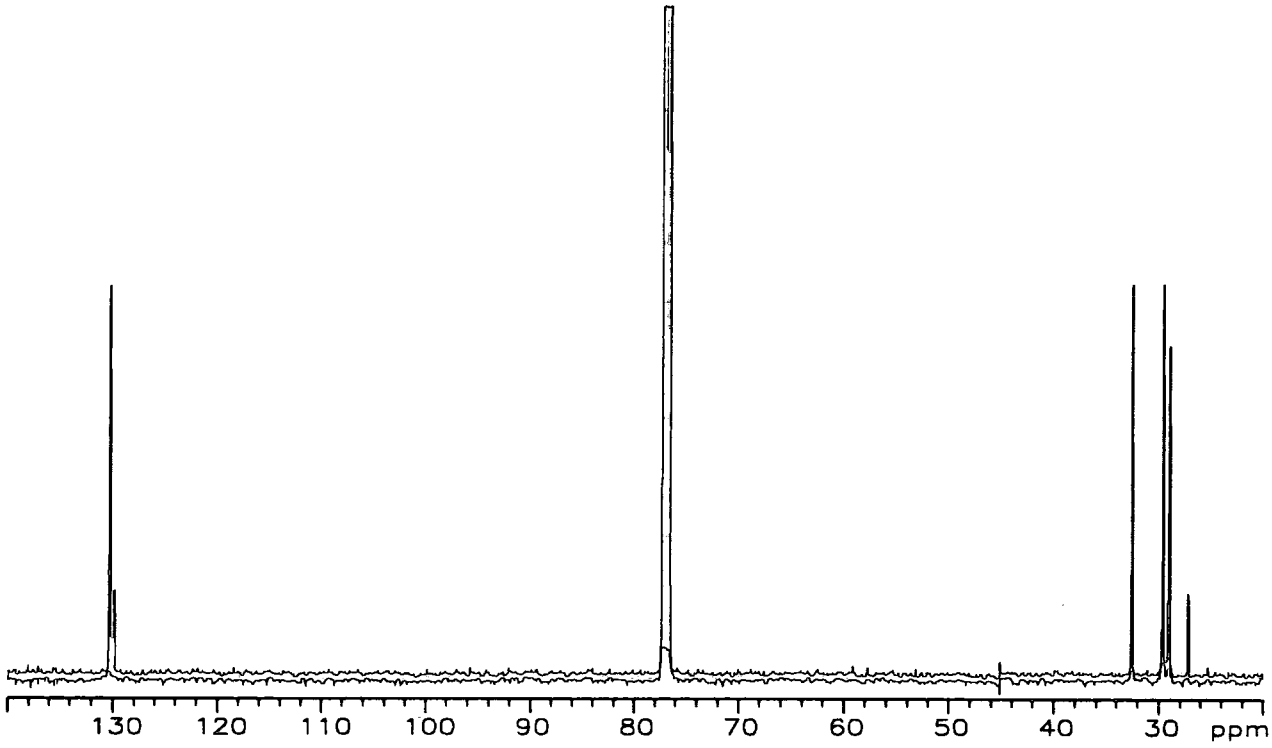

Appendix 2.16.d ^{13}C-NMR spectrum of poly(1-octenylene) initiated by $Mo(CH^tBu)(OC(CH_3)(CF_3)_2)_2(NAr)$

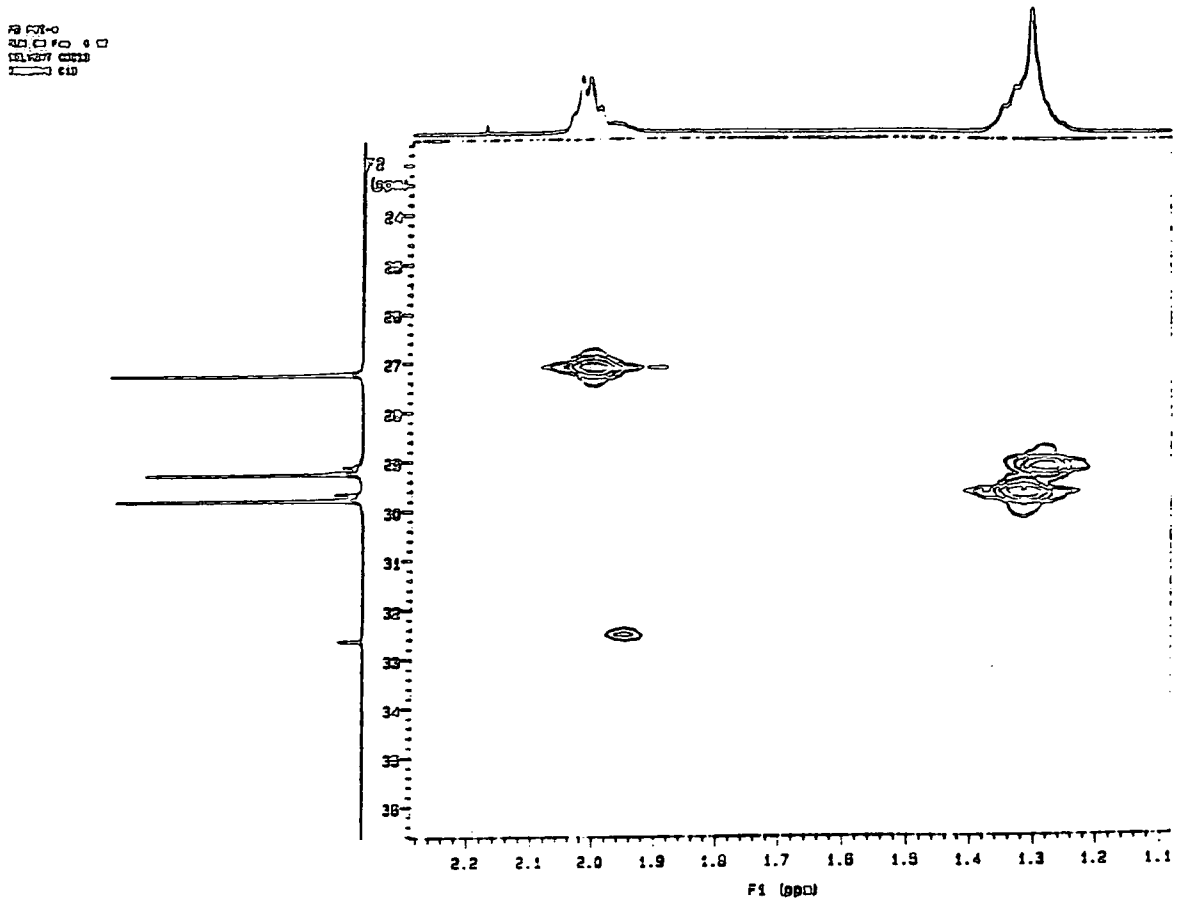

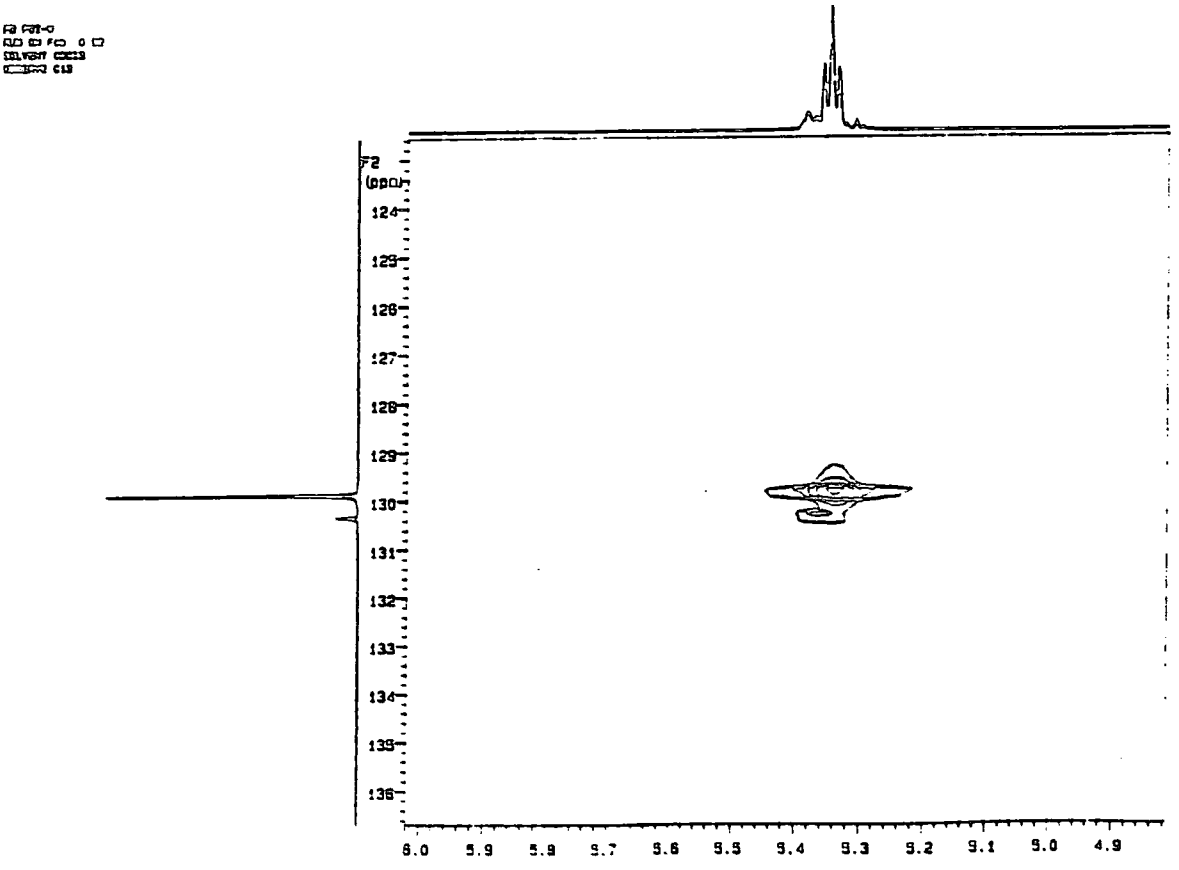

Appendix 2.17 HETCOR spectum of poly(1-octenylene) initiated with $W(CH^tBu)(O^tBu)_2(NAr)$

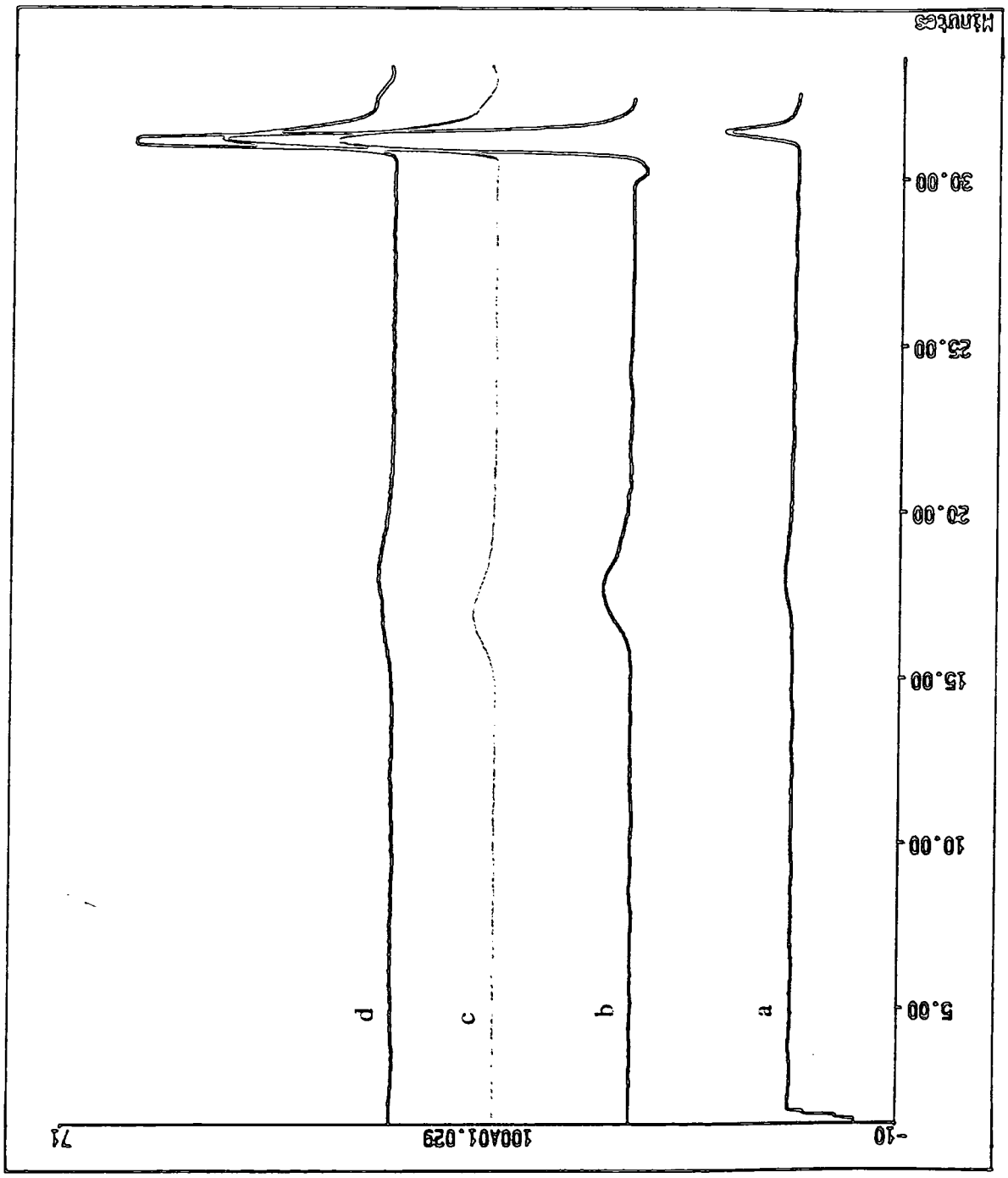

Appendix 2.18.a GPC trace of poly(1-octenylene) initiated with $W(CH^tBu)(O^tBu)_2(NAr)$

Appendix 2.18.b GPC trace of poly(1-octenylene) initiated with $Mo(CH^tBu)(OC(CH_3)_3)_2(NAr)$

Appendix 2.18.c GPC trace of poly(1-octenylene) initiated with $Mo(CH^tBu)(OC(CH_3)_2CF_3)_2(NAr)$

Appendix 2.18.d GPC trace of poly(1-octenylene) initiated with $Mo(CH^tBu)(OC(CH_3)(CF_3)_2)_2(NAr)$

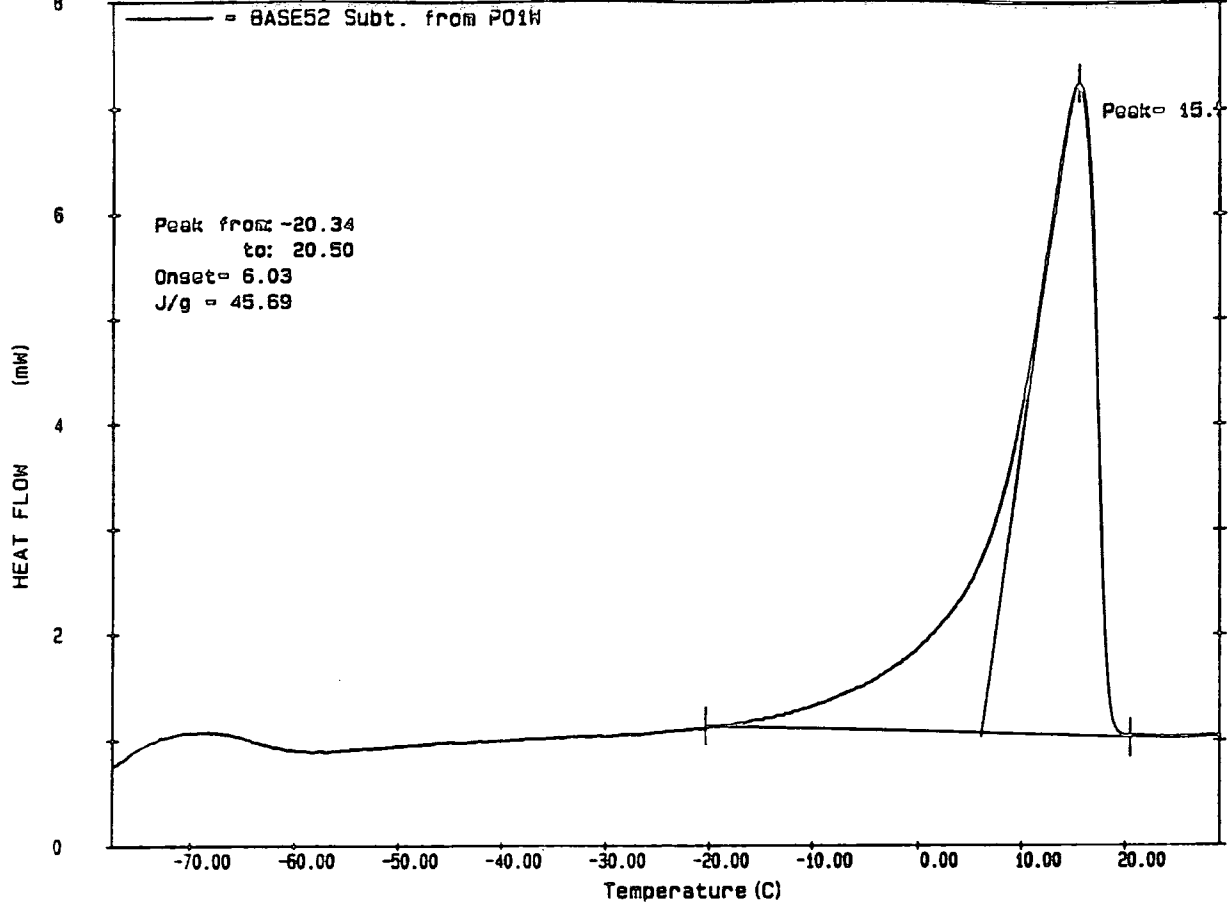

Appendix 2.19.a DSC trace of poly(1-octenylene) initiated with $W(CH^tBu)(O^tBu)_2(NAr)$

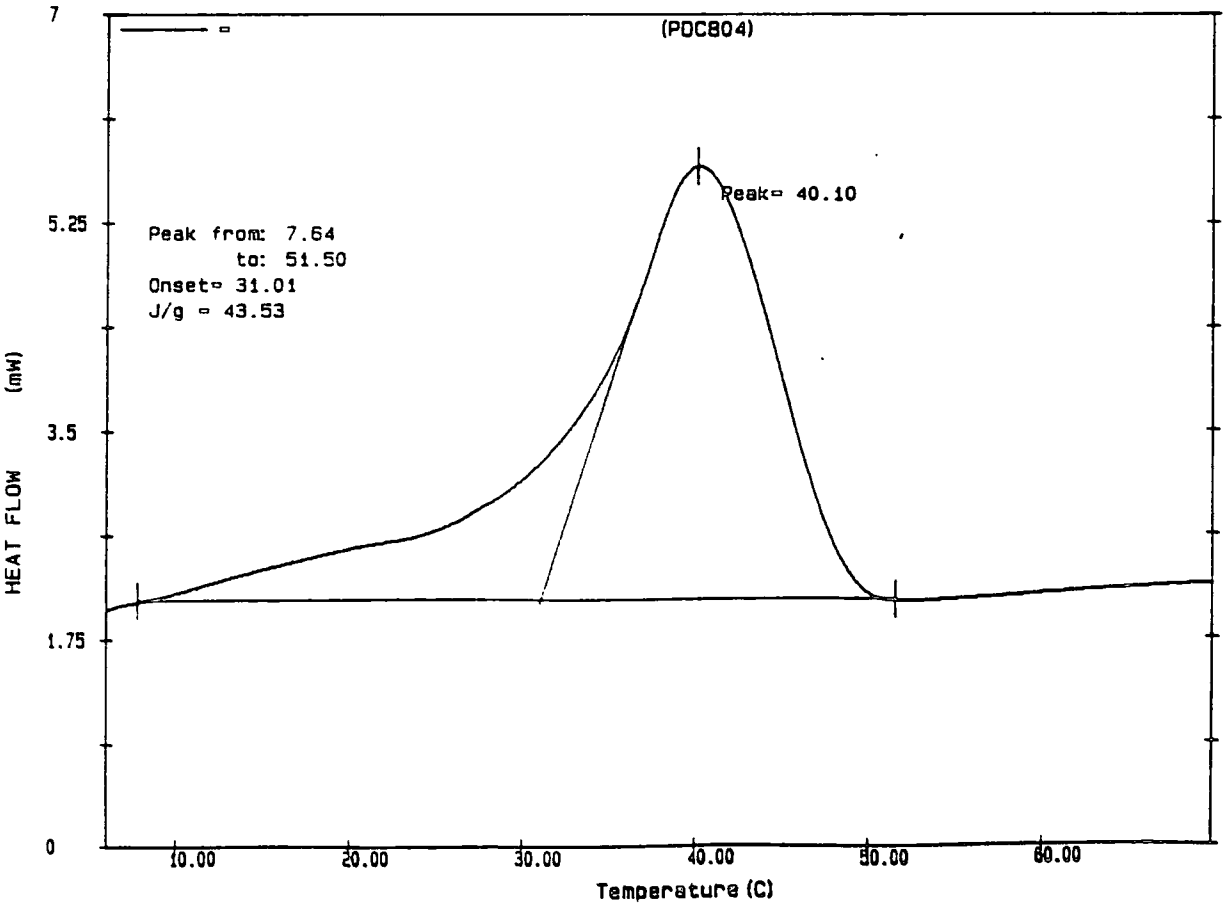

Appendix 2.19.b DSC trace of poly(1-octenylene) initiated with $Mo(CH^tBu)(OC(CH_3)_3)_2(NAr)$

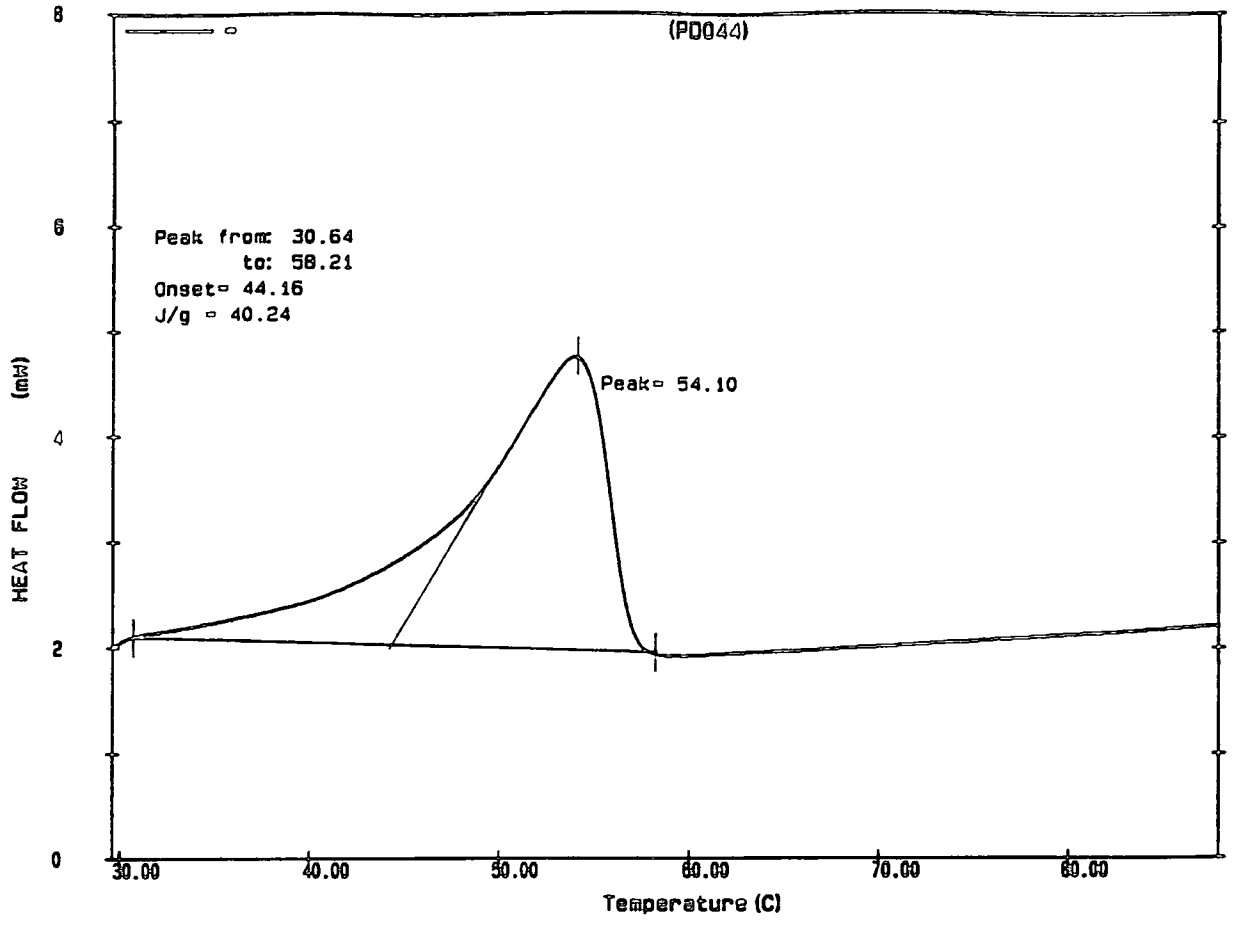

Appendix 2.19.c DSC trace of poly(1-octenylene) initiated with $Mo(CH^tBu)(OC(CH_3)_2CF_3)_2(NAr)$

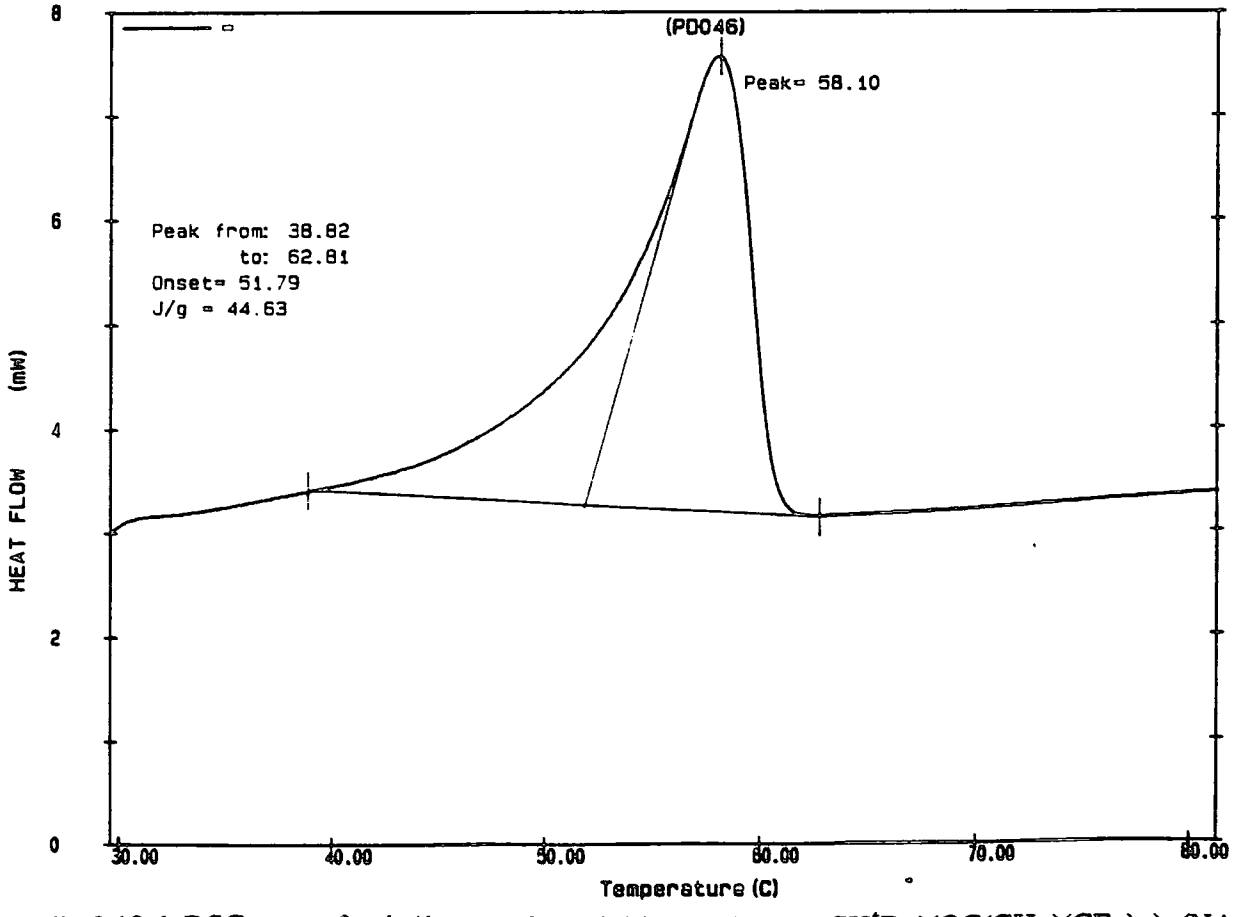

Appendix 2.19.d DSC trace of poly(1-octenylene) initiated with $Mo(CH^tBu)(OC(CH_3)(CF_3)_2)_2(NAr)$

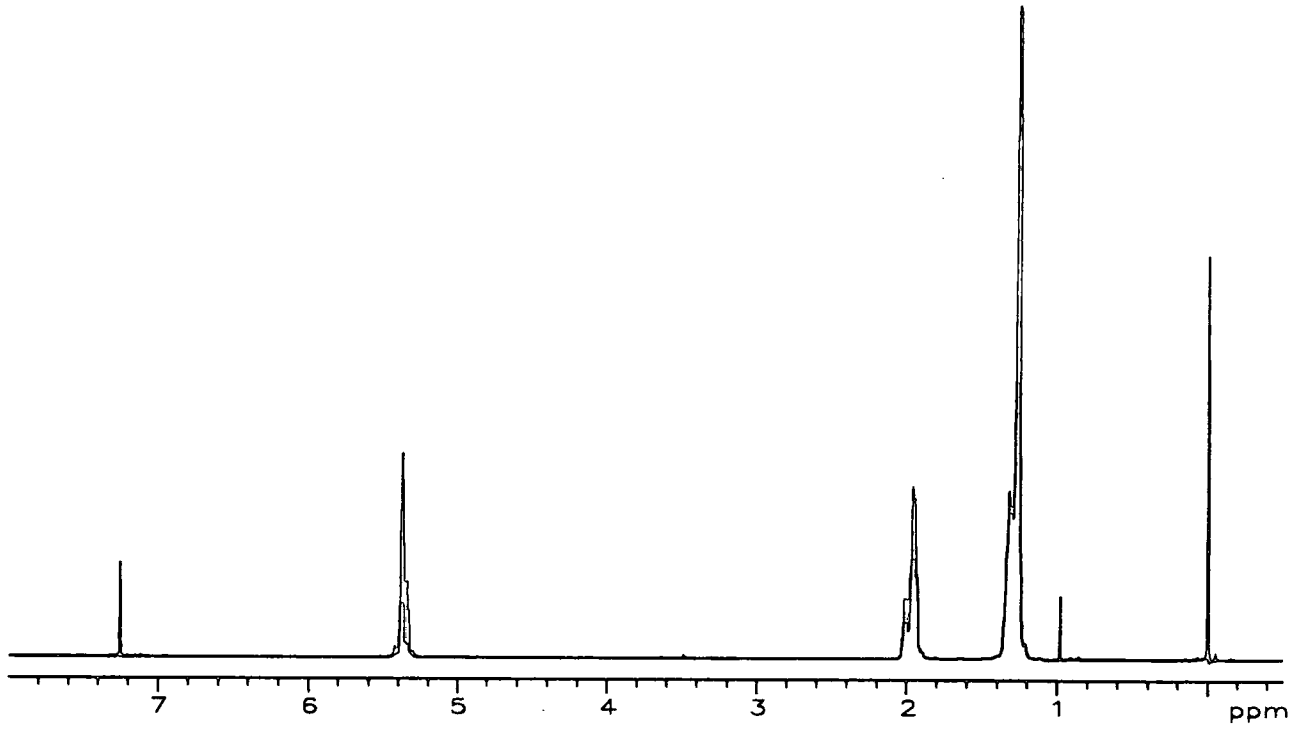

Appendix 2.20 ^{1}H-NMR spectrum of poly(1-decenylene) initiated by W(CH^{t}Bu)(O^{t}Bu)$_2$(NAr)

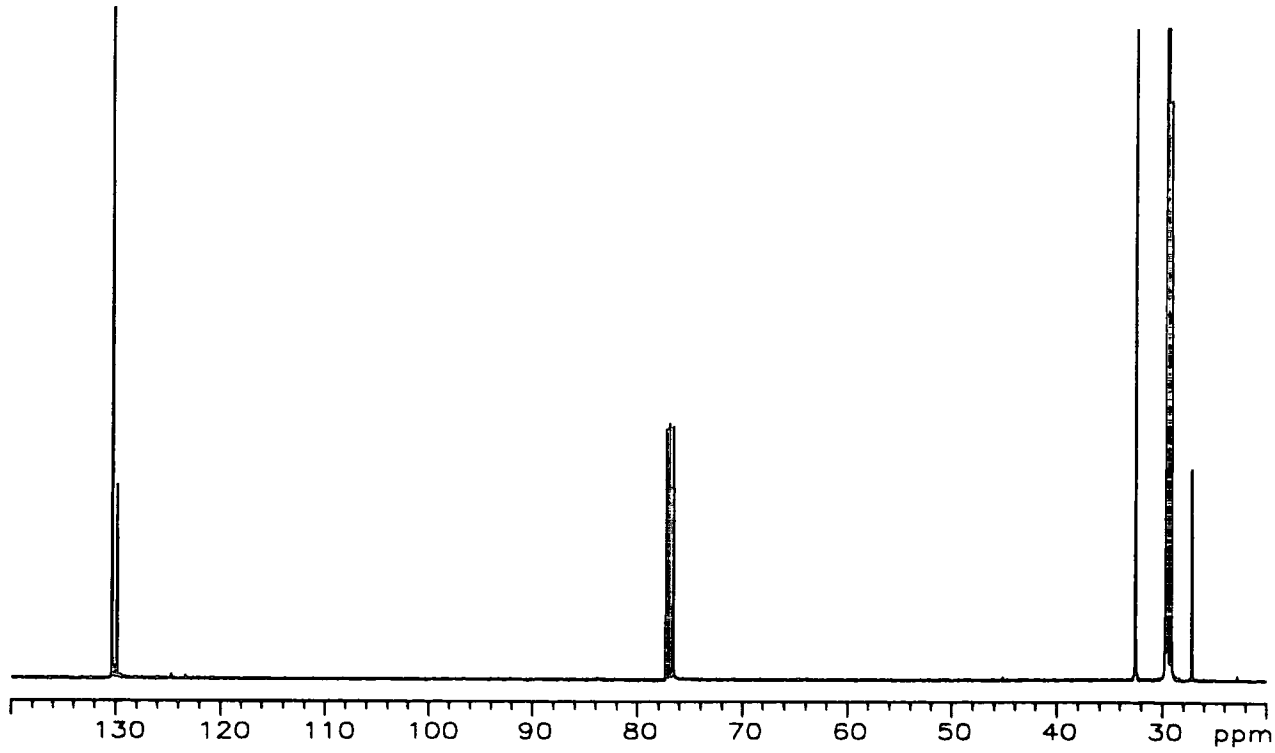

Appendix 2.21.a ^{13}C-NMR spectrum of poly(1-decenylene) initiated by W(CHtBu)(OtBu)2(NAr)

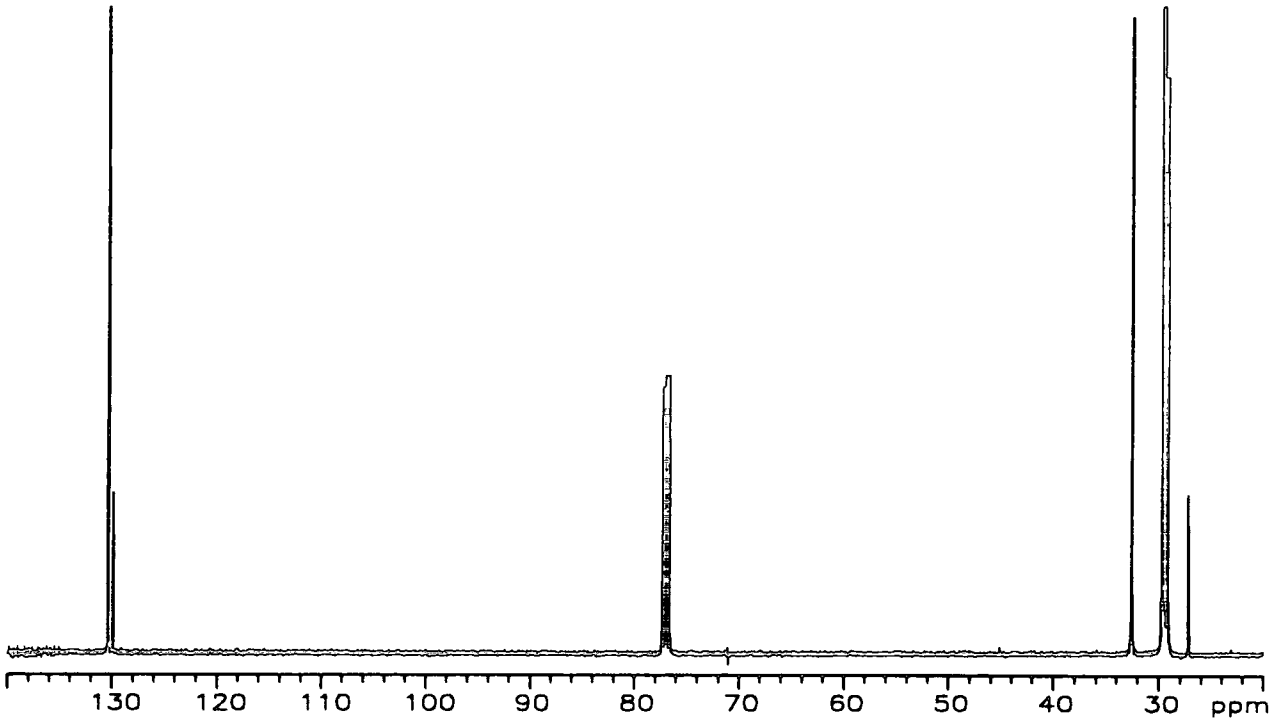

Appendix 2.21.b ^{13}C-NMR spectrum of poly(1-decenylene) initiated by $Mo(CH^tBu)(OC(CH_3)_3)_2(NAr)$

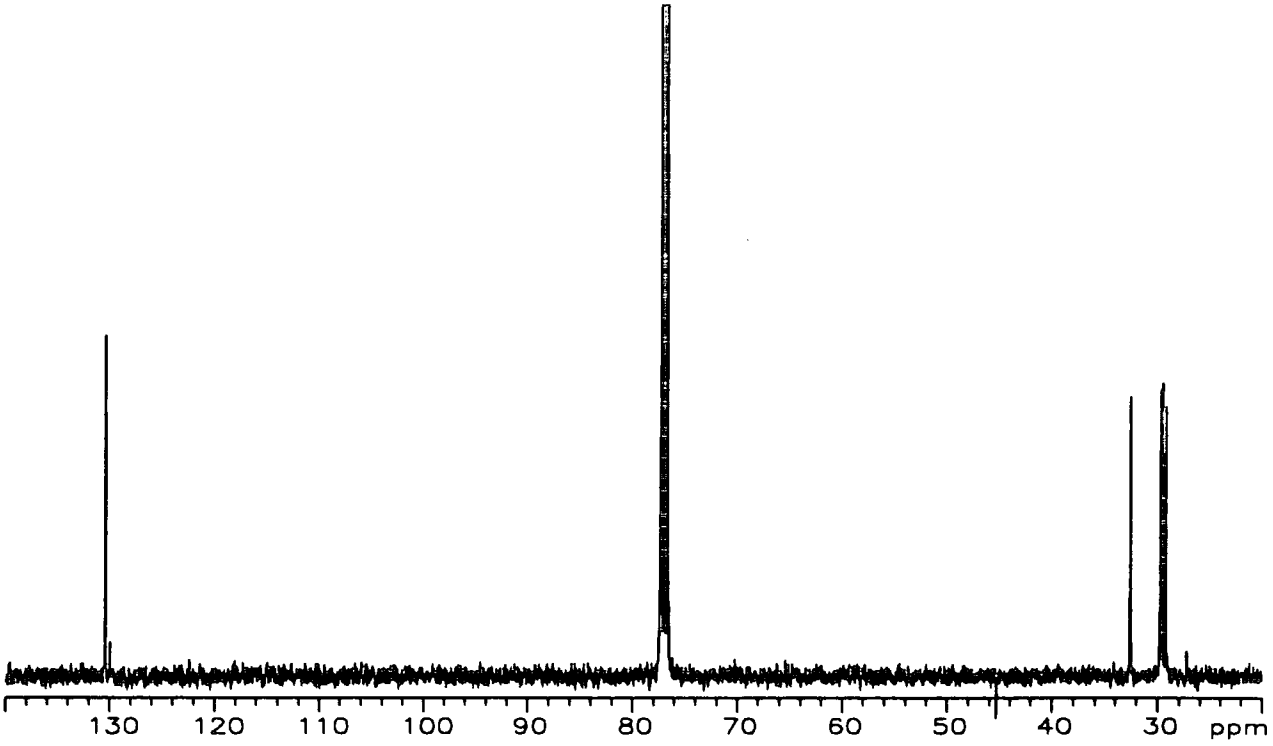

Appendix 2.21.c ^{13}C-NMR spectrum of poly(1-decenylene) initiated by $Mo(CH^tBu)(OC(CH_3)_2CF_3)_2(NAr)$

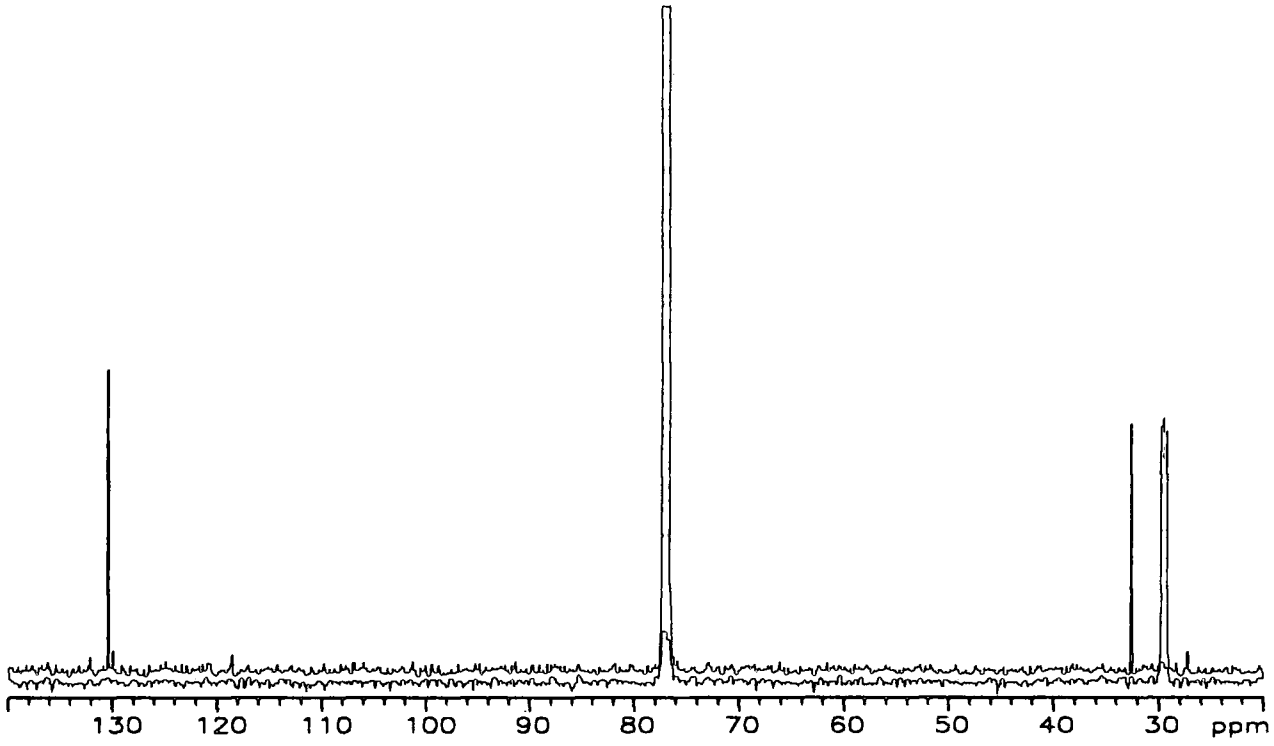

Appendix 2.21.d ^{13}C-NMR spectrum of poly(1-decenylene) initiated by $Mo(CH^tBu)(OC(CH_3)(CF_3)_2)_2(NAr)$

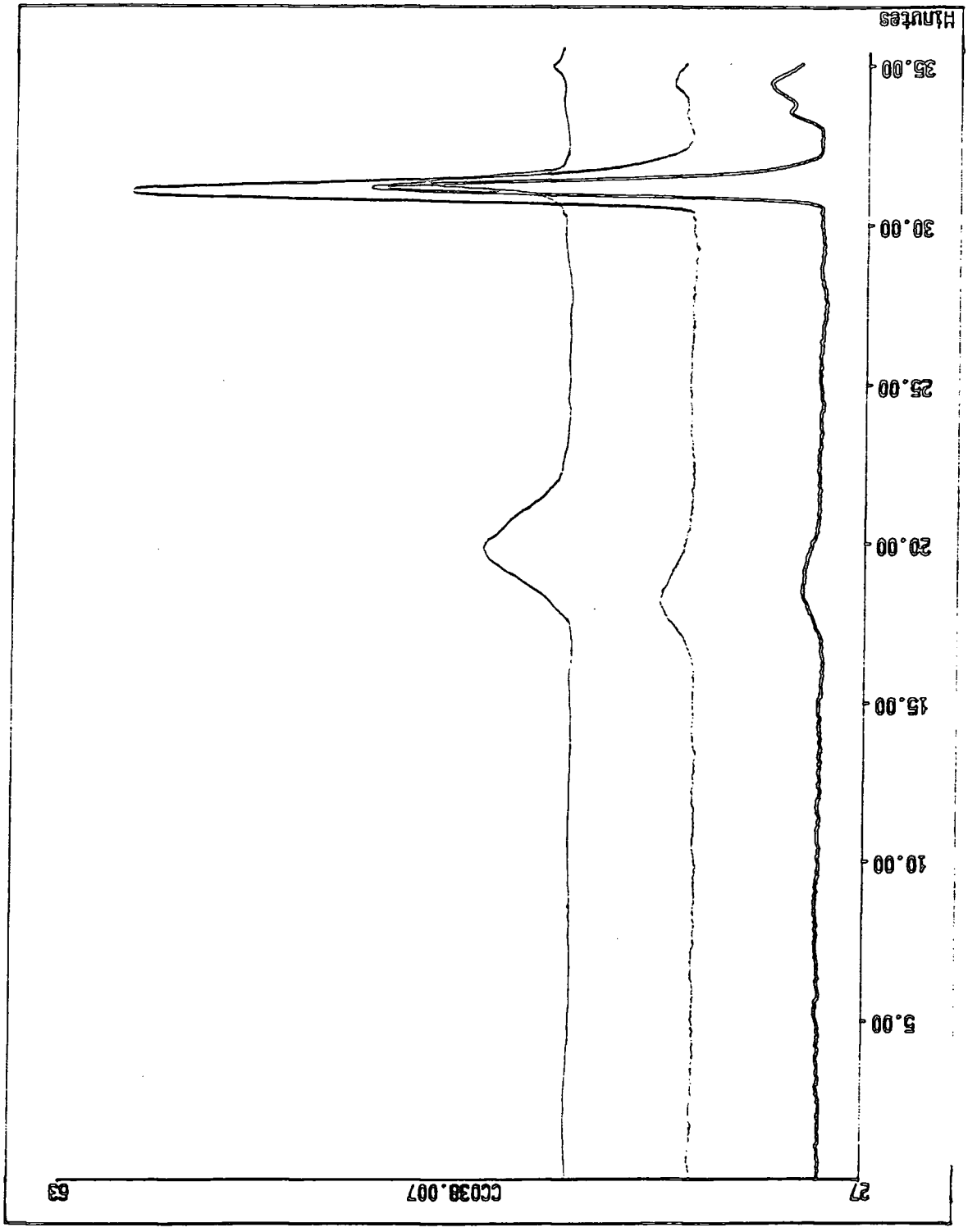

Appendix 2.22.a GPC trace of poly(1-decenylene) initiated with $W(CH^tBu)(O^tBu)_2(NAr)$

Appendix 2.22.b GPC trace of poly(1-decenylene) initiated with $Mo(CH^tBu)(OC(CH_3)_3)_2(NAr)$

Appendix 2.22.c GPC trace of poly(1-decenylene) initiated with $Mo(CH^tBu)(OC(CH_3)_2CF_3)_2(NAr)$

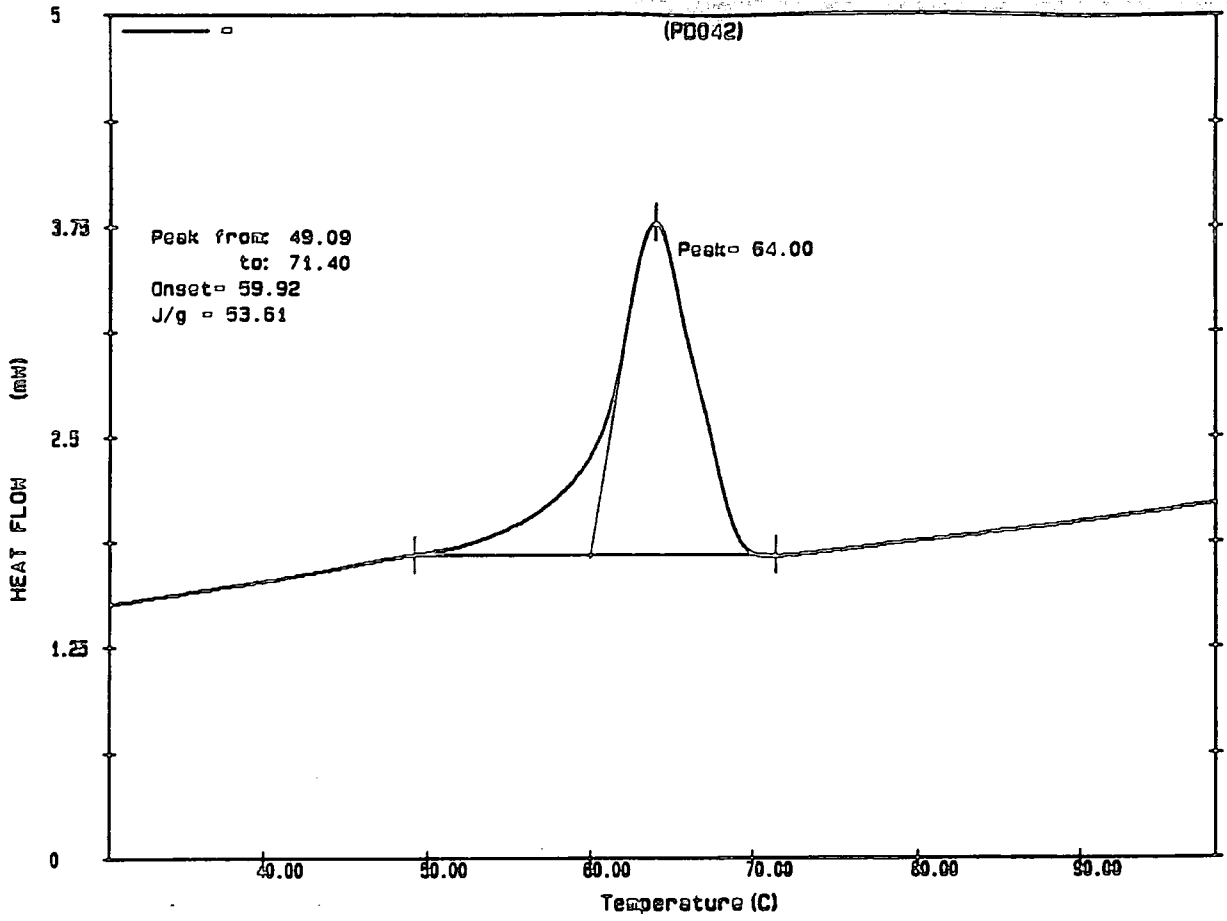

Appendix 2.23.a DSC trace of poly(1-decenylene) initiated with $W(CH^tBu)(O^tBu)_2(NAr)$

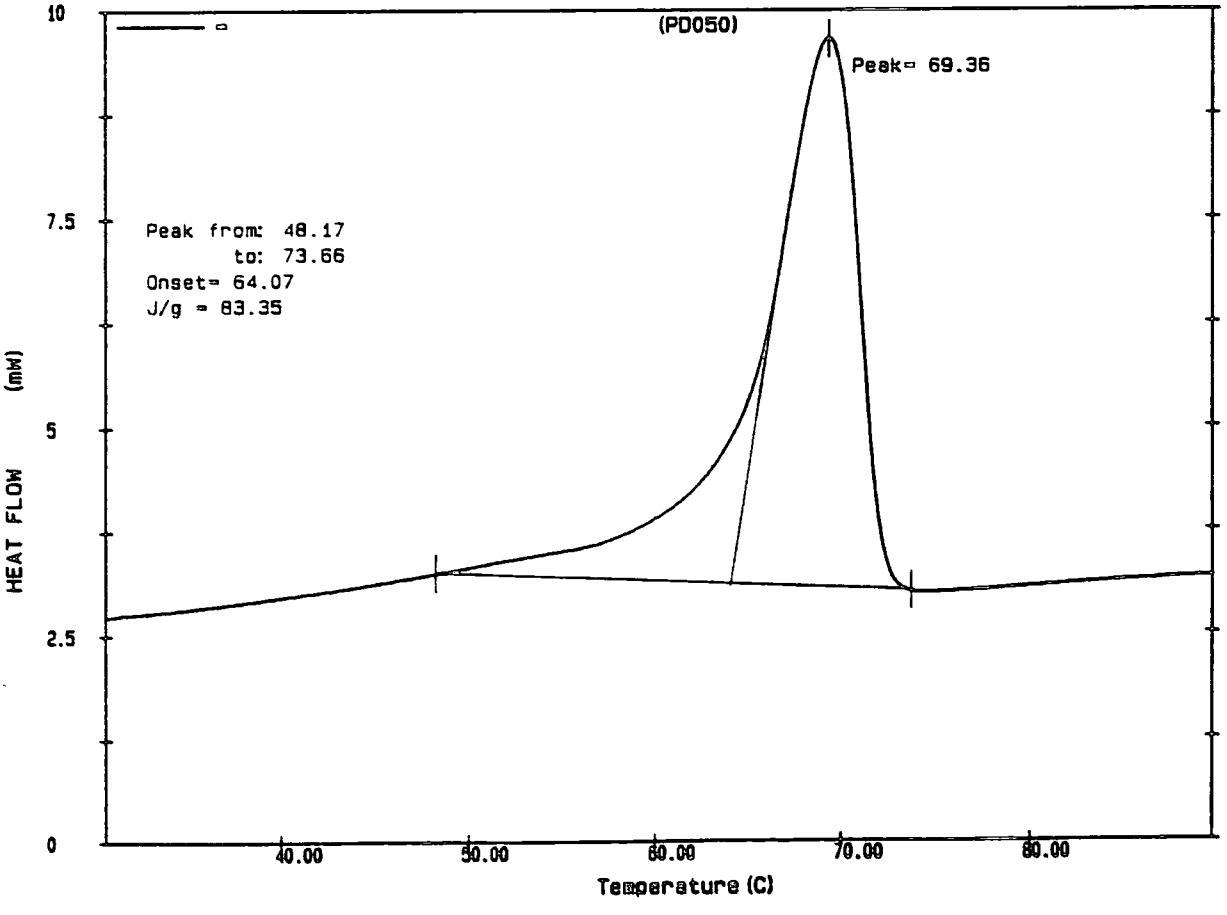

Appendix 2.23.b DSC trace of poly(1-decenylene) initiated with $Mo(CH^tBu)(OC(CH_3)_3)_2(NAr)$

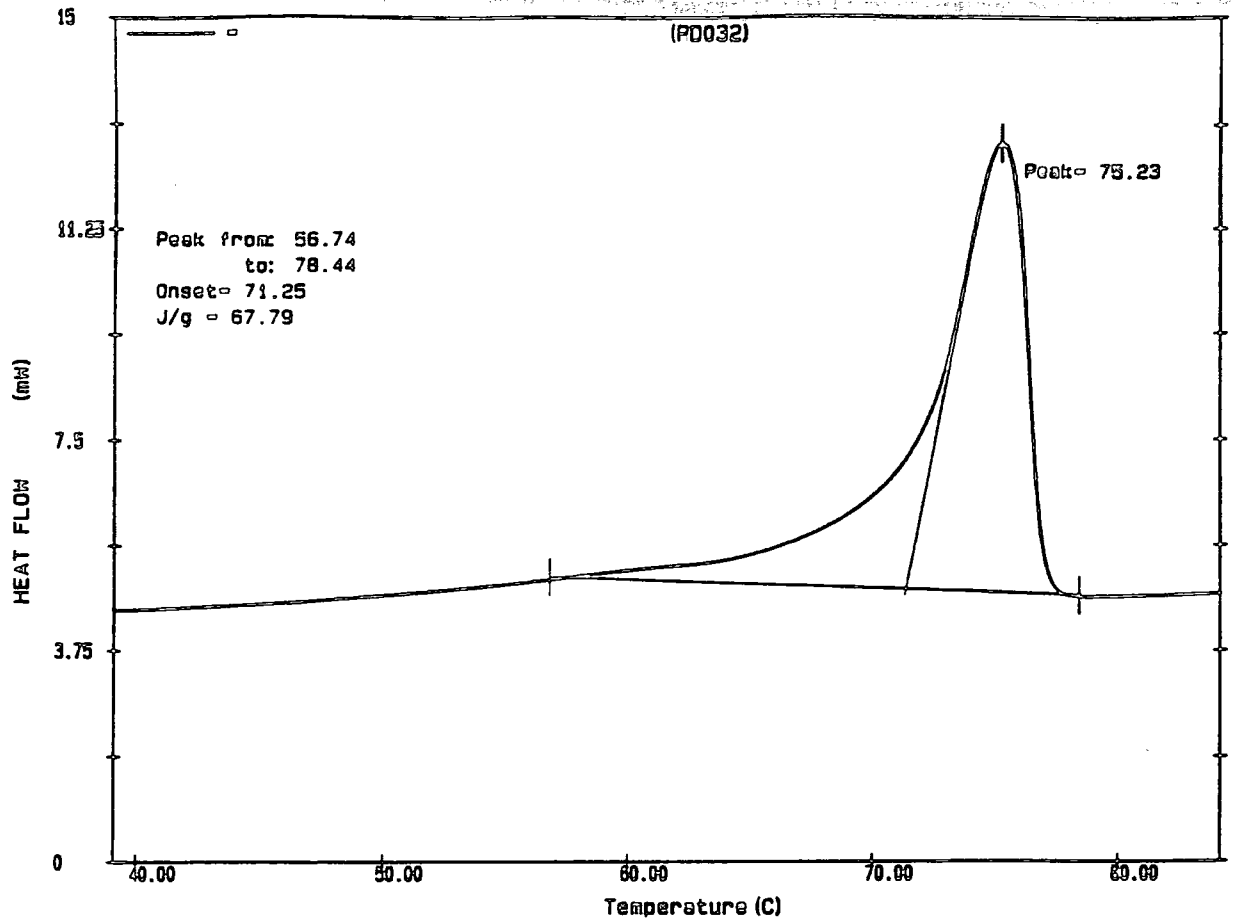

Appendix 2.23.c DSC trace of poly(1-decenylene) initiated with $Mo(CH^tBu)(OC(CH_3)_2CF_3)_2(NAr)$

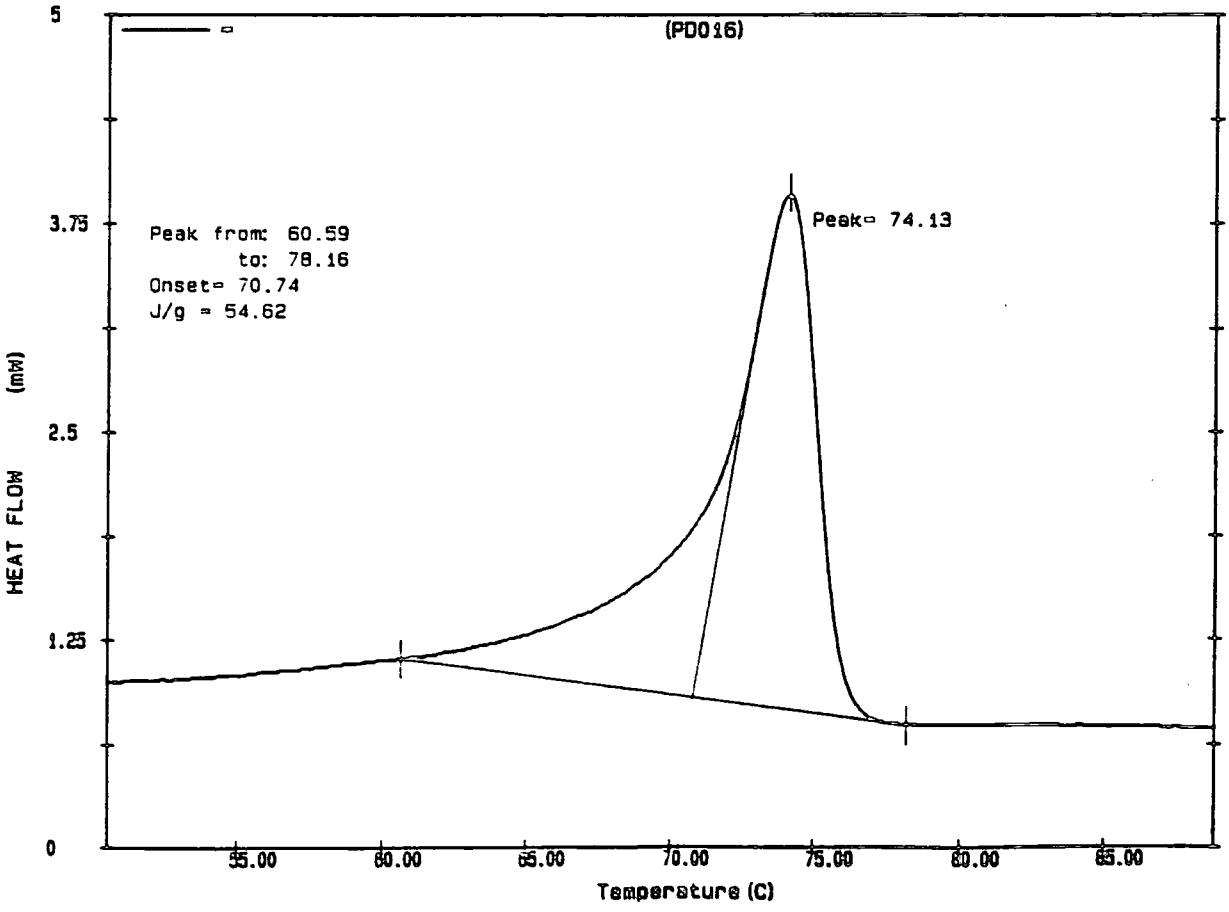

Appendix 2.23.d DSC trace of poly(1-decenylene) initiated with $Mo(CH^tBu)(OC(CH_3)(CF_3)_2)_2(NAr)$

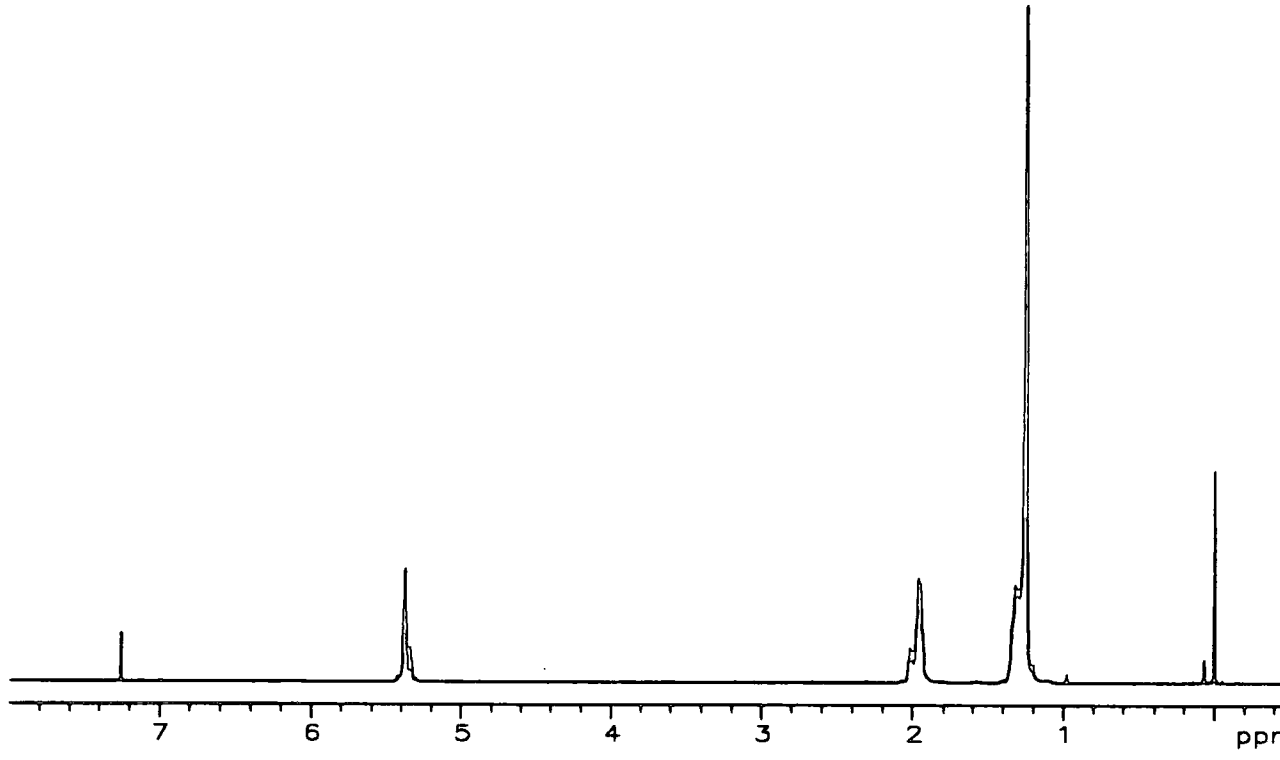

Appendix 2.24. ^{1}H-NMR spectrum of poly(1-dodecenylene) initiated by W(CH^{t}Bu)(O^{t}Bu)$_2$(NAr)

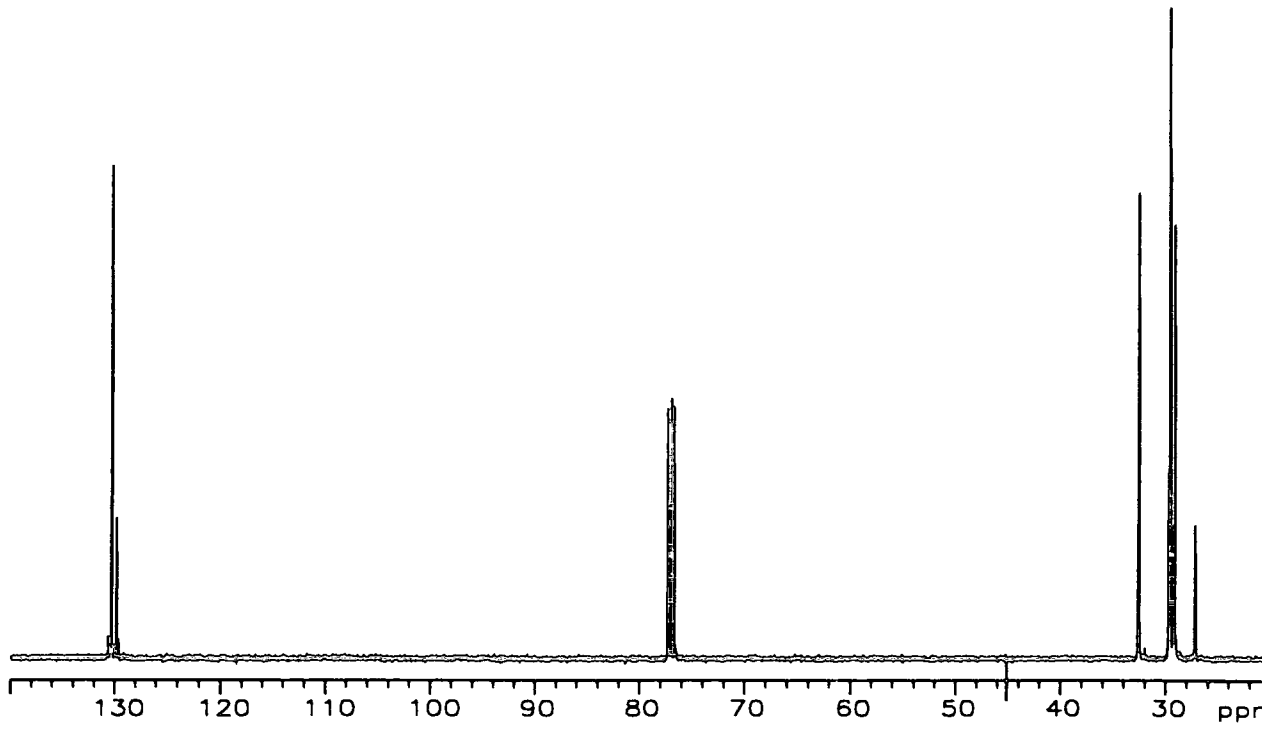

Appendix 2.25.a ^{13}C-NMR spectrum of poly(1-dodecenylene) initiated by W(CHtBu)(OtBu)2(NAr)

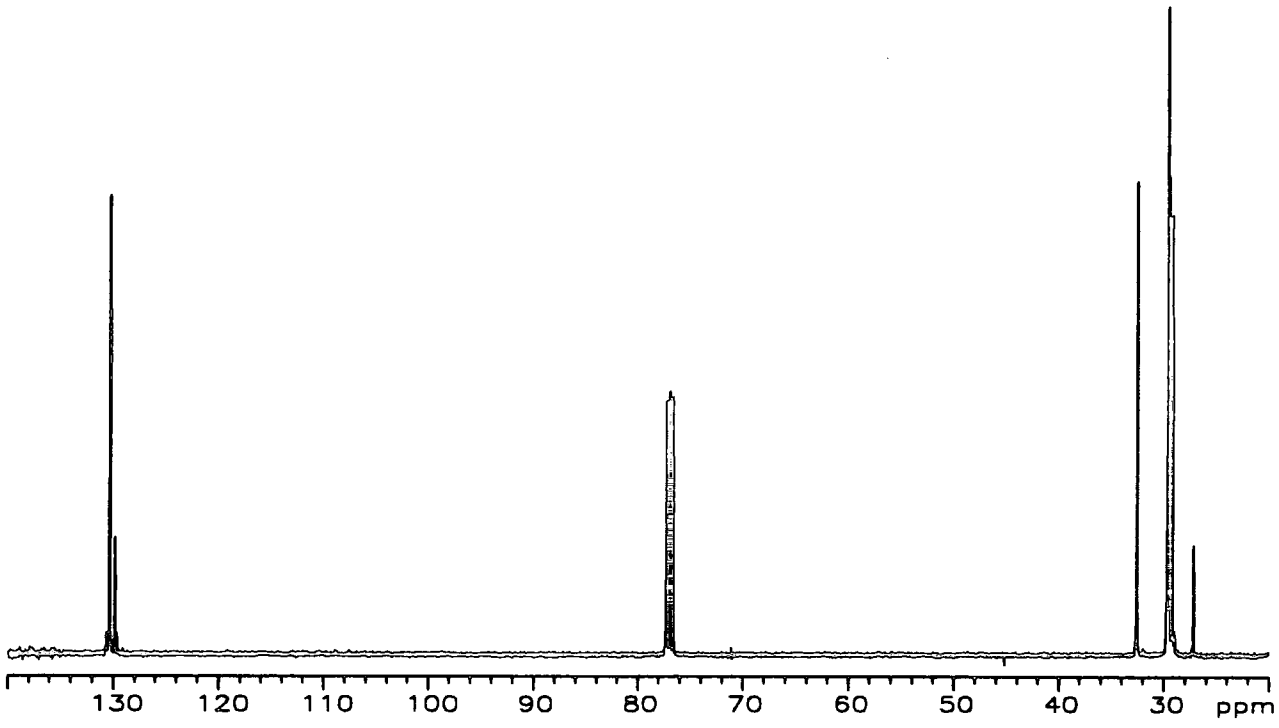

Appendix 2.25.b ^{13}C-NMR spectrum of poly(1-dodecenylene) initiated by $Mo(CH^tBu)(OC(CH_3)_3)_2(NAr)$

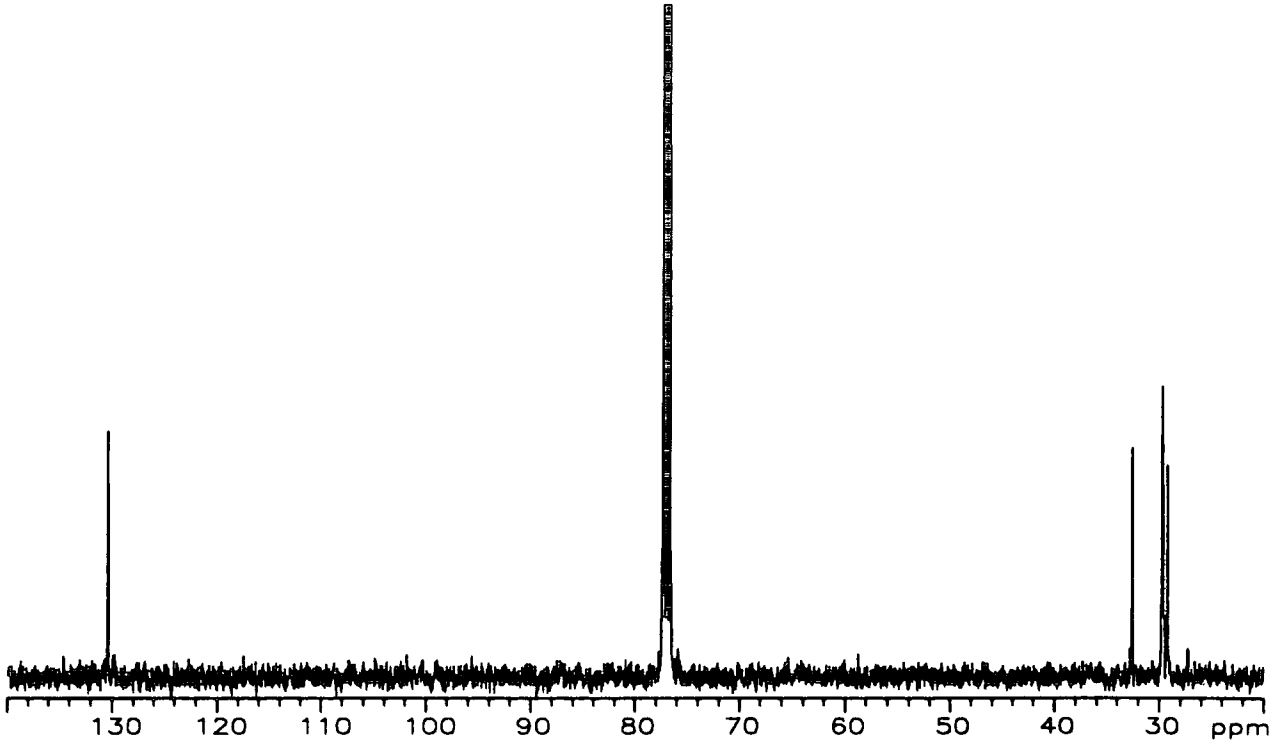

Appendix 2.25.c ^{13}C-NMR spectrum of poly(1-decenylene) initiated by $Mo(CH^tBu)(OC(CH_3)_2CF_3)_2(NAr)$

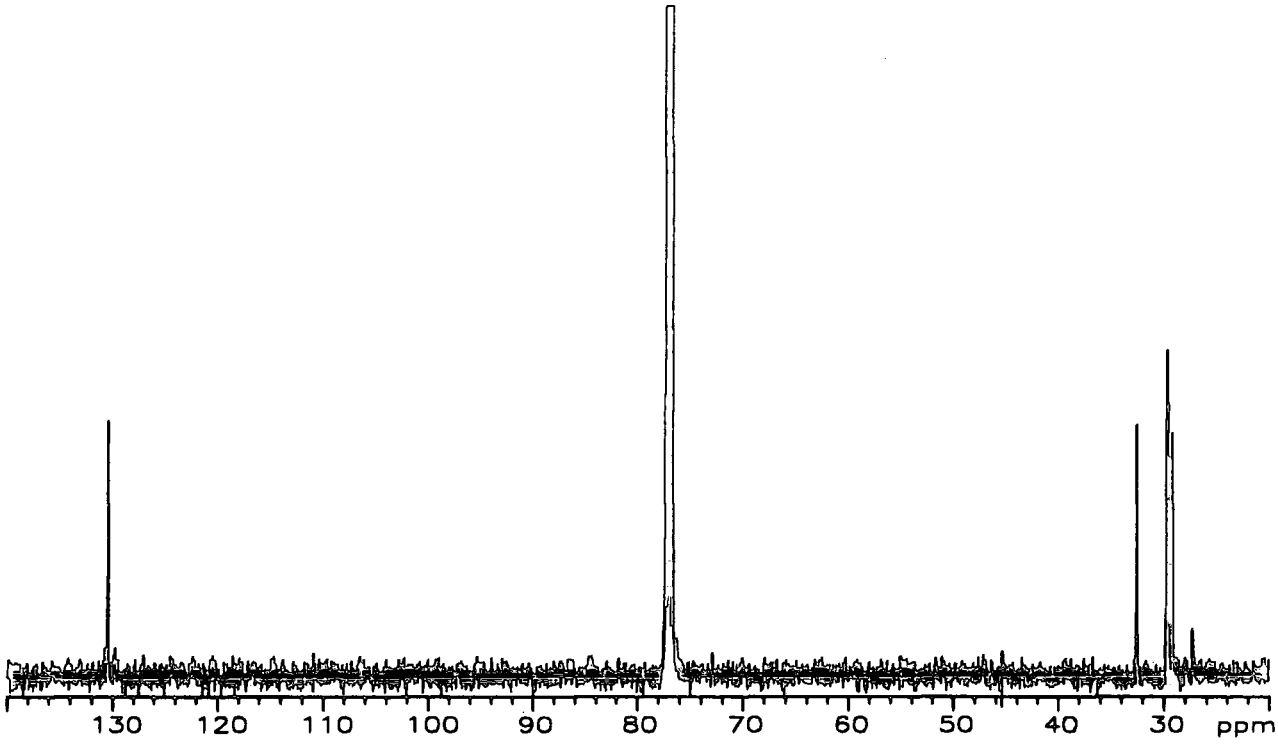

Appendix 2.25.d ^{13}C-NMR spectrum of poly(1-dodecenylene) initiated by $Mo(CH^tBu)(OC(CH_3)(CF_3)_2)_2(NAr)$

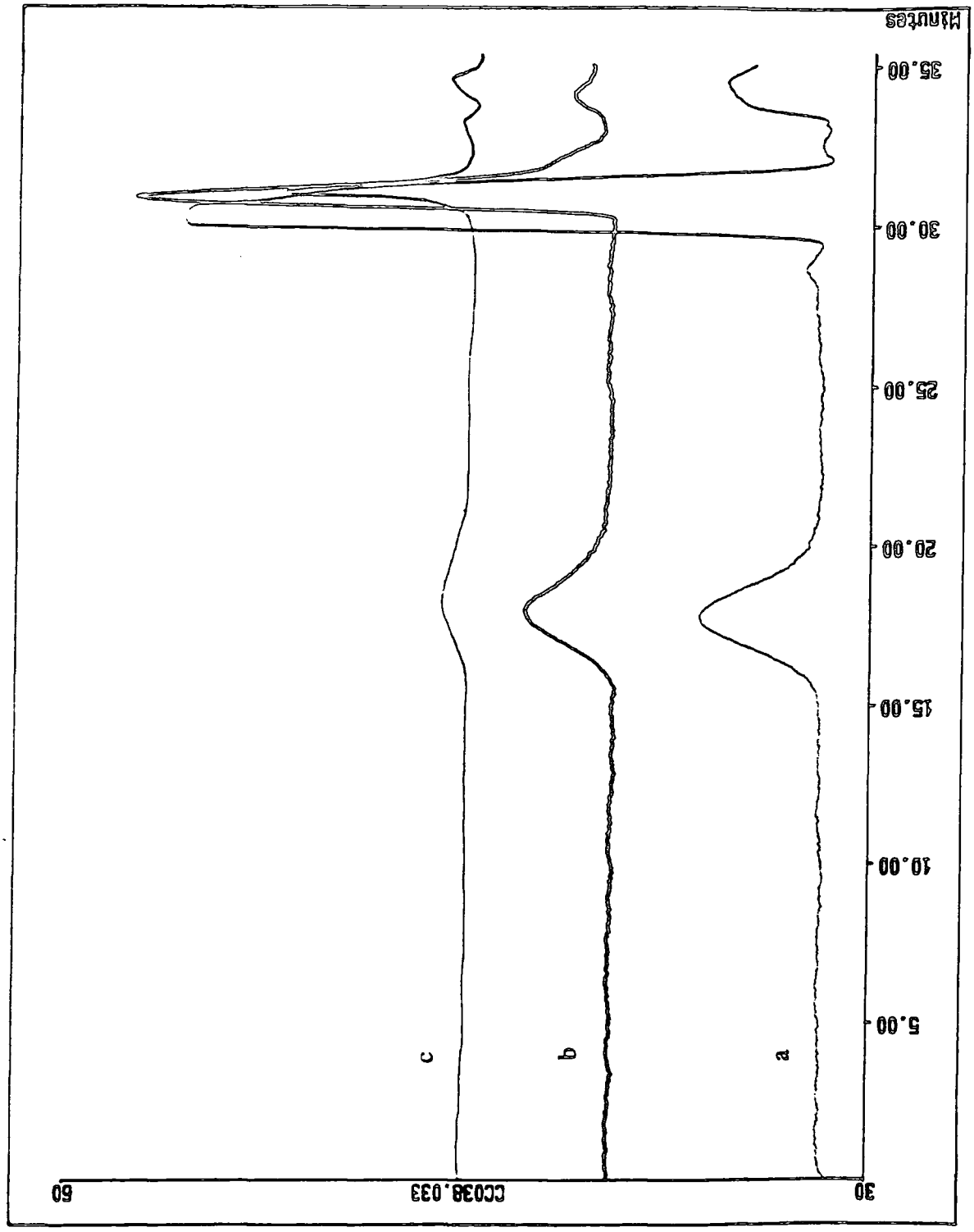

Appendix 2.26.a GPC trace of poly(1-dodecenylene) initiated with $W(CH^tBu)(O^tBu)_2(NAr)$

Appendix 2.26.b GPC trace of poly(1-dodecenylene) initiated with $Mo(CH^tBu)(OC(CH_3)_3)_2(NAr)$

Appendix 2.26.c GPC trace of poly(1-dodecenylene) initiated with $Mo(CH^tBu)(OC(CH_3)_2CF_3)_2(NAr)$

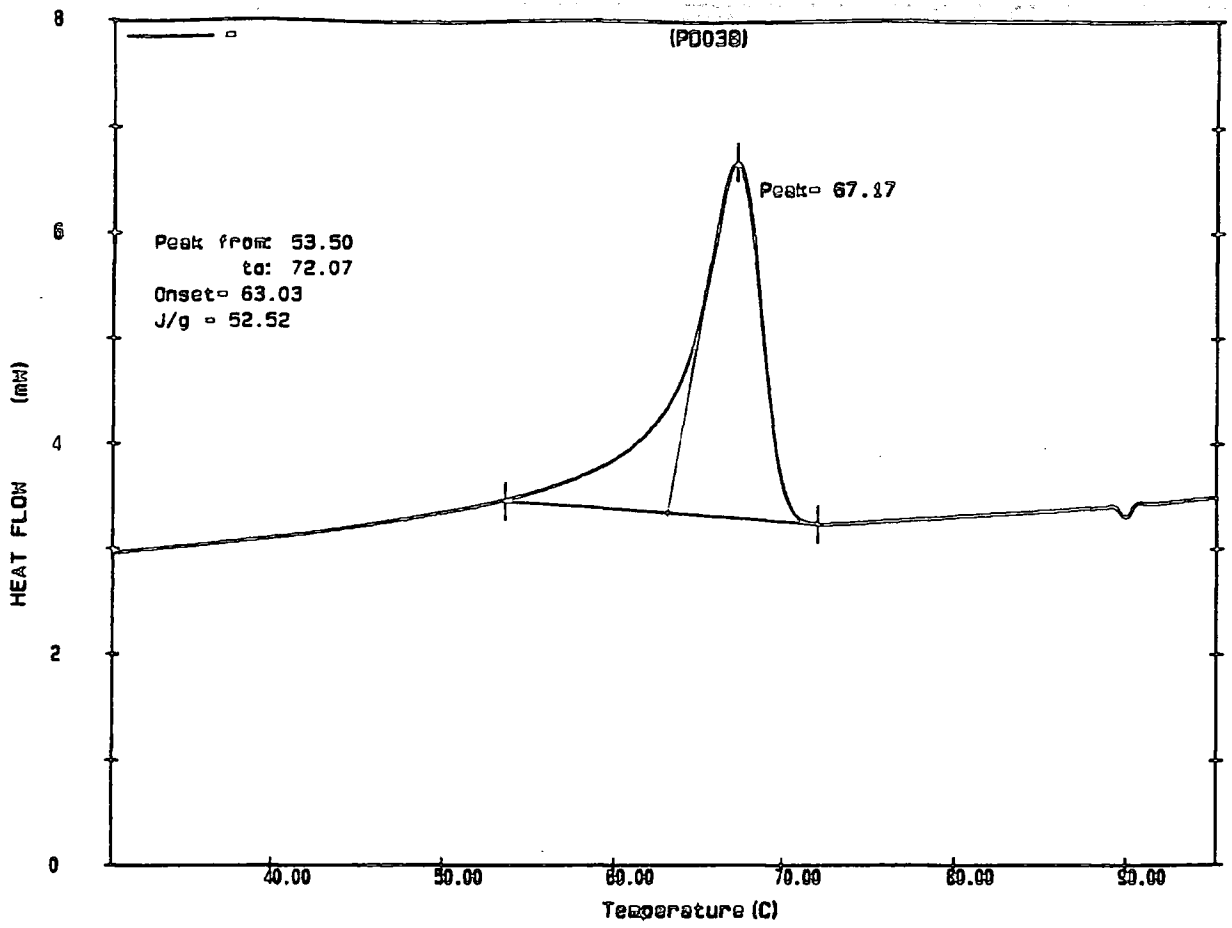

Appendix 2.27.a DSC trace of poly(1-dodecenylene) initiated with $W(CH^tBu)(O^tBu)_2(NAr)$

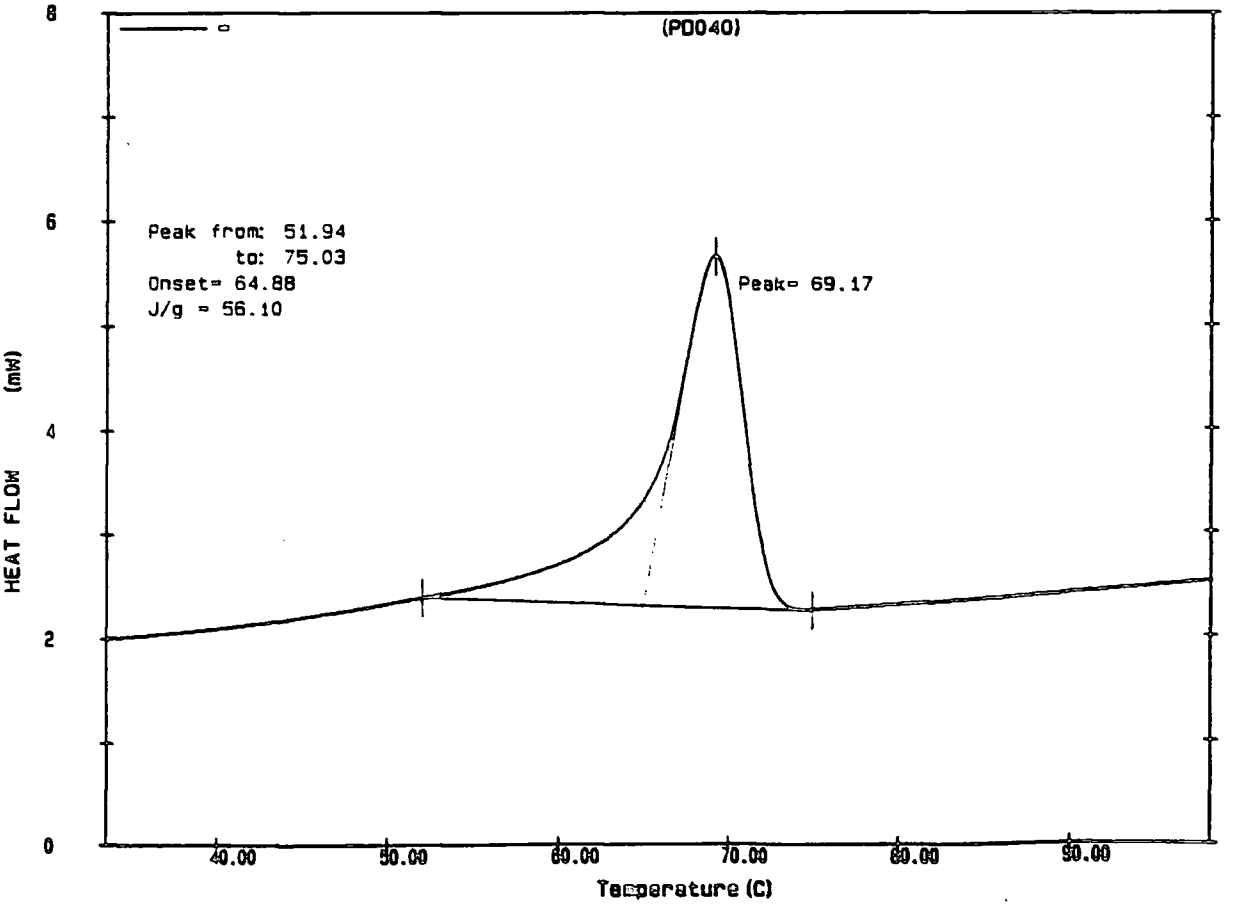

Appendix 2.27.b DSC trace of poly(1-dodecenylene) initiated with $Mo(CH^tBu)(OC(CH_3)_3)_2(NAr)$

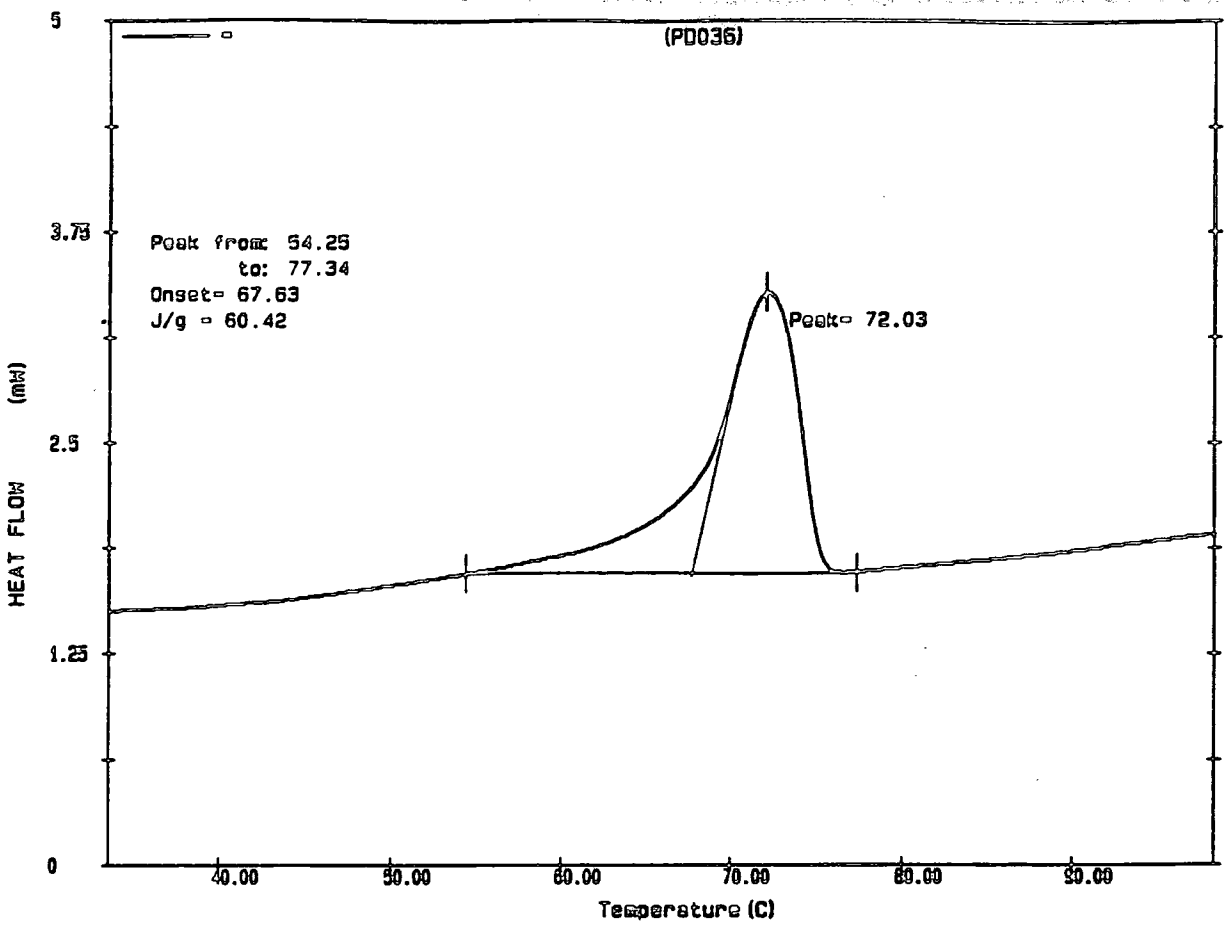

Appendix 2.27.c DSC trace of poly(1-dodecenylene) initiated with $Mo(CH^tBu)(OC(CH_3)_2CF_3)_2(NAr)$

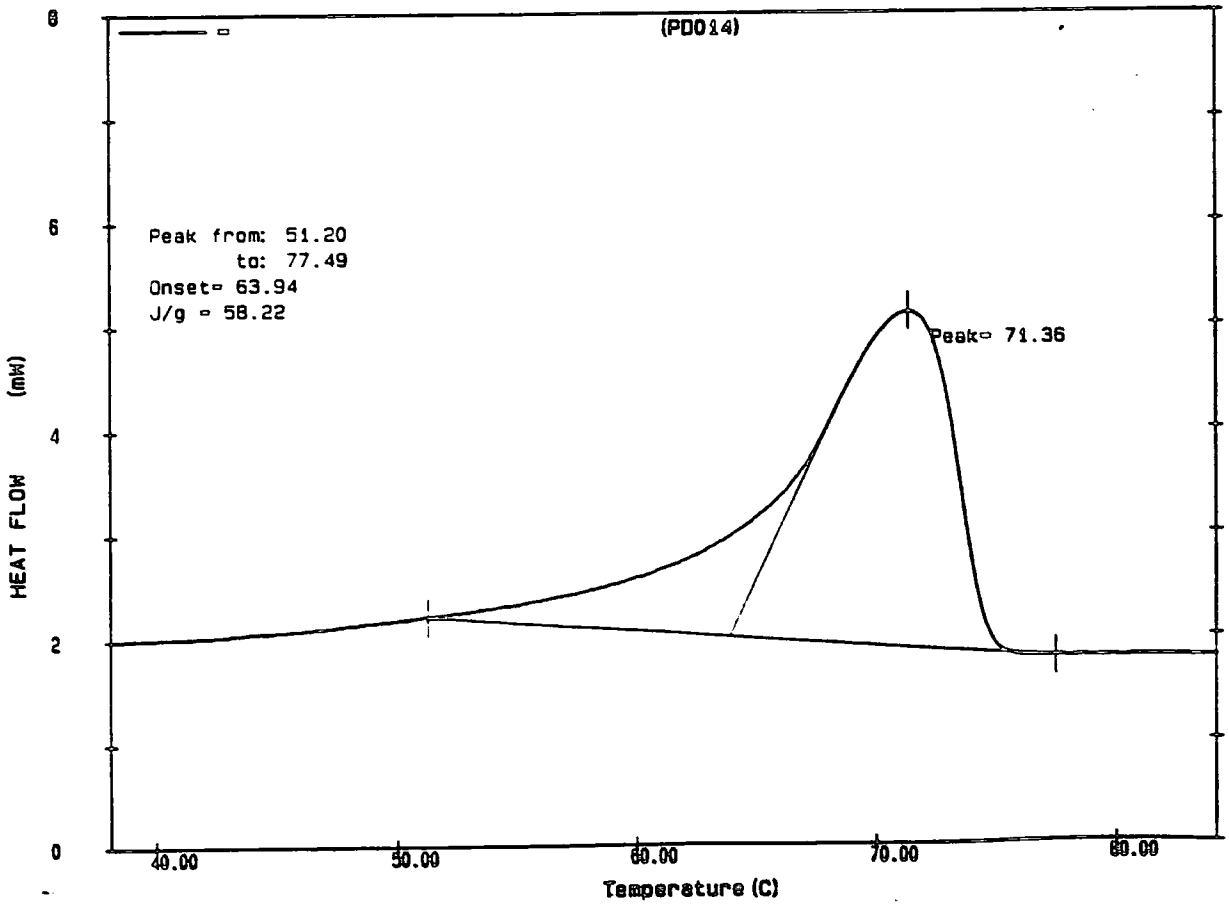

Appendix 2.27.d DSC trace of poly(1-dodecenylene) initiated with $Mo(CH^tBu)(OC(CH_3)(CF_3)_2)_2(NAr)$

APPENDIX 3

Analytical data for Chapter 3

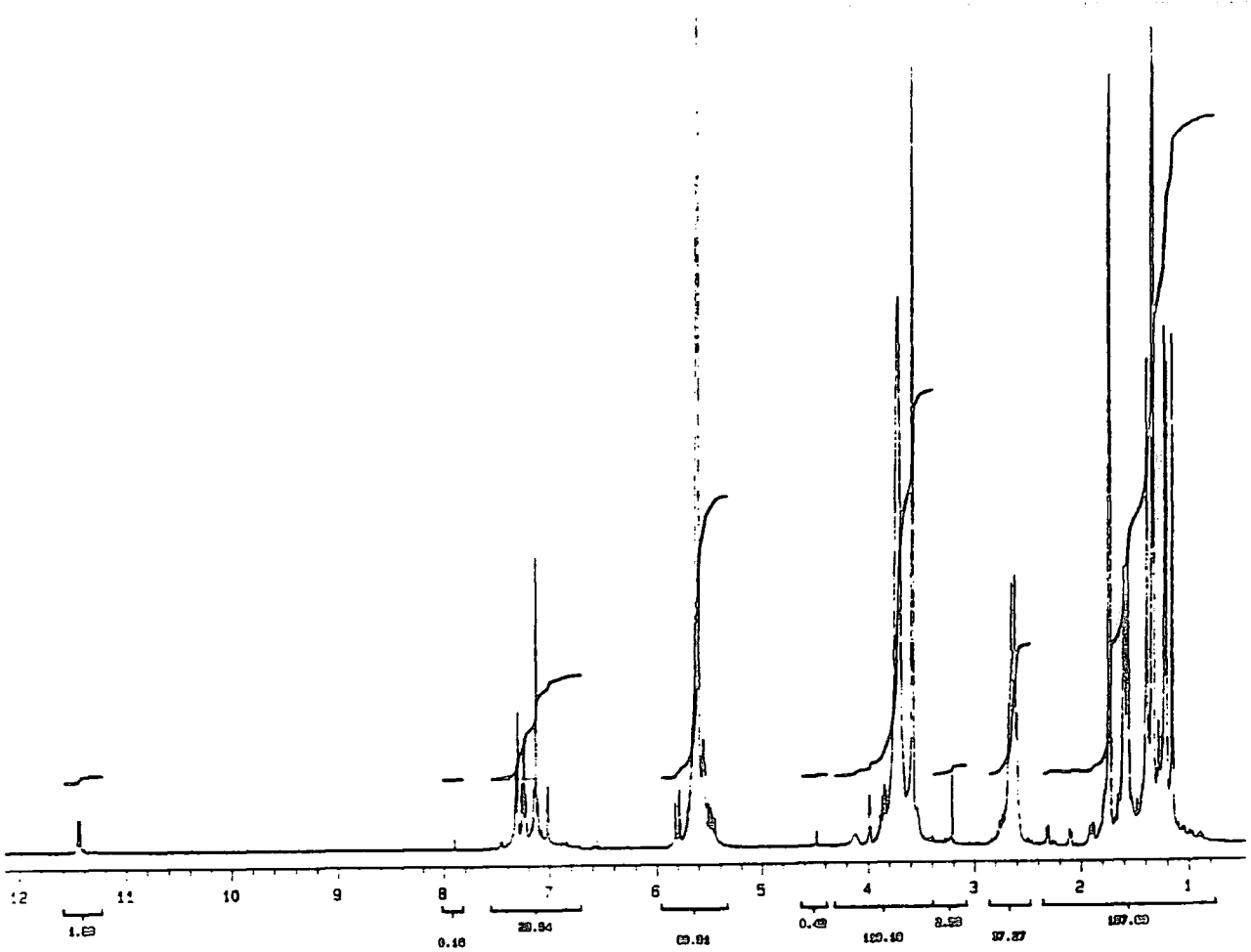

Appendix 3.1.a ^{1}H-NMR of the poly(bistrifluoromethylnorbornadiene)-*block*-poly(1-octenylene) polymerisation (1 hour after addition of bis(trilfuoromethyl)norbornadiene

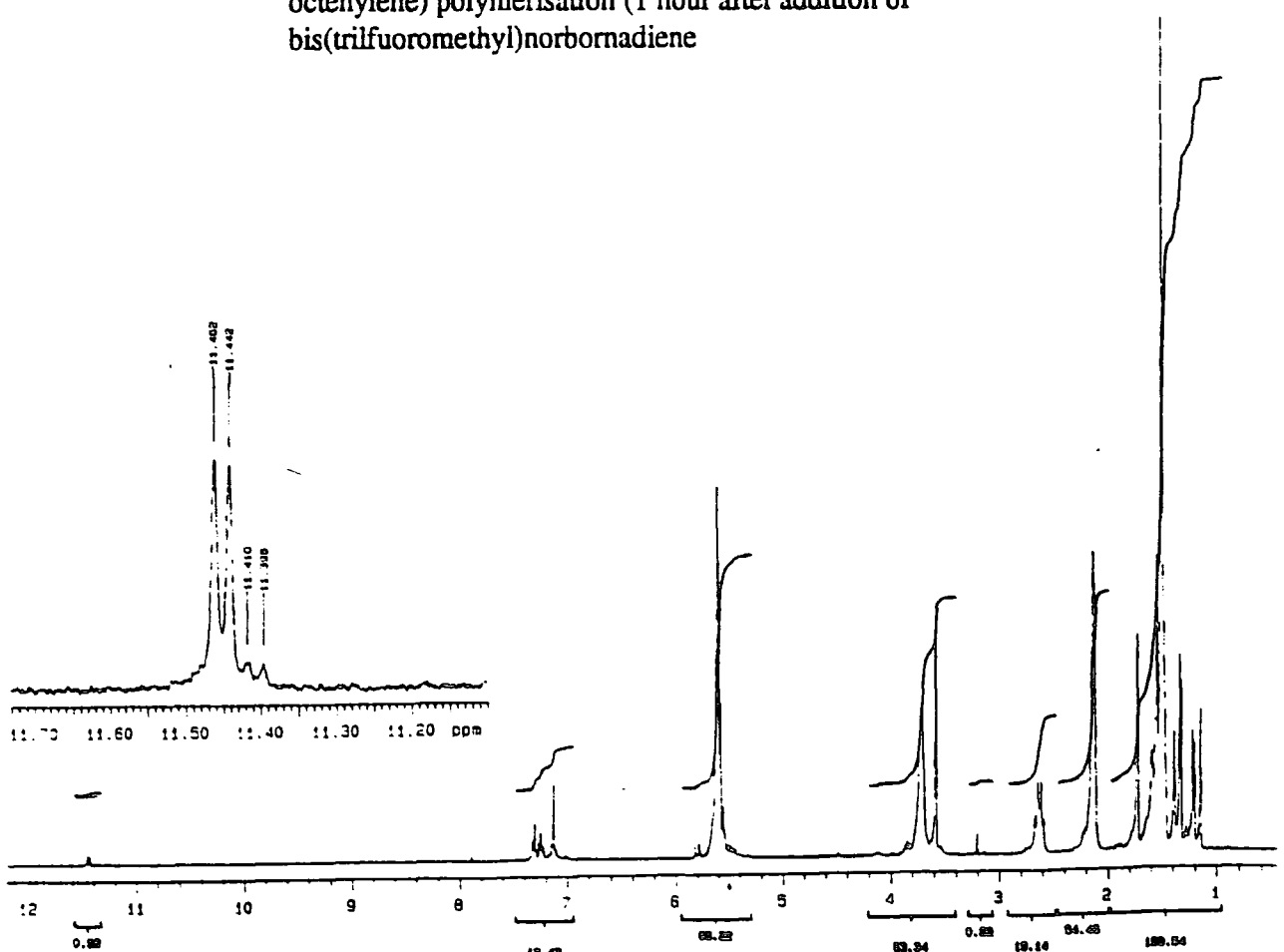

Appendix 3.1.b ^{1}H-NMR of the poly(bistrifluoromethylnorbornadiene)-*block*-poly(1-octenylene) polymerisation (15 min after addition of cyclooctene)

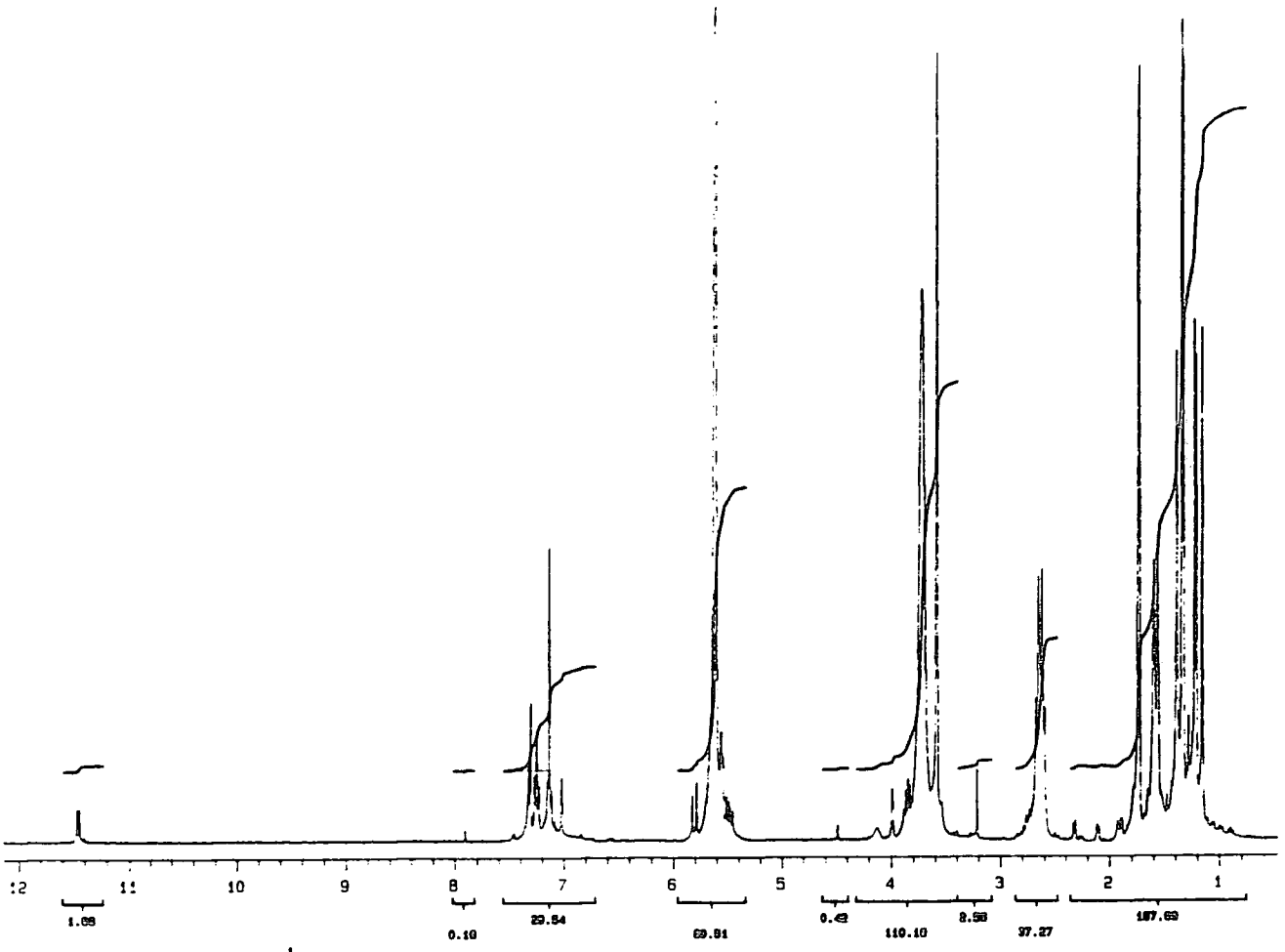

Appendix 3.1.a ^{1}H-NMR of the poly(bistrifluoromethylnorbornadiene)-*block*-poly(1-octenylene) polymerisation (1 hour after addition of bis(trilfuoromethyl)norbornadiene

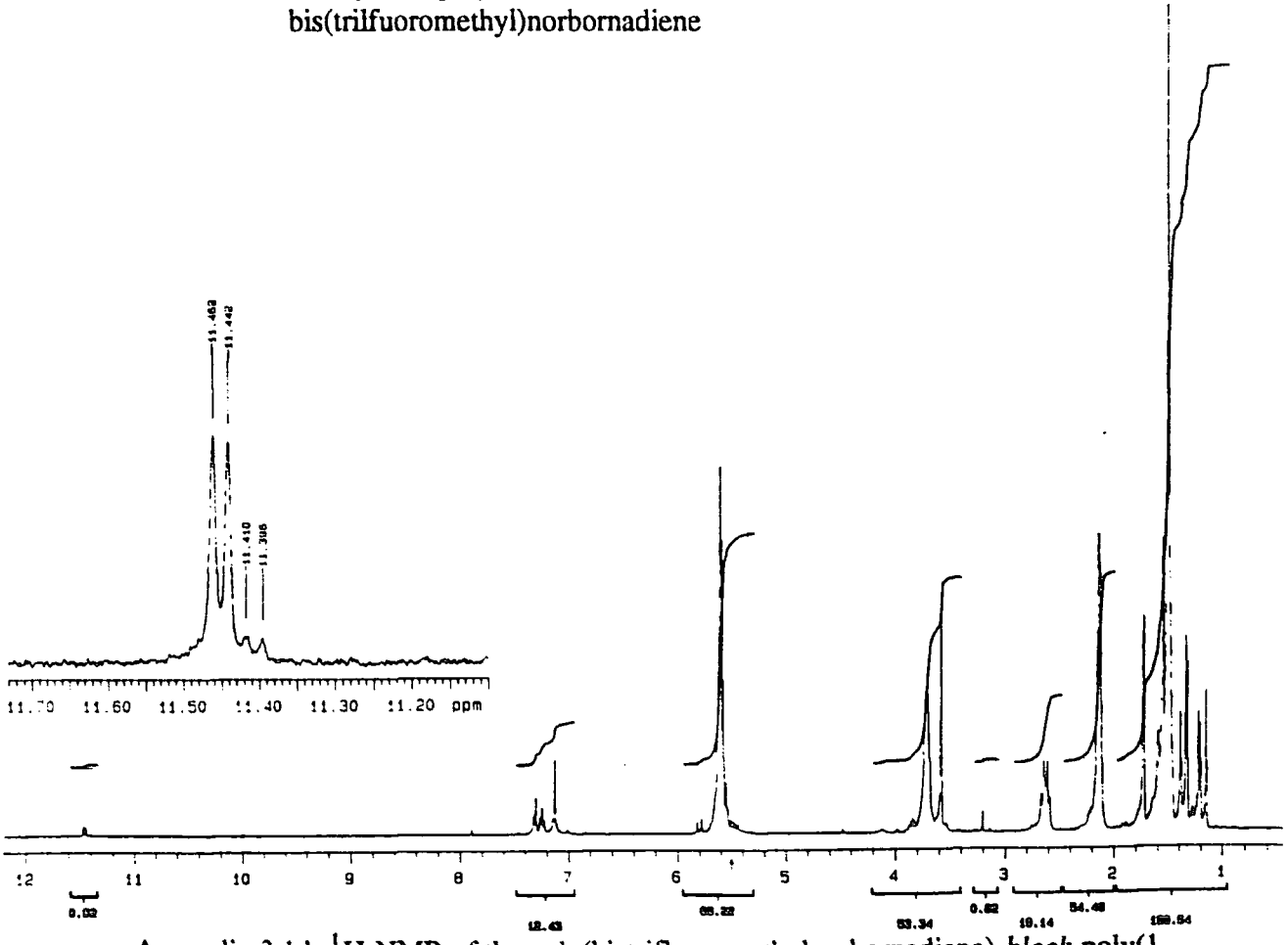

Appendix 3.1.b ^{1}H-NMR of the poly(bistrifluoromethylnorbornadiene)-*block*-poly(1-octenylene) polymerisation (15 min after addition of cyclooctene)

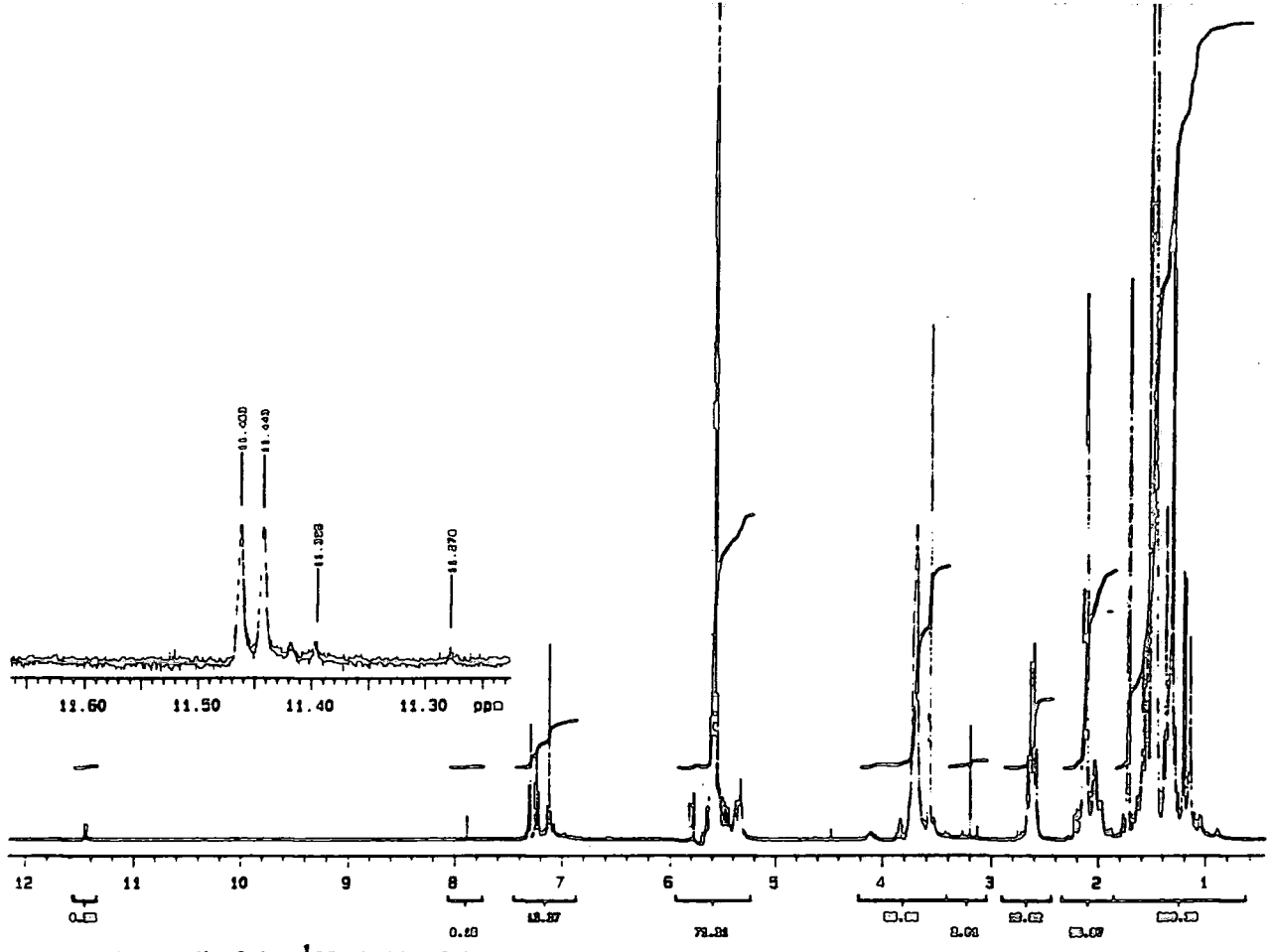

Appendix 3.1.c ^{1}H-NMR of the poly(bistrifluoromethylnorbornadiene)-*block*-poly(1-octenylene) polymerisation (3 days after addition of cyclooctene)

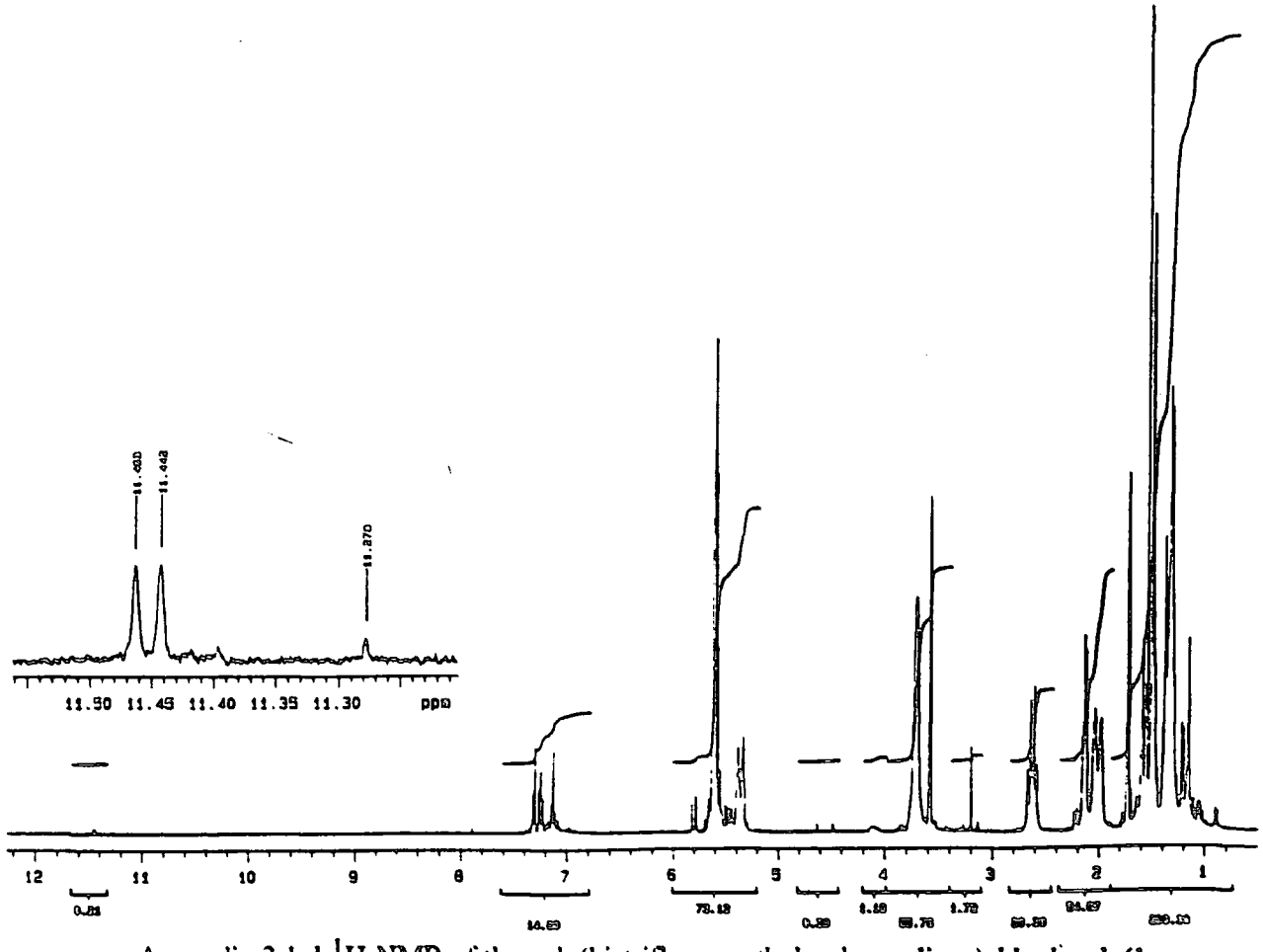

Appendix 3.1.d ^{1}H-NMR of the poly(bistrifluoromethylnorbornadiene)-*block*-poly(1-octenylene) polymerisation (7 days after addition of cyclooctene)

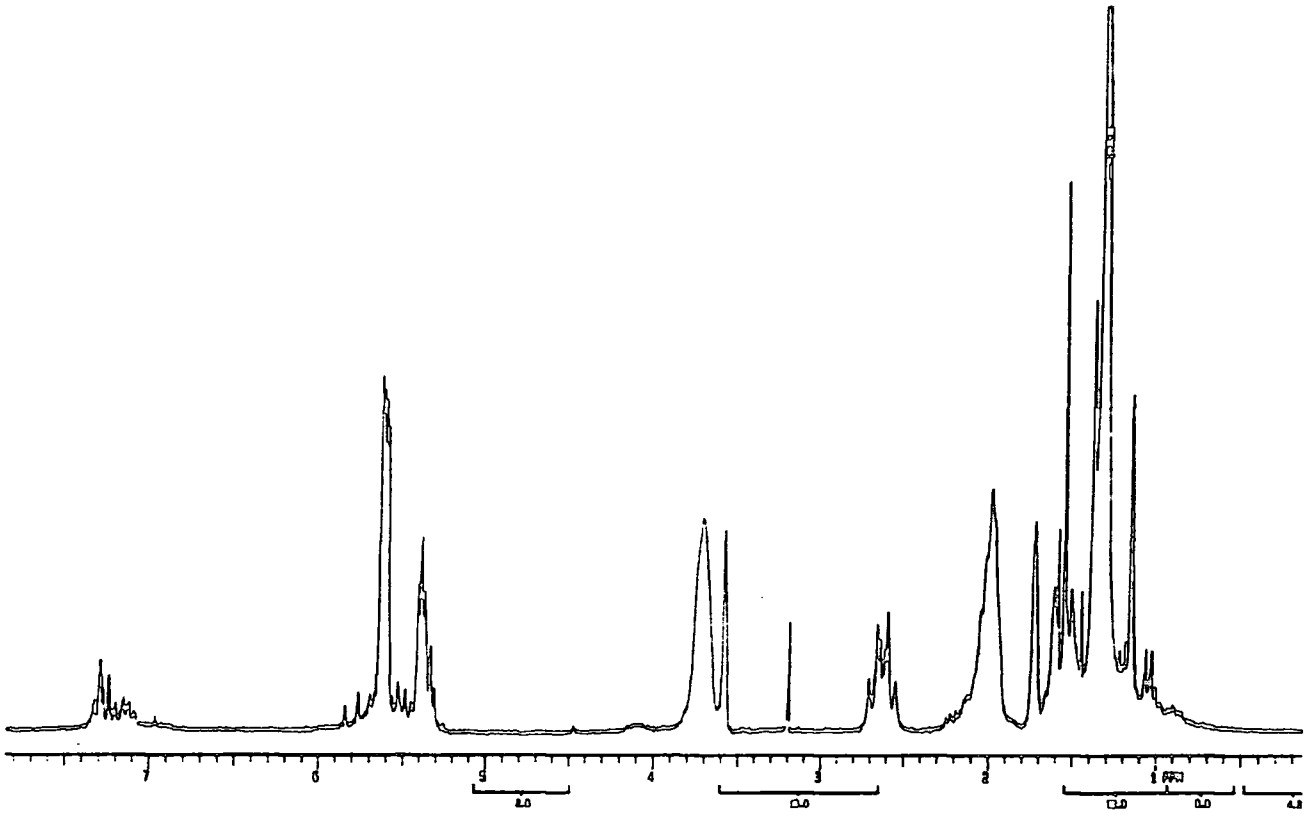

Appendix 3.1.e ^{1}H-NMR of the poly(bistrifluoromethylnorbornadiene)-*block*-poly(1-octenylene) polymerisation (10 days after addition of cyclooctene)

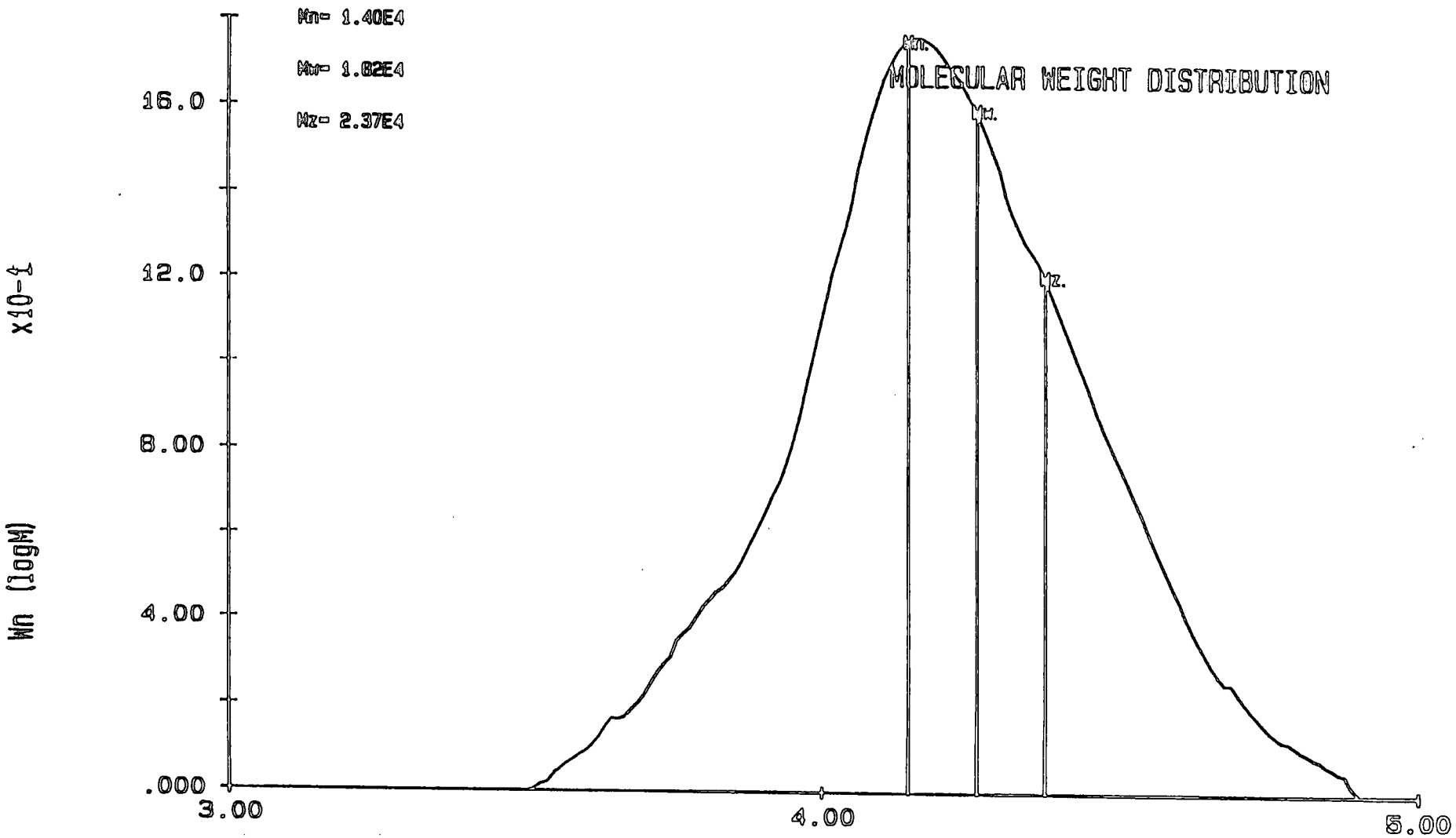

Appendix 3.2 GPC trace of poly(bistrifluoromethylnorbornadiene)-*block*-poly(1-octenylene)

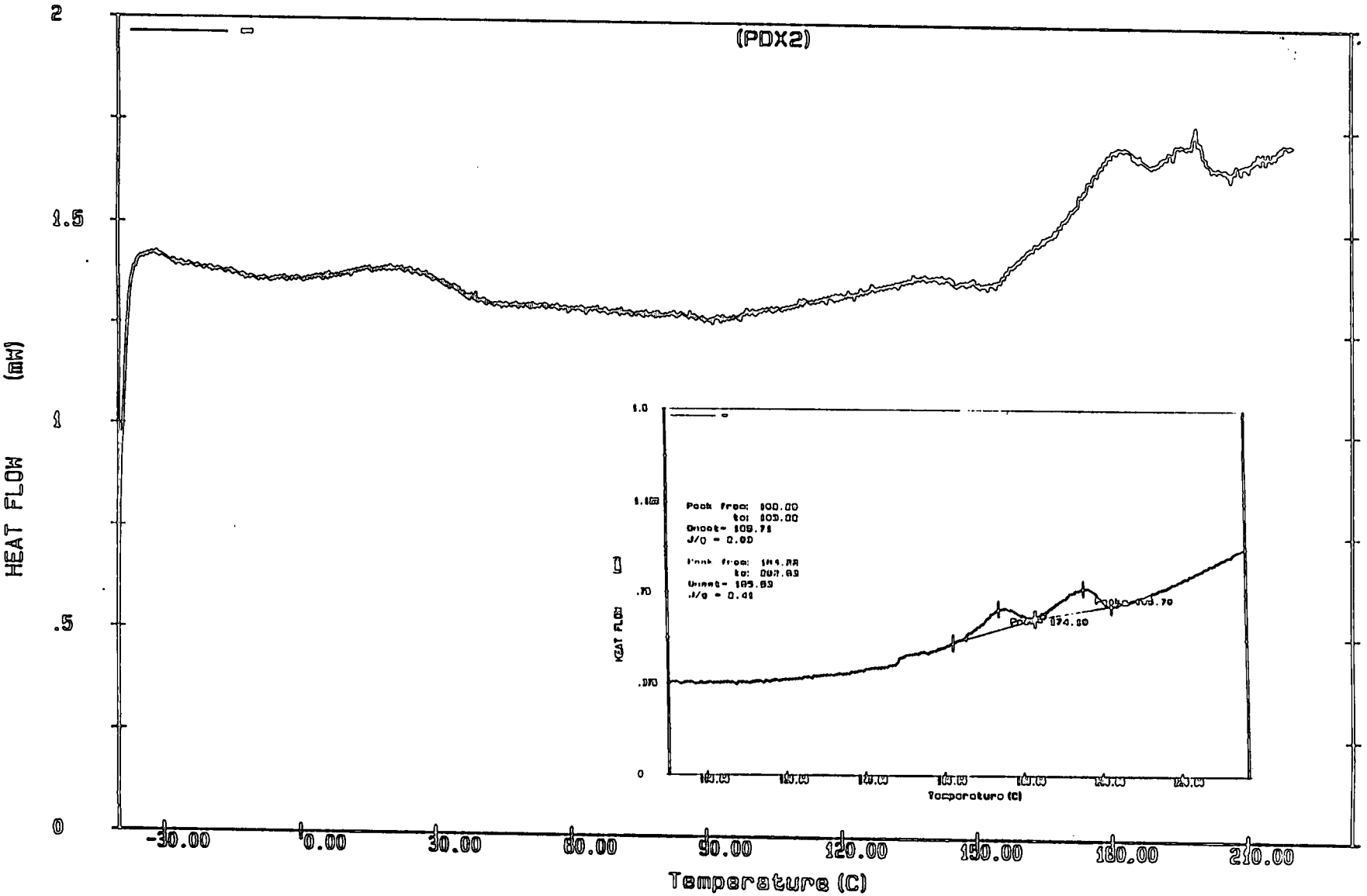

Appendix 3.3 DSC trace of poly(bistrifluoromethylnorbornadiene)-*block*-poly(1-octenylene)

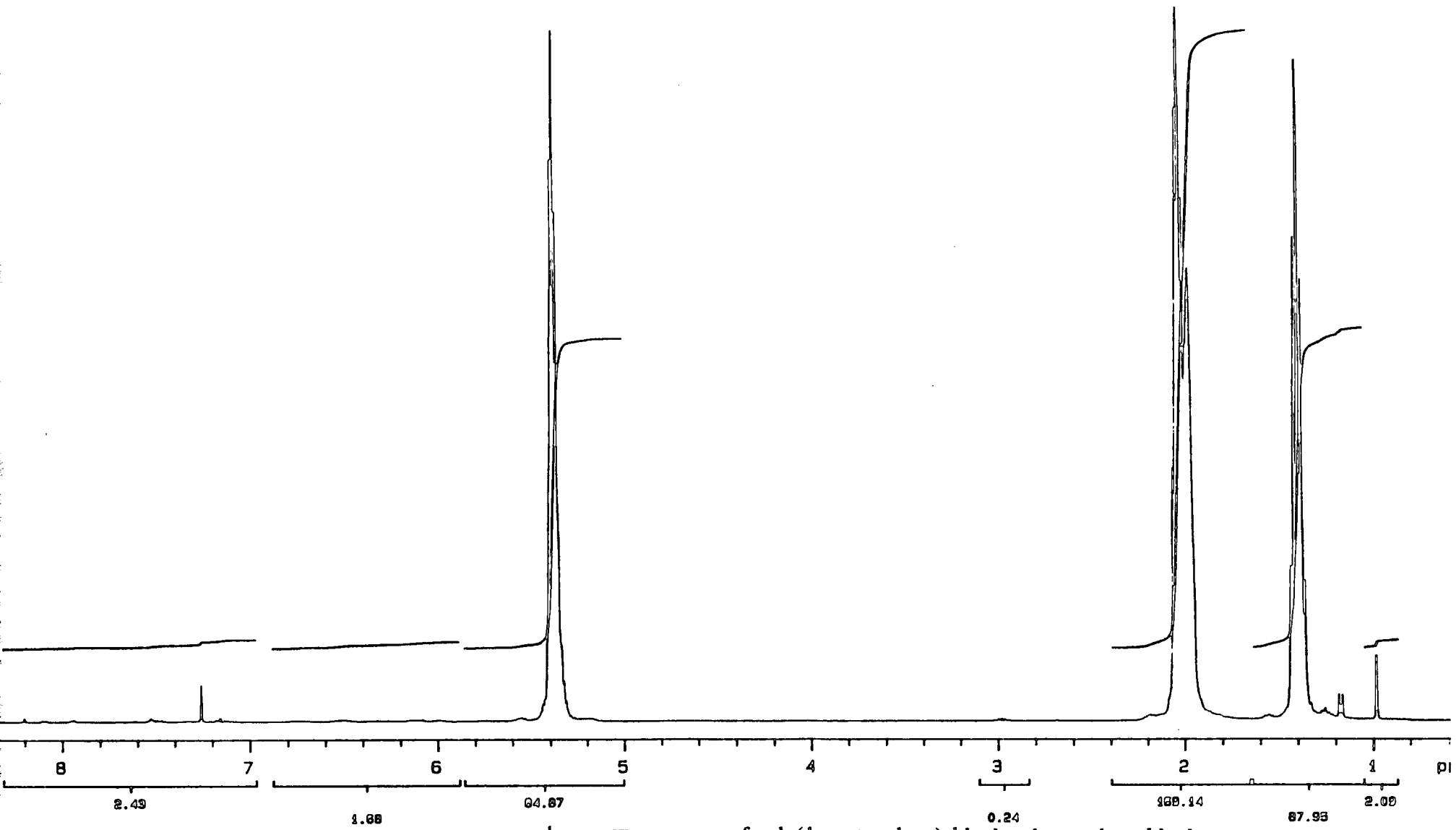

Appendix 3.4 ^{1}H-NMR spectrum of poly(1-pentenylene)-*block*-polyacetylene-*block*-poly(1-pentenylene)

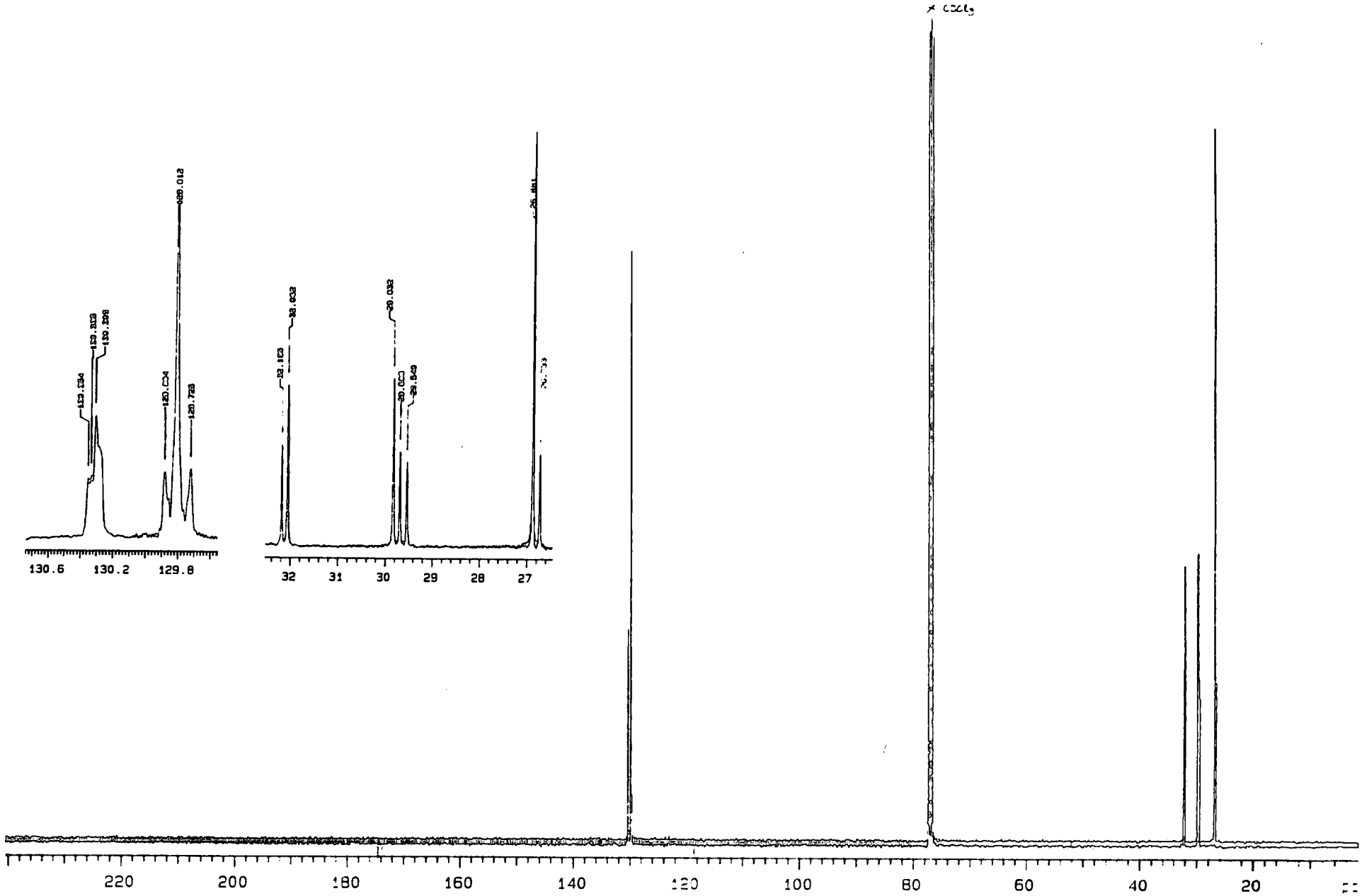

Appendix 3.5 ^{13}C-NMR spectrum of poly(1-pentenylene)-*block*-polyacetylene-*block*-poly(1-pentenylene)

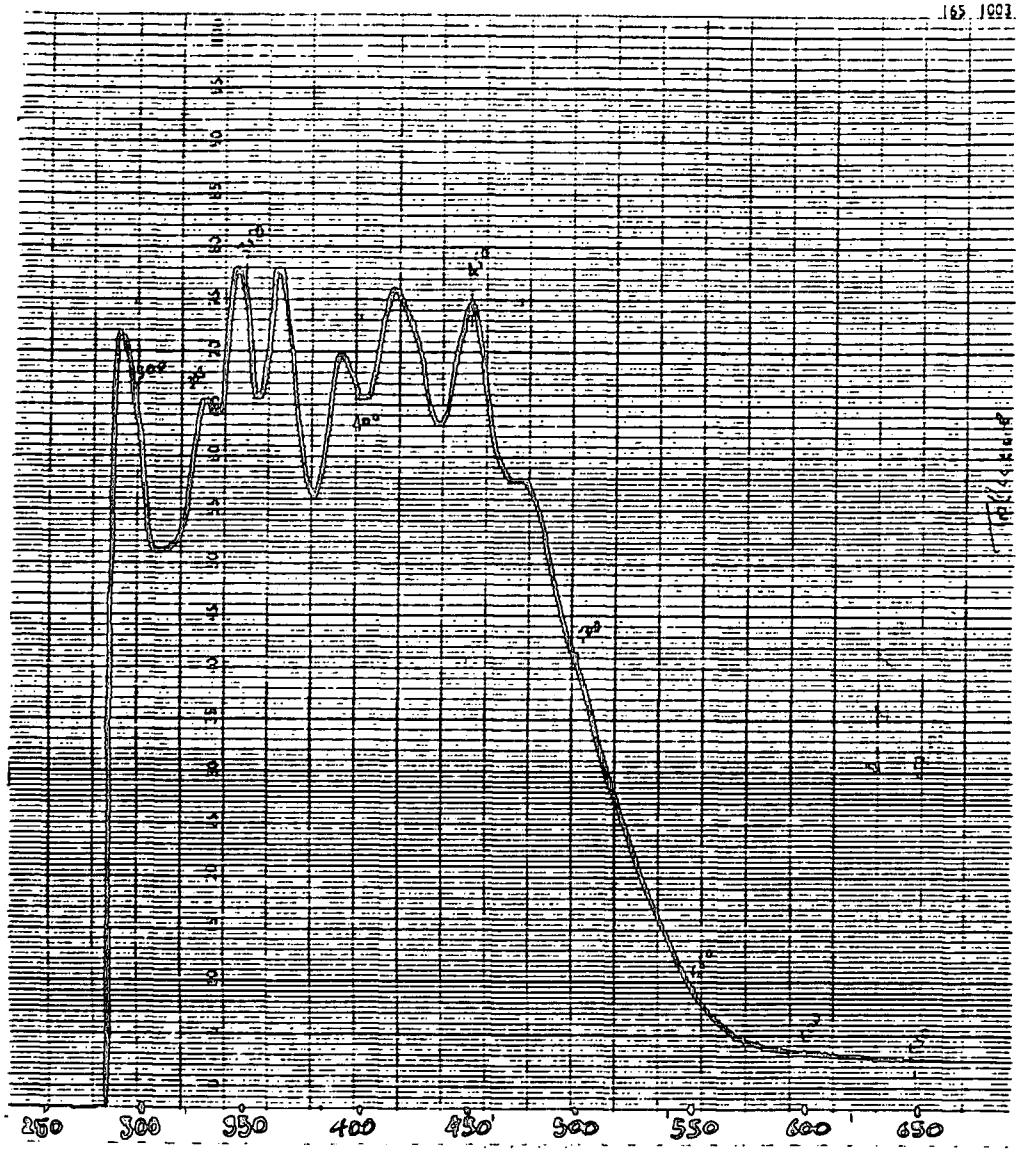

Appendix 3.6.a UV / Vis spectrum of poly(1-pentenylene)-*block*-polyacetylene-*block*-poly(1-pentenylene) in toluene

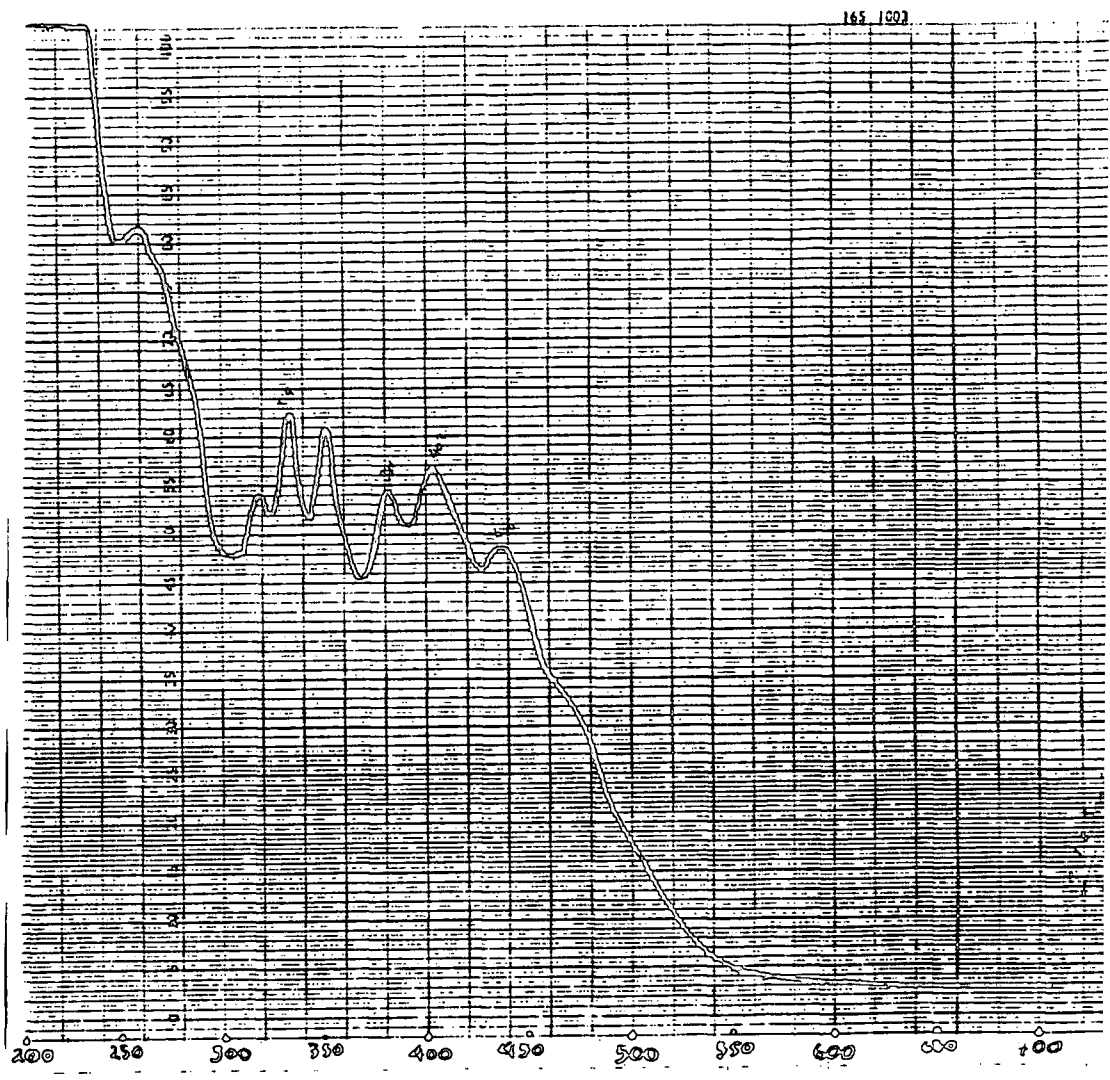

Appendix 3.6.b UV / Vis spectrum of poly(1-pentenylene)-*block*-polyacetylene-*block*-poly(1-pentenylene) in heptane

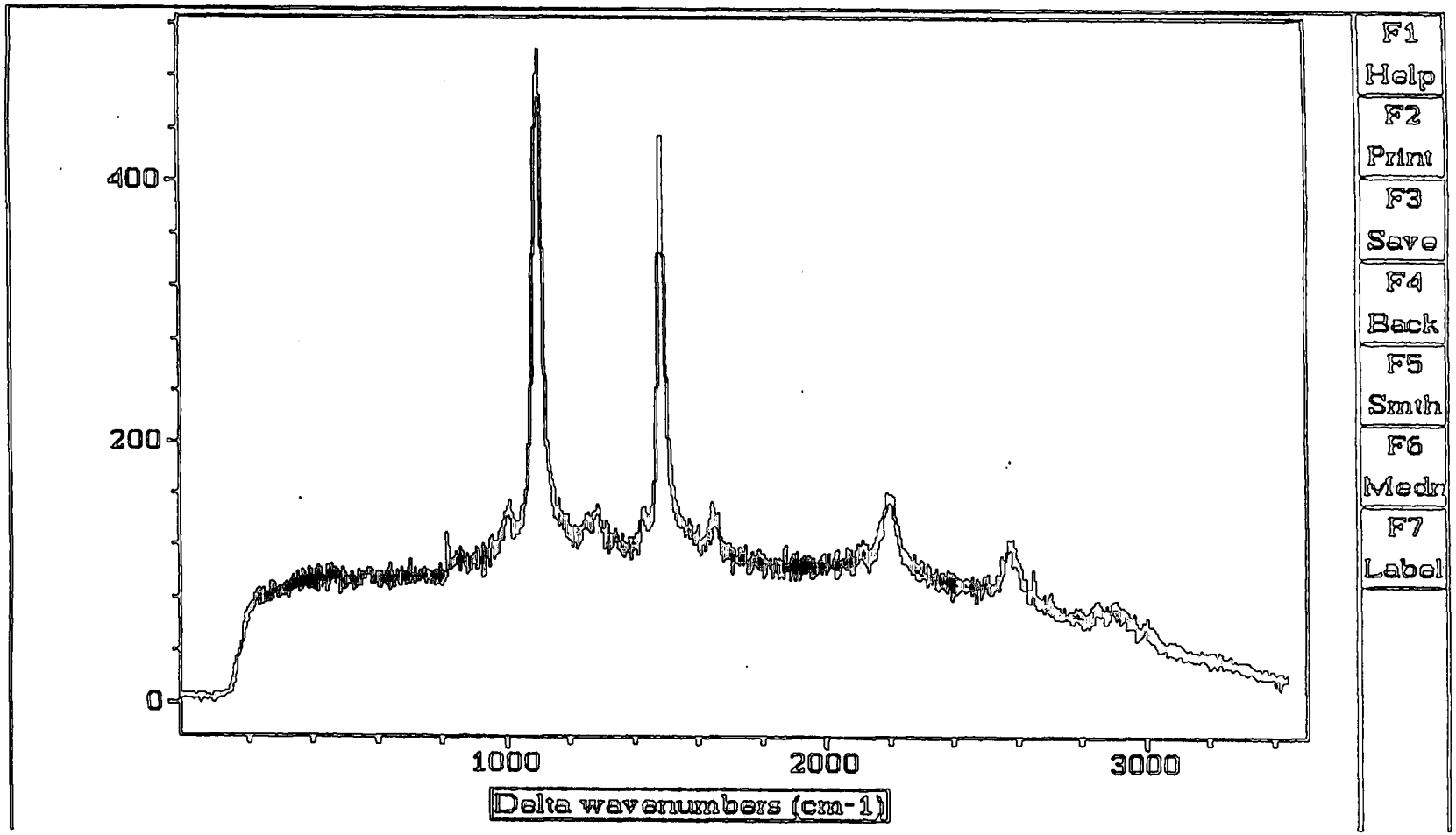

Appendix 3.7 Raman spectrum of poly(1-pentenylene)-*block*-polyacetylene-*block*-poly(1-pentenylene)

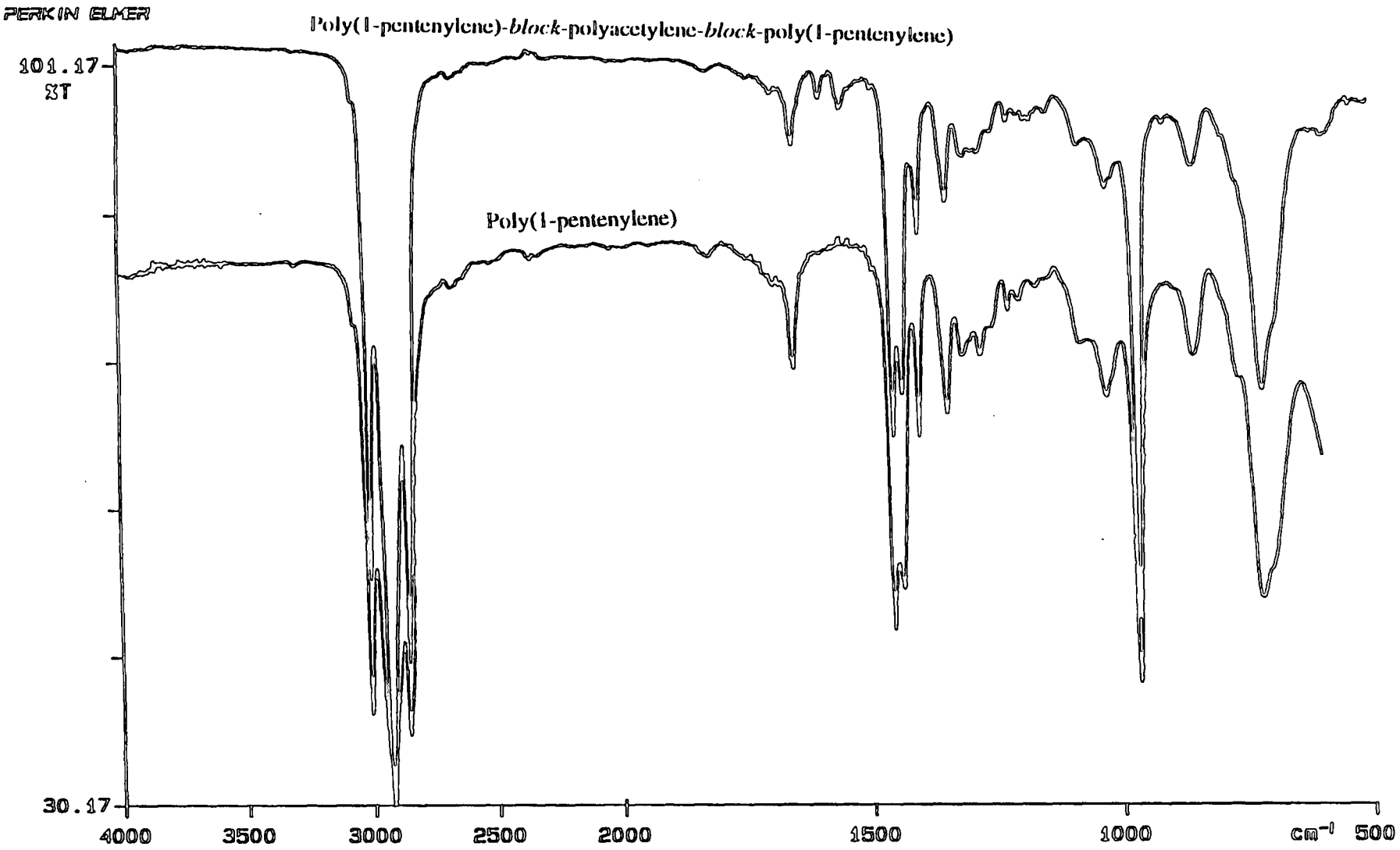

Appendix 3.8 Overlaid IR spectra of poly(1-pentenylene)-*block*-polyacetylene-*block*-poly(1-pentenylene) and poly(1-pentenylene) homopolymer

Flow Rate Marker : TOLUENE found at 31.03Min
in Standards at 31.02Min
Broad Peak Start : 18.20 End : 21.70 Mins

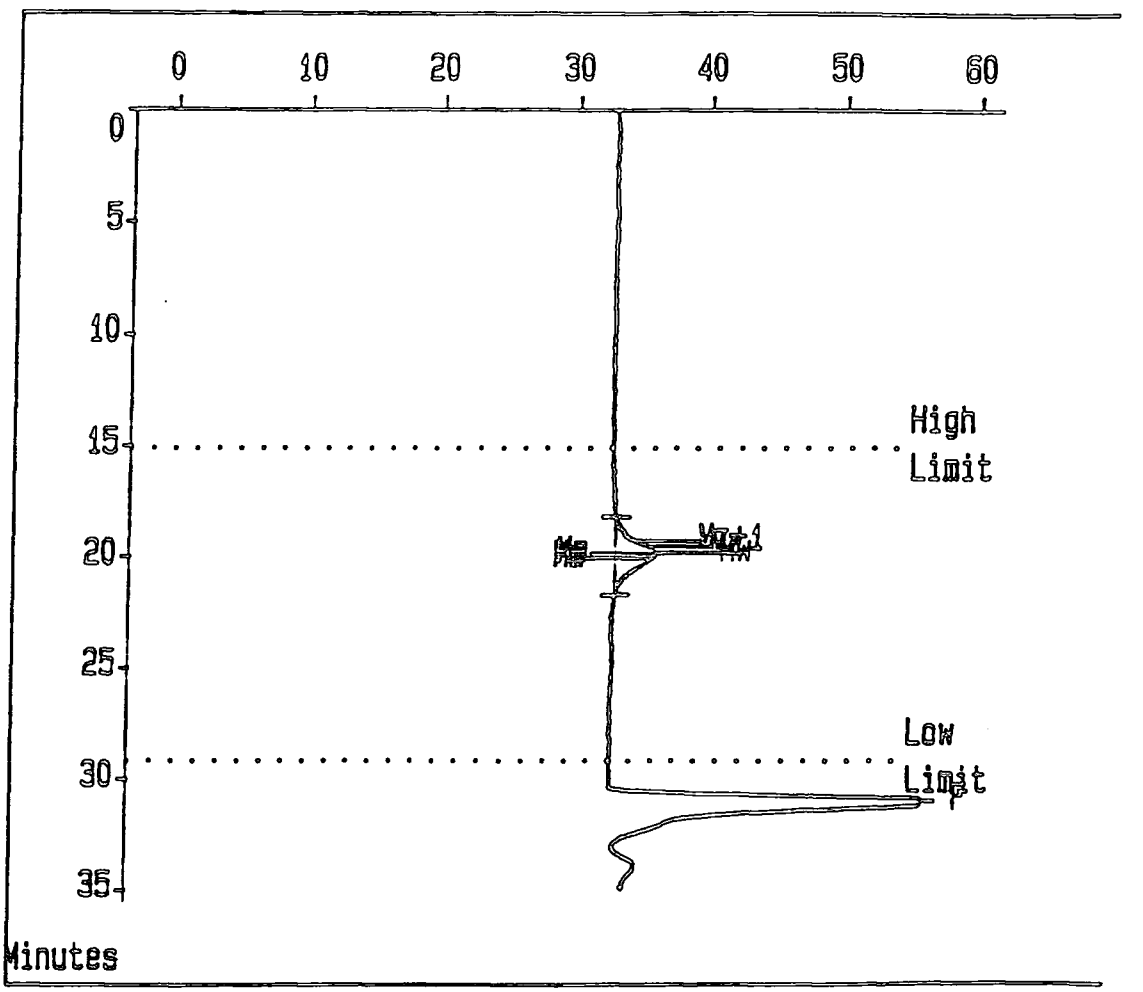

Molecular Weight Averages

Mp =	42934.8	Mz =	53888.8
Mn =	36379.0	Mz+1 =	65246.6
Mw =	44237.2	Mv =	42946.3
Polydispersity =	1.216		

Appendix 3.9 GPC trace of poly(1-pentenylene)-*block*-polyacetylene-*block*-poly(1-pentenylene

APPENDIX 4

Analytical data for Chapter 4

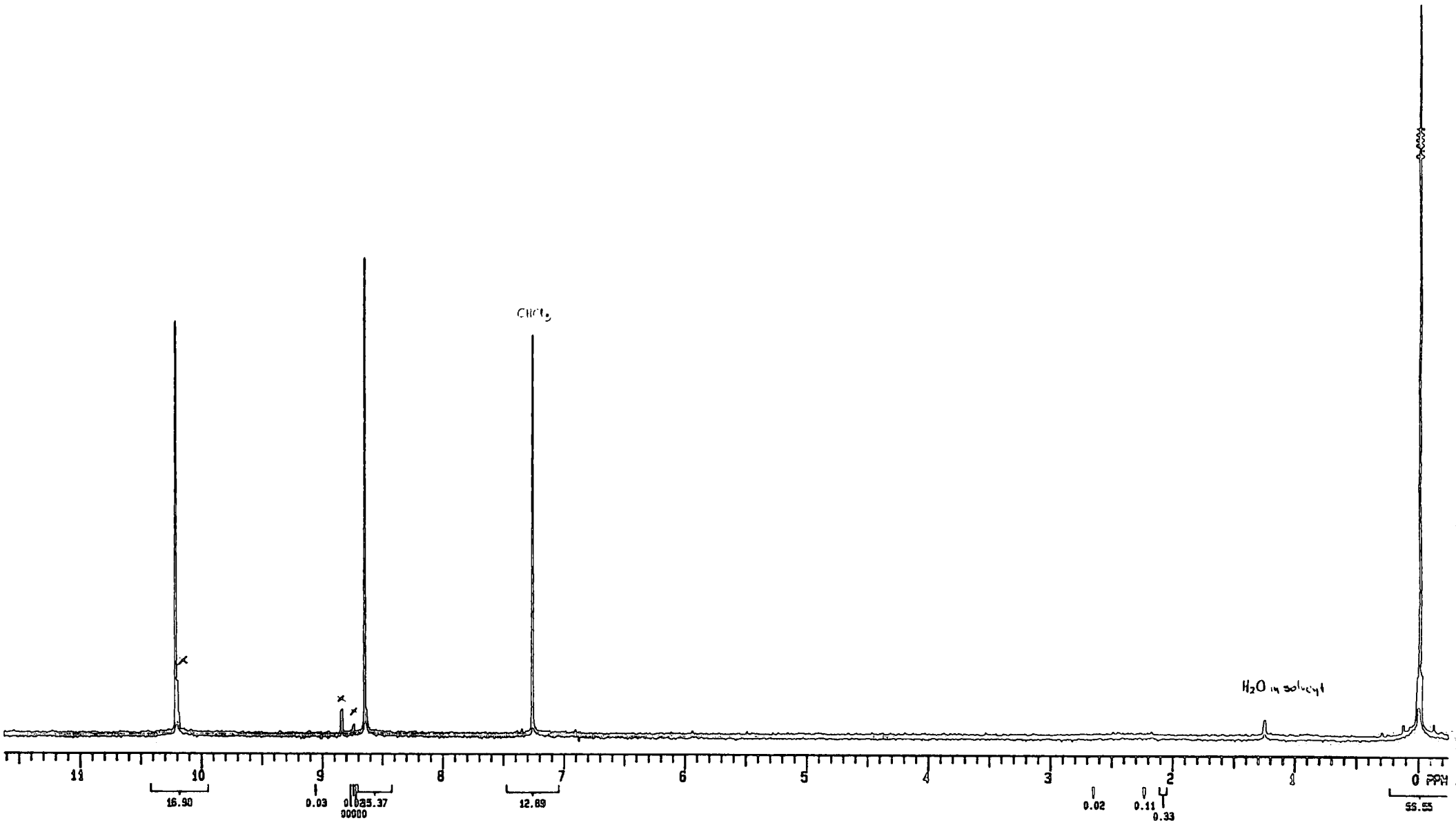

Appendix 4.1 ^{1}H NMR spectrum of 1,3,5-benzenetricarboxaldehyde

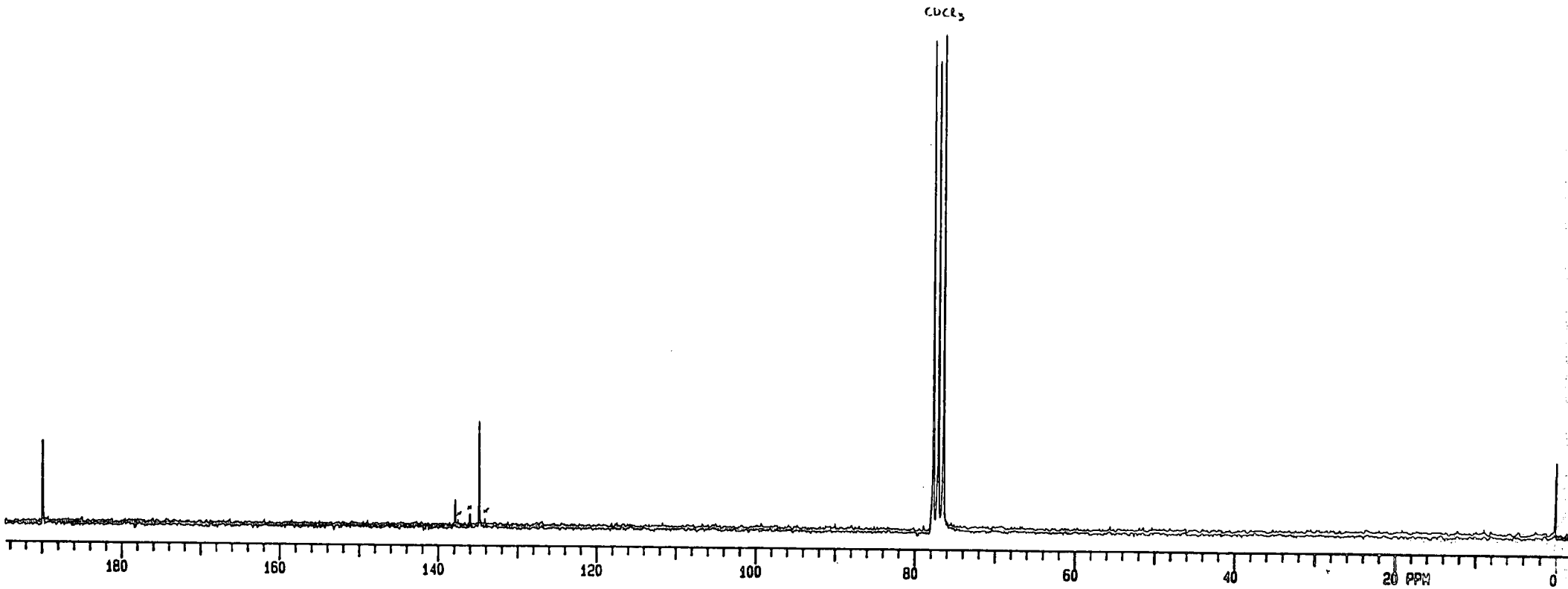

Appendix 4.2 ^{13}C NMR spectrum of 1,3,5-benzenetricarboxaldehyde

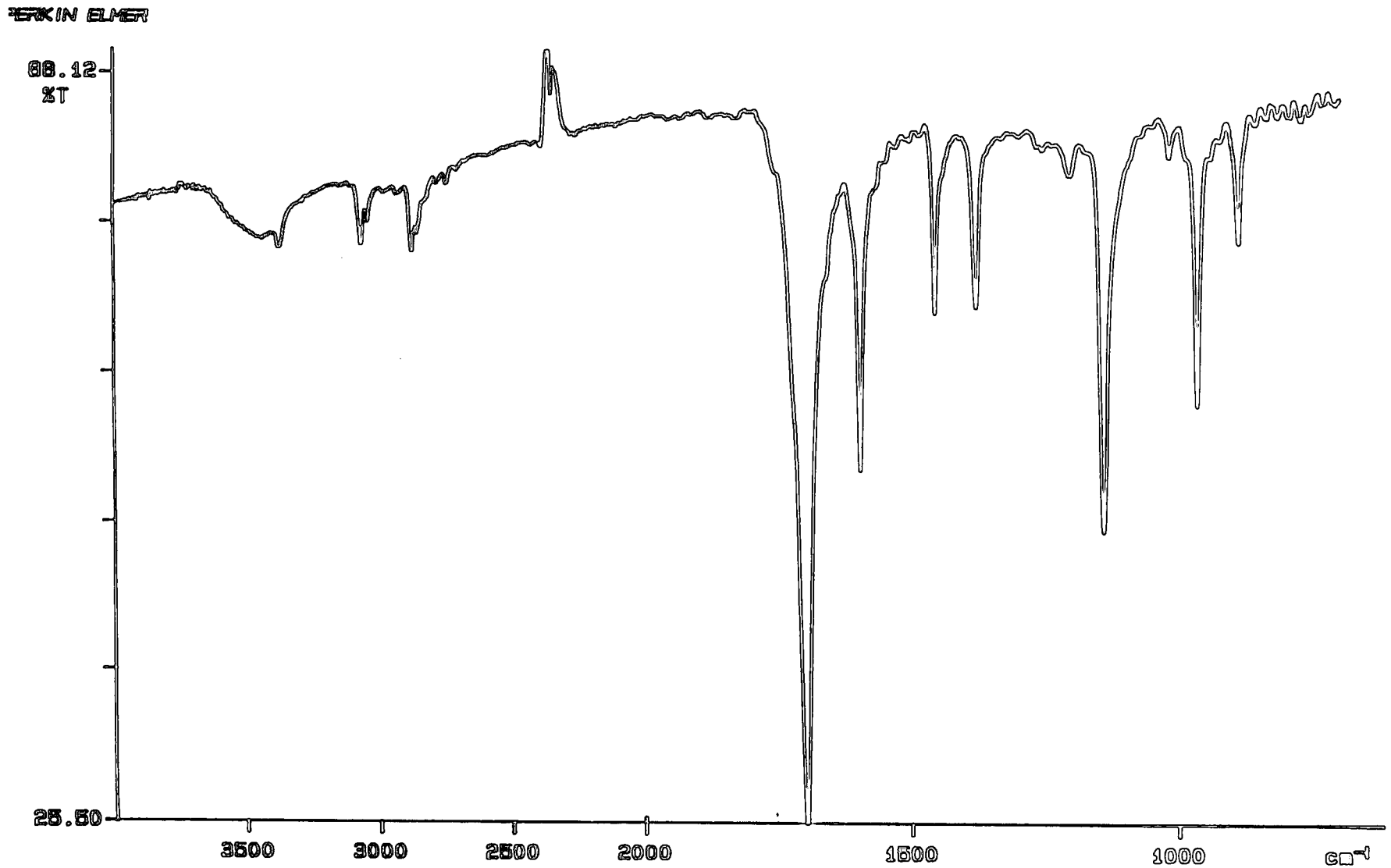

Appendix 4.3 IR spectrum of 1,3,5-benzenetricarboxaldehyde

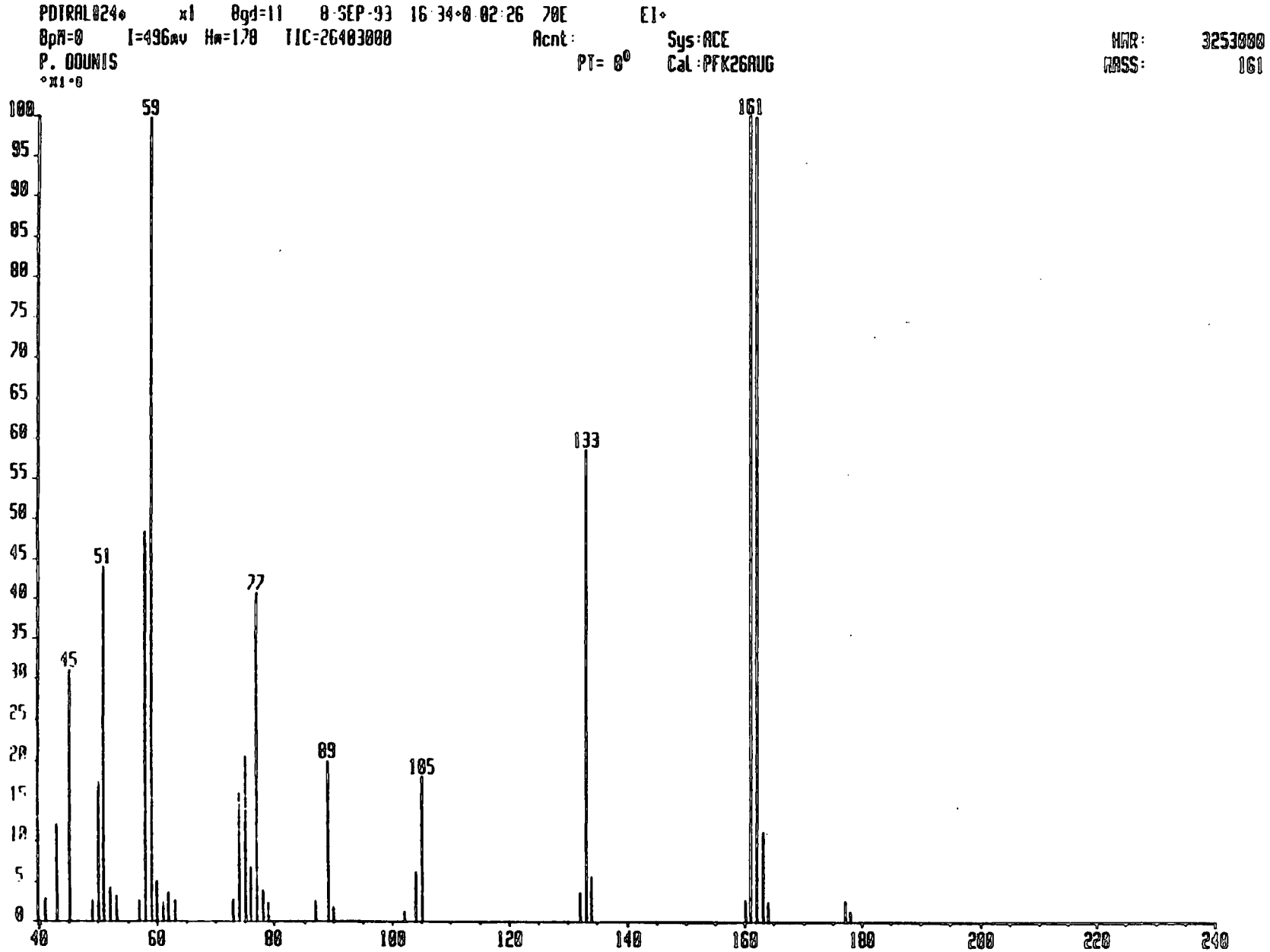

Appendix 4.4 Mass spectrum of 1,3,5-benzenetricarboxaldehyde

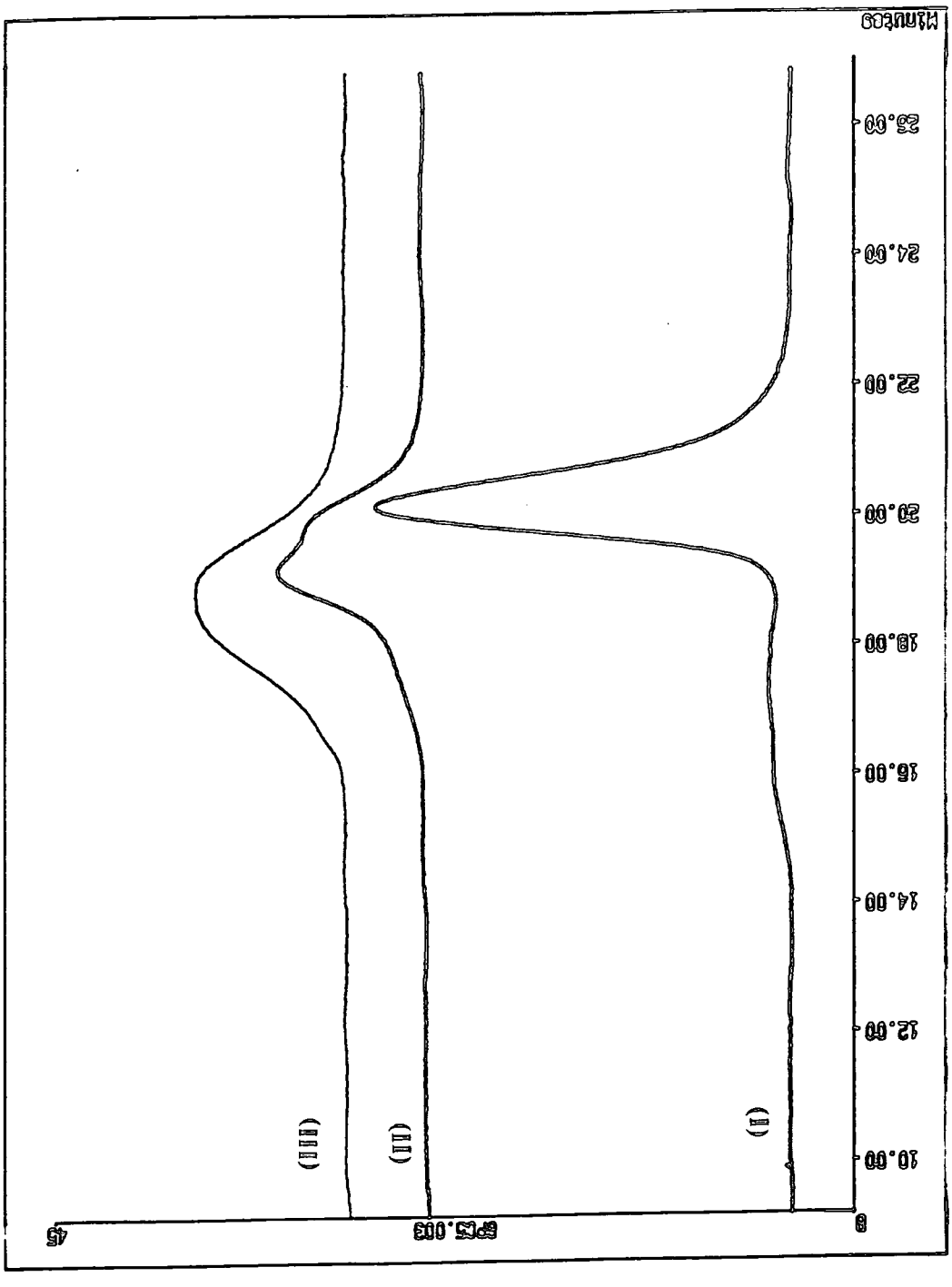

Appendix 4.5 Overlaid GPC traces of poly(1-pentenylene) capped with mono- (I), di- (II) and trifunctional (III) aldehydes

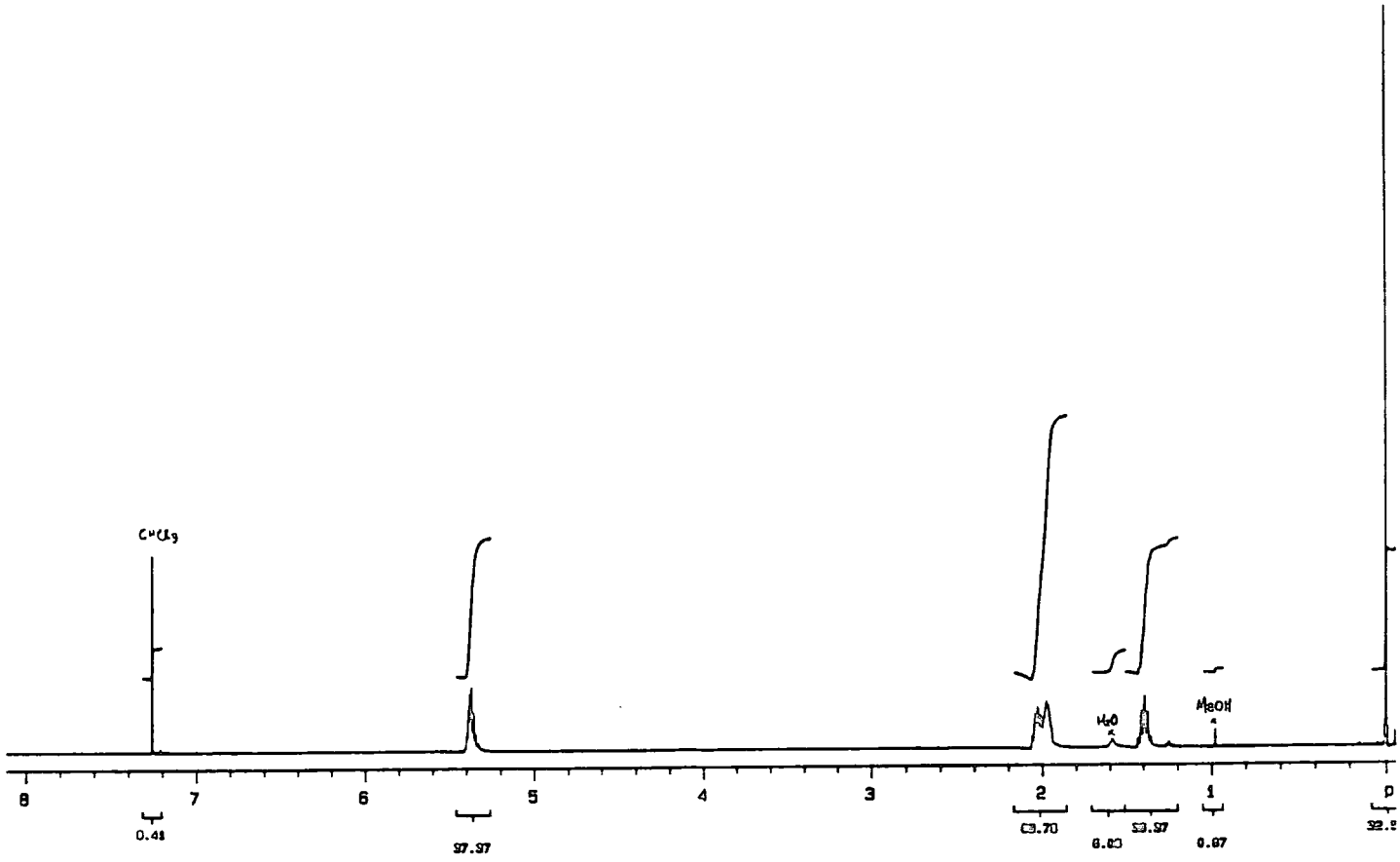

Appendix 4.6 ^{1}H NMR spectrum of star poly(1-pentenylene)

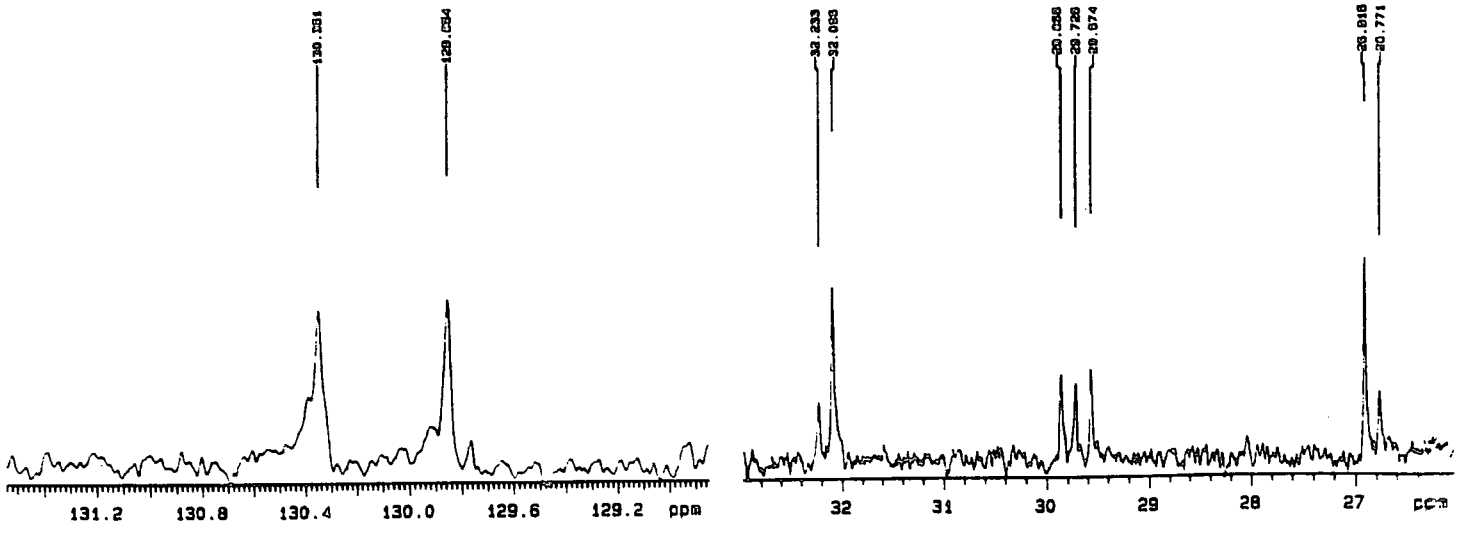

Appendix 4.7 ^{13}C NMR spectrum of star poly(1-pentenylene)

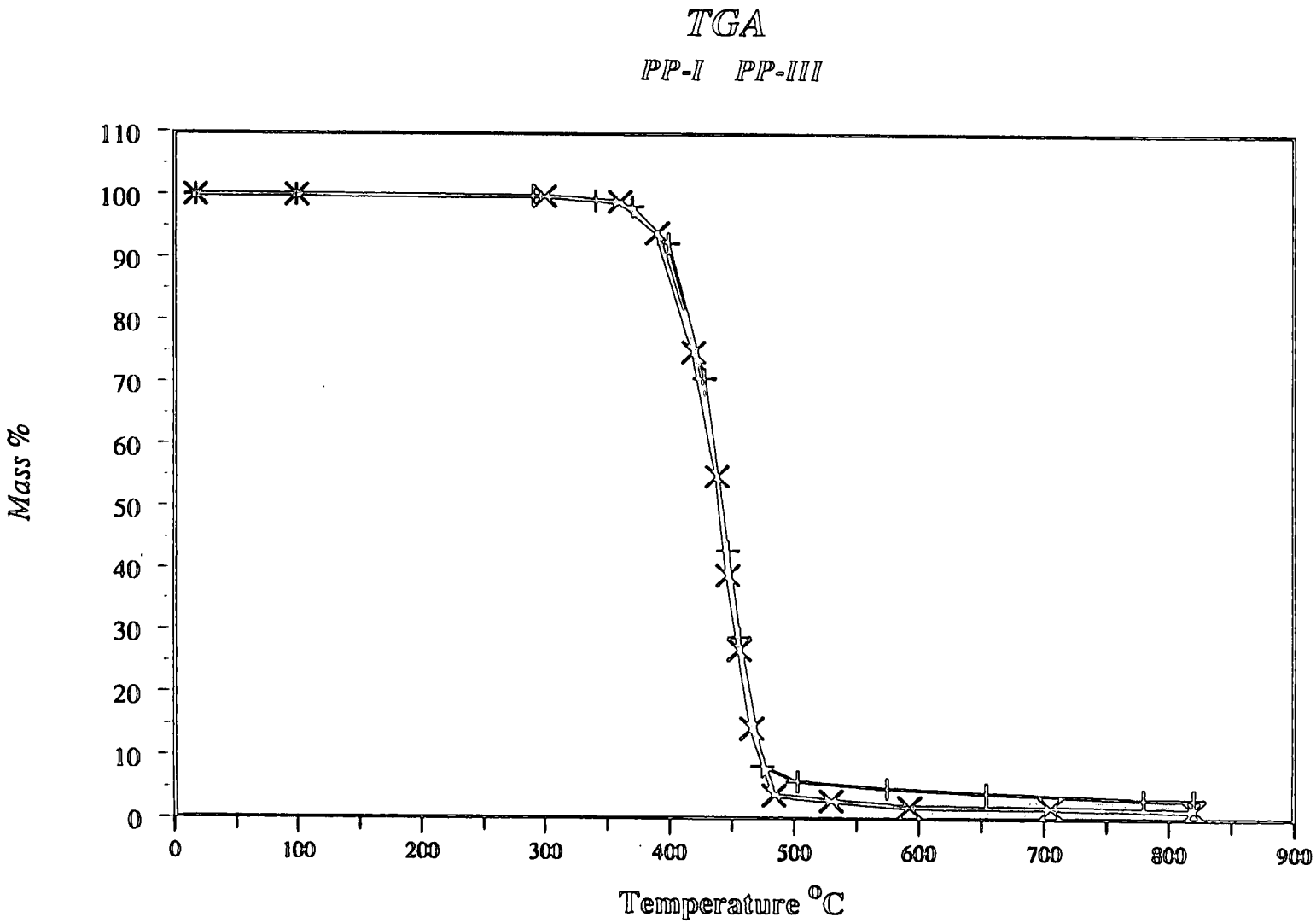

Appendix 4.8 Thermogravimetric analysis of linear and star poly(1-pentenylenes)

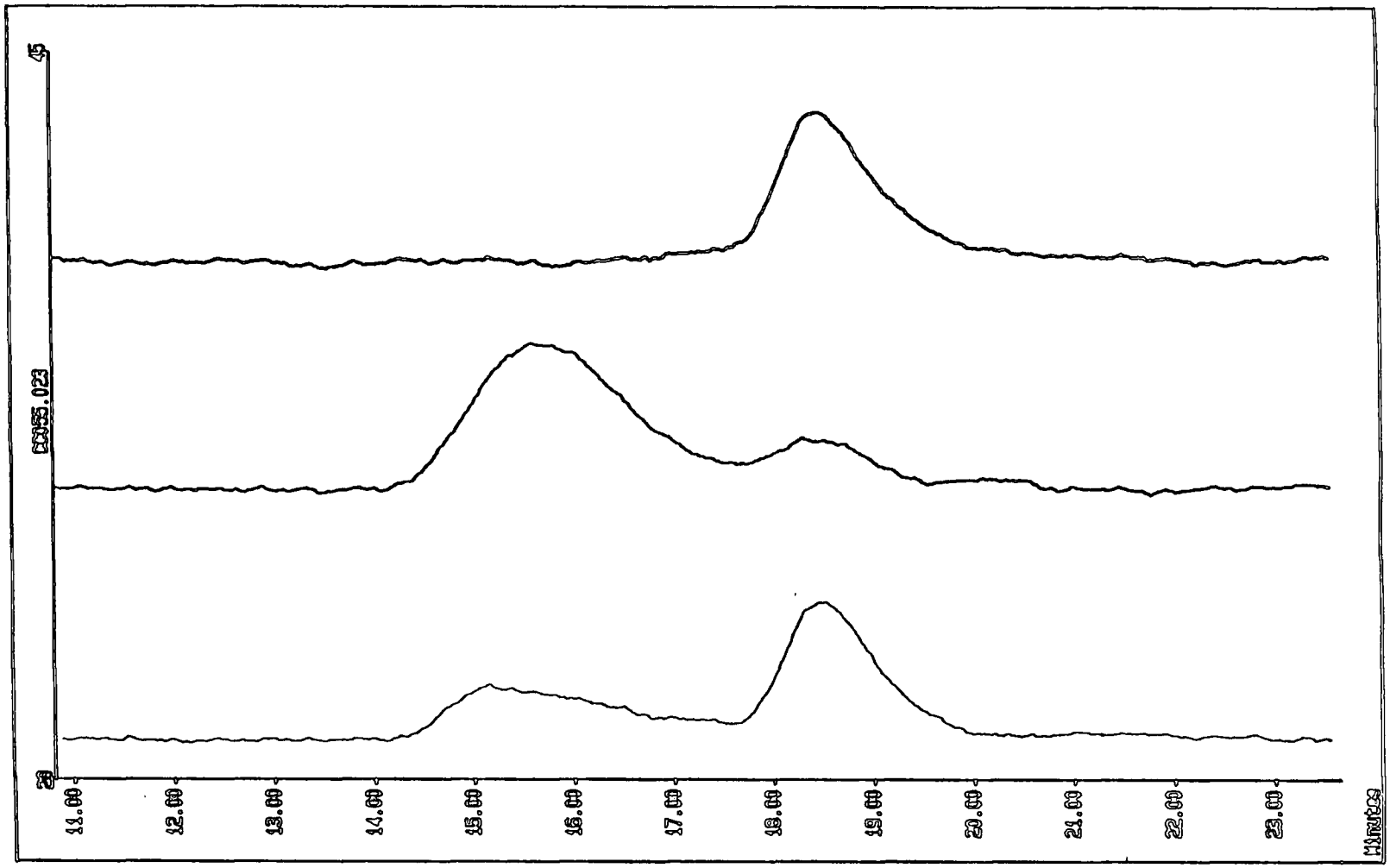

Appendix 4.9 Overlaid GPC traces of linear polymer (IV) before and after fractionation

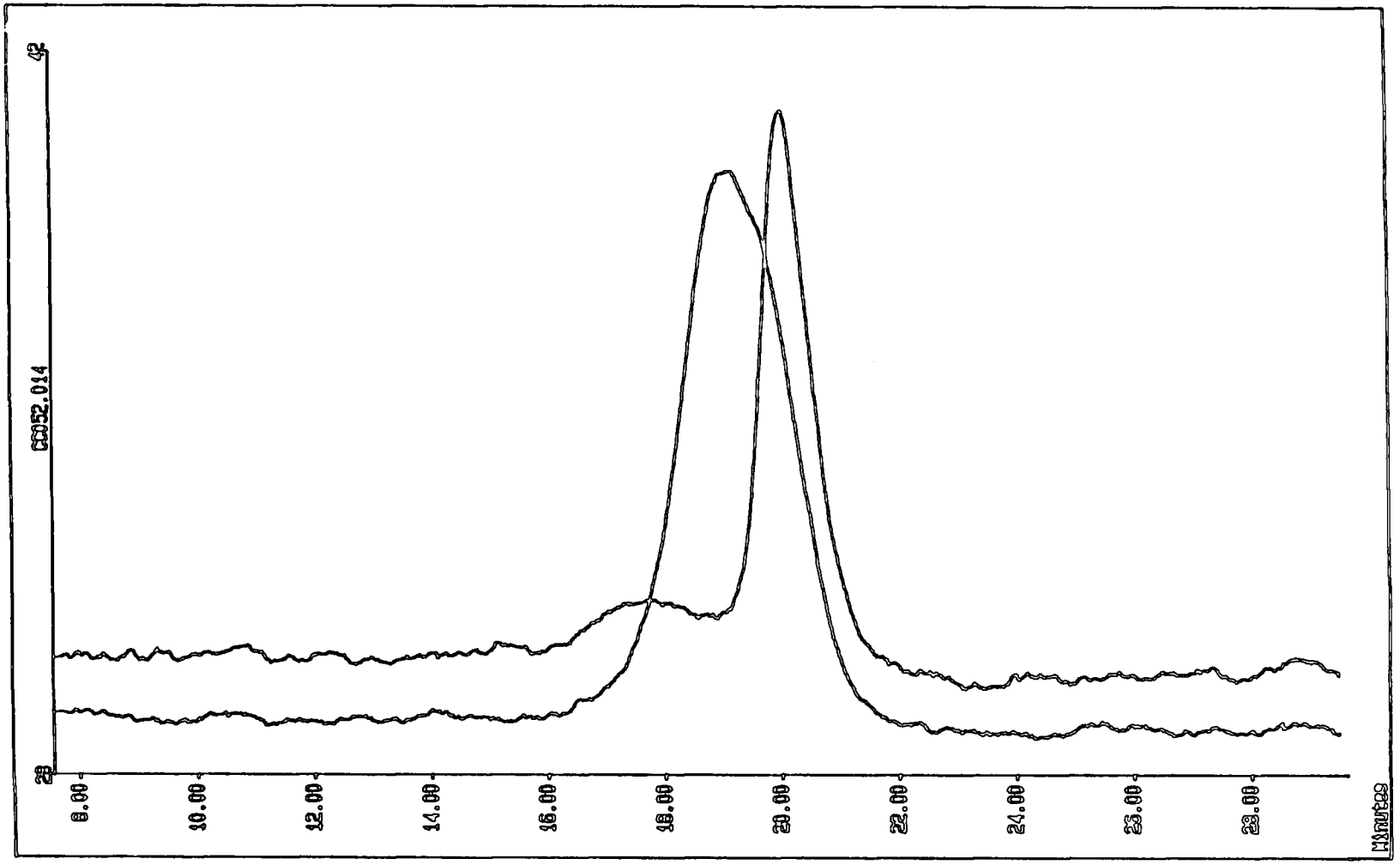

Appendix 4.10 Overlaid GPC traces of linear polymer (V) before and after the capping reaction

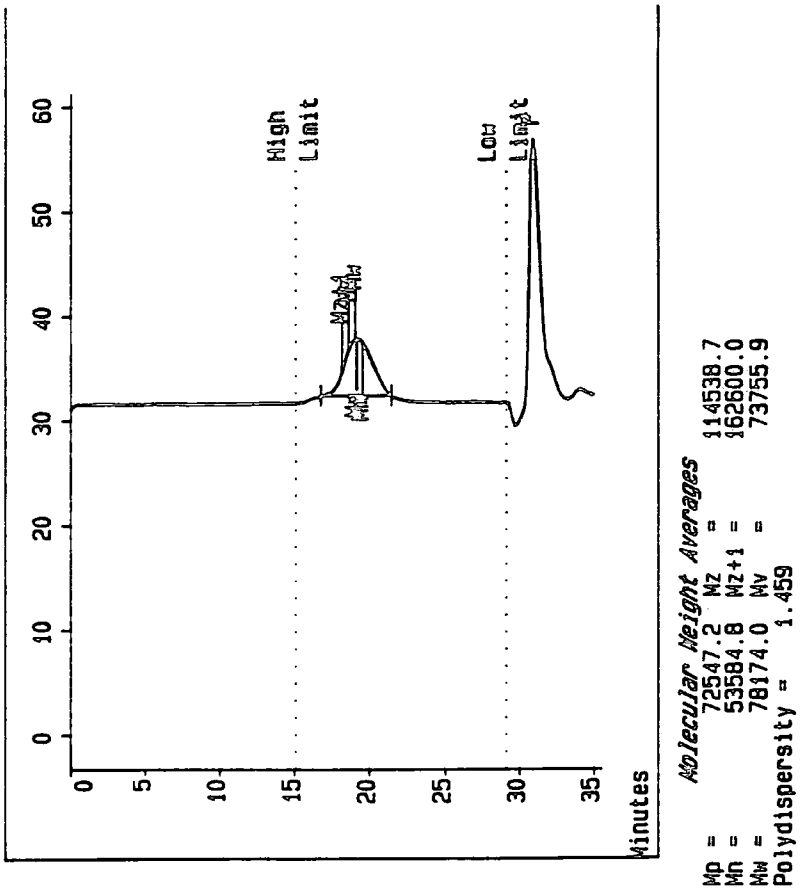

Appendix 4.11 GPC trace of star polymer (VI)

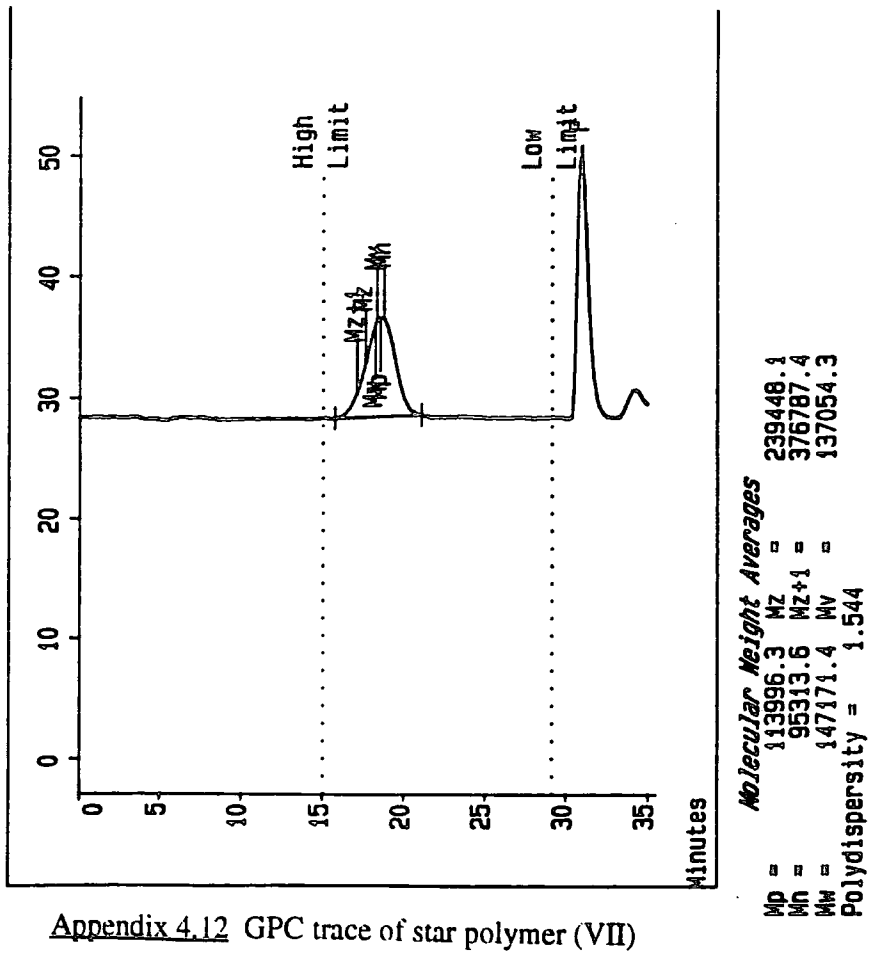

Appendix 4.12 GPC trace of star polymer (VII)

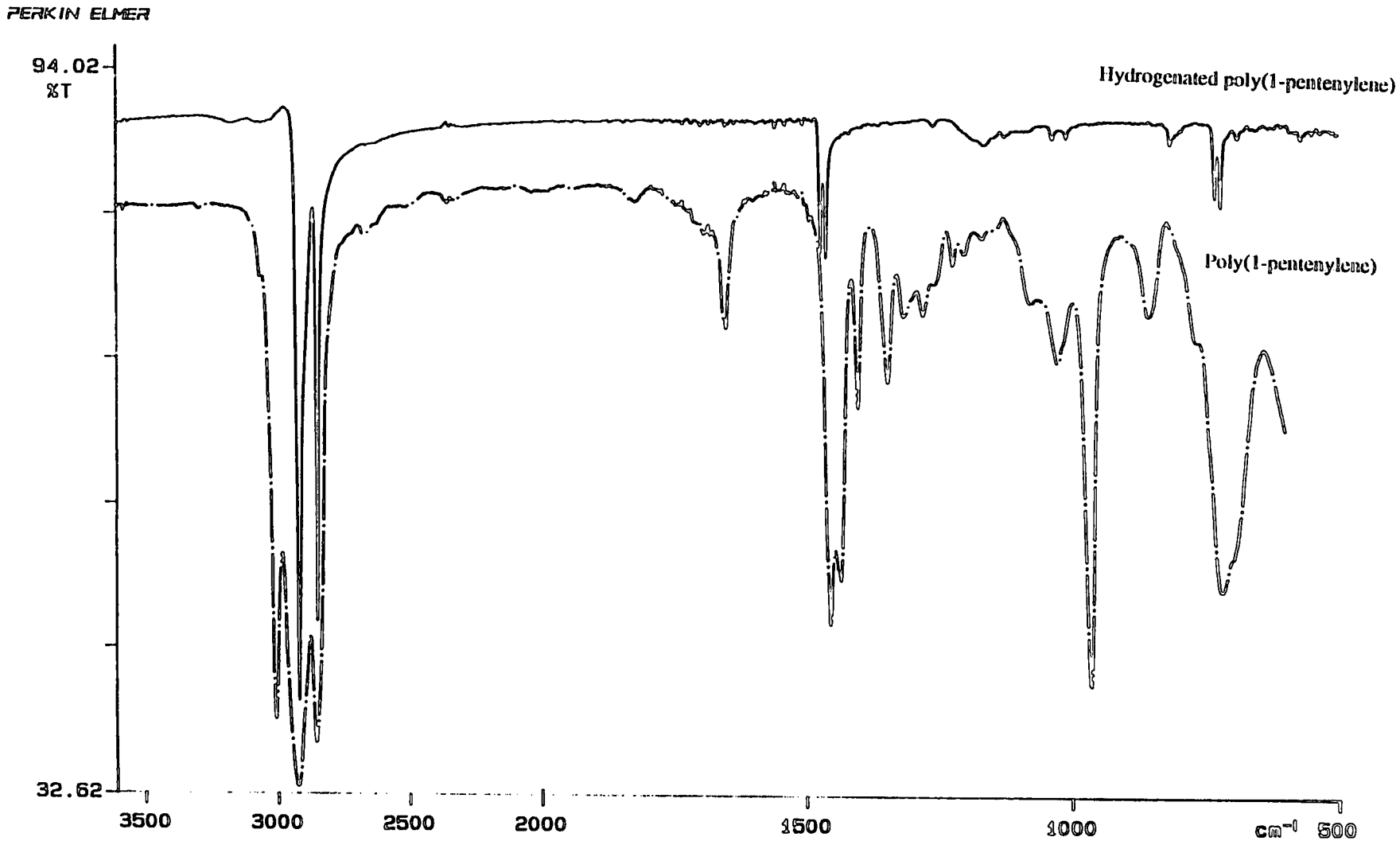

Appendix 4.13 Overlaid IR spectra of poly(1-pentenylene) and hydrogenated poly(1-pentenylene)

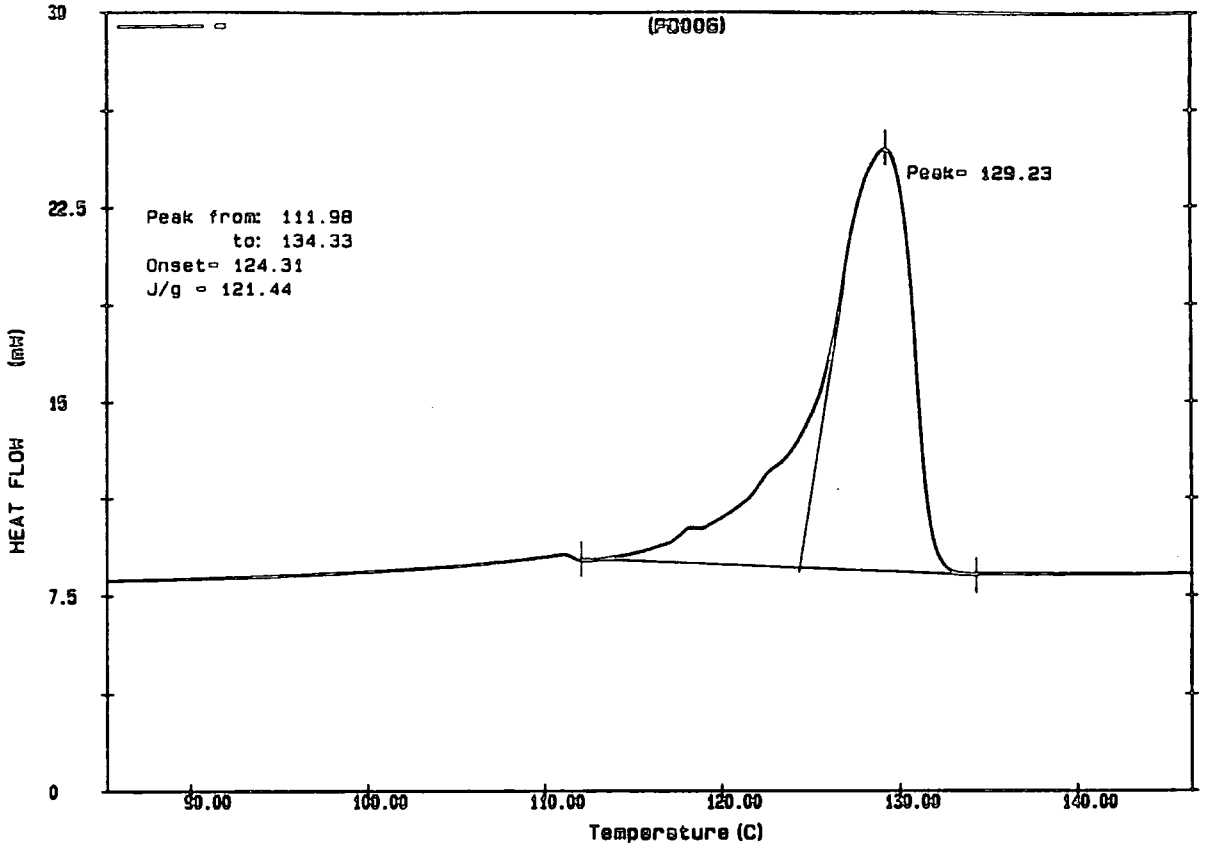

Appendix 4.14 DSC trace of star Polyethylene (Mn=49800)

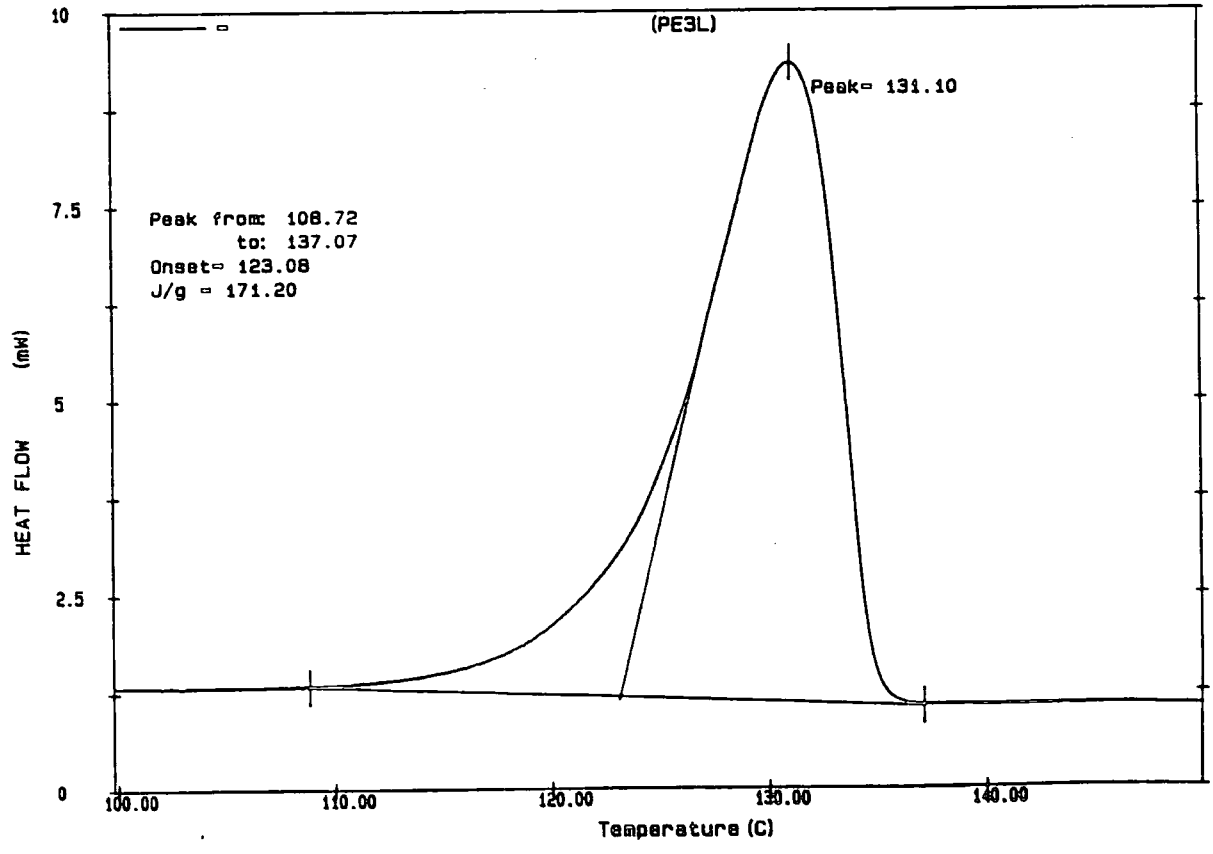

Appendix 4.15 DSC trace of star Polyethylene (Mn=62800)

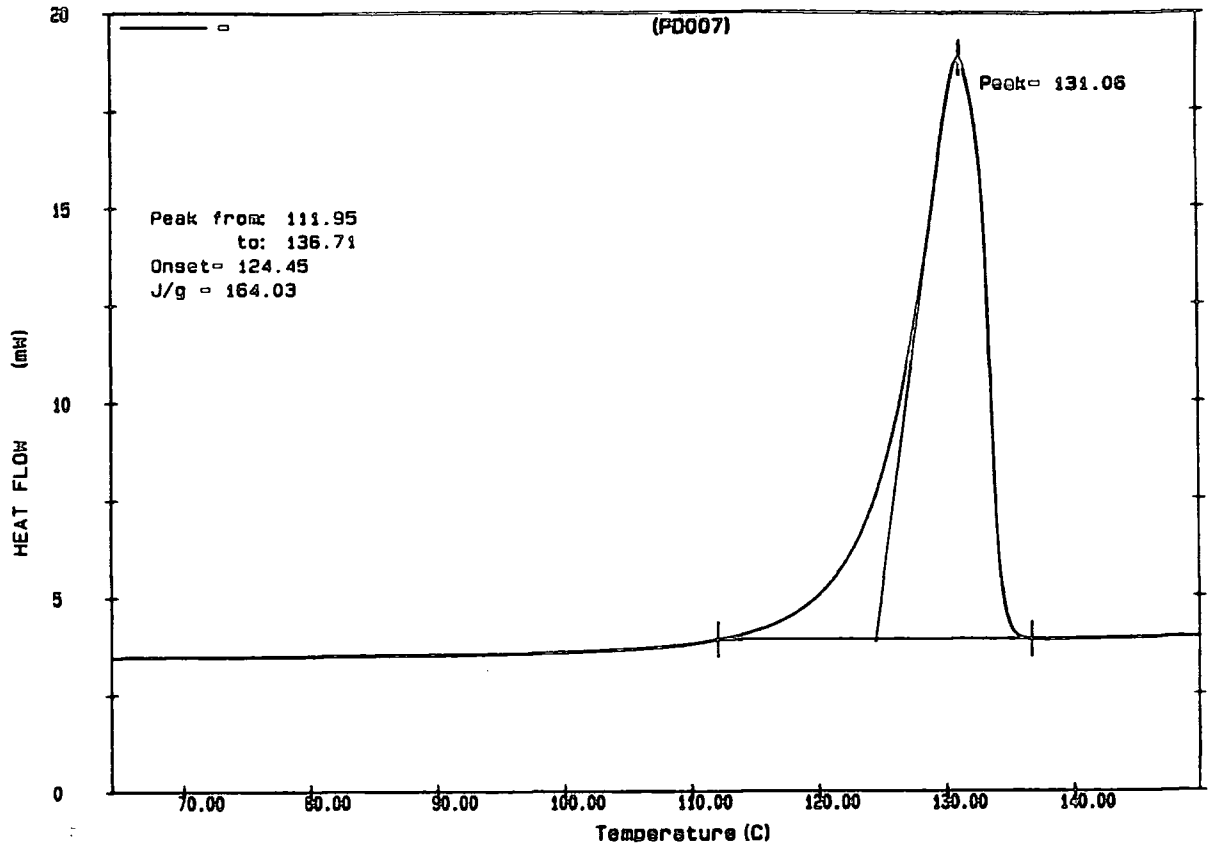

Appendix 4.16 DSC trace of star Polyethylene (Mn=95300)

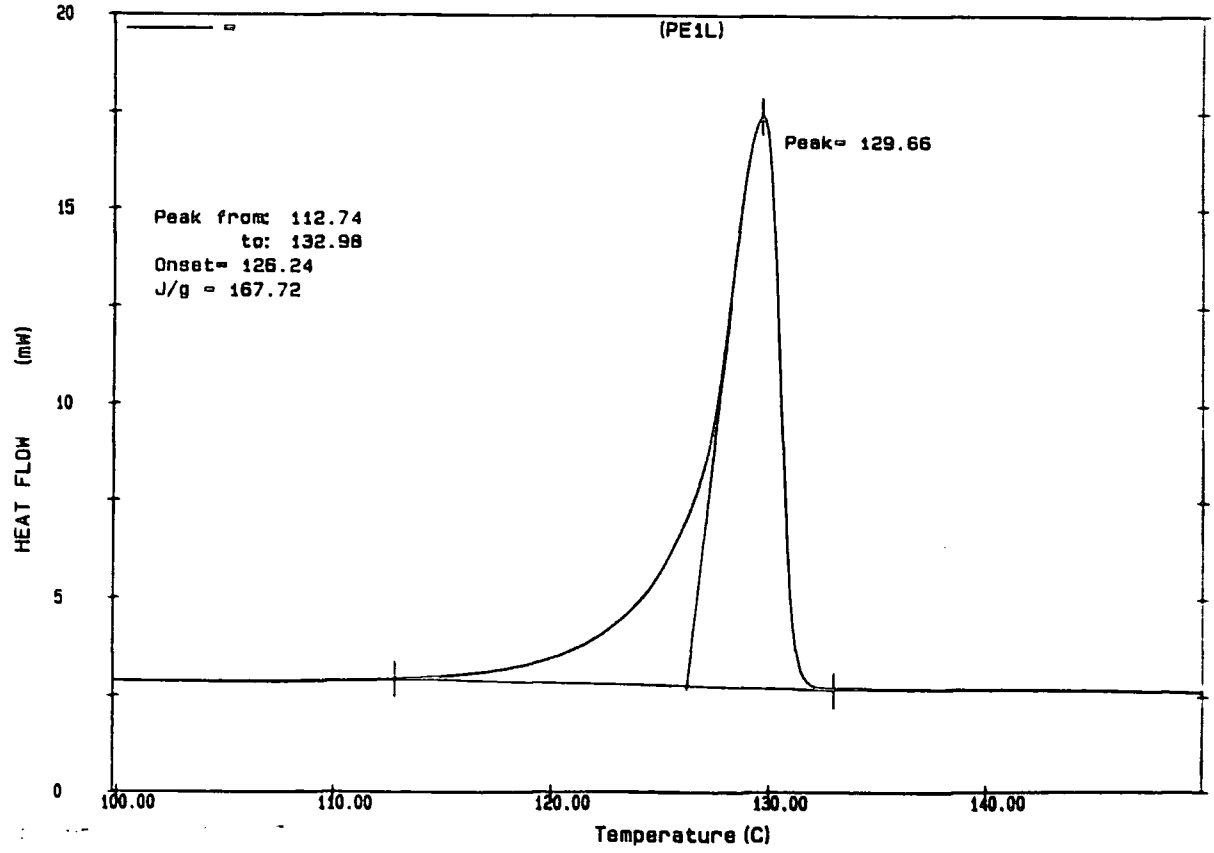

Appendix 4.17 DSC trace of linear Polyethylene (Mn=21640)

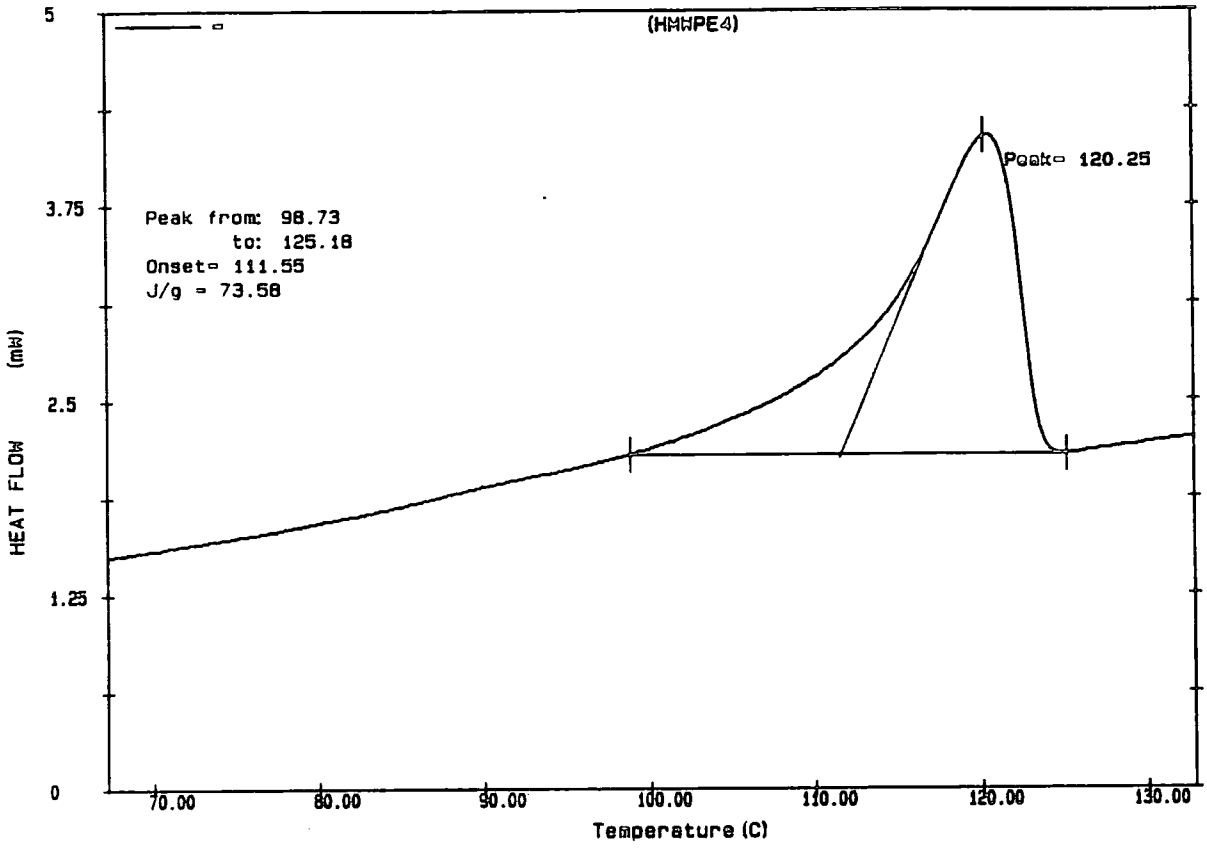

Appendix 4.18 DSC trace of linear Polyethylene (Mn=12400)

APPENDIX 5

Analytical data for Chapter 5

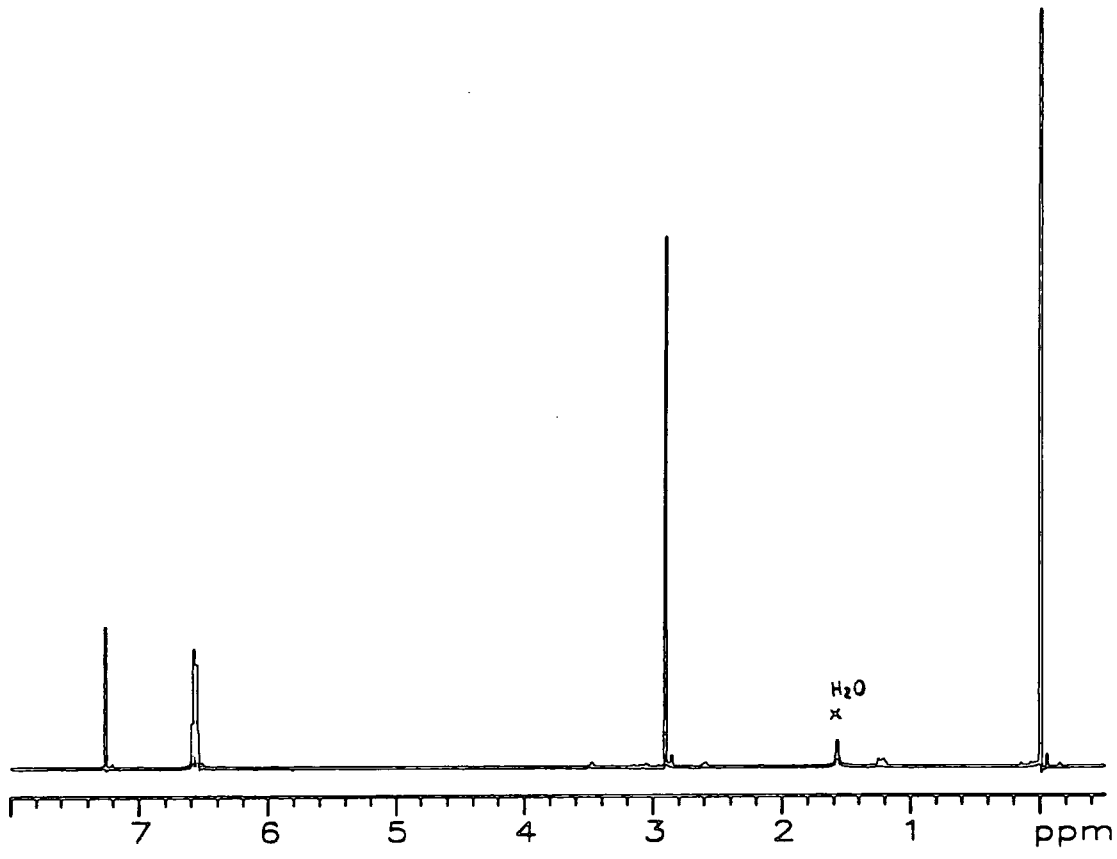

App.5.1 ^{1}H-NMR spectrum of 1,4-cyclohexanedicyclopentadienylidene

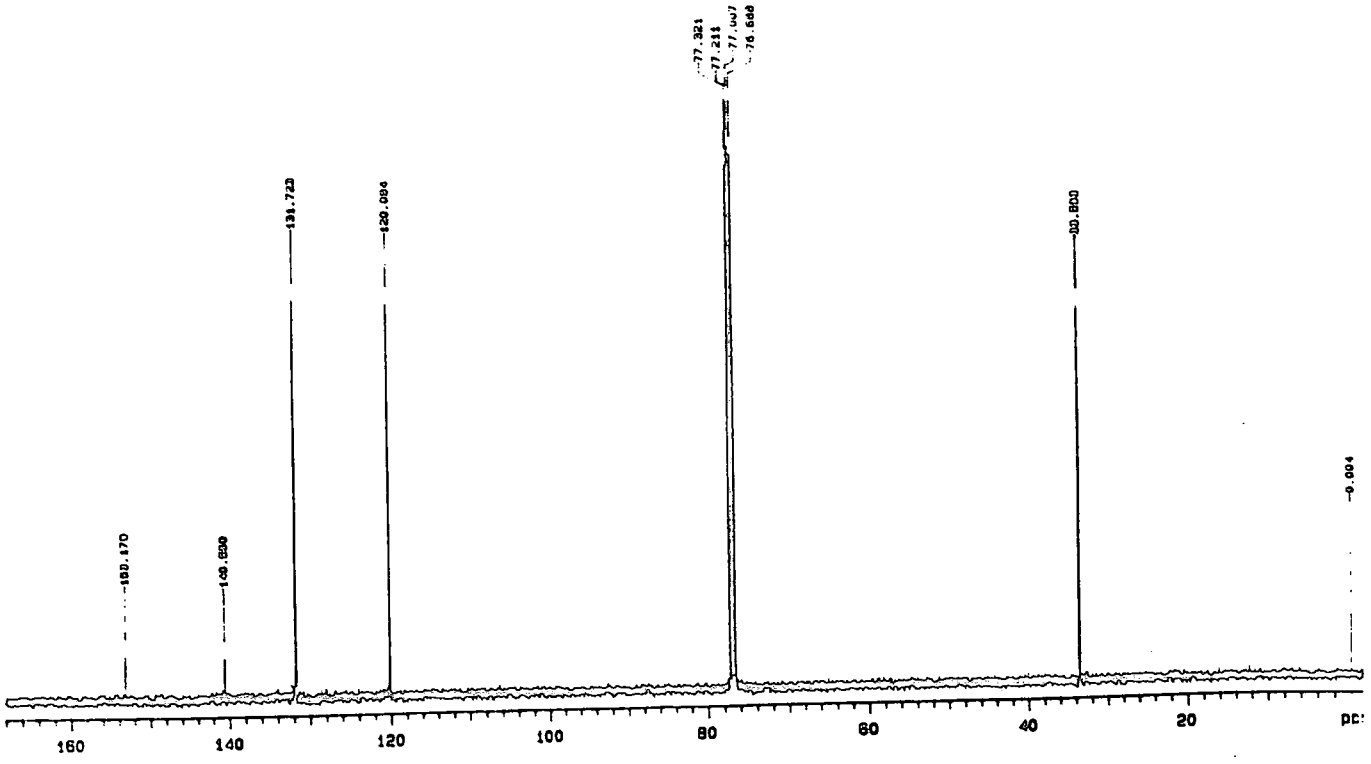

App.5.2 ^{13}C-NMR spectrum of 1,4-cyclohexanedicyclopentadienylidene

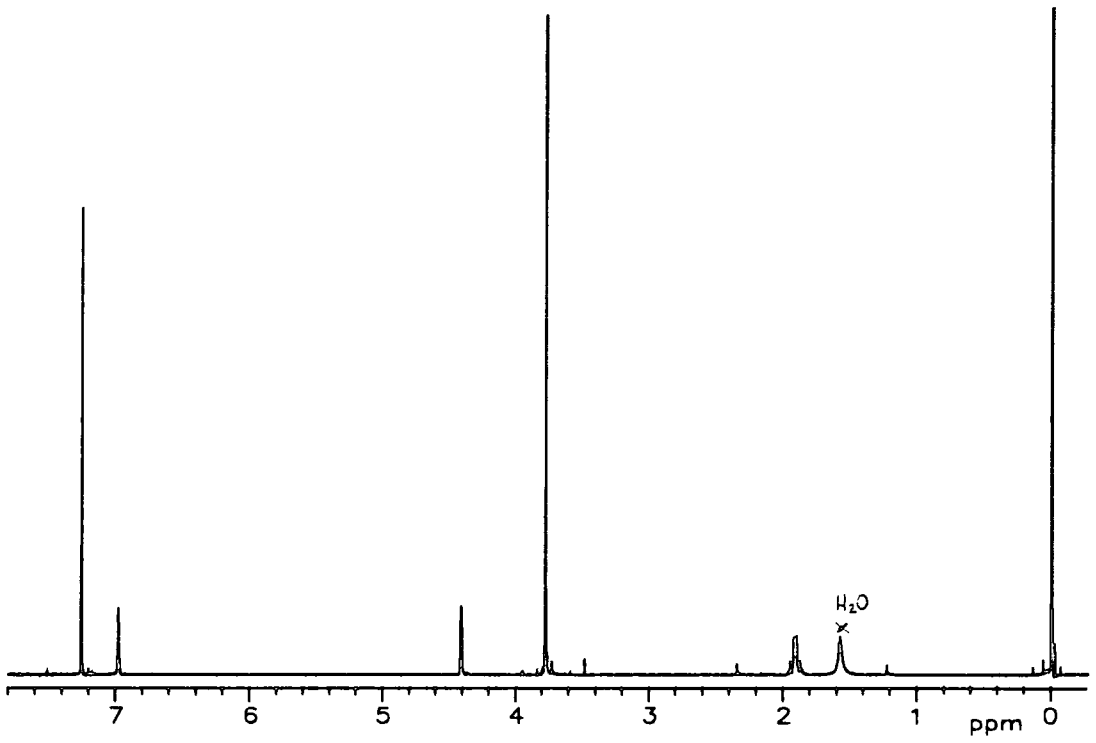

App.5.3 ^{1}H-NMR spectrum of compound (2)

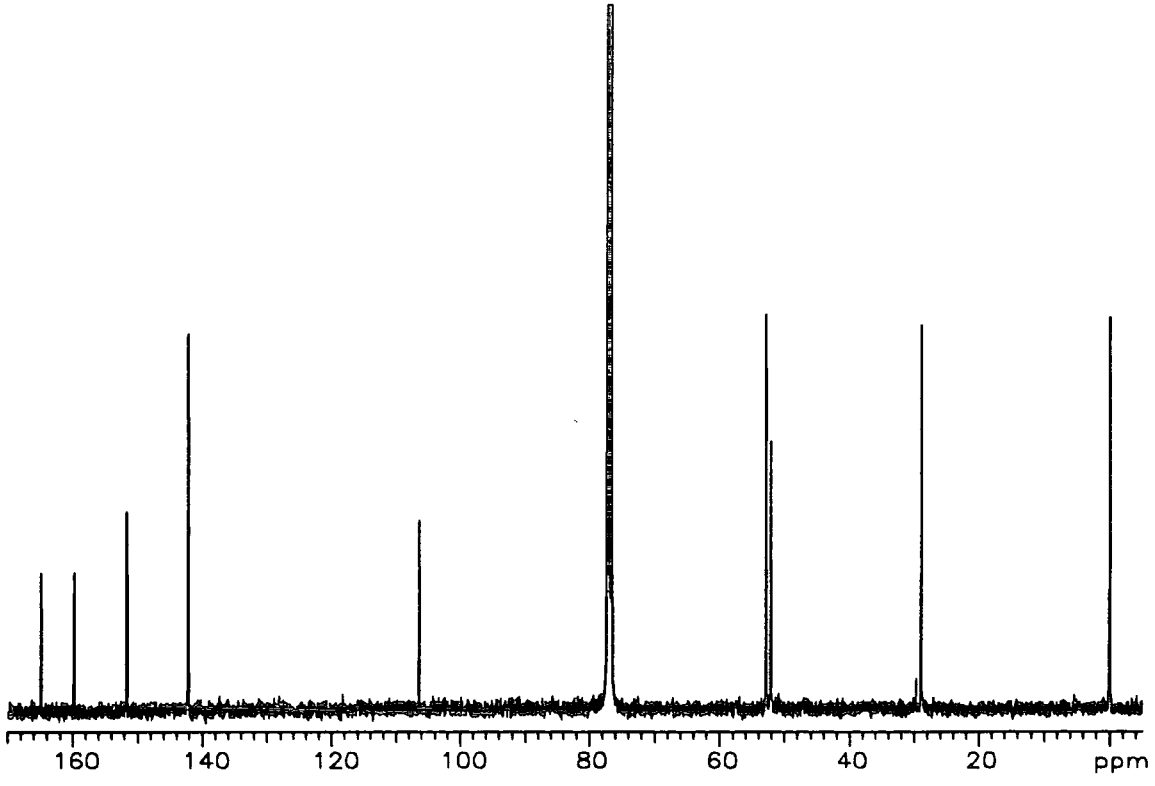

App.5.4 ^{13}C-NMR spectrum of compound (2)

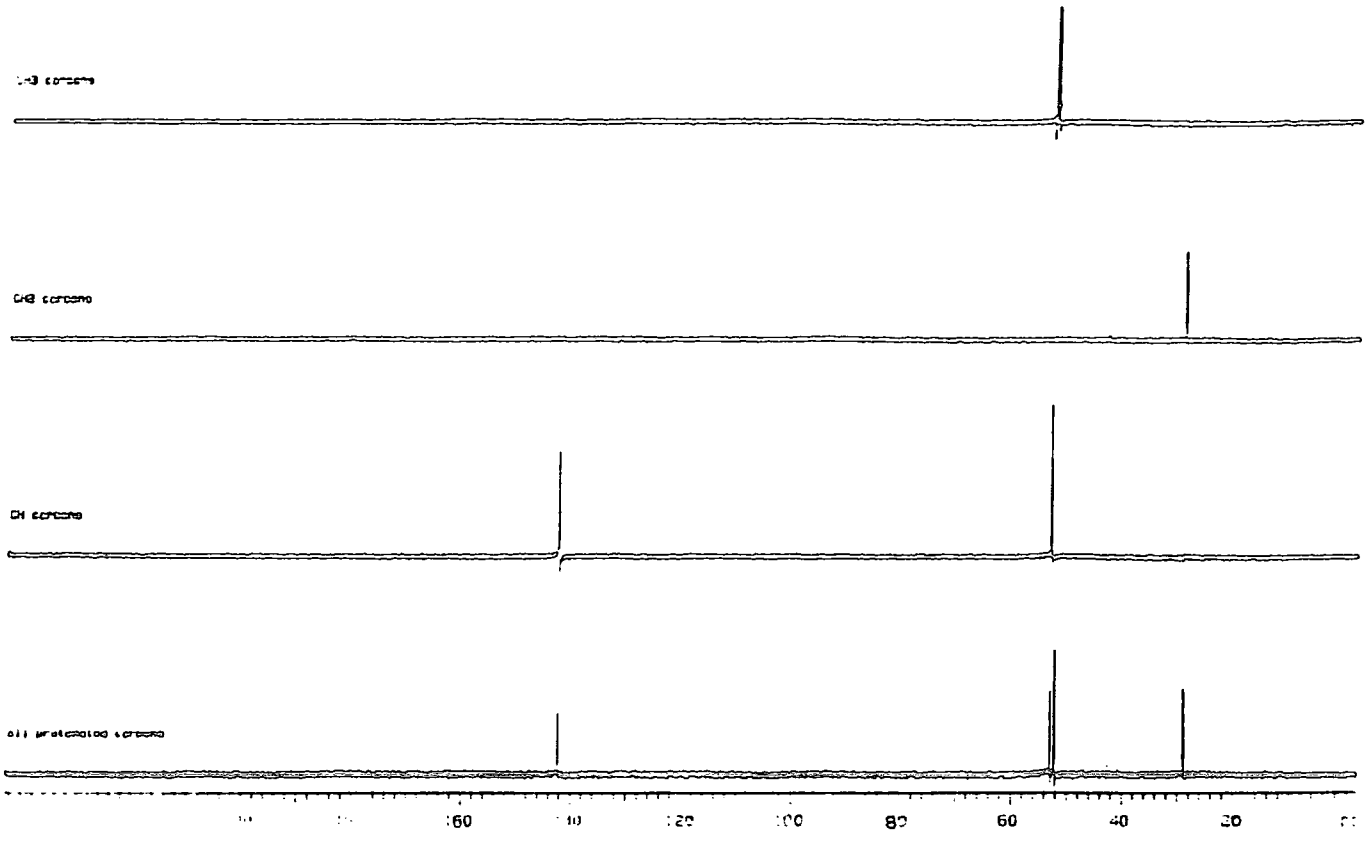

App.5.5 APT spectrum of compound (2)

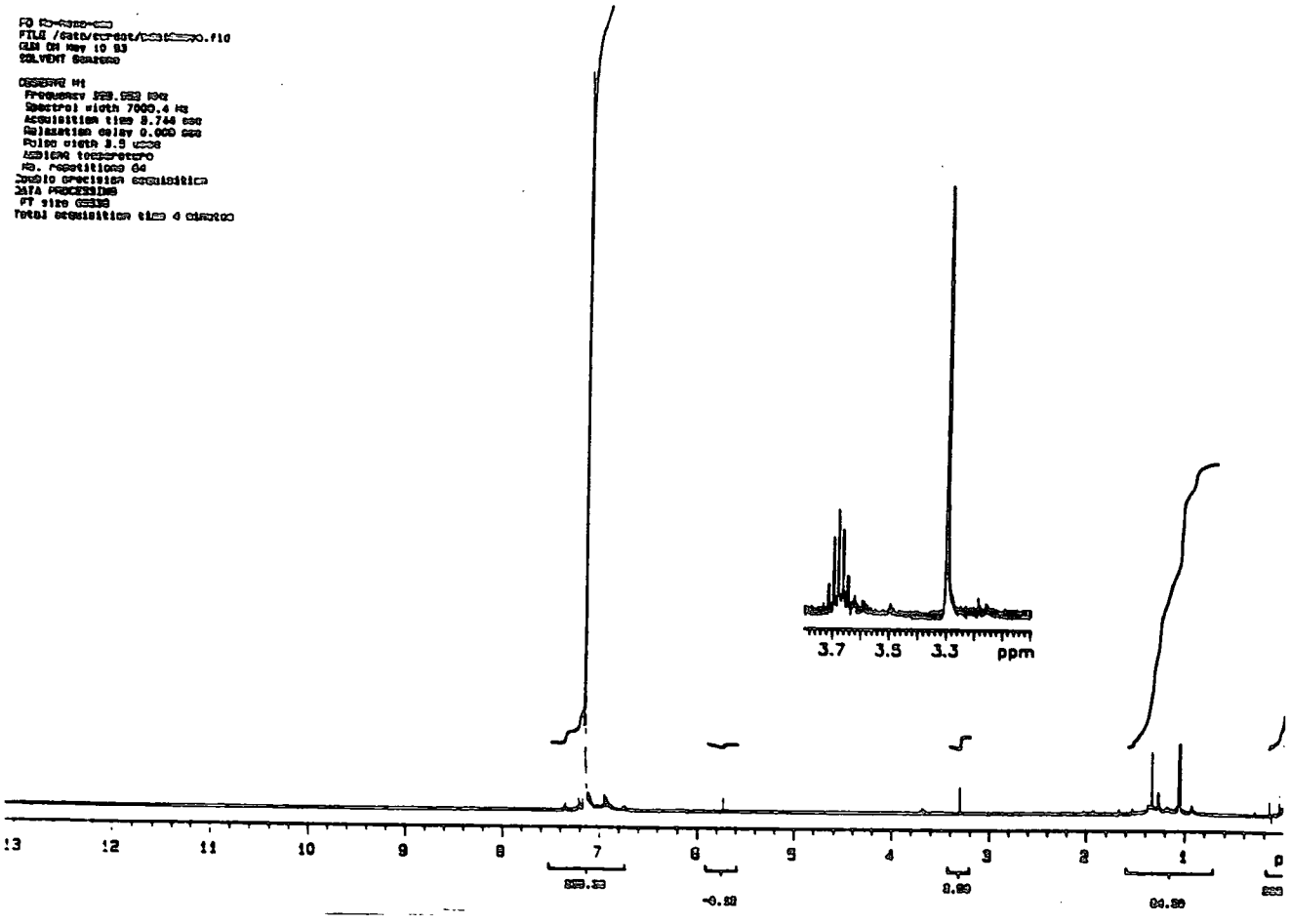

App.5.6 ^{1}H-NMR spectrum of $Mo(CCH_3Ph)(NAr)(OCCH_3(CF_3)_2)_2$

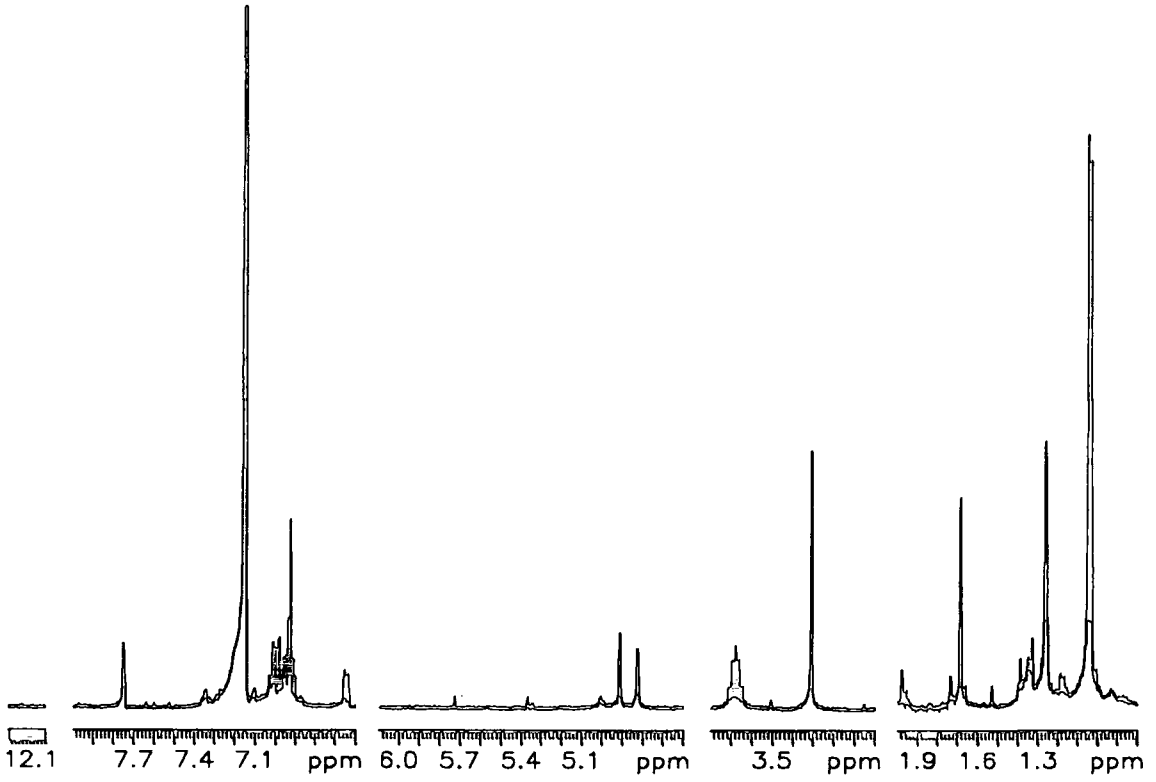

Appendix 5.7 ^{1}H-NMR spectrum of Mo(=C(CH_3)-m-$C_6H_4C(CH_3)=CH_2$)(NAr)($OCCH_3(CF_3)_2$)$_2$

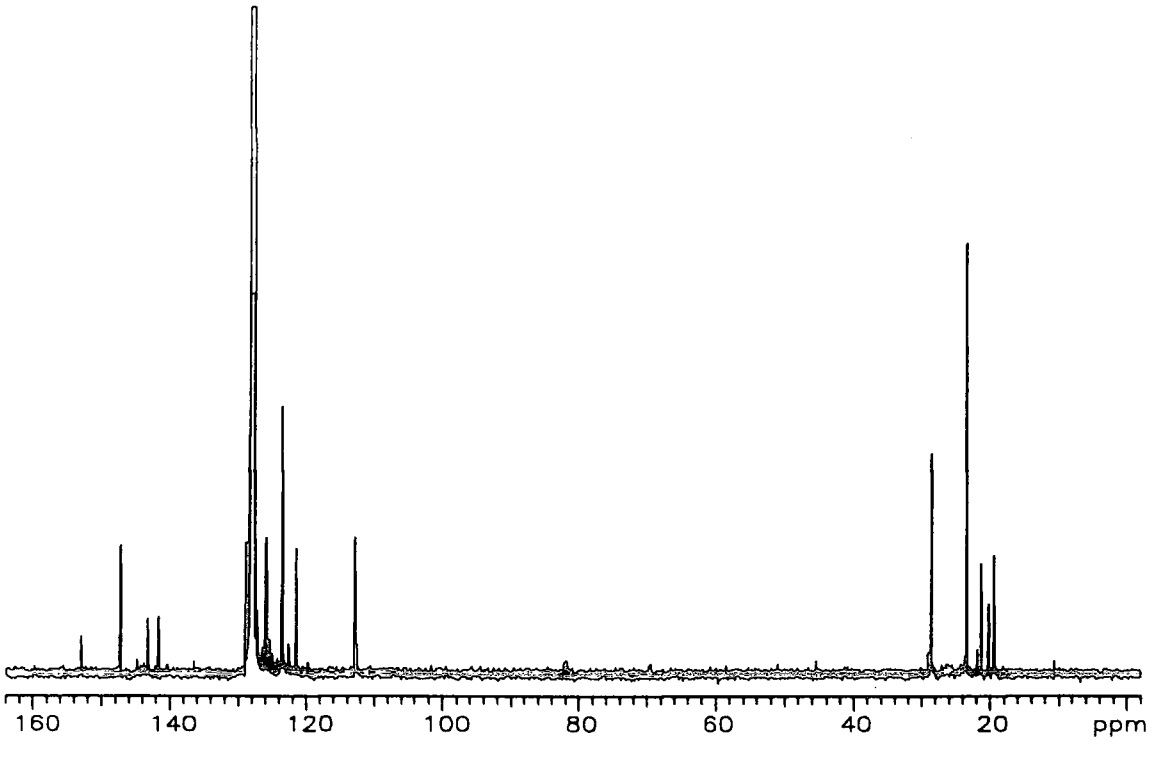

Appendix 5.8 ^{13}C-NMR spectrum ofMo(=C(CH_3)-m-$C_6H_4C(CH_3)=CH_2$)(NAr)($OCCH_3(CF_3)_2$)$_2$

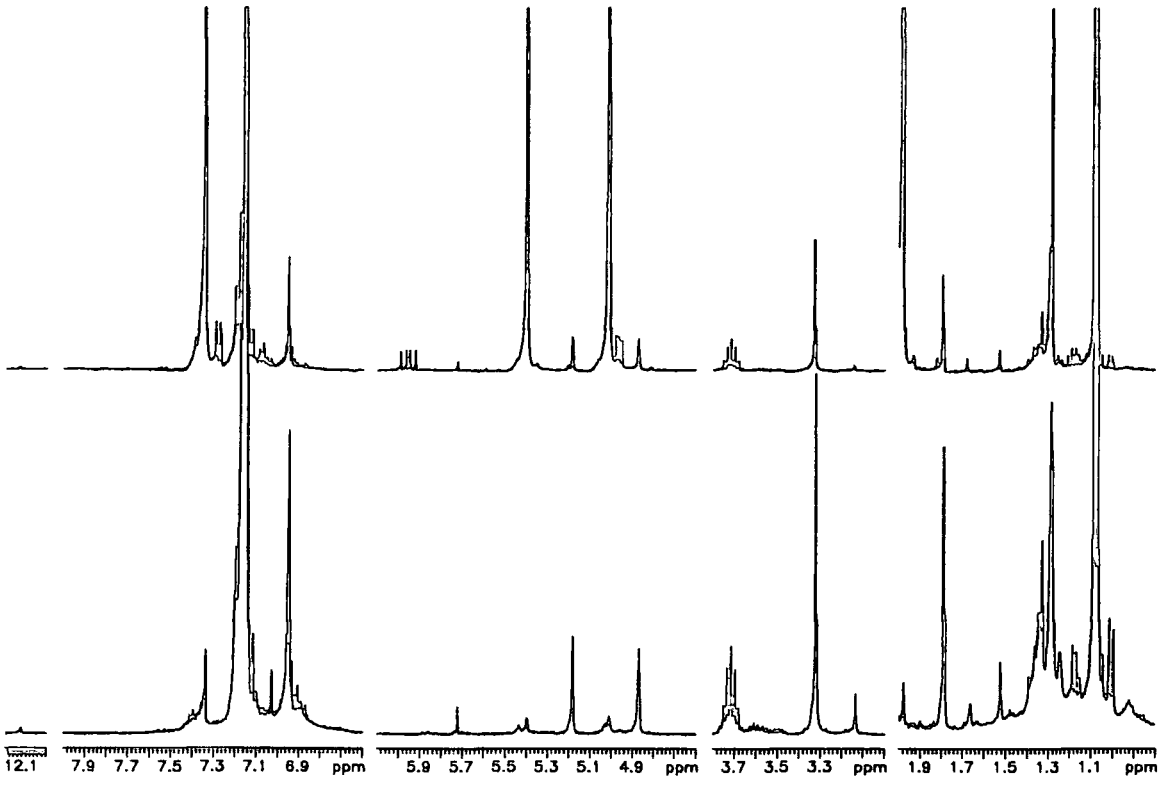

Appendix 5.9 ^{1}H-NMR spectrum of Mo(=C(CH_3)-p-$C_6H_4C(CH_3)=CH_2$)(NAr)($OCCH_3(CF_3)_2$)$_2$

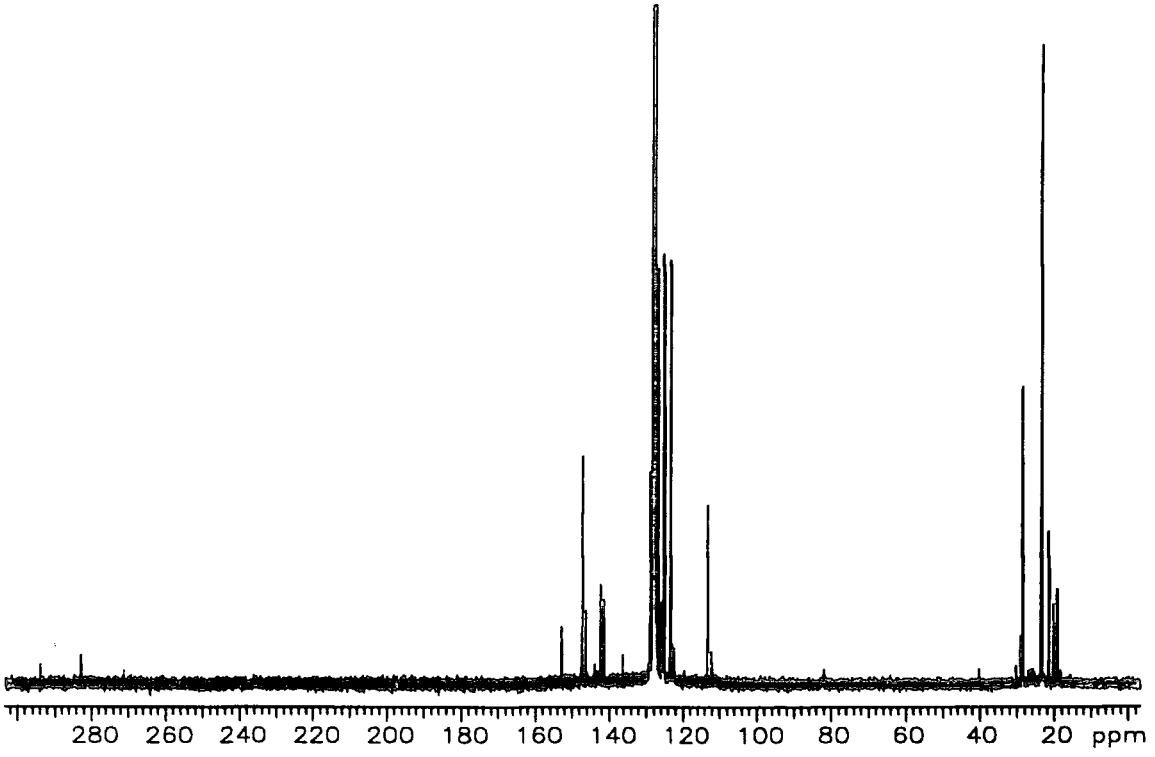

Appendix 5.10 ^{13}C-NMR spectrum of Mo(=C(CH_3)-p-$C_6H_4C(CH_3)=CH_2$)(NAr)($OCCH_3(CF_3)_2$)$_2$

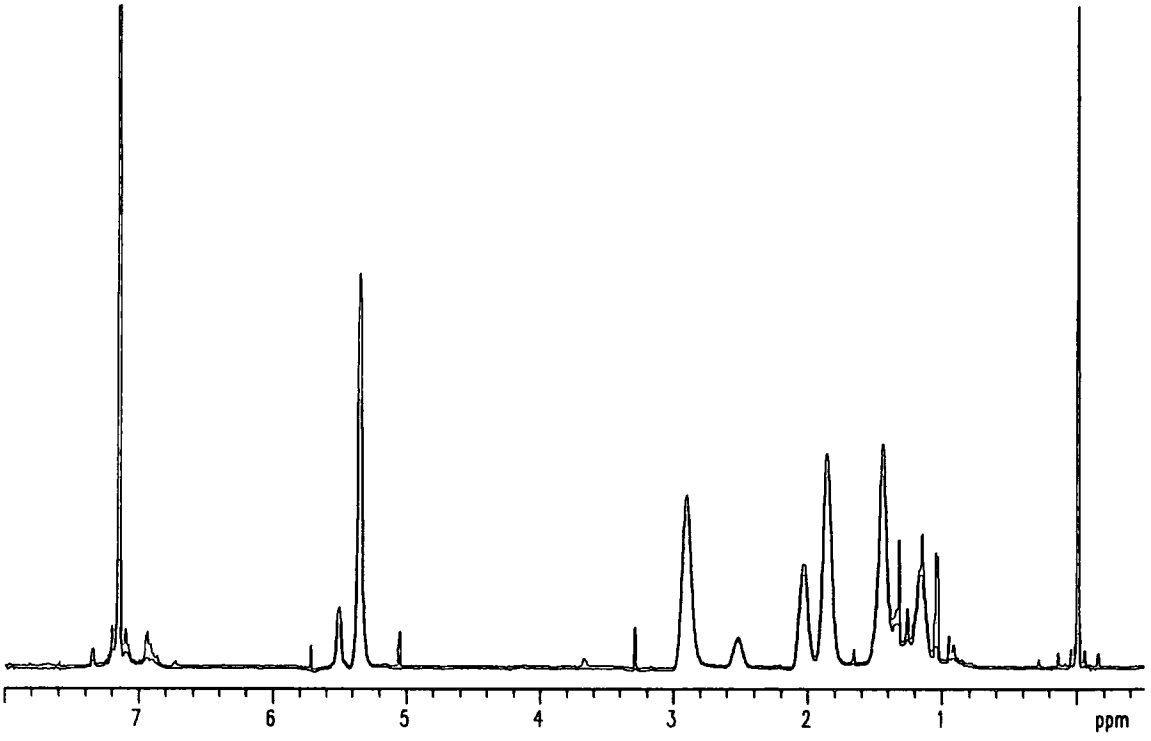

Appendix 5.11 ^{1}H-NMR of polynorbornene initiated by $Mo(=C(CH_3)Ph)(NAr)(OCCH_3(CF_3)_2)_2$

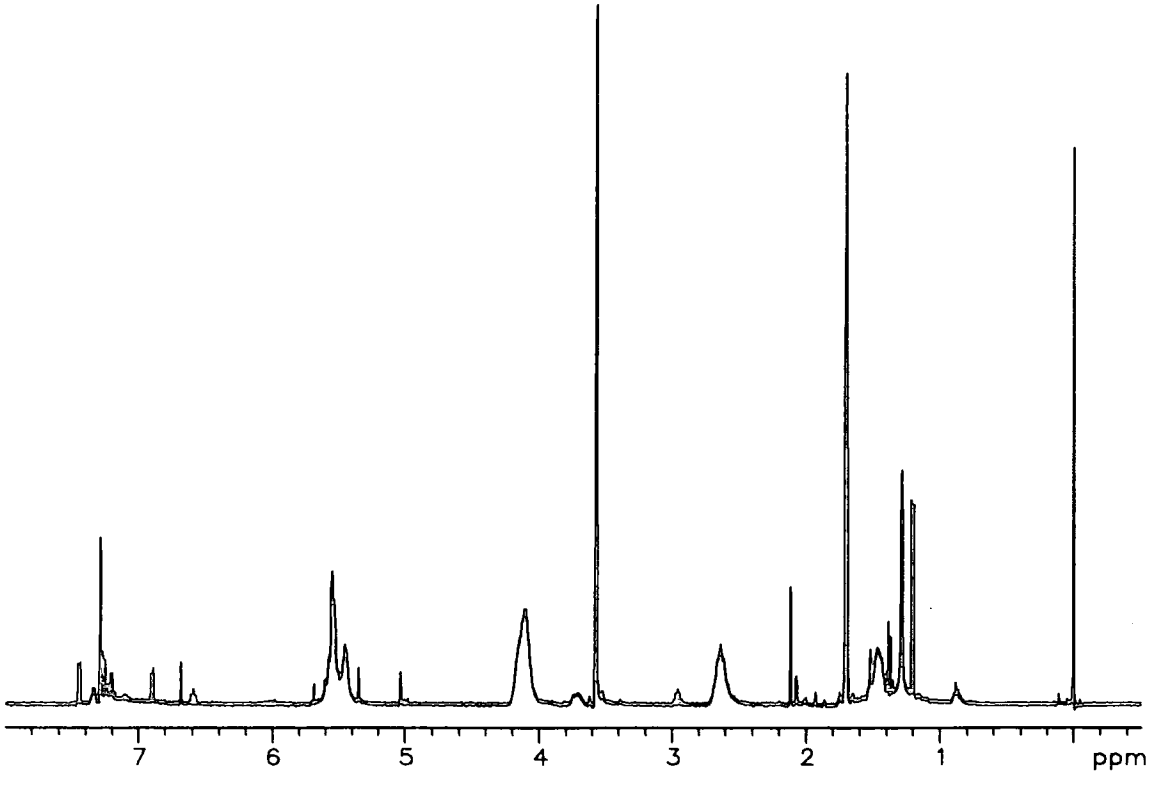

Appendix 5.12 ^{1}H-NMR of poly(bistrifluomethylnorbornadiene) obtained via $Mo(=C(CH_3)Ph)(NAr)(OCCH_3(CF_3)_2)_2$ initiation

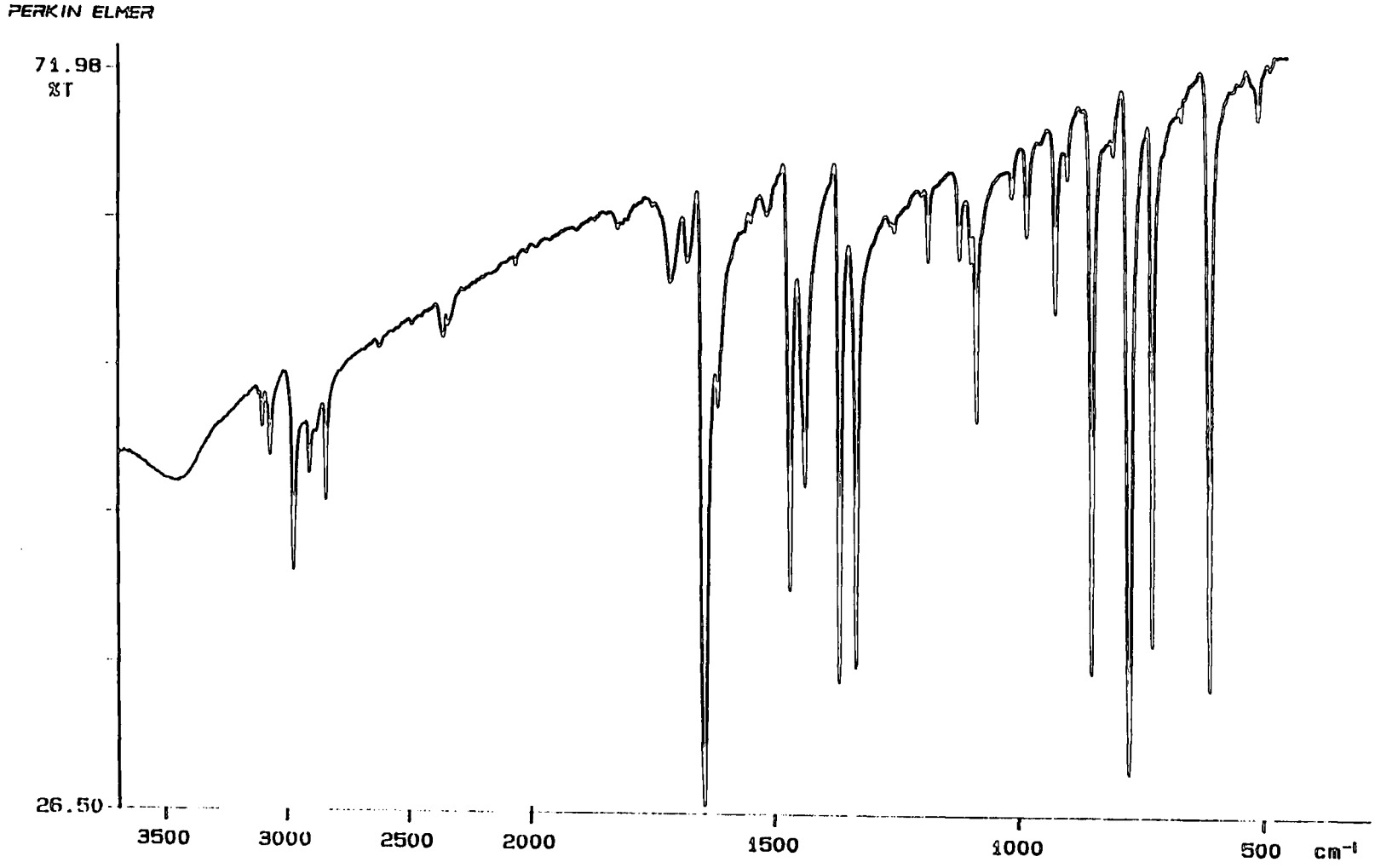

Appendix 5.13 Infrared spectrum of 1,4-cyclohexanedicyclopentadienylidene

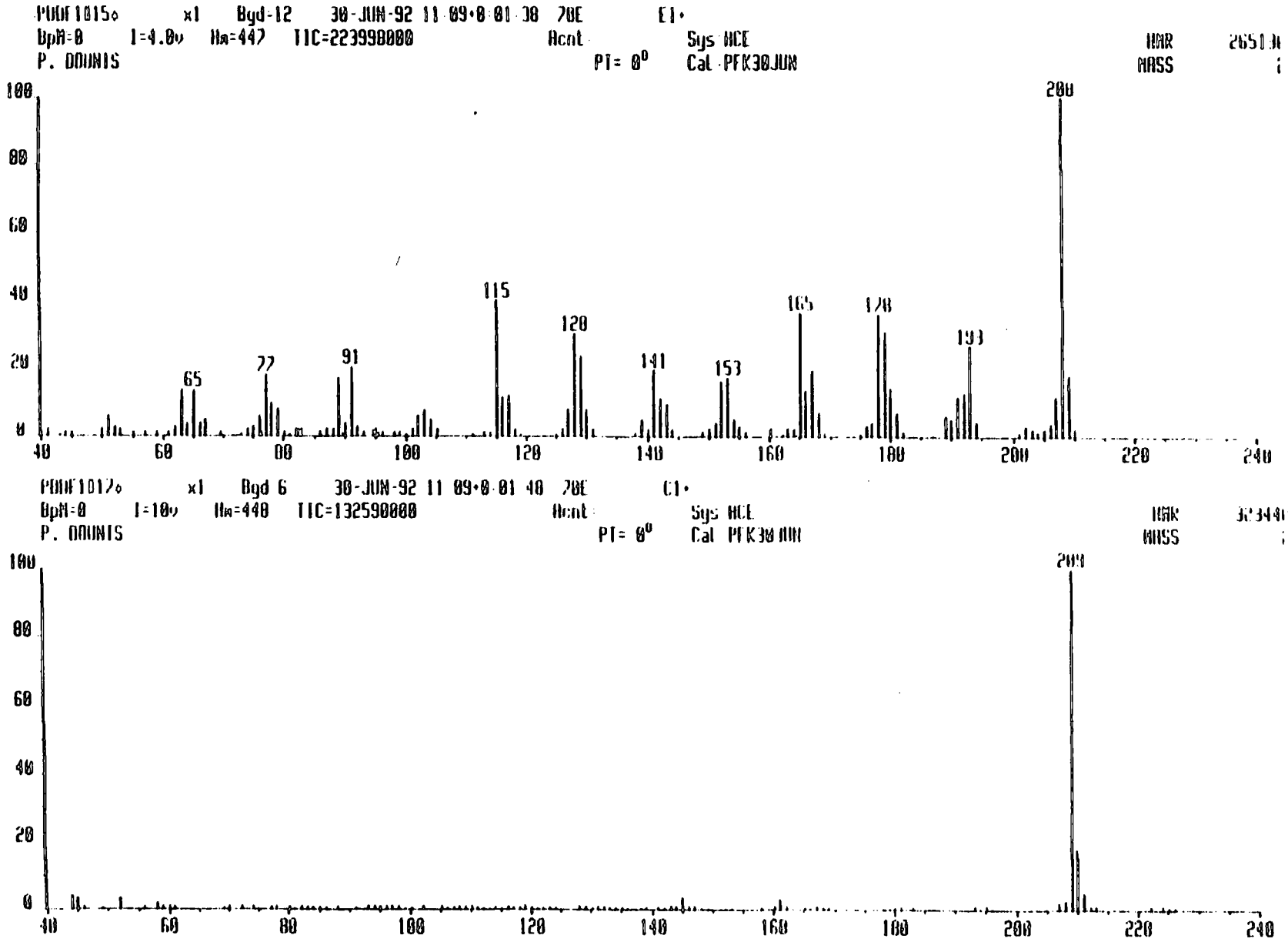

Appendix 5.14 Mass spectra of 1,4-cyclohexanedicyclopentadienylidene

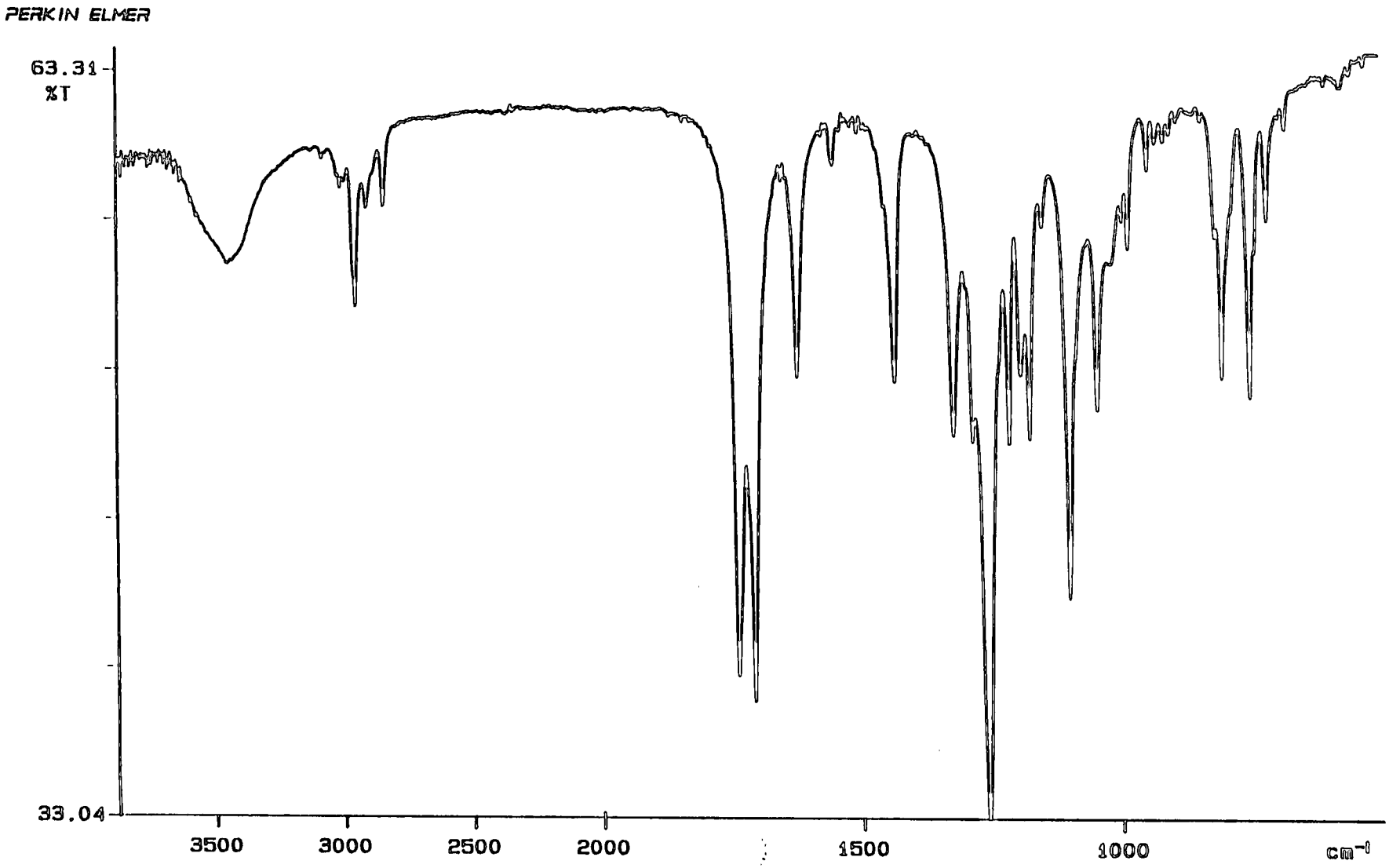

Appendix 5.15 Infrared spectrum of compound (2)

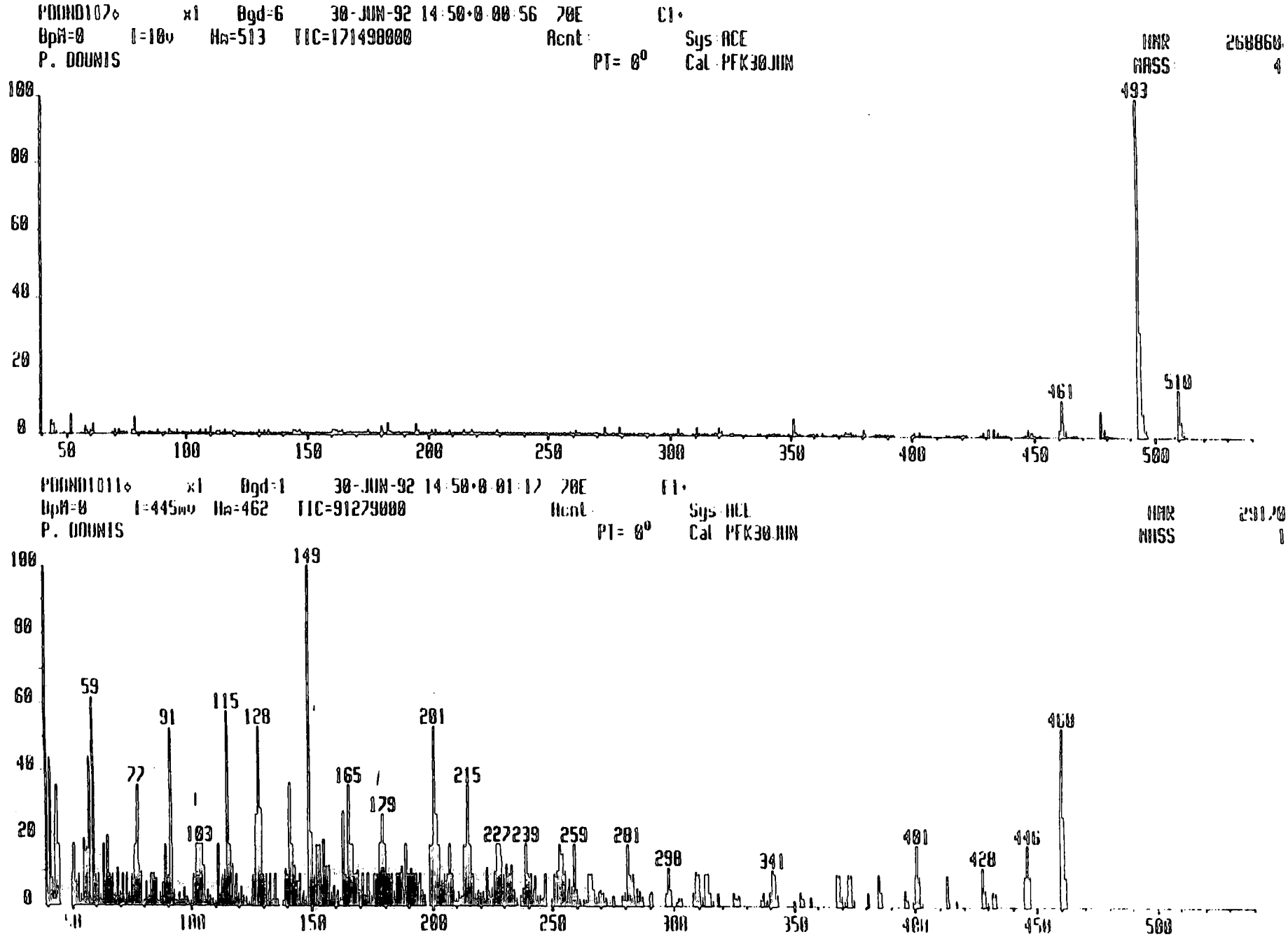

Appendix 5.16 Mass spectra of compound (2)

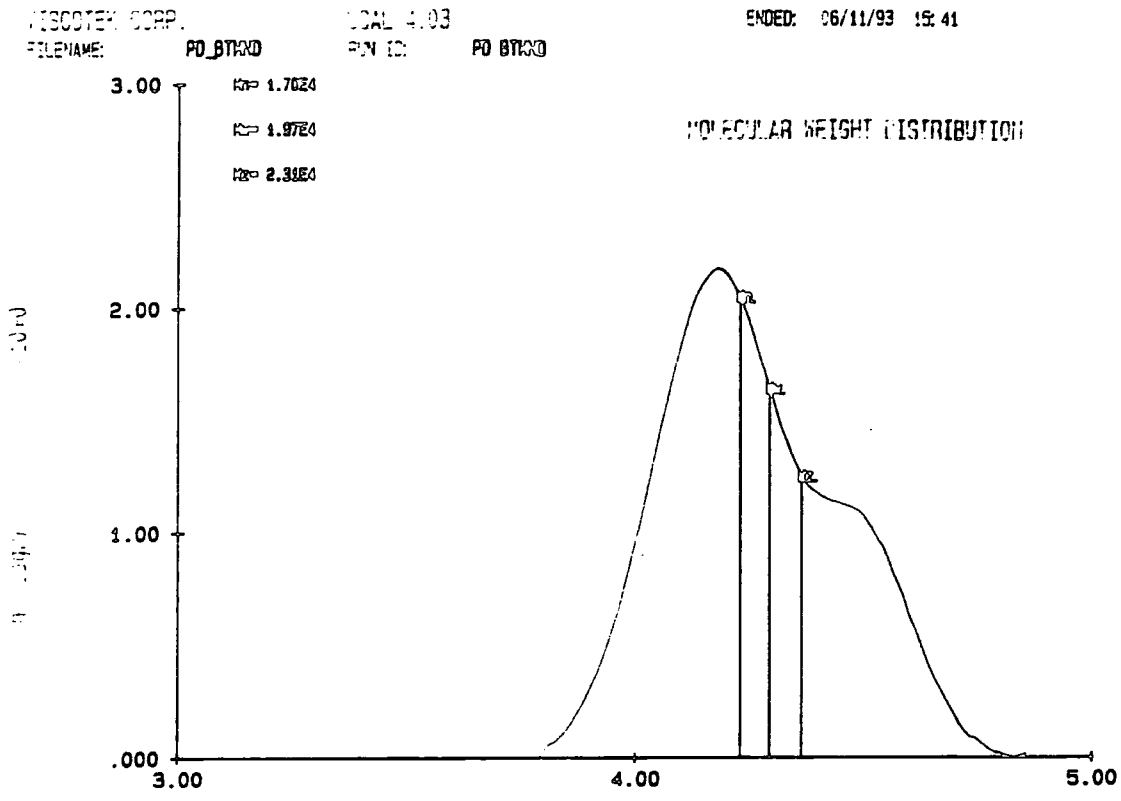

Appendix 5.19 GPC trace of poly(bistrifluoromethylnorbornadiene) initiated with $Mo(=C(CH_3)Ph)(NAr)(OCCH_3(CF_3)_2)_2$

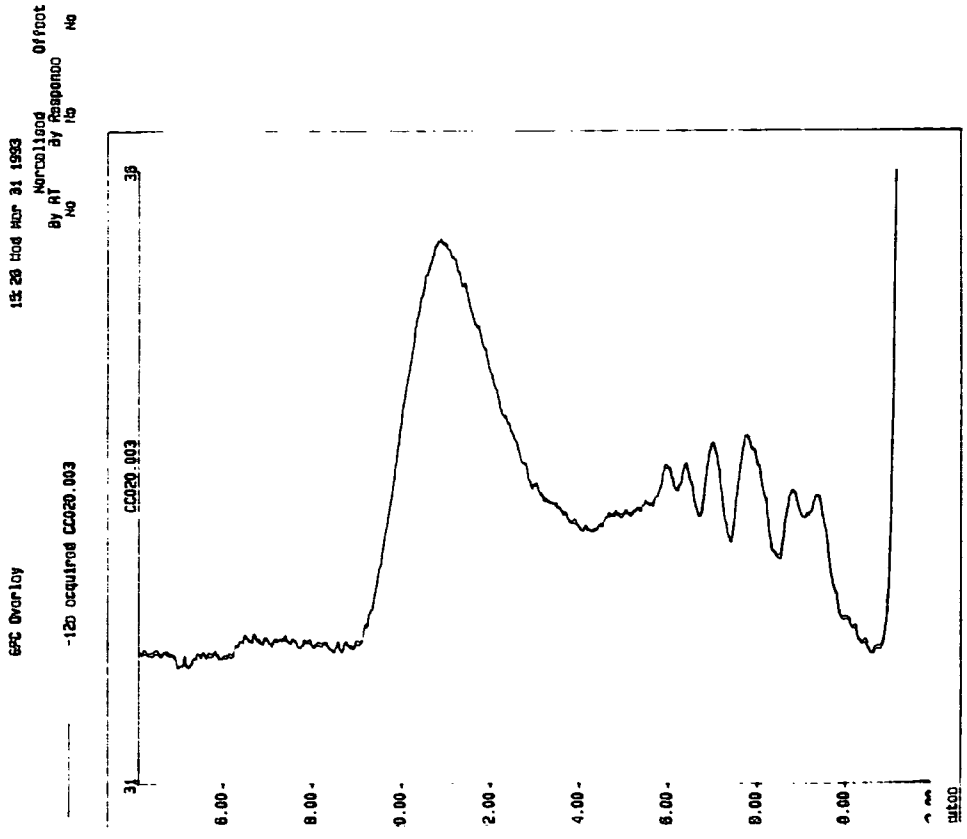

Appendix 5.17 GPC trace of poly(1-octenylene) initiated with $Mo(=C(CH_3)Ph)(NAr)(OCCH_3(CF_3)_2)_2$

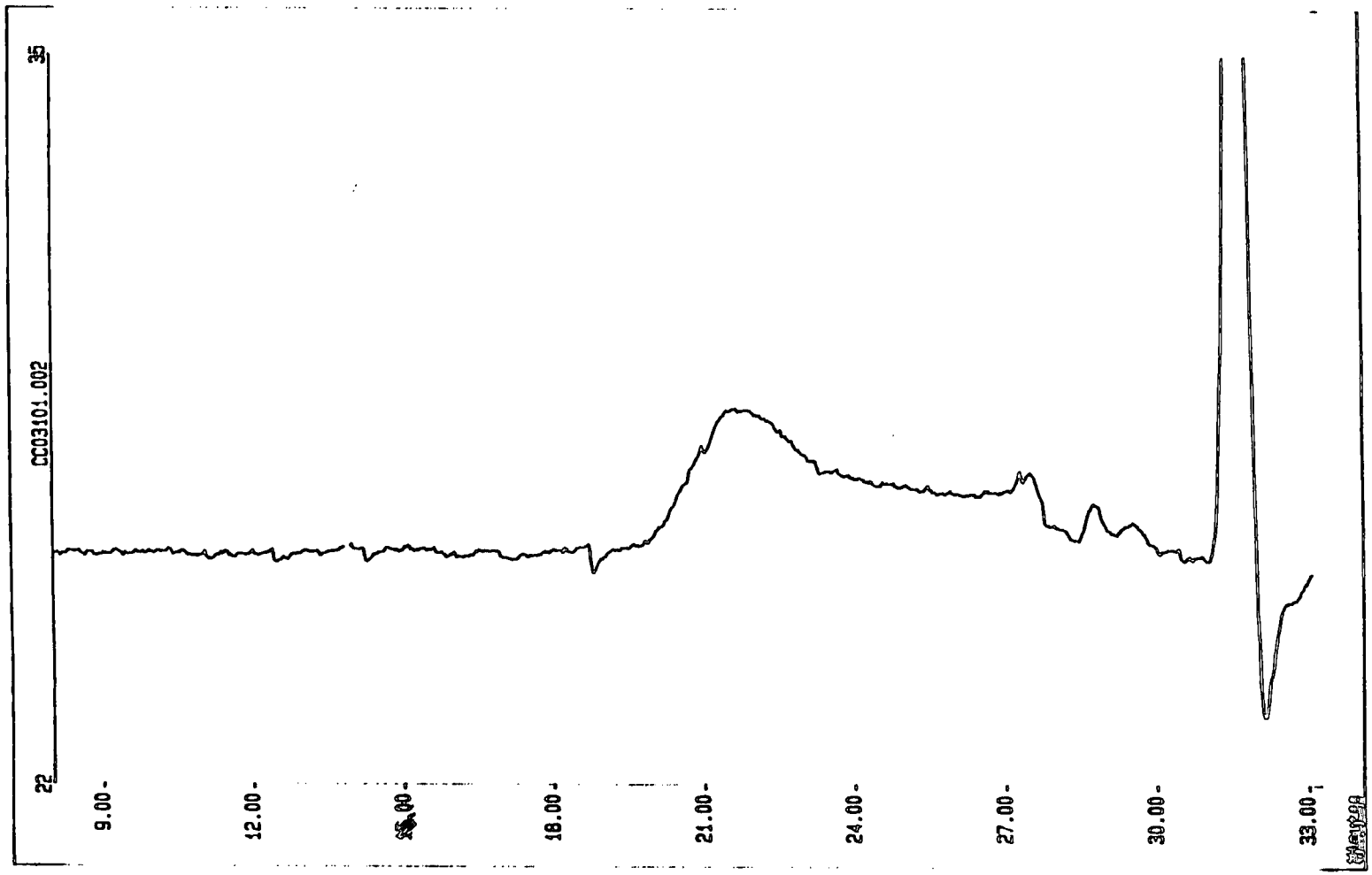

Appendix 5.18 GPC trace of polynorbornene initiated with $Mo(=C(CH_3)Ph)(NAr)(OCCH_3(CF_3)_2)_2$

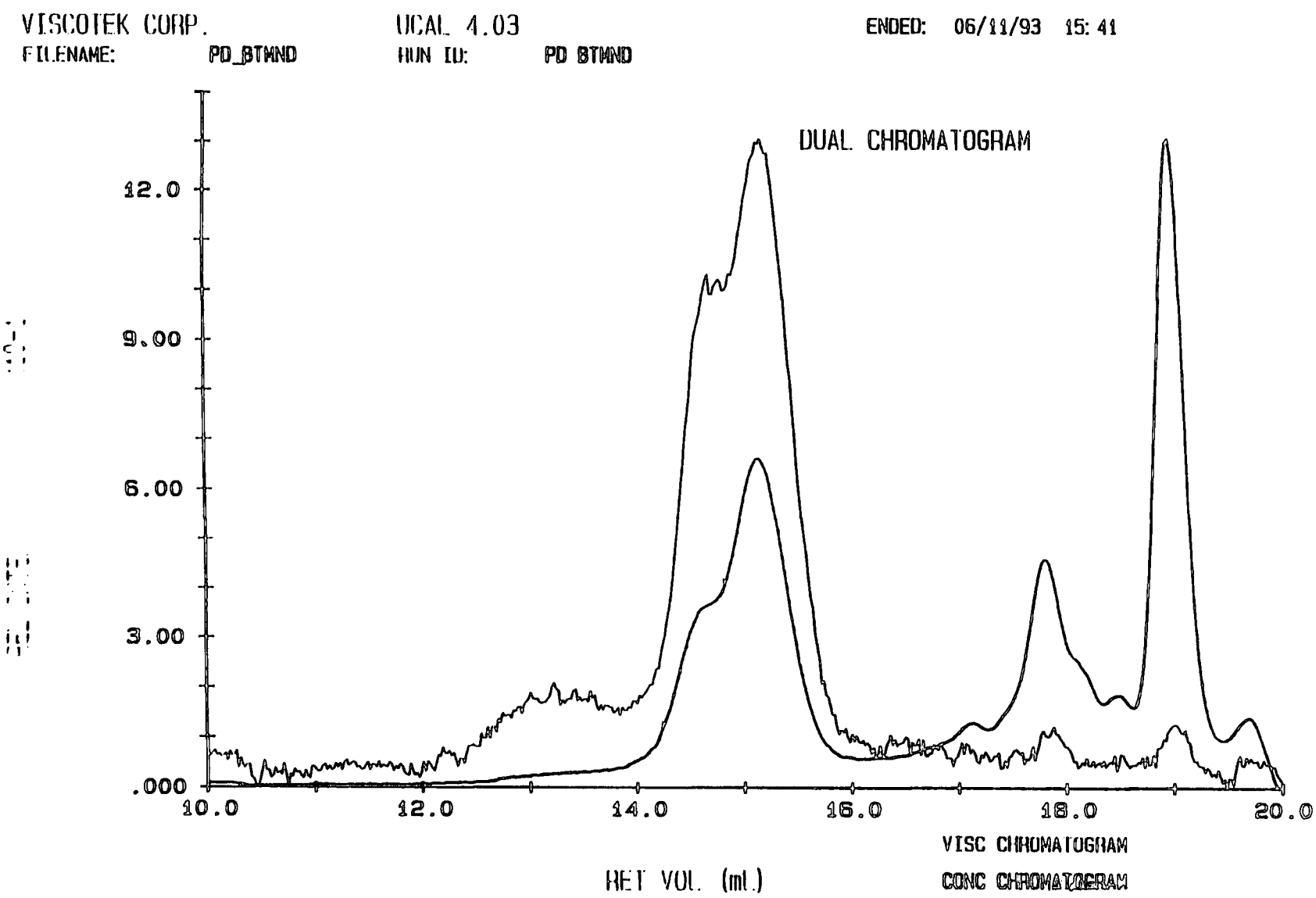

Appendix 5.19 GPC trace of poly(bistrifluoromethylnorbornadiene) initiated with $Mo(=C(CH_3)Ph)(NAr)(OCCH_3(CF_3)_2)_2$

APPENDIX 6

Lectures and conferences attended by the author

UNIVERSITY OF DURHAM
Board of Studies in Chemistry
Colloquia, Lectures and Seminars given by Invited Speakers

1990

October 11	Dr.W.A.MacDonald, (ICI, Wilton). Materials for the Space Age.
October 24	Dr.M.Bochmann, (University of East Anglia). Synthesis, Reactions and Catalytic Activity of Cationic Titanium Alkyls.
October 26	Prof.R.Soulen, (South Western University, Texas). Preparation and Reactions of Bicycloalkenes.
October 31	Dr.R.Jackson, (Newcastle University). New Synthetic Methods: α-Amino Acids and Small Rings.
November 1	Dr.N.Logan, (Nottingham University). Rocket Propellants.
November 6	Dr.P.Kocovsky, (Uppsala University) Stereo-Controlled Reactions Mediated by Transition and Non-Transition Metals.
November 7	Dr.D.Gerrard, (British Petroleum). Raman Spectroscopy for Industrial Analysis.
November 8	Dr.S.K.Scott, (Leeds University). Clocks, Oscillations and Chaos.
November 14	Prof.T.Bell, (SUNY, Stoney Brook, USA). Functional Molecular Architectures and Molecular Recognition.
November 21	Prof.J.Pritchard, (Queen Mary & Westfield College, London University). Copper Surfaces and Catalysts.
November 28	Dr.B.J.Whitaker, (Leeds University). Two-Dimensional Velocity Imaging of State-Selected Reaction Products.
November 29	Prof.D.Crout, (Warwick University). Enzymes in Organic Synthesis.
December 5	Dr.P.G.Pringle, (Bristol University). Metal Complexes with Functionalised Phosphines.
December 13	Prof.A.H.Cowley, (University of Texas). New Organometallic Routes to Electronic Materials.

1991

January 15	Dr.B.J.Alder, (Lawrence Livermore Labs. California). Hydrogen in all its Glory.
January 17	Dr.P.Sarre, (Nottingham University). Comet Chemistry.

January 24	Dr.P.J.Sadler, (Birkbeck College London). Design of Inorganic Drugs: Precious Metals, Hypertension and HIV.
January 30	Prof.E.Sinn, (Hull University). Coupling of Little Electrons in Big Molecules. Implications for the Active Site of (Metalloproteins and other) Macromolecules.
January 31	Dr.D.Lacey, (Hull University). Liquid Crystals.
February 6	D.R.Bushby, (Leeds University). Biradicals and Organic Magnets.
February 14	Dr.M.C.Petty, (Durham University). Molecular Electronics.
February 20	Prof.B.L.Shaw, (Leeds University). Syntheses with Coordinated, Unsaturated Phosphine Ligands.
February 28	Dr.J.Brown, (Oxford University). Can Chemistry Provide Catalysts Superior to Enzymes?
March 6	Dr.C.M.Dobson, (Oxford University). NMR Studies of Dynamics in Molecular Crystals.
March 7	Dr.J.Markam, (ICI Pharmaceuticals). DNA Fingerprinting.
April 24	Prof.R.R.Schrock, (Massachusetts Institute of Technology). Metal-Ligand Multiple Bonds and Metathesis Initiators.
April 25	Prof.T.Hudlicky, (Virginia Polytechnic Institute). Biocatalysts as Symmetry Based Approaches to the Efficient Synthesis of Complex Natural Products.
June 20	Prof.M.S.Brookhart, (University of N.Carolina). Olefin Polymerisations, Oligomerisations and Dimerisations using Electrophilic Late Transition Metal Catalysts.
July 29	Dr.M.A.Brimble, (Massey University, New Zealand). Synthetic Studies Towards the Antibiotic Griseusin-A.
October 17	Dr.J.A.Salthouse, (University of Manchester). Son et Lumiere-A Demonstration Lecture.
October 31	Dr.Keeley, (Metropolitan Police Forensic Science). Modern Forensic Science.
November 6	Prof.B.F.G.Johnson, (Edinburgh University). Cluster-surface Analogies.
November 7	Dr.A.R.Butler, (St.Andrews University). Traditional Chinese Herbal Drugs: A Different Way of Treating Disease.
November 13	Prof.D.Gani, (St.Andrews University). The Chemistry of PLP Dependent Enzymes.

November 20	Dr.R.More O'Ferrall, (University College, Dublin). Some Acid-Catalysed Rearrangements in Organic Chemistry.
November 28 **SCI Lecture**	Prof.I.M.Ward, (IRC in Polymer Science, Leeds University). The Science and Technology of Orientated Polymers.
December 4	Prof.R.Grigg, (Leeds University). Palladium-Catalysed Cyclisation and Ion-Capture Processes.
December 5	Prof.A.L.Smith, (Ex. Unilever). Soap, Detergents and Black Puddings.
December 11	Dr.W.D.Cooper, (Shell Research). Colloid Science: Theory and Practice.

1992

January 22	Dr.K.D.M.Harris, (St.Andrews University). Understanding the Properties of Solid Inclusion Compounds.
January 29	Dr.A.Holmes, (Cambridge University). Cycloaddition Reactions in the Service of the Synthesis of Piperidine and Indolizine Natural Products.
January 30	Dr.M.Anderson, (Sittingbourne, Shell Research). Recent Advances in the Safe and Selective Chemical Control of Insect Pests.
February 12	Prof.D.E.Fenton, (Sheffield University). Polynuclear Complexes of Molecular Clefts as Models for Copper Biosites.
February 13	Dr.J.Saunders, (Glaxo Group Research Limited). Molecular Modeling in Drug Discovery.
February 19	Prof.E.J.Thomas, (University of Manchester). Applications of Organostannanes to Organic Synthesis.
February 20 **Musgrave Lecture**	Prof.E.Vogel, (University of Cologne). Porphyrins: Molecules of Interdisciplinary Interest.
February 25 **Tilden Lecture:**	Prof.J.F.Nixon, (University of Sussex). Phosphaalkynes: New Building Blocks in Organic and Organometallic Chemistry.
February 26	Prof.M.L.Hitchman, (Strathcylde University). Chemical Vapour Deposition.
March 5	Dr.N.C.Billingham, (University of Sussex). Degradable Plastics-Myth or Magic.
March 11	Dr.S.E.Thomas, (Imperial College). Recent Advances in Organoiron Chemistry.
March 12	Dr.R.A.Hann, (ICI Imagedata). Electronic Photography-An Image of the Future.

March 18	Dr.H.Maskill, (Newcastle University). Concerted or Stepwise Fragmentation in a Deamination-type Reaction.
April 7	Prof.D.M.Knight, (University of Durham). Interpreting Experiments: The Beginning of Electrochemistry.
May 13	Dr.J-C.Gehret, (Ciba Geigy, Basel). Some Aspects of Industrial Agrochemical Research.
October 15	Dr.M.Glazer and Dr.S.Tarling, (Oxford University and Birbeck College). It Pays to be British!- The Chemist's Role as an Expert Witness in Patent Litigation.
October 20	Dr.H.E.Bryndza, (Du Pont Central Research). Synthesis,Reactions and Thermochemistry of Metal(alkyl)cyanide Complexes and Their Impact on Olefin Hydrocyanation Catalysts.
October 22 **Ingold-Albert Lecture**	Prof. A.G.Davies, (University College, London). The Behaviour of Hydrogen as a Pseudometal.
October 28	Dr.J.K.Cockroft, (Durham University). Recent Developments in Powder Diffraction.
October 29	Dr.J.Emsley, (Imperial College, London). The Shocking History of Phosphorus.
November 4	Dr.T.Kee, (University of Leeds). Synthesis and Coordination Chemistry of Silylated Phosphites.
November 5	Dr.C.J.Ludman, (University of Durham). Explosions, A Demonstration Lecture.
November 11	Prof.D.Robins, (Glasgow University). Pyrrolizidene Alkaloids: Biological Activity, Biosynthesis and Benefits.
November 12	Prof.M.R.Truter, (University College, London). Luck and Logic in Host-Guest Chemistry.
November 18	Dr.R.Nix, (Queen Mary College, London). Characterisation of Heterogeneous Catalysts.
November 25	Prof.Y.Vallee, (University of Caen). Reactive Thiocarbonyl Compounds.
November 25	Prof.L.D.Quin, (University of Massachusetts, Amherst) Fragmentation of Phosphorus Heterocycles as a Route to Phosphoryl Species with Uncommon Bonding.
November 26	Dr.D.Humber, (Glaxo, Greenford). AIDS - The Development of a Novel Series of Inhibitors of HIV.
December 2	Prof.A.F.Hegarty, (University College, Dublin). Highly Reactive Enols Stabilised by Steric Protection.
December 2	Dr.R.A.Aitkin, (University of St.Andrews). The Versatile Cycloaddition Chemistry of $Bu_3P.CS_2$.

December 3 **SCI Lecture**	Prof.P.Edwards, (Birmingham University). What is a Metal?
December 9	Dr.A.N.Burgess, (ICI Runcorn). The Structure of Perfluorinated Ionomer Membranes.
1993	
January 20	Dr.D.C.Clary, (University of Cambridge). Energy Flow in Chemical Reactions
January 21	Prof.L.Hall, (University of Cambridge). NMR - A Window to the Human Body.
January 27	Dr.W.Kerr, (University of Strathclyde). Development of the Pauson-Khand Annulation Reaction. Organocobalt Mediated Synthesis of Natural and Unnatural Products.
February 3	Prof.S.M.Roberts, (University of Exeter). Enzymes in Organic Synthesis.
February 10	Dr.D.Gillies, (University of Surrey). NMR and Molecular Motion in Solution.
February 11 **Tilden Lecture**	Prof.S.A.R.Knox, (Bristol University). Organic Chemistry at Polynuclear Metal Centres.
February 17	Dr.R.D.W.Kemmitt, (University of Leicester). Oxatrimethylenemethane Metal Complexes.
February 18	Dr.I.Fraser, (ICI, Wilton). Reactive Processing of Composite Materials.
February 22	Prof.D.M.Grant, (University of Utah). Single Crystals, Molecular Structure and Chemical-Shift Anisotropy
February 24	Prof.C.J.M.Stirling, (University of Sheffield). Chemistry on the Flat-Reactivity of Ordered Systems.
March 3	Dr.K.J.P.Williams, (BP). Raman Spectroscopy for Industrial Analysis.
March 10	Dr.P.K.Baker, (University College of North Wales, Bangor). An Investigation of the Chemistry of the Highly Versatile 7-Coordinate Complexes $[MI_2(CO)_3(NCMe)_2]$ (M=Mo,W).
March 11	Dr.R.A.Jones, (University of East Anglia). The Chemistry of Wine Making
March 17	Dr.R.J.K.Taylor, (University of East Anglia).] Adventures in Natural Product Synthesis.
March 24	Prof.I.O.Sutherland, (University of Liverpool). Chromogenic Reagents for Chiral Amine Sensors.
May 13 **Boys-Rahman Lecture**	Prof.J.A.Pople, (Carnegie-Mellon University Pittsburgh). Applications of Molecular Orbital Theory.

May 21	Prof.L.Weber, (University of Biefield). Metallo-phospha Alkenes as Synthons in Organometallic Chemistry
June 1	Prof.J.P.Konopelski, (University of California, Santa Cruz). Synthetic Adventures with Enantiomerically Pure Acetals.
June 7	Prof.R.S.Stein, (University of Massachusetts). Scattering Studies of Crystalline and Liquid Crystalline Polymers.
June 16	Prof.A.K.Covington, (University of Newcastle). Use of Ion Selective Electrodes as Detectors in Ion Chromatography.
June 17	Prof.O.F.Nielsen, (H.C.Ørsted Institute, University of Copenhagen). Low-Frequency IR - and Raman Studies of Hydrogen Bonded Liquids.
October 4	Prof.F.J.Fehler, (University of California at Irvine). Bridging the Gap Between Surfaces and Solution with Sessilquioxanes.
October 20	Dr.P.Quayle, (University of Manchester). Aspects of aqueous ROMP Chemistry.
October 23	Prof.R.Adams, (University of S.Carolina) The Chemistry of Metal Carbonyl Cluster Complexes Containing Platinum and Iron, Ruthenium or Osmium and the Development of a Cluster Based Alkyne Hydrogenation Catalyst
October 27	Dr.R.A.L.Jones, (Cavendish Laboratory) Perambulating Polymers
November 10	Prof.M.N.R.Ashfold, (University of Bristol) High Resolution Photofragment Translational Spectroscopy: A New way to Watch Photodissociation
November 17	Dr.A.Parker, (Laser Support Facility) Applications of Time Resolved Resonance Raman Spectroscopy to Chemical and Biochemical Problems
November 24	Dr.P.G.Bruce, (University of St. Andrews) Synthesis and Applications of Inorganic Materials
December 1	Prof.M.A.McKervy, (Queen University, Belfast) Functionalised Calixirenes

The author has also attended the following lectures in the IRC in Polymer Science and Technology International Seminar Series.

1991

March 18	Prof.G.Wegner,(Max-Planck-Institut for Polymerforschung, Mainz), at Leeds University. New Developments in Main Chain Liquid Crystal Polymers
May 9	Prof.P.G.de Gennes, (Laboratoire de Physique de la Matiere Condensee, College de France, Paris), at Leeds University. Polymer-Polymer Interfaces
September 16	Dr.A.Griffin, (Melville Laboratory, University of Cambridge), at Leeds University. Photoactive Liquid Crystalline Polyacrylcinnamates.

1992

March 17	Prof.Sir S.Edwards, (Cavendish Laboratory, University of Cambridge), at Leeds University. Phase Dynamics and Phase Changes in Polymer Liquid Crystals
March 25	Prof.H.Chedron, (Hoechst AG, Frankfurt am Main), at Durham University. Structural Concepts and Synthetic Methods in Industrial Polymer Science.
May 11	Prof.W.Burchard, (University of Freiburg),at Durham University. Recent Developments in the Understanding of Reversible and Irreversible Network Formation.
September 21	Prof.E.L.Thomas, (MIT, Cambridge, Massachusetts),at Leeds University. Interface Structures in Copolymerr-Homopolymer Blends.

1993

April 1	Prof. H.W.Speiss, (Max-Planck Institut for Polymerforschung, Mainz), at Durham University. Multidimensional NMR Studies of Structure and Dynamics of Polymers.
June 2	Prof.F.Ciardelli, (University of Pisa), at Durham University. Chiral Discrimination in the Stereospecific Polymerisation of α-olefins.
June 8	Prof.B.E.Eichinger, (BIOSYM Technologies Inc. San Diego), at Leeds University. Recent Polymer Modeling Results and a Look into the Future.
July 6	Prof.C.W.Macosko, (University of Minnesota, Minneapolis), at Bradford University. Morphology Development in Immiscible Polymer Polymer Blending.

CONFERENCES/MEETINGS ATTENDED BY THE AUTHOR

October 1990-March 1991
The Basics of Polymer Science and Technology-An Introductory Course in the Physics, Chemistry and Engineering of Polymers (15 days) Hugh Ripley Hall Ripon.

March 26-28 1991
Macro Group (UK) Polymer Conference, Lancaster University.

June 25 1991
Macro Group (UK) Transistion Metal Mediated Polymerisations Conference, SCI London.

July 22-26 1992
Polymer Surfaces and Interfaces (II), Durham University,

March 26-28 1992
Macro Group (UK) Polymer Conference Durham University.

September 7-11 1992
RSC/SCI Macro Group (UK) and the ACS Division of Polymer Chemistry Inc., "Macromolecules '92" 3rd Euro-American conference on "Functional Polymers and Biopolymers", University of Kent, Canterbury.

June 27-July 2 1993
Tenth International Symposium on Olefin Metathesis, Tihany-University of Vesprem, Hungary.

APPENDIX 7

References

References

1. R.L.Banks and G.C.Bailey, Ind.Eng.Chem.Prod.Res.Develop., 3, 170, (1964)
2. Calderon et al, Chem.Eng.News., 45, 51, (1967)
3. A.W.Anderson and N.G.Merckling, U.S.Pat. 2,721,189 , (1955)
4. I.M.Robinson and W.L.Truett, U.S.Pat. 2,932,630 ,(1960)
5. W.L.Truett, D.R.Johnson, I.M.Robinson and B.A.Montague, J.Am.Chem.Soc., 82, 2337, (1960)
6. H.S.Eleuterio, U.S.Pat. 3,074,918 , (1957), Chem.Abst. 55:16005, (1961)
7. G.Dall'Asta, G.Mazzanti, G.Natta and G.Mortoni, Makromol.Chem., 69, 163, (1964)
8. G.Dall'Asta, G.Mazzanti and G.Natta, Angew.Chem., 76, 765, (1964)
9. N.Calderon and H.Y.Chen, U.S.Pat. 3,535,401 , (1970)
10. N.Calderon, H.Y.Chen and K.W.Scott, Tetrahedron Lett., 3327, (1967)
11. N.Calderon, E.A. Ofstead, J.P.Ward, W.A.Judy and K.W.Scott, J.Am.Chem.Soc., 90, 4133, (1968)
12. K.J.Ivin: "Olefin Metathesis", Academic Press, London, (1983)
13. V.Drugatan, A.T.Balaban, M.Dimonie: "Olefin Metathesis and Ring Opening Polymerization of Cyclo-olefins", 2nd edition, Wiley-Interscience, (1985)
14. T.Seagusa and E.Goethals: "Ring Opening Polymerization", ACS Washington, (1977)
15. B.M.Novak, W.Risse and R.H.Grubbs, Advances in Polymer Science, 102, (1992)
16. R.H.Grubbs, in 'Comprehensive Organometallic Chemistry', 8th edition, Wilkinson, Abel and Stone (Eds.), Pergamon Press, Oxford (1982)
17. K.J.Ivin: 'Metathesis Polymerisation' in 'Encyclopedia of Polymer science and Engineering' 2nd edition, Vol 9, p.634, Wiley-Interscience, (1985)
18. R.H.Grubbs, C.R.Hoppin, J.Chem.Soc.,Chem.Comm., 634, (1977)
19. T.T.Denisova, A.I.Syatkovskii and T.B.Skyratova, Polym.Sci.USSR, A25, 798, (1983)
20. J.Kress, M.Wesolek, J.A.Osborn, J.Chem.Soc.,Chem.Comm., 514, (1982)
21. C.P.Casey and T.J.Burkhardt, J.Am.Chem.Soc, 95, 5833, (1973)
22. C.P.Casey and T.J.Burkhardt, J.Am.Chem.Soc, 96, 7808, (1974)
23. E.O.Fisher and A.Maasbol, Angew.Chem., Inter.Ed., 3, 580, (1964)
24. R.R.Schrock, J.Feldman, C.F.Cannizo and R.H.Grubbs, Macromolecules, 20, 1169, (1987)

25. R.R.Schrock, R.T.DePue, J.Feldman, K.B.Yap, W.M.Davies, L.Parks, M.DiMare, M.Schofield, J.Anhaus, E.Walborsky, E.Evitt, C.Kruger and P.Batz, Organometallics, 9, 2262, (1990)
26. R.H.Crabtree, 'The organometallic chemistry of the transition metals', Wiley-Interscience, New York, (1988)
27. R.H.Grubbs, L.K.Johnson, B.M.Novak, D.M.McGarth, A.Benedicto, M.France, S.T.Guyen, M.Cagne, Abs of papers ACS, 204, Aug 1992
28. A.J.Amass, T.A.McGourtney, Eur.Polym.J., 16, 235, (1980)
29. J.S.Hamilton, K.J.Ivin and J.J.Rooney, Brit.Pol.J.,16, 21, (1984)
30. *a)*P.M.Blackmore, Ph.D Thesis, Durham University (1986), *b)*W.J.Feast, V.C.Gibson and E.L.Marshall, J.Chem.Soc.,Chem.Comm., 16, 1157, (1992) and *c)* G.R.Davies, W.J.Feast, V.C.Gibson, H.V.S.Hubbard, K.J.Ivin, A.M.Kenwright, J.P.Mitchell, I.M.Ward, B.Wilson, Makrom.Chem., Macrom.Symp., 66, 289, (1993)
31. P.R.Marshall and B.J.Ridgewell, Eur.Polym.J., 5, 29, (1969)
32. K.W.Scott, N.Calderon, E.A.Ofstead, W.A.Judy, and J.P.Ward, ACS Adv.Chem.Ser., 91, 399, (1969)
33. J.Herisson and Y.Chauvin, Macromol.Chem., 141, 161, (1970)
34. E.Thorn-Csanyi, Angew.Macromol.Chem., 94, 181, (1985)
35. E.Thorn-Csanyi, J.Mol.Cat., 28, 49, (1985)
36. E.Thorn-Csanyi and H.Timm, J.Mol.Cat., 28, 37, (1985)
37. M.L.H.Green, G.J.A.Adam, S.G.Davies, K.P.Ford, M.Ephritikhine and P.F.Todd, J.Mol.Cat., 8, 15, (1980)
38. L.R.Gillion and R.H.Grubbs, J.Am.Chem.Soc, 108, 733, (1986)
39. R.R.Schrock, Acc.Chem.Res, 23, 158, (1990)
40. J.S.Murdzek, R.R.Schrock, Macromolecules, 20, 2642, (1987)
41. R.M.E.Green, K.J.Ivin, J.J.Rooney, J.Kress and J.A.Osborn, Makromol.Chem., 189, 2797, (1988)
42. F.Stelzer, O.Leitmer, K.Pressl, G.Leising and R.H.Grubbs, Synthetic.Metals, 41-43, 991, (1991)
43. a)J.Mitchel, Ph.D Thesis, Durham University (1991) and *b)*J.P.Mitchell, V.C.Gibson, R.R.Schrock, Macromolecules, 24,5, 1220, (1991)
44. *a)*Z.Wu, L.K.Johnson, R.A.Fisher and R.H.Grubbs, Abs. of papers A.C.S.,201, 129, (Apr. 1992) and *b)*Z.Wu, D.R.Wheeler and R.H.Grubbs, J.Am.Chem.Soc., 114, 146, (1992)
45. C.A.Smith, Ph.D Thesis, Durham University(1993)
46. R.J.Michak and H.Tucker, Am.Chem.Soc., Polym.Prep., 13, 885, (1972)

47. K.J.Ivin, J.H.O'Donnell, J.J.Rooney and C.D.Stewart, Makromol.Chem., 180, 1975, (1979)
48. F.Imaizumi, K.Enyo and Y.Nakata, Jpn.Kokai Tokkyo Koho 7745697 (Apr.11, 1977)
49. Y.Kobayashi, R.Jio and T.Ueshima, Jpn.Kokai Tokkyo Koho 7976700 (June 19, 1979)
50. T.J.Katz, JMcGinnis and C.Altus, J.Am.Chem.Soc, 98, 606, (1976)
51. V.A.Kormer, E.R.Dolinskaya and A.S.Katchaturov, Macrom.Chem., Rapid.Comm., 1, 531, (1980)
52. H.Sato, K.Okimoto and Y.Tanaka, J.Macrom.Sci.Chem., A11, 767, (1977)
53. J.G.Hamilton, K.J.Ivin, J.J.Rooney and L.C.Waring, J.Chem.Soc.,Chem.Comm., 159, (1983)
54. T.J.Katz, S.J.Lee and N.Acton, Tetrahedron Letters, 47, 4247, (1976)
55. T.J.Katz, S.J.Lee and M.A.Shippey, J.Mol.Cat., 8, 219, (1980)
56. L.R.Gillion, Ph.D Thesis, California Institute of Technology, (1986), cited in 44b
57. R.R.Schrock, R.T.DePue, J. Feldman, C.J.Schaverien, J.C.Dewan, A.H.Liu, J.Am.Chem.Soc, 110, 1423, (1988)
58. R.R.Schrock, K.B.Yap, D.C.Yang, H.Sitzmann, L.R.Sita and G.C.Baazan, Macromolecules, 22, 3191, (1989)
59. I.Pasquon and V.Giannini: "Stereoregular linear polymers" in Encyclopedia of Polymer Science and Engineering, 2nd edition, V.15, p.632, Wiley-Interscience, (1985)
60. G.Dall'Asta and P.Scaglione, Rubber Chem.Techn., 42,1235, (1969)
61. G.Natta, G.Dall'Asta and G.Mazzanti, Angew.Chem.Int.Ed.Engl., 3(11), 723, (1964)
62. G.Natta, G.Dall'Asta, I.W.Bassi and G.Carella, Makromol.Chem., 91, 87, (1966)
63. C.P.Casey and T.J.Burkhardt, J.Am.Chem.Soc, 95, 5833, (1973)
64. C.P.Casey, L.D.Albin and T.J.Burkhardt, J.Am.Chem.Soc, 99, 2533, (1977)
65. G.Dall'Asta and R.Manetti, Eur.Pol.J., 4, 154, (1968)
66. L.M.Vardanyan, Y.V.Korshak, M.P.Peterina and B.A.Dolgoplosk, Dokl.Akad.Nauk.SSSR, 207, 345, (1972)
67. A.E.Tonnelli, "NMR Spectroscopy and Polymer Microstructure, the conformational connection.", AT&T Bell Laboratories, VCH Publishers Inc., N.Y., (1989)
68. L.Hocks, D.Berck, A.J.Hubert and P.Teyssié, J.Polym.Sci.,Polymer Lett., 13, 391, (1975)
69. J.H.Edwards and W.J.Feast, Polymer, 21, 595, (1991)
70. J.L.Brédas and R.Silbey, "Conjugated Polymers", Kluwer Academic Publishers, Dordreht, (1991)
71. L.Y.Park, R.R.Schrock, S.G.Stieglitz and W.E.Crowe, Macromolecules, 24, 3489, (1991)

72. G.Bazan, E.Khosravi, R.R.Schrock, W.J.Feast, V.C.Gibson, M.B.O'Reagan, J.K.Thomas and W.M.Davies, J.Am.Chem.Soc., 112, 8378, (1990)
73. S.A.Krouse and R.R.Schrock, Macromolecules, 21, 1885, (1988)
74. H.E.Schaffer, R.R.Chanche, R.J.Silbey, K.Knoll, and R.R.Schrock, J.Chem.Phys., 94, 4161, (1991)
75. E.Khosravi, M.A.Mohsin, W.J.Feast, T.F.Johnson and V.C.Gibson, Conference preceedings, 10th International Symposium on Olefin Metathesis, Tihany, Hungary, (1993)
76. G.C.Bazan and R.R.Schrock, Macromolecules, 24, 4, 817-822, (1991)
77. H.C.Brown, R.F.McFarlin, J.Am.Chem.Soc., 78, 252, (1956)
78. W.P.Cochrane, P.L.Pauson and T.S.Stevens, J.Chem.Soc., (c), 630, (1968)
79. W.Ried and R.F.Königstein, Chem.Ber., 92, 2532, (1959)
80. J.Roovers, "Branched polymers" in 'Encyclopedia of Polymer science and Engineering' 2nd edition, Vol 2, p.478, Wiley-Interscience, (1985)
81. M.E.Brown, Introduction to thermal analysis, Chapman & Hall Ltd., London, (1988)
82. J.P.Runt, "Crystallinity determination" in Encyclopedia of Polymer Science and Engineering 2nd edition, Vol.4, p.487, Wiley-Interscience, (1985)
83. J.G.Hamilton, K.J.Ivin and J.J.Rooney, Brit.Pol.Journal, **16**, 21, (1984)
84. H.J.Harwood, D.B.Russel, J.J.A.Verthe and J.Zymonas, Macromol.Chem., **163**, 1, (1973)
85. W.Risse, D.R.Wheeler, L.F.Canizzo and R.H.Grubbs, Macromolecules, **22**, 3205, (1989)
86. K.J.Stone and R.D.Little, J.Org.Chem., **49**, 1849, (1984)
87. H.O.Kalinowski, S.Berger and S.Braun, "^{13}C-NMR spectroscopy", (1988)
88. A.Wasserman, "Diels-Alder reactions", Elsevier, N.Y.,(1965)
89. K.Alder, Ann.Chem., **1**, 566, (1950)
90. H.H.Fox, J.Lee, L.Y.Park and R.R.Schrock, Organometallics, **12**, 759, (1993)
91. R.H.Wiley, J.I.Jin, Y.Kamath, J.Polymer.Science, A-1, **6**, 1065, (1968)
92. E.L.Marshall, Unpublished results
93. W.J.Feast, V.C.Gibson, E.Khosravi, E.L.Marshall and J.P.Mitchell, Polymer Comm., **33**, 872, (1992)